Supplementary file S6 to: Grimm, V. et al. (2020) 'The ODD Protocol for Describing Agent-Based and Other Simulation Models: A Second Update to Improve Clarity, Replication, and Structural Realism' *Journal of Artificial Societies and Social Simulation* 23 (2) 7: http://jasss.soc.surrey.ac.uk/23/2/7.html [10.18564/jasss.4259]

# S6: Example TRACE documents

In this supplement, example TRACE documents from the literature are compiled. We acknowledge permission of the authors to do so. In case you want to use specific parts of these documents (e.g., certain submodels, approaches, parameterizations), please cite the corresponding publicaton of the TRACE document:

Nabe-Nielsen, J., van Beest, F. M., Grimm, V., Sibly, R. M., Teilmann, J., & Thompson, P. M. (2018). Predicting the impacts of anthropogenic disturbances on marine populations. *Conservation Letters*, e12563.

Ayllón, D., Railsback, S. F., Vincenzi, S., Groeneveld, J., Almodóvar, A., & Grimm, V. (2016). InSTREAM-Gen: Modelling eco-evolutionary dynamics of trout populations under anthropogenic environmental change. *Ecological Modelling*, *326*, 36-53.

# TRACE document

This is a TRACE document ("TRAnsparent and Comprehensive model Evaludation"), which provides supporting evidence that our model presented in:

> **Nabe-Nielsen J., van Beest F.M., Grimm V., Sibly R.M., Teilmann, J. & Thompson, P.M. (2018). Predicting the impacts of anthropogenic disturbances on marine populations. *Conserv. Lett.* 11(5), e12563.**

was thoughtfully designed, correctly implemented, thoroughly tested, well understood, and appropriately used for its intended purpose.

The rationale of this document follows:

> Schmolke A., Thorbek P., DeAngelis D.L., Grimm V. (2010). Ecological modelling supporting environmental decision making: a strategy for the future. *Trends Ecol. Evol.* 25, 479-486.

and uses the updated standard terminology and document structure in:

> Grimm V., Augusiak J., Focks A., Frank B., Gabsi F., Johnston A.S.A., Liu C., Martin B.T., Meli M., Radchuk V., Thorbek P., Railsback S.F. (2014). Towards better modelling and decision support: documenting model development, testing, and analysis using TRACE. *Ecol. Modell.* 280, 129–139.

and

> Augusiak J., Van den Brink P.J., Grimm V. (2014). Merging validation and evaluation of ecological models to 'evaludation': a review of terminology and a practical approach. *Ecol. Modell.* 280, 117–128.

# Contents

# 1 Problem formulation

**This TRACE element provides supporting information on**: The decision-making context in which the model will be used; a precise specification of the question(s) that should be answered with the model, including a specification of necessary model outputs; and a statement of the domain of applicability of the model, including the extent of acceptable extrapolations.

**Summary:**

**Anthropogenic noise can induce behavioral responses in marine mammals, which may influence the individual animals' foraging success and, ultimately, the dynamics of the population. Pile-driving noise associated with construction of offshore wind farms can have pervasive effects on the harbor porpoise (*Phocoena phocoena*). In this study we present an agent-based model, the DEPONS model, for assessing population consequences of such pile-driving noise on the porpoise population in the North Sea. Population dynamics emerge from the individuals' competition for a dynamically replenishing food resource and from altered movements in the presence of pile-driving noise. Model predictions are influenced by the exact timing and spatial location of individual pile-driving events.**

Marine populations experience increasing levels of noise from offshore renewable energy developments, seismic surveys, military sonars and ship traffic (Tyack 2008; Slabbekoorn et al. 2010; Nowacek et al. 2015). A comprehensive assessment of the effects of human noise on marine populations is increasingly demanded for management of marine ecosystems in Europe and the U.S. (EU Marine Strategy Framework Directive 2008; White House Executive Order 2010). Many types of offshore activities (including wind farm construction) require an environmental impact assessment (EIA) to be conducted prior to development. EIAs are particularly focused at fragile and protected populations, and in European waters the species mentioned on the Habitats Directive (EU 1992) are of concern. Critically, they often require a cumulative assessment of the population level impacts of the primary development in combination with other human activities in the region. The model we present here can be used for conducting spatial planning to ensure that offshore activities affect the population as little as possible and conduct EIAs of planned projects. The model has been developed for the harbor porpoise (*Phocoena phocoena*), a small cetacean listed on the Habitats Directive Annexes II and IV, but the principles behind the model can be applied for any marine species.

Noise can travel over long distances in marine environments and induce behavioral responses of affected individuals (DeRuiter et al. 2013; Miller et al. 2015). This can lead to disruption of natural foraging behavior and habitat displacement, with potential consequences for individual survival and population dynamics. Pile-driving of wind turbine foundations, which is one of the most pervasive sources of noise in many areas, is known to affect harbor porpoise densities at distances >20 km (Tougaard et al. 2009; Brandt et al. 2011). The modeling framework we present here links the dynamics of harbor porpoise populations directly with the response of individuals to pile-driving noise. Model predictions depend on the exact timing and location of pile-driving events. Population densities and the time it takes the population to recover after pile-driving stops can be measured either locally or for the entire population.

TRACE document: Nabe-Nielsen et al. 2018. Individual-based model of habor porpoise.

The model takes a data-driven, mechanistic approach to management of marine populations. Population dynamics emerge from the individuals' competition for a dynamically replenishing food resource and from altered movements and foraging success when pile-driving noise is present. The model framework is currently parameterized for assessing effects of wind farm construction on the North Sea harbor porpoise population, but can be parameterized for other populations and other types of impulsive noise. The use of general relationships between population regulation and resource availability (Sinclair 2003; Goss-Custard et al. 2006) is likely to cause the model to generate robust predictions for a wide range of environmental conditions (Grimm & Railsback 2005; Stillman et al. 2015).

Although the model is likely to be robust to variations in environmental conditions, it should be noted that it was developed for the North Sea population. As population dynamics are tightly linked to animal foraging behavior and space use (home ranges), the model can only be extrapolated to areas outside the North Sea if there are empirical data available for re-calibrating the movement patterns. We consistently used the simplest possible implementation of the different processes and behaviors in the model (i.e. the submodels that involved the smallest number of parameters) if there were no data to suggest that particular parameters could play a role for harbor porpoise movement, energetics or population dynamics in nature.

# 2 Model description

**This TRACE element provides supporting information on**: The model. Provides a detailed written model description. For individual/agent-based and other simulation models, the ODD protocol is recommended as standard format. For complex submodels it should include concise explanations of the underlying rationale. Model users should learn what the model is, how it works, and what guided its design.

**Summary:**

**Here we present the complete description of the DEPONS model for simulating population effects of pile-driving noise (version 1.1). The description follows the updated ODD (Overview, Design concepts, Details) protocol (Grimm et al. 2010). The model extends an existing agent-based model (Nabe-Nielsen et al. 2014). The present documentation includes both elements previously described for the original model, an overview of the underlying fine-scale movement model (Nabe-Nielsen et al. 2013b) and the novel behaviors related to large-scale movement and to changes in movements in the presence of noise. The model, which was implemented in Repast Simphony 2.3.1 (http://repast.sourceforge.net), is open-source and published under the GNU General Public License v2. It can be downloaded from https://doi.org/10.5281/zenodo.556455.**

Section contents

## 2.1 Purpose

The model simulates how harbor porpoise population dynamics are affected by pile-driving noise associated with construction of offshore wind farms. The animals' survival is directly related to their energy levels, and the population dynamics are affected by noise through its impact on the animals' foraging behavior. By ensuring that the animals' movement patterns, space use and reactions to noise are realistic, the population dynamics in the model should have the same causal drivers in the model as in nature.

## 2.2 Entities, state variables, and scales

The model includes four kinds of entities: porpoises, wind turbines, landscape grid cells and cell groups. The porpoise agents are characterized by their location, speed, movement direction, age, age of maturity, energy level, pregnancy status, lactation status and preferred dispersal distance. Each porpoise agent is a 'super individual' (Scheffer et al. 1995) representing several real-world female porpoises. The wind turbine agents are characterized by their location, noise source level, the start time and end time for their construction.

Simulations are based on a 835.2 km × 870 km landscape covering the North Sea. The landscape is divided into 2088 × 2175 grid cells, each covering 400 m × 400 m, and into cell groups covering 2 km × 2 km. The choice of cell sizes was arbitrary. Cell groups do not have state variables, but are characterized exclusively by their location. They enable porpoises to navigate back to the places where they experienced the highest energy intake rates. Grid cells are characterized by their coordinates, average water depth, food level, maximum food level, distance to land and by whether they are used as food patches or not. The landscape includes land and bodies of water with unknown food levels (northern part of the North Sea; Figure 1), i.e. areas that are not used by simulated porpoises (42.0% of the grid cells), food patches

(0.67%) and water without food (57.3%). Each of the 30549 food patches covers one grid cell. Food level and maximum food level are always zero for grid cells that are not used as food patches. The distribution of the food patches is identical to the one used by Nabe-Nielsen et al. (2013b), i.e. it included on average 1000 food patches per 100 km × 100 km. The number of food patches is arbitrary, but sufficiently large to enable simulated porpoises to develop realistic movement patterns. The only other environmental parameter in the model is the time of year.

### 2.3 Process overview and scheduling

The model proceeds in time steps of half an hour and simulations typically last for 30 years. At the beginning of each time step porpoises detect noise originating from active pile-driving operations. This permits porpoises within a certain radius from pile-driving operations to know the direction of the noise source and the received sound level. The radius depends on the sound source level.

The animals' fine-scale movements are controlled by a combination of correlated random walk (CRW) behavior (Turchin 1998), their ability to move towards known food patches (directed by a spatial memory) and the extent to which they are deterred by noise. CRW movements predominate as long as energy intake is high, else animals gradually become more directed towards patches where they have previously found food (Nabe-Nielsen et al. 2013b). The animals turn and slow down if there is land ahead. Animals turn away from noise, and the strength of the bias away from the noise source depends on the received sound level. The noise level does not affect the length of their fine-scale moves. Animals can remain deterred for some time after the pile-driving stops, although to a decreasing extent (by default this behavior is turned off). The updating of this 'residual deterrence' takes place at the end of each time step.

The animals' energy levels and mortality are tightly coupled in the model. An animal's energy level (scaled to lie in the range 0–20) increases when it encounters food in a food patch, but decreases with every move. Animals consume a decreasing fraction of the food as their energy levels increase from 10 to 20, assuming that there is a limit to how much energy they can store. Consumption of food causes their energy levels to increase equivalently. Their energy expenditure per time step depends on the season and whether they are lactating. The lower their energy levels, the higher their risk of dying. Animals with lactating calves do not die, but abandon their calves instead. Individual energy budgets were constructed following established principles of physiological ecology (Sibly et al. 2013). The animals move one at a time in an order that is randomized after each half-hour time step. Animals whose energy levels have been decreasing for some time stop using fine-scale movements, and start dispersing towards more profitable areas (cell groups) instead.

Food is only found in the food patches, which are randomly distributed across the seascape. The maximum amount of food (energy) varies among patches and seasons. It is derived from seasonal maps of the relative porpoise densities in the North Sea (Figure 1; Gilles et al. 2016), assuming that porpoises are only observed in areas with sufficient food. Updating of the food distribution map takes place four times per year. The actual amount of food in the patches changes dynamically: When a porpoise visits a patch, it consumes all or part of the food found there, but afterwards the food (energy) level increases logistically until reaching the maximum level. The updating of patch energy levels, i.e. replenishment of food, takes place at the end of every simulation day, after porpoises have moved and consumed food.

At the end of each day a number of life-history processes take place: Porpoises die if they reach their maximum age. They may mate, depending on the time of the year and their age. If

they are already pregnant, they may give birth. If accompanied by a lactating calf they may wean the calf, which results in the creation of a new, independent individual in the model (if the calf is a female). Independent male porpoises are not included in the model, as the number of males was not considered a limiting factor for reproduction. The number of males is therefore not expected to affect population dynamics. Once every year, new mating dates are calculated.

The different variables in the model are updated asynchronously, i.e. immediately after a process has been executed.

## 2.4 Design concepts

*2.4.1 Basic principles:* The model builds on the assumption that the porpoise population is food limited, at least in the absence of noise. Noise acts by scaring porpoises away and by causing habitat fragmentation, thereby reducing the animals' foraging efficiency. The animals' foraging efficiency is also influenced by their ability to return to high quality areas they have previously visited, which assumes that they have a spatial memory (see Nabe-Nielsen et al. 2013b). The animals' energy budget is represented using the model presented by Sibly et al. (2013).

*2.4.2 Emergence:* The equilibrium population size (carrying capacity) emerges from a Balance between mortality and reproduction, where mortality is linked to the energy levels of individual animals (i.e. porpoise agents). The energy levels, in turn, emerge from a balance between energy expenditure and food intake. Animals adapt their foraging behavior to increase food intake and fitness when they have not found food in the recent past. The animals' spatial distribution in the landscape emerges from their tendency to disperse towards more profitable parts of the landscape and their age class distribution emerges from their starvation-related mortality.

The rate at which local porpoise densities recover after a pile-driving operation ends emerges from the animals' decision to either return to previously visited food patches close to the pile-driving area, to utilize food patches in the area they were displaced to, or to start dispersing. Their choice between these three alternatives depends on their energetic state and their success finding food in the area they were displaced to (partially related to chance events and partially to fitness-optimizing behavior).

*2.4.3 Adaptation:* Animals react to decreasing food levels in particular patches by being less attracted to them. They react to decreasing energy levels by dispersing towards parts of the landscape (i.e. cell groups) where they have previously experienced a high energy intake rate.

*2.4.4 Objectives:* Animals attempt to optimize their foraging behavior, and hence maximize their fitness, by returning to previously visited food patches when correlated random walk movements result in a low food acquisition rate. They also attempt to optimize foraging by dispersing towards more profitable areas when fine-scale movements do not enable them to sustain their energy levels.

*2.4.5 Learning:* Animals do not learn from what other animals have experienced. They do remember the location of previously visited food patches for some days (Nabe-Nielsen et al. 2013b), which enables them to adapt their fine-scale movements. They also have a persistent memory of the profitability (i.e. the energy intake rate) of all cell groups they have visited since they were born, so they gradually learn about the quality of different parts of the landscape. This guides their dispersal behavior. The animals learn/inherit their preferred dispersal distance from their mother before entering the model as independent individuals, but they do not inherit their mothers' knowledge of where the most profitable cell groups are.

*2.4.6 Prediction:* Animals base their prediction of how much food they can gather in different areas on their previous visits to those areas.

*2.4.7 Sensing:* Animals are able to sense if there is land in the direction they are about to move, which permits them to turn towards deeper water to avoid the coast. They also sense noise, which causes them to turn away from the noise emitting object(s). The animals know when their energy levels decrease, which causes them to disperse and to be more likely to abandon their lactating calves, or to die.

*2.4.8 Interaction:* The modeled animals only interact indirectly via competition for food.

*2.4.9 Stochasticity:* Fine-scale movement, mating date and mortality involve stochastic events. The probability of surviving increases with increasing energy levels.

*2.4.10 Collectives:* Social structure is not included in the model, but each agent represents several real animals.

*2.4.11 Observation:* The number of animals, their energy levels and the total amount of food in the landscape are recorded daily. The number of animals in different parts of the landscape can be counted (based on the 'blocks file'), and the movement tracks of a specified number of animals can be recorded to analyze for variations in home range sizes etc. The extent to which animals react to noise (i.e. the length of the deterrence vector, $|\mathbf{V}_D|$, see Eqn. 3) can be recorded for each half-hourly position. The age-class distribution and age specific mortalities are recorded yearly.

## 2.5 Initialization

The model was initialized by creating 10,000 randomly distributed porpoise agents. Their age-class distribution corresponded to that of stranded and by-caught animals (Lockyer & Kinze 2003), and 68% of the adults in the model were pregnant (corresponding to parameter *h* in Table 1). The energy level, $E_p$, of each porpoise was initially modeled as a random normal variable with mean 10 and standard deviation one (parameter $E_{\text{init}}$). Mating date was a random normal variable with mean 225 and standard deviation 20. Simulations were set to start on 1 January 1981. They included 3900 piling operations distributed on 65 wind farms that were planned to be built in the period 2011–2020 as part of the European Union 2020 goals (Directive 2009/28/EC, http://eur-lex.europa.eu/legal-content/EN/ALL/?uri=CELEX%3A32009L0028, summarized in http://www.ewea.org/fileadmin/ewea_documents/documents/publications/reports/Seanergy_2020.pdf). The food levels in the patches were set to the location specific maximum food levels for 1 January.

The model simulations can be initialized and executed through a Graphical User Interface (GUI) or through a batch procedure. The GUI allows for one simulation run at a time where the user can view the porpoise movements and distribution across the landscape, the location and construction period of wind farms, the population size, energy levels of porpoise agents, energy levels in food patches distributed across the landscape, as well as the age class distribution of the population. In the batch procedure the user can initialize multiple simulations that run simultaneously, but the user cannot see the aforementioned components on the screen or obtain information on age class distribution. Once the simulation(s) has completed the model output is automatically written out for both the GUI and batch procedure.

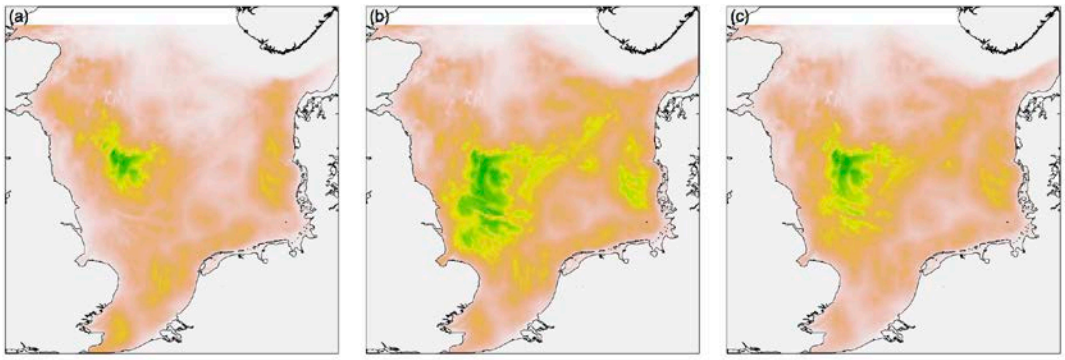


Figure 1. Food distribution maps derived from seasonal maps of porpoise densities in the North Sea for (a) spring, (b) summer, and (c) autumn (Gilles et al. 2016). Green shows areas with high porpoise densities, grey shows land and white indicates missing data. No porpoise density map was available for the winter, so the map from the autumn was used instead.

## 2.6 Input data

Eight different background maps are used in the model: The maximum amount of food in each food patch was derived from a map of the porpoise densities in the different parts of the North Sea (see Gilles et al. 2016 for details). These are included as four raster files with a spatial resolution of 400 m × 400 m, one for each season (Figure 1). No food was found outside the food patches. The raster file for the winter season (December–February) is read in from the file 'quarter1.asc' at the start of simulations. The ETRS89 - EPSG:3035 projection is used throughout. As there was no map available for porpoise densities in the winter, the map from the autumn season was used during winter. The raster maps were standardized to have a mean value of 0.3914, corresponding to the mean food level previously used in simulations of the Inner Danish Waters population (Nabe-Nielsen et al. 2014). Four additional raster files with the same extent and resolution are used: a 'patches' file describing the location of the food patches, a 'bathymetry' file that allows animals to avoid water depths $<w_{min}$ (see parameter list), a 'distance-to-coast' file (allowing animals to turn when approaching land) and a 'blocks' file that makes it possible to count the number of porpoises in user defined areas.

The simulations include details about pile-driving events. These are provided in a tab separated 'wind-farms' text file with columns id (identifier), x, y (coordinates), impact (sound source level, dB SEL @1m), start and end (timing of pile-driving, measured in number of half-hour time steps since the beginning of the simulation). Noise is emitted during both the start and the end time step. The sound source level was 234 dB SEL for pile-driving in all scenarios, corresponding to the value calculated for the Gemini wind farm (see below). See

the Submodels section for details on how noise from wind turbine agents was represented in the model.

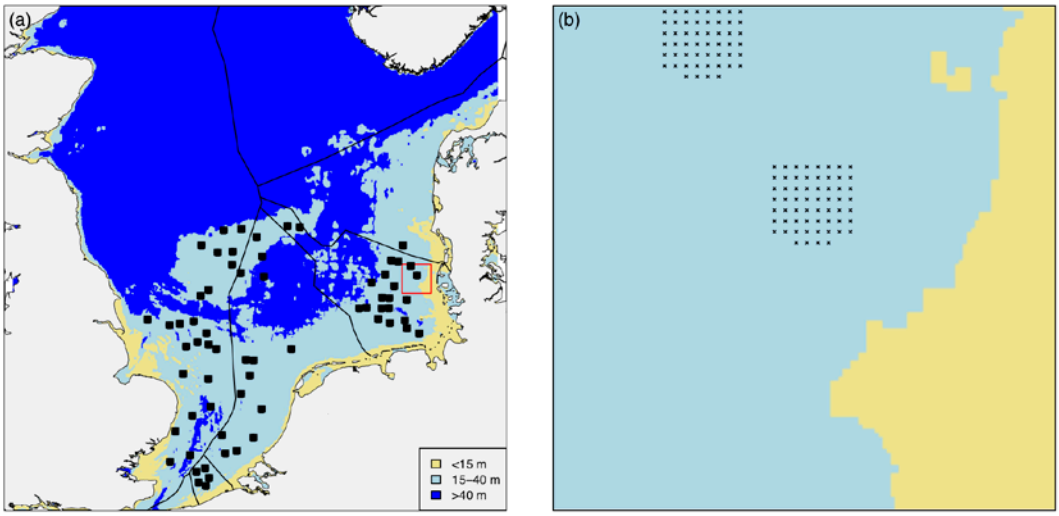


Figure 2. Positions of wind turbines in the three pile-driving scenarios used in this study. The red square on (a) indicates the 50 km × 50 km area shown in greater detail in (b).

Three different scenarios were used for investigating the population effect of wind farm construction in the North Sea. All scenarios included 65 wind farms with the same spatial distribution (Figure 2). A pre-specified number of wind farms were selected per country (Denmark: 1 wind farm; Germany: 21; Netherlands: 14; Belgium: 5; UK: 24), which enabled the individual countries to meet the EU 2020 target for renewable energy development (EU 2009). Wind farms were selected in areas with water depths between 15–40 m and >4 km from any neighboring wind farm. Aside from these rules wind farms were placed at random. Each wind farm included 60 wind turbines distributed in a regular 1078 m x 1078 m grid. 6 MW turbines constructed with monopile foundations was assumed throughout. Turbines were installed using pile-driving, which took two hours for each pile. No noise mitigation or soft start was included in the scenarios. The turbines were constructed in the 10-year period starting 1 January 2011, with 6–7 farms being built per year. In Scenario 1, the parks were constructed in random order, in Scenario 2 the parks in the eastern North Sea were built first, followed by the ones in the western North Sea (starting in the north in each area). In Scenario 3 parks were constructed in the same order as in Scenario 1, but the time between individual pilings within the wind farms was halved (from 48 hours to 24 hours). The start time of the first pilings in the different wind farms were the same in scenarios 1 and 3. In addition to these scenarios, we used a reference scenario without any wind farms to establish the population size in the absence of noise.

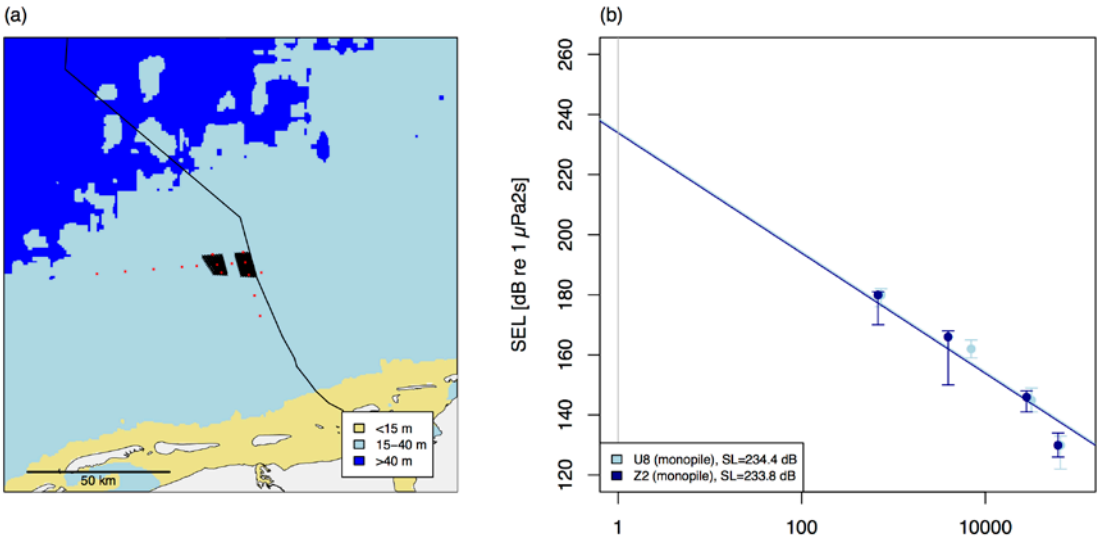


Figure 3. Data from the Gemini wind farm construction site used for calibration of the porpoises' response to noise. (a) Virtual landscape including wind turbine construction sites (black dots) and CPODS (red dots). The black line shows the border to Germany. (b) Received sound levels recorded using hydrophones at different distances [m] from two pilings. Sound source levels (*SL*) and sound transmissions were modeled assuming spherical spreading of the noise.

A different landscape, combined with a different set of pile-driving events, was used for calibration of the parameters *c* and *T* (see parameter list). The landscape was a 400 × 400 cell subset of the North Sea landscape covering the area around the Gemini wind farm construction site in the Netherlands (Figure 3). The landscape included a number of virtual CPODS (i.e. acoustic monitoring stations that detect the presence of porpoises based on the clicks they emit while foraging and navigating) whose positions corresponded to those of real CPODS deployed during wind farm construction. The 160 pile-driving events had the exact same positions as those of the real pile-driving events. Their sound source levels ('impact'; 234 dB SEL @1m) were calculated based on data from four hydrophones placed near two of the pile-driving locations (Figure 3b). See details on calibration of the porpoises' response to noise in the section 'Data evaluation'.

## 2.7 Submodels

The different submodels are executed in the order they are listed below (see overview in 'Process overview and scheduling'). Names of variables and parameters are retained from Nabe-Nielsen et al. (2013b, 2014).

### *2.7.1 Porpoises detect noise*

At the beginning of each time step, porpoises register the noise from active pile-driving operations. This is done by letting the wind turbine agents emit noise if they are under construction, thus producing a dynamic soundscape. Noise source levels (*SL*), positions and timings of pile-driving events are provided as input data. Animals react to noise only up to a certain distance from a pile-driving event. This distance is determined by the response threshold (*T*) and the extent to which sound is transmitted in water. Here *T* was determined based on data from the Gemini wind farm using pattern-oriented modeling. The sound level received by the animals (*R*) was modeled assuming spherical spreading (Figure 4a; Urick 1983), so

$$R = SL - 20 \log_{10}(\text{dist}(p,k)) \quad \text{Eqn. A1}$$

where dist($p$,$k$) is the distance from the porpoise $p$ to the pile-driving event $k$. Noise emitted by a pile-driving operation only influences animals out to a certain distance, $dist_{max}$, where $R = T$. By rearranging Eqn. 1 we get

$$dist_{max} = 10^{(SL - T) / 20} \quad \text{Eqn. A2}$$

Each pile-driving event equips all porpoise within the distance $dist_{max}$ with a deterrence vector that points directly away from the noise source (Figure 4). The length of the deterrence vector $\mathbf{V}_D$ is determined by

$$|\mathbf{V}_D| = c(R - T) \quad \text{Eqn. A3}$$

assuming a linear relationship between the received sound level and the strength of reaction. Here $c$ is the deterrence coefficient. Each animal's fine-scale movements are only influenced by the pile-driving event that yields the largest deterrence vector. This is usually without any practical implications, as wind farms are generally constructed by piling one turbine foundation at a time.

Animals can be assumed to sense the distance to anthropogenic noise sources, (as demonstrated by DeRuiter et al. 2013) and to stop being deterred when they are further away from the noise than a certain distance. When dist($p$,$k$) > $d_{max\_deter}$ the length of the deterrence vector is therefore set to 0. When using the default value of $d_{max\_deter}$ (Table 2), this parameter does not affect population dynamics. The parameter is only included to make it possible to assume a maximum deterrence distance in other studies.

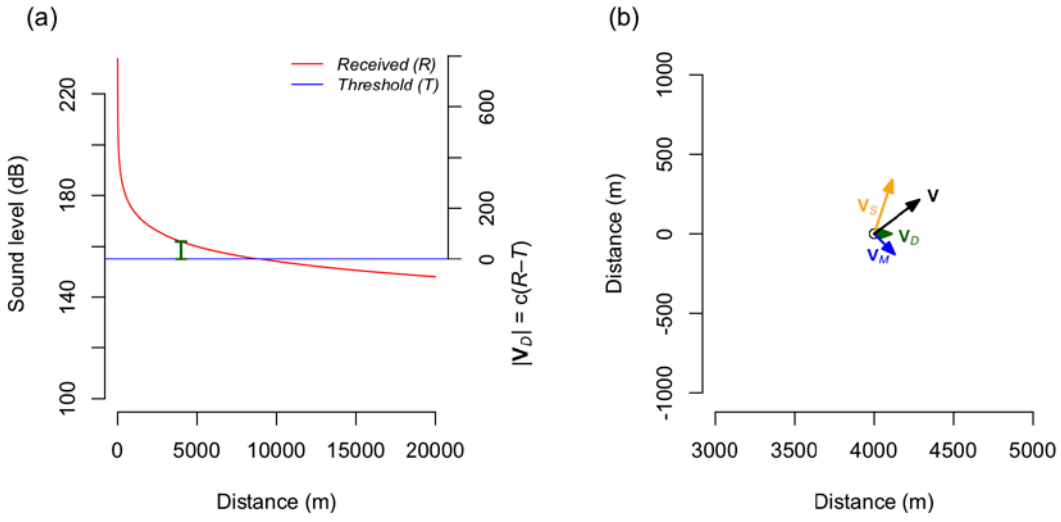


Figure 4. Relationship between received sound level ($R$) and deterrence behavior in the model. (a) Decrease in $R$ with distance assuming spherical spreading for pile-driving in Gemini, without noise mitigation ($SL$=234 dB SEL). The green bar shows the length of the deterrence vector for a porpoise located 4 km from the pile-driving, $|\mathbf{V}_D|$, i.e. the bias away from the noise. (b) Vector $\mathbf{V}_S$ represents the correlated random walk during **one** 30-min time step, $\mathbf{V}_M$ represents the spatial memory move and $\mathbf{V}_D$ represents the deterrence from North Sea pile-driving noise. $\mathbf{V}$ is the standardized resultant vector, i.e. the actual move in the presence of noise. Here shown for $c$=10 (deterrence coefficient; arbitrary value) and Threshold ($T$)=155 dB SEL. Here $dist_{max}$= 8913 m.

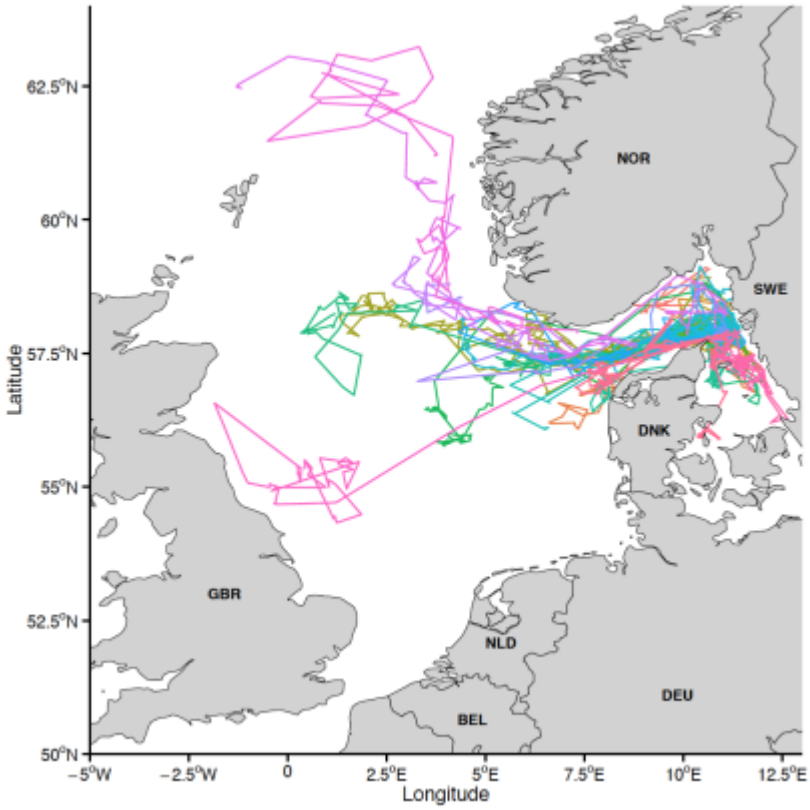


Figure 5. Tracks of 25 free-ranging porpoises equipped with ARGOS satellite tags providing a position every 1–3 days. All animals were tagged at Skagen, northern Denmark (DNK). Each track shows positions from a maximum of 150 days.

### *2.7.2 Disperse*

We distinguish large-scale movements/dispersal from the fine-scale movements described in section 2.7.3. In each time step each porpoise agent takes either a dispersal step or a fine-scale movement step depending on whether it is in dispersal mode (turned on in the submodel '[Life history processes]'').

When an animal agent disperses, it is guided by a persistent spatial memory (PSM) of the energy intake rate it has achieved in each of the different parts (cell groups) of the landscape that it has visited since it was born. Fine-scale movements, in contrast, are guided by a gradually decreasing memory of the foraging success in recently visited food patches. The rationale for introducing PSM to guide large-scale movements is that satellite tagged animals tend to return to the same general part of the landscape after having been elsewhere for several weeks or months (Figure 5). Such behavior must be guided by a spatial memory. Often such dispersal moves gradually switch from being relatively directed to becoming increasingly exploratory, which would enable animals to search for new foraging grounds in the vicinity of areas where they previously experienced a high food intake rate. Most animals keep moving back and forth over the same area, thus maintaining a constant dispersal distance.

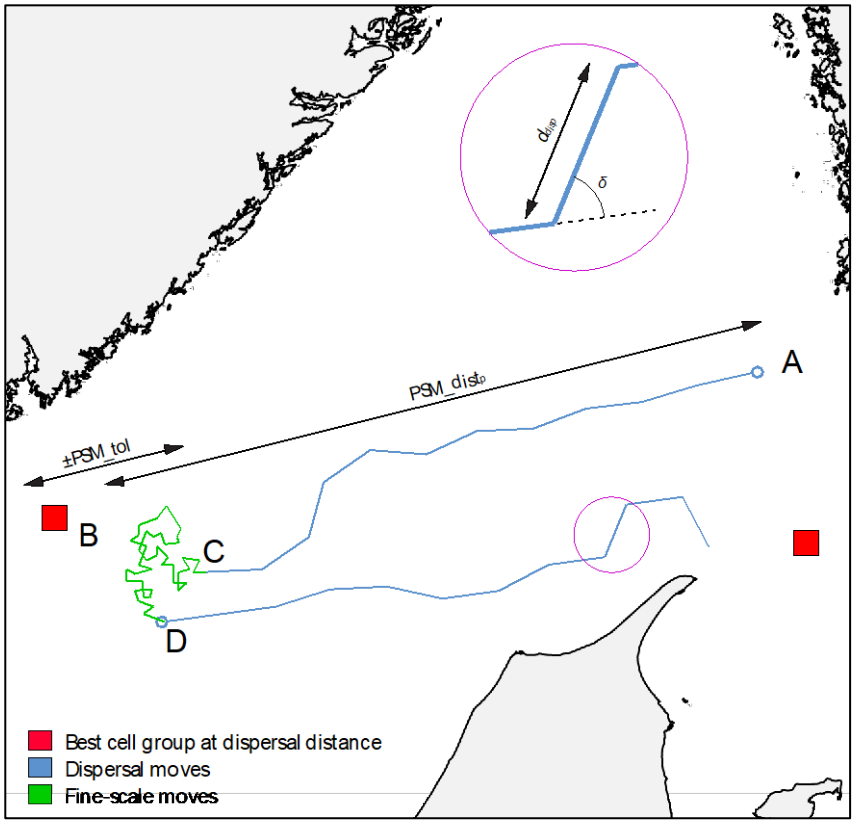


Figure 6. Dispersal behavior. When dispersal starts (A), the porpoise agent starts moving towards the most profitable 2 km × 2 km cell group (B) at its preferred dispersal distance. The distance from A to B is $d_{target}$. All dispersal steps have the length $d_{disp}$ and the total distance dispersed in a particular dispersal event is $d_{cum}$. After each dispersal step, the porpoise makes a random turn $\delta$. The turning angle increases the further the porpoise has dispersed. It stops dispersing when $d_{cum}$=0.95 $d_{target}$ (at point C), but may start dispersing again at a later point (D).

To incorporate PSM dispersal behavior into the model, the entire landscape was divided into 2 km × 2 km cell groups. Each animal is equipped with a preferred, fixed dispersal distance ($PSM\_dist_p$) at birth. Initially its value is drawn from a normal distribution, *PSM_dist*, but calves subsequently inherit the preferred dispersal distance from their mothers. Animals whose energy levels have been decreasing for $t_{todisp}$ days stop using fine-scale movements and start dispersing (Figure 6).

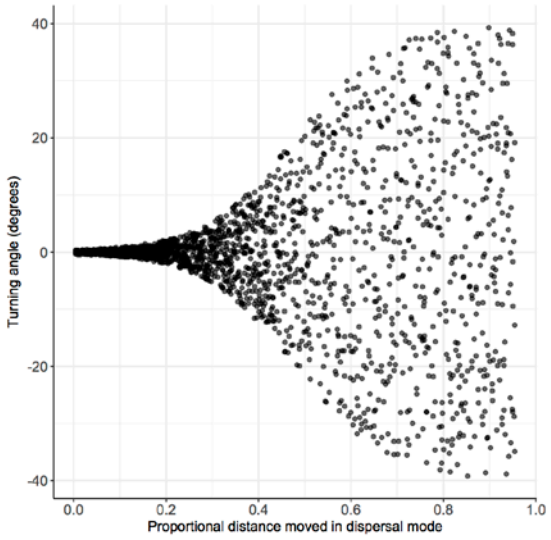


Figure 7. Simulated change in turning angle distribution as the porpoise agent approaches the dispersal target. In this example, PSM_angle was set to 40 and each dot represents a dispersal step (1987 steps within 26 distinct dispersal events). Angles are larger for animals that have dispersed a larger proportion of the initial distance to their dispersal targets.

When an animal starts dispersing, it turns towards the most profitable cell group at its preferred dispersal distance ($PSM\_dist_p \pm PSM\_tol$, see Table 2), i.e. the group where it has previously obtained the highest energy intake rate (calculated as total amount of food eaten divided time spent in each cell group). The distance to this cell group is $d_{target}$. Animals that have visited <50 cell groups disperse towards a random cell group at their preferred dispersal distance (burn-in behavior). All dispersal steps have the same length $d_{disp}$. Turning angles $\delta$ between consecutive steps increase logistically,

$$\delta = PSM\_angle\ \omega_2/(1+e^{-z/PSM\_log}) \qquad \text{Eqn. A4}$$

where $\omega_2$ is a random number in the range -1–1 and $z$ is determined by

$$z = (3 \times d_{cum} / d_{target}) - 1.5 \qquad \text{Eqn. A5}$$

Here $d_{cum}$ is the cumulated distance moved using dispersal moves during the current dispersal event, $d_{target}$ is the initial distance to the center of the selected cell group and *PSM_log* is >0 (see Table 2). Turning angles gradually increase from a value close to 0 (depending on the choice of *PSM_log*) to a maximum of *PSM_angle* (see Figure 7). The animals remember the amount of food they encounter while dispersing and the amount of time they spend in different cell groups. This enables them to navigate back towards these cell groups during subsequent dispersal events.

An animal stops dispersing (a) once it has moved $0.95 \times d_{target}$ using dispersal steps, or (b) if the next step would have caused it to move on land (i.e. to an area with water depth<$w_{disp}$) or (c) across the edge of the landscape, or (d) if its daily average energy level increases to a level that is higher than any of the daily energy levels they have experienced over the previous seven days, or (e) if it moves into an area with high noise levels (where $R>T$).

New independent calves inherit their preferred dispersal distance from their mother (but not their knowledge about relative profitability of different parts of the landscape). See Section 3.2.2 for details regarding calibration of dispersal parameters.

### *2.7.3 Fine-scale movement*

All animals that are not dispersing take a fine-scale move in each step.

The length and direction of a fine-scale move is determined by the sum of three vectors: $\mathbf{V}_S$, which describes a correlated random walk (CRW) move (Turchin 1998), $\mathbf{V}_M$, which describes a spatial memory move, and $\mathbf{V}_D$, which describes the deterrence from noise. The CRW behavior introduces a positive correlation between the lengths of consecutive steps and a negative correlation between consecutive turning angles. This corresponds to the behavior described in detail in the appendix of (Nabe-Nielsen et al. 2013b). Here

$$\mathbf{V}_S = \mathbf{x}(k + E) \qquad \text{Eqn. A6}$$

where $\mathbf{x}$ is a vector defining an unweighted CRW move and $k$ is an 'inertia constant' (see list of parameters related to movement, Table 2). $E$ is a measure of the benefit of using an undirected search for food, which is determined by how much food the animal remembers that it has found in the recent past. This is controlled by the actual amount of food encountered and the satiation memory decay rate $r_S$ (see details in Nabe-Nielsen et al. 2013b). As $k$ is small, the length of $\mathbf{V}_S$ is mostly related to $E$, which is used as a proxy for how much food the animal should expect to find if taking an undirected CRW step. The vector $\mathbf{x}$ allows the autocorrelation in turning angles and in step length, and the variance in these variables, to be controlled through the parameters $a$, $b$, $m$ and $R_1$–$R_3$. The equations describing these relationships are provided in Nabe-Nielsen et al. (2013b).

Fine-scale movements, in contrast to large-scale dispersal, are guided by a gradually decreasing memory of its foraging success in recently visited food patches. The animals' tendency to move towards previously visited food patches is determined by their memory of where they have found food in the past, and how much. This spatial memory move, $\mathbf{V}_M$, is determined by

$$\mathbf{V}_M = \sum M[c]\, \mathbf{i}[c] \qquad \text{Eqn. A7}$$

where $M$ is a measure of the amount of food that the animal remembers that it has found in patch $c$, weighed by the costs of going there (i.e. a measure of the benefit of returning to patch $c$). The animal's memory of previously visited patches decreases logistically with time. The shape of the logistic function is controlled by the reference memory decay rate $r_R$. $\mathbf{i}$ is a unity vector pointing in the direction of patch $c$ (Nabe-Nielsen et al. 2013b). The calculation of the deterrence vector is explained in Eqn. A3. The standardized resultant vector, i.e. the fine-scale move taken in the presence of noise, is then determined by

$$\mathbf{V}^* = \frac{\mathbf{V}_M + \mathbf{V}_S + \mathbf{V}_D}{\|\mathbf{V}_M + \mathbf{V}_S + \mathbf{V}_D\|} \times \|\mathbf{V}_S\| \qquad \text{Eqn. A8}$$

This equation is equivalent to Eqn. A2 of Nabe-Nielsen et al. (2014). In Eqn. A8 $\mathbf{V}^*$ has been standardized to have the same length as $\mathbf{V}_S$, so the length of the step is not affected by the noise level.

If the move defined by $\mathbf{V}^*$ would cause the porpoise to move to an area with too shallow water ($<w_{\min}$) it turns in the direction with deepest water (40°, 70°, 120° or 180° as needed).

### *2.7.4 Update energy level and mortality*

Porpoises increase their energy levels $E_p$ when moving through food patches and reduce the amount of food (energy) in the patches equivalently. They never eat more than 99% of the food they encounter in a patch, and always leave at least $U_{min}$ food units (see Table 1) to allow food levels to replenish (see section 2.7.6). Their energy levels are scaled to lie in the range 0–20. The animals consume a smaller proportion of the food as their energy levels increase from 10–20, and animals with an energy level of 20 do not consume any of the food they encounter (Nabe-Nielsen et al. 2014).

Porpoises use a season-dependent amount of energy $E_{use}$ in every step. They spend more energy during the summer ($E_{use} \times E_{warm}$ in the months May–September and $E_{use} \times (0.5 \times (1 - E_{warm}) + 1)$ in April and October) and when they are lactating ($E_{use} \times E_{lact}$).

The porpoises' risk of dying increases as their energy levels decrease. The yearly survival probability $s_y$ (Figure 8) is calculated as

$$s_y = 1 - e^{-\beta E_p} \qquad \text{Eqn. A9}$$

which is subsequently converted to a per-step survival probability

$$s_s = e^{log(s_y)/(360 \times 48)} \qquad \text{Eqn. A10}$$

If $\omega_1$ is a random number in the range 0–1 and the animal is lactating, the calf is abandoned if $\omega_1 > s_s$ (calves do not appear as independent individuals in the model). If $\omega_1 > s_s$ and the animal is not lactating, it dies (following the principles described by Sibly et al. 2013).

These processes take place in every time step.

### *2.7.5 Update food distribution map*

Every 3rd month (on simulation day 60, 150, 240 and 300), a new seasonal food distribution map is loaded. The map is used for determining the maximum amount of food that can be present in food patches in different parts of the landscape (Figure 1). The spatial distribution of the patches remains constant.

### *2.7.6 Update patch energy level*

Takes place every day.

$$E_k[t+1] = E_k[t] + r_U \times E_k[t] \, (1 - E_k[t] / M_k[t]) \qquad \text{Eqn. A11}$$

where $r_U$ is the food replenishment rate, $E_k[t]$ is the food level in patch $k$ at time $t$ and $M_k[t]$ is the maximum amount of food in each patch (derived from season-specific map of porpoise densities in the different parts of the North Sea; Gilles et al. 2016). This is equivalent to Eqn. A4 of Nabe-Nielsen et al. (2014).

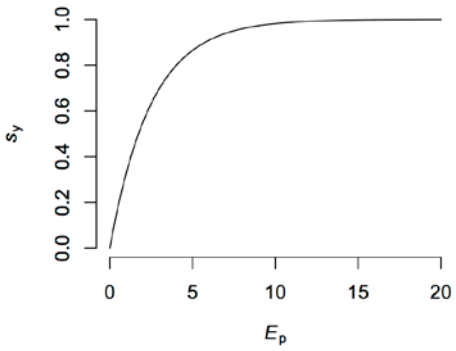


Figure 8. Relationship between energy level and yearly mortality for $\beta$=0.4.

### *2.7.7 Calculate mating dates*

Takes place every year, on 1 January. Each porpoise's mating date, $t_{mating}$, is drawn from a normal distribution.

### *2.7.8 Life-history processes*

This submodel is executed at the end of every day, i.e. every 48$^{th}$ time step.

Update the animals' dispersal status based on their daily average energy level. Animals start dispersing when their energy levels decrease for $t_{todisp}$ consecutive days.

Die of old age: Animals older than $t_{maxage}$ years are removed from the simulation.

Mate and become pregnant: If the simulation date is $t_{mating}$ the animals that are not already pregnant mate and become pregnant with a probability $h$.

Give birth: Animals that have been pregnant for $t_{gest}$ days give birth to a calf and start lactating.

Wean calf: Lactating animals stop nursing their calves after $t_{nurs}$ days. This results in the creation of a new independent individual in the model with probability 0.5 (assuming equal sex ratios). From the time of weaning male porpoises are omitted from the model.

See Table 1 for list of parameters related to animal life history.

### *2.7.9 Update residual deterrence*

Animals may keep being deterred by a noise source for some time after the noise stops. This is termed 'residual deterrence'. At the end of each step their movements become less biased by these noises that they are no longer exposed to. The decrease in residual deterrence is controlled by $\psi_{deter}$, so

$$|\mathbf{V}_D|_{t+1} = |\mathbf{V}_D|_t \, (100 - \psi_{deter})/100 \qquad \text{Eqn. A12}$$

After $t_{deter}$ time steps animals are assumed to stop being deterred by noise sources that no longer emit noise. By default $t_{deter}$ is set to 0 (see Table 2).

(Go to process overview).

# 3 Data evaluation

**This TRACE element provides supporting information on**: The quality and sources of numerical and qualitative data used to parameterize the model, both directly and inversely via calibration, and of the observed patterns that were used to design the overall model structure. This critical evaluation will allow model users to assess the scope and the uncertainty of the data and knowledge on which the model is based.

**Summary:**

**There is a total of 45 parameters in the DEPONS model, all of which can be specified by the user. Thirteen are related to animal life history and energetics, 23 are related to animal movement and reactions to noise, and 9 are related to general model behavior (specification of input and output files etc.). Seven of the parameters related to animal movement and reactions to noise are not currently used, but maintained to increase model flexibility and facilitate easy re-parameterization for other applications. The 36 parameters related to animal life history, energetics and movement are region-specific. Values are obtained from the literature for six parameters; four parameters controlling the animals' response to noise and dispersal movements were calibrated following a pattern-oriented modeling approach.**

Section contents



## 3.1 Parameters and data related to animal life history and energetics

The processes and parameter names of the DEPONS model related to birth and death of animals and to how animal survival is related to their energetic status are identical to the ones in the model described in Nabe-Nielsen et al. (2014).

Seven of the 13 parameters related to life history and energetics were obtained from the literature (Table 1). The parameter values for $h$ and $t_{mature}$ were based on data collected in the northwest Atlantic, off the coast of Maine (United States). The parameters are inherently hard to estimate due to difficulties studying harbor porpoises in the wild, and may vary among regions and among years. The parameters $t_{gest}$ and $t_{nurs}$ are based on a Danish study of captive animals and on studies of harbor porpoises in Danish waters. There are no data on how much the parameters vary among populations. The parameter $t_{maxage}$ is an upper limit for how old porpoises are likely to get, based on records of stranded animals in Denmark. The parameter $t_{mating}$ may vary among populations and years, but again this is difficult to assess due to the limited number of studies of porpoises in the wild. The parameter $E_{warm}$ was obtained from a

study of captive animals, based on their food consumption. It is difficult to assess to what extent the parameter varies among animals and depending on the size and health of the animals.

Six parameters related to energetics were either obtained from unpublished studies or calibrated based on general considerations regarding animal energetics (Sibly et al. 2013). The parameter $E_{lact}$ was obtained from a study of Danish captive animals. This is unlikely to vary much among populations due to energetic constraints related to animal energy consumption, but is likely to vary depending on the age of the lactating calf. The parameter $U_{min}$ is the minimum amount of food in a patch. The unit is scalable to kJ and other measures of energy content (hence we use the term 'relative unit' for energy-related variables). $U_{min}$ influences how fast food recovers in a patch after being nearly depleted. $E_{use}$ was calibrated to ensure that the population reached a dynamic equilibrium size, assuming that food recovered after approximately 2 days. This is based on the observation that satellite tagged porpoises in the inner Danish waters often return to the same area after approximately two days (J Nabe-Nielsen, unpubl. data). As porpoises have a high energetic demand (Wisniewska et al. 2016), we take such repeated returns to the same area as an indication that food has recovered. Details of the calibration procedure are provided in the appendix of Nabe-Nielsen et al. (2014). When letting the maximum amount of food in a patch be 1 during winter in the Inner Danish Waters simulations, the average food level in the patches was 0.3914 (Nabe-Nielsen et al. 2014). In the current study, the average food level in the patches was scaled to be the same (see input data), i.e. the average food level was assumed to be the same in the North Sea and the inner Danish waters. One unit of food in a patch is equivalent to one unit of energy available for the porpoise agents, and it is assumed that no energy is lost when food is consumed. The value of $\beta$ determines the relationship between the animals' energetic status and their risk of dying (Eqn. A9). The value used in this study was obtained through calibration (see details in Nabe-Nielsen et al. 2014). The relationship between the animals' energetic status and mortality is likely to vary among populations, but the use of a slightly different value of $\beta$ has a very small impact on population dynamics and carrying capacity (appendix of Nabe-Nielsen et al. 2014 and sensitivity analyses in chapter 7). The value of $r_U$ was calibrated to ensure that the population reached a stable population size (Nabe-Nielsen et al. 2013a, 2014). Unfortunately, there are no field studies that allow us to determine how $r_U$ varies among geographic regions.

| Parameter | Standard value | Code name | Description [units] (reference) |
|---|---|---|---|
| $h$ | 0.68 | h | Probability that adult females become pregnant (Read & Hohn 1995). |
| $t_{gest}$ | 300 | tgest | Gestation time [days] (Lockyer et al. 2003). |
| $t_{nurs}$ | 240 | tnurs | Nursing time [days] (Lockyer 2003; Lockyer & Kinze 2003). |
| $t_{maxage}$ | 30 | tmaxage | Maximum age of porpoises [years] (Lockyer & Kinze 2003). |
| $t_{mature}$ | 3.44 | mage | Age of maturity [years] (Read 1990). |
| $t_{mating}$ | N(225, 20) | randomMatingDayNormal | Mating day [day of year] (peaking in August; Lockyer |

| Parameter | Standard value | Code name | Description [units] (reference) |
|---|---|---|---|
| | | | 2003). |
| $E_{lact}$ | 1.4 | Elact | Energy use multiplier for lactating mammals [unitless] (Magnus Wahlberg, unpubl. data). |
| $E_{warm}$ | 1.3 | Ewarm | Energy use multiplier in warm water [unitless] (Lockyer 2003). |
| $E_{use}$ | 4.5 | Euse | Energy use per half-hour step in May–September [relative unit] (calibrated, Nabe-Nielsen et al. 2014). |
| $E_{init}$ | N(10, 1) | porpInitEnergyNormal | Initial energy level for porpoises [relative unit] (arbitrary). |
| $r_U$ | 0.1 | rU | Food replenishment rate; the rate that food recovers after being eaten [unitless] (calibrated, Nabe-Nielsen et al. 2014). |
| $U_{min}$ | 0.001 | regrowthFoodQualifier | Minimum food level in a patch; the starting value for logistic replenishment of the food [relative unit] (arbitrary). |
| $\beta$ | 0.4 | beta | Survival probability constant [unitless] (calibrated, Nabe-Nielsen et al. 2014). |

Table 1. Model parameters related to life history and energetics. The parameter names and parameter values are the same as used in Nabe-Nielsen et al. (2013b, 2014). The 'code names' are the names used in the Repast Java code in the current version of the model. Standard values of parameters written as N(x,y) indicate random values drawn from a Gaussian distribution with mean x and standard deviation y. In the input parameter files x and y are separated by ';'. The units of the parameters $E_{use}$, $E_{init}$ and $U_{min}$ are scaled by the same factor relative to Joule, hence the term 'relative unit'.

## 3.2 Parameters and data related to animal movements and response to noise

### *3.2.1 Parameters related to fine-scale movements*

The parts of the DEPONS model related to simulation of fine-scale movements are identical to the model described by Nabe-Nielsen et al. (2013b, 2014), except that the model has now been ported from NetLogo to the Repast framework to increase simulation speed. Fine-scale movements are influenced by the first 10 parameters in Table 2. Parameter names are kept the same as in Nabe-Nielsen et al. (2013b).

Fine-scale movements are simulated using a mixture of correlated random walk (CRW) behavior and spatial memory moves. The parameterization of the fine-scale movement model was done after $\log_{10}$ transforming the distance moved per 30-minutes step, as step lengths were approximately log-normally distributed in the movement data that was used for parameterization. The CRW is specified using the parameters $a$, $b$, $m$, $R_1$, $R_2$, and $R_3$, where $R_x$, provide mean and variation in distance moved per step, turning angles and in the relationship between turning angle and distance moved. The spatial memory behavior is

controlled by the parameters $r_S$, $r_R$, and $k$. All parameters were calibrated to ensure realistic fine-scale movement behavior (see Nabe-Nielsen et al. 2013b).

| Parameter | Standard value | Code name | Description [units] (reference) |
|---|---|---|---|
| $r_S$ | 0.2 | rS | Satiation memory decay rate [unitless] (Nabe-Nielsen et al. 2013b). Value used in (Nabe-Nielsen et al. 2014). |
| $r_R$ | 0.1 | rR | Reference memory decay rate [unitless] (Nabe-Nielsen et al. 2013b). Value used in (Nabe-Nielsen et al. 2014). |
| $k$ | 0.001 | k | Inertia constant; the animal's tendency to keep moving using CRW irrespective of foraging success [unitless] (arbitrary). |
| $a$ | 0.94 | a | Autocorrelation constant for $\log_{10}(d/100)$, where $d$ is distance moved per time step [unitless] (Nabe-Nielsen et al. 2013b). |
| $b$ | 0.26 | b | Autocorrelation constant for turning angles in CRW [unitless] (Nabe-Nielsen et al. 2013b). |
| $m$ | 0.74 | m | Value of $\log_{10}(d/100)$ where turning angles stop decreasing with speed. $d$ is distance moved per time step [m] (Nabe-Nielsen et al. 2013b). |
| $R_1$ | N(0.42, 0.48) | r1 | $\text{Log}_{10}(d/100)$, where $d$ is distance moved per time step [m] (Nabe-Nielsen et al. 2013b). |
| $R_2$ | N(0, 38) | r2 | Turning angle between steps [degrees] (Nabe-Nielsen et al. 2013b). |
| $R_3$ | N(96, 28) | r3 | Relationship between turning angle and $\log_{10}$ step length [unitless] (Nabe-Nielsen et al. 2013b). |
| $d_{maxmove}$ | 1.18 | dmax_mov | Maximum value of $\log_{10}(d/100)$ while using fine-scale moves. Here $d$ is distance moved per time step [m]. |
| $d_{disp}$ | 1.25 | ddisp | Dispersal distance per time step [km] (calibrated in current study). |
| $t_{todisp}$ | 3 | tdisp | Time before onset of dispersal [days]. Standard value based on the observations that captive porpoises appear to starve after not eating for three days (Magnus Wahlberg, unpubl. data). |
| *PSM_angle* | 20 | psmType2RandomAngle | Maximum absolute turning angle after each persistent spatial memory (PSM) dispersal step [degrees] (calibrated in current study). |
| *PSM_dist* | N(210, 50) | psmDistancePreference, psmDistanceStddev | Preferred distance to dispersal target. [km] (calibrated in current study). |
| *PSM_log* | 0.3 | psmLogDecrease | Parameter controlling logistic increase in turning angle during dispersal [unitless] |

| Parameter | Standard value | Code name | Description [units] (reference) |
|---|---|---|---|
| | | | (calibrated in current study). |
| *PSM_tol* | 5 | psmDistancePreferenceTolerance | Tolerance band within which the dispersal cell is selected (PSM dist±PSM tol) [km] (calibrated in current study). |
| $w_{disp}$ | 4 | wdisp | Minimum water depth when dispersing [m] (Nabe-Nielsen et al. 2014). |
| $w_{min}$ | 1 | wmin | Minimum water depth [m] required by porpoises (J. Tougaard, pers. obs). |
| *T* | 155 | drespthreshold | Response threshold; received sound level above which porpoises start getting deterred [dB] (calibrated in current study). |
| *c* | 0.07 | c | Deterrence coefficient [unitless] (calibrated in current study). |
| $d_{max\_deter}$ | 1000 | dmax_deter | Maximum deterrence distance [km]. Animals that are more than this far from the noise source should stop being deterred (worst-case scenario based on Brandt et al. 2012). |
| $t_{deter}$ | 0 | tdeter | Residual deterrence time; number of time steps the deterrence effect lasts when the animal is no longer exposed to noise [time steps] (arbitrary). |
| $\psi_{deter}$ | 50 | ddecay | Deterrence decay constant; decrease in deterrence per time step after noise has stopped [percent] (arbitrary). |

Table 2. Model parameters related to animal movements and response to noise. Parameter names and parameter values are the same as used in Nabe-Nielsen et al. (2013b, 2014), except for parameters that were introduced and calibrated in the current study. The 'code names' are the names used in the Repast computer code. Standard values of parameters written as N(x,y) indicate random values drawn from a Gaussian distribution with mean x and standard deviation y. In the input parameter files x and y are separated by ';'. The three last parameters in the table are not used (i.e. they are turned off) in the current study.

The CRW movement behavior of real porpoises, i.e. the animals' tendency to zig-zag and their speed while doing so, is likely to vary among animals and to depend on local environmental conditions. In the DEPONS model (version 1.1) the CRW behavior was calibrated based on data from a single animal equipped with a dead reckoning tag[†] in the inner Danish waters (Figure 9; J. Teilmann, unpublished data). Its movements are unlikely to be representative for all animals in all parts of the North Sea, but these were the only data available at the time the model was parameterized.

The spatial memory allows animals to navigate back to patches where they have found food in the past, which enables them to remain in the same area for several days or weeks. The

[†] Dead reckoning provides a means for calculating animal movements by integrating the speeds and headings for consecutive small segments of a movement path to construct the entire path, see (Wilson et al. 2007) for details.

behavior is controlled by the parameters $r_S$ (satiation memory decay rate, controlling whether animals keep using a correlated random walk), $r_R$ (reference memory decay rate, controlling animals' ability to navigate back to previously visited patches), $k$ and $w_{\text{min}}$. Here $k$ is a constant that only influences animal movements in the rare cases where they do not have any memory of previously visited food patches (e.g. in the beginning of simulations). $w_{\text{min}}$, which determines the minimum water depth required by porpoises, influences animal movements in the vicinity of the coast only. $r_S$ and $r_R$ were calibrated using pattern-oriented modeling (POM; Grimm et al. 2005; Kramer-Schadt et al. 2007) to ensure that animals developed movement tracks that closely resembled those observed for satellite-tracked animals in the inner Danish waters, i.e. with the same home range sizes, mean residence times and displacement distances (Nabe-Nielsen et al. 2013b). Again, these movements are unlikely to be representative for animals in all parts of the North Sea. The spatial memory behavior may therefore be improved by obtaining values of $r_S$ and $r_R$ that enable simulated animals to move similarly to North Sea animals equipped with satellite tags.

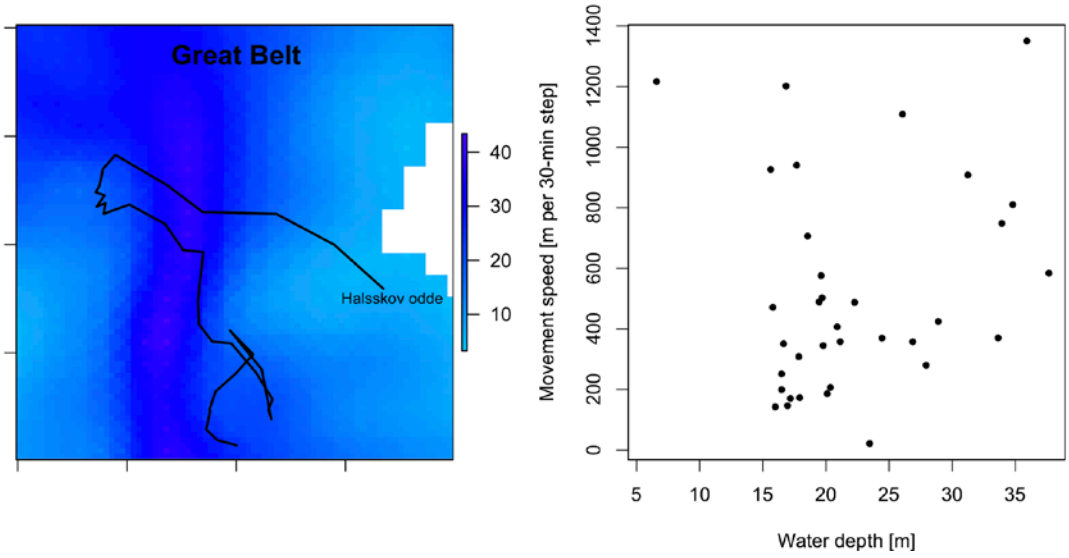


Figure 9. Movement track used for calibration of fine-scale movements (from animal equipped with Dead Reckoning tag). Each line segment shows a 30-min step. The legend shows the bathymetry in the area. The distance moved per step was weakly correlated with bathymetry ($r$=0.17). The same was the case for absolute turning angles ($r$= –0.23).

The fine-scale movements are not only influenced by the movement-related parameters themselves, but also by the spatial distribution of food patches and the average food levels in the patches. On the average, the food levels were the same in the current study as those used in the inner Danish waters (Nabe-Nielsen et al. 2013b, 2014) and the animals' fine-scale movements are therefore, on the average, the same as those previously documented for the inner Danish waters. The food levels were derived from maps of the spatial distribution of porpoises in the North Sea (see Figure 1). Further refinements of these maps can be expected to make fine-scale movements even more realistic for North Sea conditions. In order to use the model in other regions of the world similar maps must be produced for the entire area used by the population of interest.

### *3.2.2 Parameters related to dispersal*

Dispersal behavior was modeled based on a persistent spatial memory (PSM) movement behavior that enabled animals to navigate back to the 2 km × 2 km cell group where they had previously obtained the highest energy intake rate and that was located at their preferred dispersal distance. The seven parameters used for controlling dispersal are listed in Table 2.

To find the optimal values of the parameters $d_{disp}$ (distance moved per dispersal step), *PSM_angle* (maximum turning angle after each step) and *PSM_dist* (preferred dispersal distance) we simulated animal movement tracks based on a range of parameter values. The aim was to enable the model to produce tracks similar to those observed for 25 satellite-tracked porpoises (Figure 5). For $d_{disp}$ we considered the range 0.3–0.9 km 30 $min^{-1}$ (with 0.2 km 30 $min^{-1}$ increments), for *PSM_angle* we considered the values 20°, 40° and 60°, and for *PSM_dist* we considered mean values in the range 50–300 km (with 50 km increments). The standard deviation in *PSM_dist*, which controlled the variation in preferred dispersal distances among porpoise agents, was calibrated visually. The selected value allowed the variation in home range size of simulated animals to resemble that of satellite-tracked animals (Figures 5 and 11). All possible combinations of $d_{disp}$, *PSM_angle* and *PSM_dist* were tested. For each combination we recorded the movements of 25 porpoise agents over a 3-year period. All agents were initialized at Skagen (northern Denmark), which was where the satellite-tracked animals were tagged. We discarded the tracks for the first 2 simulation years, which was the time it took the agents to develop their spatial memory.

We compared the tracks of simulated animals with those of satellite-tracked animals based on three statistics: home range size, home range length and cumulative distance moved. The different statistics were calculated for day 150 of each track. The median value for the 25 satellite-tracked animals was compared to the corresponding median value for 25 simulated animals for each statistic. The procedures for calculating the different statistics are provided in TRACE Appendix A.

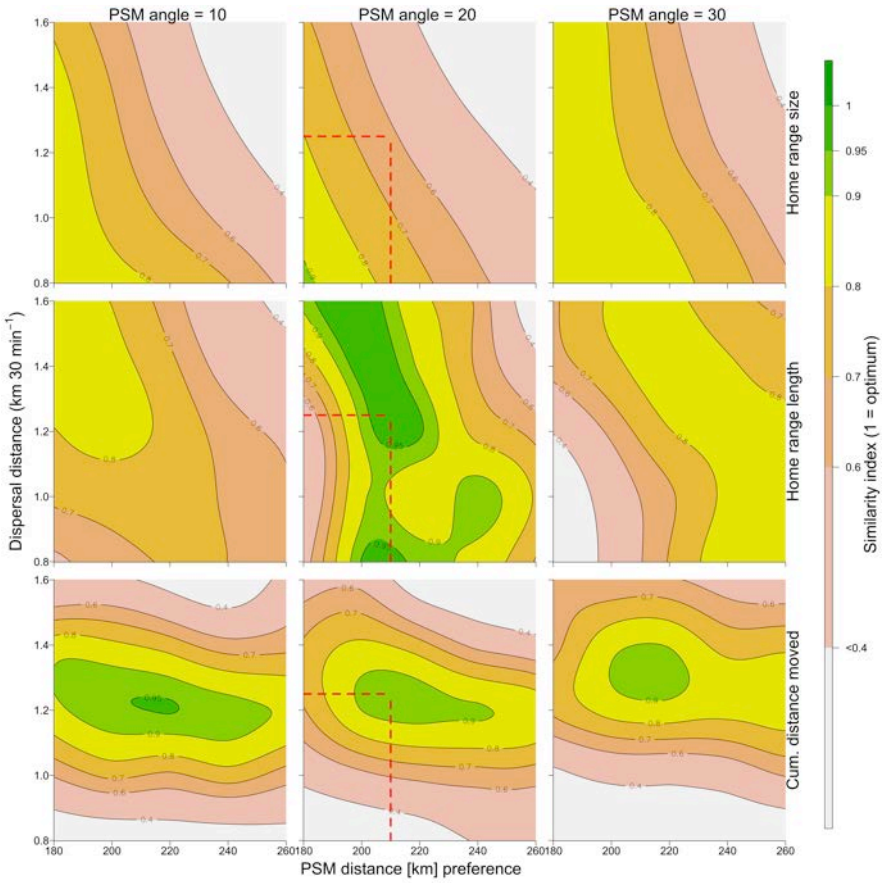


Figure 10. Calibration of the dispersal parameters *PSM_dist*, $d_{disp}$ and *PSM_angle* using pattern-oriented modeling. Each row in the figure represents one of the patterns observed for 25 satellite-tracked animals. Green regions indicate parameter values that enabled the simulation model to produce patterns similar to those observed for free-ranging animals. The similarity index is calculated as $1–(abs(x_{nature}–x_{simulated})/max(x_{nature}, x_{simulated}))$, where x is one of the three patterns. The axes values at the dashed red lines provided the highest similarity with those observed in the field and are therefore used in all simulations.

Two of the remaining parameters used for controlling dispersal behavior (*PSM_log* and *PSM_tol*) were calibrated visually to make the simulated tracks resemble those of satellite-tracked animals as closely as possible. This was done both before and after calibrating $d_{disp}$, *PSM_angle*, and *PSM_dist*. For *PSM_log*, a simple one-parameter logistic function (Eqn. A4) was used to enable animals to gradually become less directed the longer they dispersed. The movement statistics were relatively insensitive to the choice of *PSM_log*. *PSM_tol* defined the tolerance band within which a porpoise agent should find the most profitable PSM-cell when starting to disperse.

The parameter $t_{todisp}$ determines the number of days with decreasing average energy levels before the animal starts dispersing. The default value is based on the observations that captive porpoises lose weight after not eating for three days, which in nature would probably cause them to disperse to more profitable foraging areas. The parameter $w_{disp}$ determines the minimum depth at which porpoises were allowed to disperse. The value was visually assessed based on satellite-tracking data.

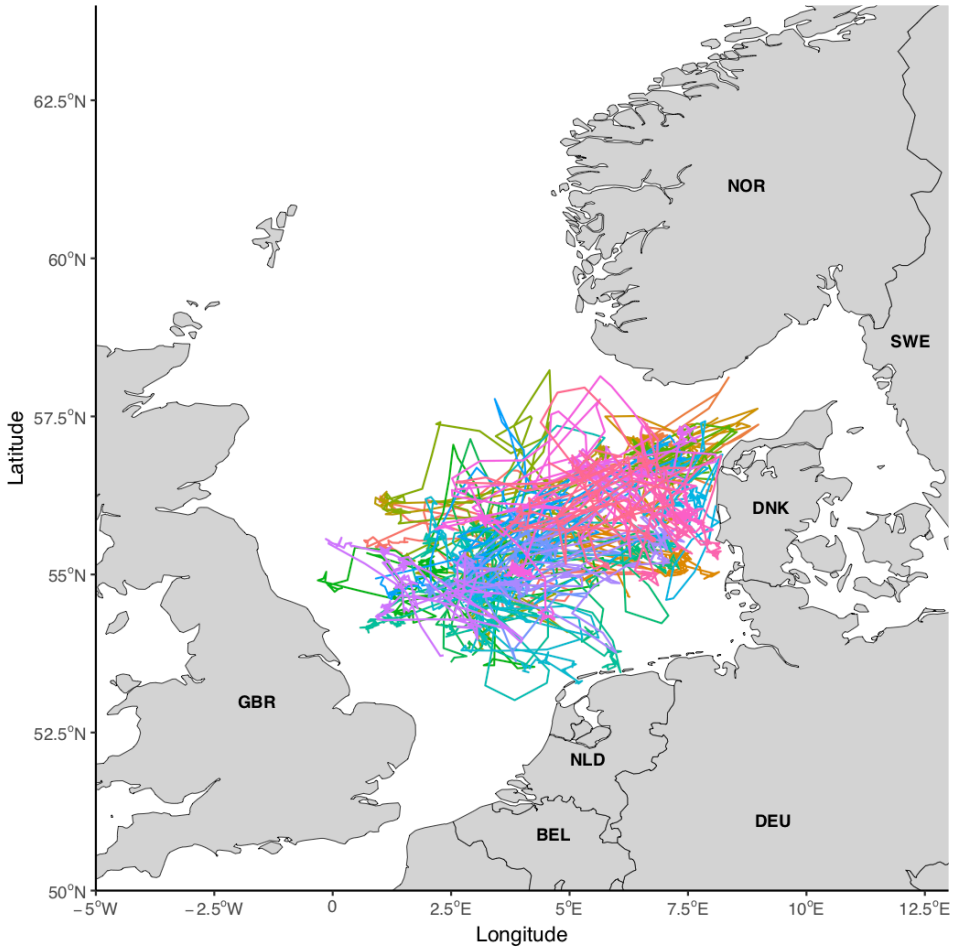


Figure 11. Daily movements of 25 simulated porpoises using values of $d_{disp}$, *PSM_angle*, and *PSM_dist* that caused their median home range length and cumulated distance moved after 150 days to closely match those of satellite tracked animals.

The dispersal tracks produced by the calibrated model resembled those of free-ranging animals in several respects. Animals developed home ranges with the same length (measured at day 150 of the tracking period), and with the same cumulated distance moved, as satellite-tracked animals (Figure 10). Their movement speeds also matched those observed in nature (see TRACE Appendix A – Calibration of dispersal behavior). Simulated home ranges were, however, more rounded, and therefore larger, than those observed in nature. Examples of tracks generated with the calibrated model (with parameters as in Table 2) are shown in Figure 11.

The parameters used for defining dispersal movements in this study are not necessarily suitable for other geographic regions. The majority of the parameters were obtained through inverse parameterization (using pattern-oriented modelling; Grimm et al. 2005; Kramer-Schadt et al. 2007; Grimm & Railsback 2012) based on animal tracks observed in the north-eastern part of the North Sea. The shapes of these tracks are influenced by the food distribution (defined as background maps; see Input data) and by proximity to land. As many of the simulated animals moved into the central part of the North Sea, their movements were less constrained by land than those of the satellite-tracked animals tagged by Skagen. This enabled them to develop more rounded, and therefore larger, home ranges than the ones

observed for free-ranging animals (Figure 10). Animals may also be influenced by other environmental conditions than proximity to land, which could cause them to disperse differently in other parts of the North Sea and elsewhere (other prey species, presence of predators etc.). Unpublished data for satellite-tracked porpoises reveal larger dispersal distances for animals in South Greenland waters (N. Nielsen, pers. comm.), suggesting that it may be important to re-parameterize the model based on local movement data when using it for populations outside the North Sea. The differences between the tracks of simulated and free-ranging animals are discussed further in the section 'Assumptions regarding dispersal'.

### *3.2.3 Parameters related to response to noise*

The porpoise agents' response to noise is controlled by the parameters $T$, $c$, $d_{max\_deter}$, $t_{deter}$, and $\psi_{deter}$ (Table 2). The first two parameters determine the length of the deterrence vector ($\mathbf{V}_D$ in Figure 4). $T$ determines the maximum distance at which porpoise movements are influenced by noise for a given sound source level, whereas $c$ determines the strength of their response at close ranges. The other parameters determine the maximum distance at which porpoises can be influenced by noise and the 'residual deterrence', i.e. the animals' tendency to move away from an area for some time after the noise has stopped.

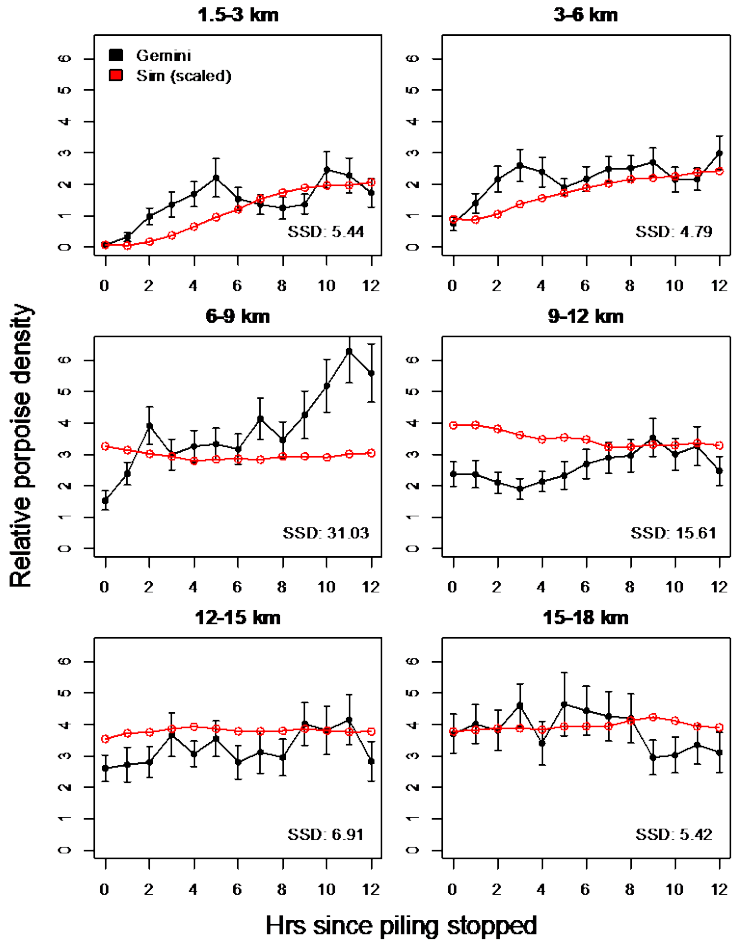


Figure 12. Recovery of porpoise densities after end of pile-driving. Black lines show changes in porpoise densities (mean % porpoise positive minutes±1SE) at different distances from closest pile-driving in the Gemini wind farm. The red lines show the corresponding relative number of porpoises in simulations based on $c$=0.07 and $T$=155 dB.

The parameters *T* and *c* were calibrated to make recovery of simulated porpoise densities resemble those observed during construction of the Gemini wind farm (Figure 12; Luuk Folkerts, unpubl. data). In the field, the relative porpoise densities were measured using CPODS that recorded the clicks emitted by echo-locating porpoises. Sound source levels were calculated based on noise data collected at different distances from two of the pile-driving sites using hydrophones (Figure 3). This was done using linear regressions, assuming spherical spreading of noise (Eqn. A1). Simulations were based on a landscape that included virtual CPODS (each covering 2 × 2 cells) placed in the exact same positions as those used in the field. The simulations included pile-driving events with the same timings and sound source levels as the real ones (Figure 3). Due to the limited size of the landscape, dispersal was turned off. We ran simulations using a range of parameter combinations (*c* in the range 0.00–0.15 and *T* in the range 151–158 dB SEL). The simulated porpoise densities were standardized to obtain the same overall mean and variance as observed around Gemini. The aim was to find the values of *c* and *T* that simultaneously minimized the squared difference between field and simulated data across a range of different distances from the nearest pile-driving. The optimal values of *c* and *T* were therefore the ones that yielded the smallest value of $\varepsilon$ in

$$\epsilon(c,T) = \sum_{d,t}(n_{d,t}(c,T) - p_{d,t})^2 = \sum_{d} SSD_d \qquad \text{Eqn. A13}$$

Here *n* is the number of simulated porpoises observed at a particular distance interval *d* from a virtual CPOD and *p* is the number of porpoises observed at the same distance interval from a pile-driving at Gemini and *t* is time since end of pile-driving. We used the distance intervals *d* shown in Figure 12.

The smallest value of $\varepsilon$ was obtained for *T*=155 dB SEL and *c*=0.07 (Figure 13). In Figure 13, $\varepsilon$ is referred to as 'Sum of Squared Deviation'.

The parameter $d_{\text{max\_deter}}$ defines an upper boundary for the distance at which porpoises can react to noise. It is only influencing model behavior if sound source levels (*SL*) are so high that they would otherwise have caused animals to react at very long distances. The reason for introducing the parameter $d_{\text{max\_deter}}$ is, that a study of Cuvier's beaked whale suggests that the way cetaceans respond to noise may depend on the distance to the noise source rather than on the received sound level (DeRuiter et al. 2013), at least for relatively low received levels. The parameter $d_{\text{max\_deter}}$ makes it possible to ensure that simulated animals are only deterred out to a certain distance, irrespective of the noise level. When $d_{\text{max\_deter}}$ is set to 1000 km (default), the parameter has no impact on the animals' response to noise, as this is far beyond the area where $R > T$ (see Figure 4).

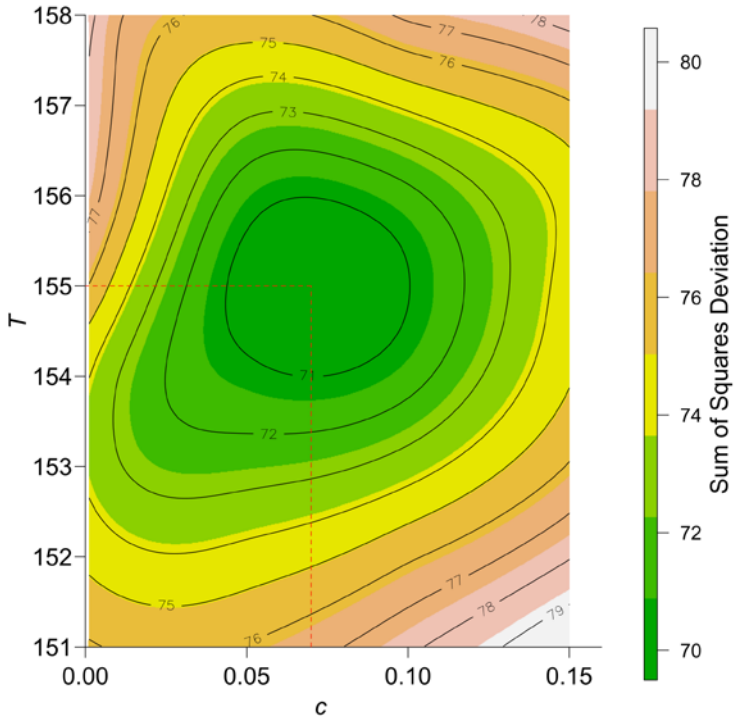


Figure 13. Calibration of *c* and *T* using pattern-oriented modeling. The target was to find values of *c* and *T* that enabled the model to produce porpoise recovery rates that resembled those observed at different distances from real pile-driving. This was obtained for *c*=0.07 and *T*=155 (red dotted line).

The parameters $t_{deter}$ and $\psi_{deter}$ determine how long porpoises keep moving away after the sound that deterred them has stopped, i.e. their 'residual deterrence' behavior. $t_{deter}$ determines the number of 30-minute time steps that porpoises remain deterred and $\psi_{deter}$ determines the reduction in deterrence after each time step (in percent, i.e. a reduction relative to the deterrence that remained prior to the step). Our knowledge of how free-ranging porpoises respond to loud noises is limited to one study (van Beest et al. 2018 subm.). Here some porpoises appeared to remain slightly deterred up to ca. 10 hours after being exposed to loud impulsive noises, whereas others did not respond. As there is limited evidence that animals remain deterred when they are no longer exposed to noise, we use a default value of $t_{deter}$=0 (i.e. no residual deterrence).

The parameters related to the animals' response to noise are likely to be site-specific. The way porpoises and other cetaceans respond to noise may depend on their condition, on whether the area where the disturbance takes place is an important foraging ground and on whether they have become habituated to noise (Richardson & Würsig 1997; Bejder et al. 2006). These factors are likely to cause the optimal values of *c* and *T* to vary among different wind farm construction sites. In Gemini porpoises only respond to noise out to a distance of 6–9 km (Figure 11), which is less than reported in most studies. Diederichs et al. (2009) found reduced porpoise numbers at 14–18 km from active pilings during construction of the Alpha Ventus wind farm, and Tougaard et al. found animals to respond at distances >20 km from Horns Reef I (Tougaard et al. 2009) in the eastern North Sea. Brandt et al. (2011) reported negative effects out to a distance of 17.8 km from the Horns Reef II wind farm, but no effect at 22 km. This suggests that *T* values that would cause animals to respond approximately 20 from the piling zone might be more representative for simulating population effects of pile-driving in the North Sea.

### 3.3 Parameters controlling general model behavior

The DEPONS model can run simulations using any landscape provided by the user, or one of the four built-in landscapes (parameter: 'landscape'). It requires eight different background maps to run simulations with any given landscape (see input data). The default landscape is the North Sea (Figure 1). This landscape was used for assessing the impact of pile-driving noise on the porpoise population. The Gemini landscape was created for parameterizing the animals' response to noise (see section Parameters related to response to noise). Simulations can also be run in the DanTysk landscape, in a Homogeneous landscape, which has no land/coast line, and where habitat quality and bathymetry are constant, or in a user defined landscape.

Although DEPONS simulations use realistic landscapes, agents that hit the edge of a landscape are unable to exit or disappear. It is sometimes (e.g. during model development and testing) useful to allow the landscape to wrap (i.e. using a non-bounded landscape). Wrapping of landscape borders is only possible in the Homogeneous landscape (parameter: 'wrapBorderHomo').

The DEPONS model can run a wide variety of wind farm construction scenarios (parameter: 'turbines'), including the three North Sea scenarios used in this study (Figure 2), the Gemini scenario (Figure 3) and the DanTysk scenario (not shown). It is possible to run simulations with alternative scenarios by selecting the 'User-def' turbines file after modifying the accompanying file (see input data). The default option is to run simulations without construction (with 'turbines' set to 'off').

The number of simulation years is set with the parameter "simYears". The default value is 50 simulation years, which allows for a 20 year burn in period, a 10 year period at carrying capacity prior to wind farm construction, a 10 year period with pile-driving noise, and a 10 year recovery period post wind-farm construction.

The number of porpoise agents to be created at the start of a simulation is set with the parameter 'porpoiseCount'. The default value of 10 000 will produce a stable population size in the North Sea landscape within the first 20 years of simulation.

Movement data of porpoise agents can be recorded by specifying how many porpoises to track using the parameter 'trackedPorpoiseCount'. Two options are available to track movements of porpoise agents. First, the user can record movement data for an unlimited number of agents from the very start of the simulation. To do so, the user must provide the starting position (x, y coordinates), and heading of the first step for each porpoise agent to track in a comma separated text file (trackedporpoise.txt; file without headers) stored in the data/landscape directory. If the file is empty, the tracked porpoise agents will have random starting locations. The second option to track movements of porpoise agents allows the user to set a delay in the start of the recording (i.e. starting from a specified time step during the simulation). This is done by writing a single line, in a semicolon separated .txt file (trackedporpoise.txt; file without headers) stored in the data/landscape directory, starting with the text delayedSelection; followed by the time step when recording should initiate; followed by the starting position (x, y coordinates). Here only one starting position can be specified, and movements of porpoise agents closest to the specified starting location are recorded. The two options of tracking the movements of porpoise agents cannot be combined.

The harbor porpoise population is subject to multiple anthropogenic disturbances and stressors, including by-catch in commercial gillnet fisheries (Read et al. 2006; van Beest et al. 2017). Although by-catch was not considered in the current study, it is possible to assess the impact of by-catch on the population in the DEPONS model (parameter: 'bycatchProb'). The

parameter was first introduced by Nabe-Nielsen et al. (2014) and ported directly into the DEPONS model (as part of the one-to-one conversion from NetLogo to Repast).

Two different parameters are used for code testing. The parameter 'randomSeed' makes it possible to repeatedly reproduce the exact same simulation (when not set to 'random'). This option should not be selected when investigating population effects of pile-driving noise. A range of built-in testing options were included to test model output under various conditions (parameter 'debug', see details in the section 'Implementation verification').

| Parameter | Standard value | Code name | Description [units] |
|---|---|---|---|
| Landscape | NorthSea | landscape | The landscape that is used in a simulation. Can take the values "NothSea", "Homogeneous", "Gemini", "DanTysk" or "UserDefined". |
| Turbines | off | turbines | The wind farm construction scenario that is used in a simulation. It reads in the selected text file that defines the turbine locations and period of activity etc. Can take the values "off", "DanTysk-construction", "Gemini-construction", "NorthSea_scenario1", "NorthSea_scenario2", "NorthSea_scenario3", and "User-def". |
| simYears | 50 | simYears | Number of simulation years. |
| porpoiseCount | 10000 | porpoiseCount | Number of porpoise agents in the simulation when initiated. |
| trackedPorpoise Count | 1 | trackedPorpoiseCount | Number of porpoise agents for which to track the xy coordinates (to monitor their movements). |
| bycatchProb | 0 | bycatchProb | Randomly selected proportion of the population to remove each year. Can take any value in range 0–1. [unitless] |
| wrapBorderHomo | true | wrapBorderHomo | Whether the border of the landscape should wrap. Can take the values "false" or "true". The landscape is without borders when "wrapBorderHomo"="true" and "landscape"="Homogeneous". |
| randomSeed | random | randomSeed | Allows the user to reproduce simulation output of earlier model runs by using the same random seed as previously used. Can take any integer |

| Parameter | Standard value | Code name | Description [units] |
|---|---|---|---|
| | | | value. |
| debug | 0 | debug | Built-in code testing parameter (values 0–5). When set to 0 no code testing/debugging occurs (see details in section 'Implementation verification'). |

Table 3. Model parameters controlling general model behavior and output types. The 'code names' are the names used in the Repast code in the current version of the model.

# 4 Conceptual model evaluation

**This TRACE element provides supporting information on**: The simplifying assumptions underlying a model's design, both with regard to empirical knowledge and general, basic principles. This critical evaluation allows model users to understand that model design was not ad hoc but based on carefully scrutinized considerations.

**Summary:**

**The DEPONS model builds on an existing model that simulates harbor porpoise movements and population dynamics in the inner Danish waters. We discuss the simplifying assumptions underlying the submodels that control animal movement, energetics and responses to noise in the existing model. We further discuss the assumptions underlying the dispersal behavior that was introduced when extending the model to become suitable for simulating effects of pile-driving noise in the North Sea. The rationale for the design and choice of simplifying assumptions are discussed.**

## 4.1 Assumptions regarding fine-scale movements

The fine-scale movement behavior builds on the assumption that animals attempt to optimize their foraging when not exposed to noise. Although fine-scale movements are influenced by the animals' energetic status and proximity to places where they have previously found food, it is unaffected by social behavior, animal age and whether they are nursing. The movements were parameterized based on data collected for one animal (Nabe-Nielsen et al. 2013b). At the time when the model was parameterized, the available fine-scale movement data (i.e. data on a 30-min resolution or finer) did not suggest that the distance moved per 30-minutes or turning angles between steps were strongly related to environmental variation (Figure 9), fine-scale movements are therefore assumed to be independent of environmental variability in DEPONS model version 1.1.

The values of $r_R$ and $r_S$, estimated for animals in the inner Danish waters, were assumed to be representative for North Sea animals. These parameters controlled the animals' ability to return to previously visited food patches based on a spatial memory (Nabe-Nielsen et al. 2013b).

### 4.2 Assumptions regarding effects of noise

Noise from pile-driving operations is assumed to influence the fine-scale movements of harbor porpoises by introducing a bias to their moves (Figure 4). This type of response to noise enables the model to reproduce the decline in population densities often observed in the vicinity of pile-driving (Brandt et al. 2011; Dähne et al. 2013), but the results of the only study where wild porpoises were exposed to noise did not yield a clear indication that noise introduces a consistent noise-level dependent bias to the fine-scale movements in wild animals (van Beest et al. 2018 subm.). As such, there might be considerable variation in how individual porpoises respond to noise in terms of their tendency to move away from noise. Such variation was not incorporated in DEPONS model version 1.1.

In the DEPONS model the parameters *c* and *T* were assumed to be constant. This may not be the case for wild animals, where habituation to noise may cause either *c* to decrease or *T* to increase in the habituated animals. Such habituation to noise may be prevalent in cetaceans (Richardson & Würsig 1997; Nowacek et al. 2007). The way wild animals react to noise may also depend on their energetic status and the quality of the area where the noise exposure takes place (Bejder et al. 2006). This is to some extent accounted for in the DEPONS model: animals that get disturbed in an unfavorable area are more likely to get permanently displaced than the animals that get disturbed in a favorable area. This results from the simulated animals' tendency to return to places where they have previously found food when they have not been able to find food for some time.

### 4.3 Use of constant vital rates

The animals' probability of becoming pregnant, the gestation time, nursing time and mating day are all assumed to be constant. In reality, they may be influenced by the animals' health, which in turn depends on a number of environmental parameters, and they may also be influenced by the age structure of the population. The choice of using temporally constant parameter values was based on a lack of empirical data indicating otherwise.

### 4.4 Assumptions regarding energetics

Population dynamics are directly linked to the balance between individuals' energy expenditure and their ability to replenish their energy reserves by finding patches with food. Assumptions regarding the animals' energy balance and availability of food in the landscape are therefore crucial to the behavior of the model.

The energy balance of individual animals depends on their energy use, which is assumed to be constant (except for increases associated with lactation and with high water temperatures in the summer months). This is likely to be realistic, as animals must maintain a fairly constant speed to forage enough to meet their high energy requirements (Kastelein et al. 1997; Wisniewska et al. 2016).

The dynamics of the food patches is influenced by how fast food replenishes after being consumed. This is influenced by the food growth rate ($r_U$) and by how much food that is left in a patch when it is nearly depleted ($U_{min}$). The selected value of $r_U$ (which allowed food to replenish after approx. two days with the selected value of $U_{min}$) was based on the observation that satellite-tracked animals in the inner Danish waters often returned to the same place

several times over a period of a few weeks. As the porpoise depends on a continuously high food intake (Kastelein et al. 1997) this was thought to indicate that food had replenished in the areas visited.

Both the animals' food intake rates and the amount of time they spend within a confined area depend on the spatial distribution of the food patches. There is currently no data on the spatial distribution of the fish that porpoises forage on in the North Sea (or in the inner Danish waters). The only indication that the spatial distribution of food patches used in our simulations is sensible comes from the similarity of the simulated movement tracks and those of satellite-tracked animals (Nabe-Nielsen et al. 2013b). When using landscapes with a low patch density in the simulations, animals return to the same area less often than they do in nature, causing them to develop larger home ranges than they do in nature (whereas animals maintained realistic home ranges in our simulations).

### 4.5 Assumptions regarding dispersal

The dispersal behavior included in the DEPONS model is based on the assumption that animals have a persistent memory of places they have previously visited. Although it has not been demonstrated that harbor porpoises have a persistent spatial memory (PSM), the ability to repeatedly return to the same area is common across a wide range of animal species (Berger-Tal & Bar-David 2015). The satellite tracks for porpoises tagged by Skagen in northern Denmark suggest that porpoises also have the ability to navigate back to places they have not visited for weeks or months (Figure 5). These tracks suggest that North Sea porpoises prefer to forage in particular areas, although it is unclear if they move over long distances in order to reach areas where they can maximize their food intake rate. The dispersal behavior implemented in the model assumes that animals disperse towards the area where they have previously obtained the highest energy intake rate, i.e. they are assumed to attempt to forage optimally, but to not take the costs of travelling to a new area into account when deciding where to go. Similar optimal foraging behavior has been demonstrated for several other species (e.g. Austin et al. 2004; Fagan et al. 2013). The dispersal behavior also builds on the assumption that animals gradually drift away from the route that would take them straight to the place where they previously experienced the highest energy intake rate. This allows them to gradually become more exploratory when approaching a region with high food availability.

The calibration of dispersal behavior is based on the assumption that home ranges of simulated animals and free-ranging animals are influenced in the same way by environmental variations. This is not always the case. Some of the satellite-tracked animals moved out of the area used in the simulation model, and as their movements were not constrained by the presence of a landscape border, their home ranges were potentially larger than those of simulated animals. The satellite-tracked animals also remained in the easternmost part of the landscape longer than the simulated animals, presumably due to the presence of local high-quality food patches that were not included in the simulation landscape. The simulated animals often moved out of this area and into the central parts of the North Sea. This enabled their home ranges to become more rounded and larger than those of the satellite-tracked animals (Figure 5 vs. Figure 11).

# 5 Implementation verification

**This TRACE element provides supporting information on**: (1) whether the computer code for implementing the model has been thoroughly tested for programming errors and (2) whether the implemented model performs as indicated by the model description.

**Summary:**

**The computer code was continually tested during model development to ensure that each consecutive step in development was only initiated after the model had passed a wide range of visual and statistical tests. Visual inspection of movement tracks was continuously carried out using the NetLogo and Repast graphical user interfaces (GUIs). The majority of the program code was initially developed and tested in NetLogo and subsequently scrutinized and re-implemented in Repast by independent programmers. Only the animals' response to noise and dispersal behavior was not part of this first version of the model.**

## 5.1 Testing the fine-scale movement model and reactions to noise

The fine-scale movement model was the first component of the DEPONS model to be developed. The structure of this submodel is described in the section 'Fine-scale movement'. All aspects of the model (including default parameter values) were kept exactly as described in the original publication (Nabe-Nielsen et al. 2013b), which described how a spatial memory could enable animals to stay in the same area for several weeks. The landscapes used during development of this model included food patches, but no other types of environmental variation. The simulated tracks were inspected visually in the homogeneous landscape as well as in landscapes including land (Figure 14). A wide range of movement statistics were calculated based on simulations in a homogeneous landscape (Nabe-Nielsen et al. 2013b). After porting the model to Repast, it was tested that the new version of the model produced movement tracks identical to those of the original NetLogo model. This was done by comparing the coordinates, spatial memory variables and energy levels of simulated animals that had been initiated on the same location in the two versions of the models (using fixed randomSeed parameter values).

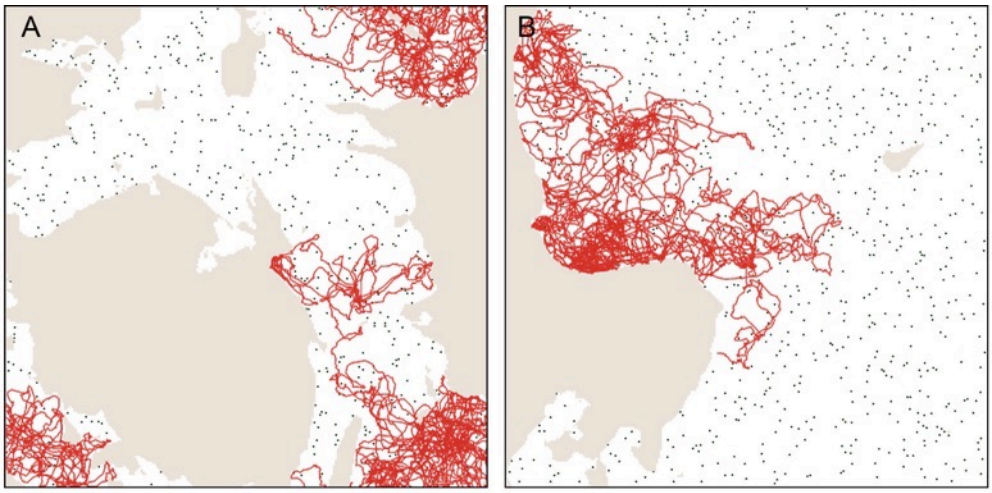


Figure 14. Tracks simulated with fine-scale movement model in landscapes with land and identical, randomly distributed food patches, but no other types of environmental variation. The tracks were produced using the porpoise movement model developed in NetLogo (doi: 10.5281/zenodo.53149). The spatial distribution of the patches was retained in the DEPONS model version 1.1.

Dedicated code was developed for testing the different submodels in the fine-scale movement model (controlled with the parameter 'debug'). This was used for developing the NetLogo version of the code (DOI:10.5281/zenodo.53097). The debug value 1 was used for developing and testing the porpoises' behavior when approaching land and to develop code that enabled them to back-track in rare situations where they got trapped by land. When setting the debug parameter to 2, the porpoises' behavior when approaching land was tested to ensure that animals turned as little as possible, while still avoiding land (distance to land, positions and turning angles were written to the console for a subset of the simulated animals). Debug value 3 was used for debugging turning angles related to CRW behavior. Debug value 4 enabled inspection of the length of the porpoises' attraction to previously visited food patches by writing the perceived/remembered value of the patch and the direction of the attraction vector to the console. Debug value 5 was used for writing out the position of the porpoise and the length of the contribution of the CRW and spatial memory moves to the console (Eqns. A5 and A6), allowing a close inspection of whether turning angles and the direction of the vector that characterized fine-scale movement were related to food availability and proximity to the visited patch as expected. This dedicated debugging code was used in combination with stress tests, where simulations were run with extreme parameter values, to identify errors that would be difficult to detect with the default/realistic parameter values.

The reaction to noise was verified by checking that the length of the deterrence vector $\mathbf{V}_D$ was exactly as specified in Figure 4 and the ODD. We used a visual inspection of the simulation to double-check that simulated porpoises reacted to noise out to the distance specified in Eqn. A1 in the submodel 'Porpoises detect noise' (see also Figure 15).

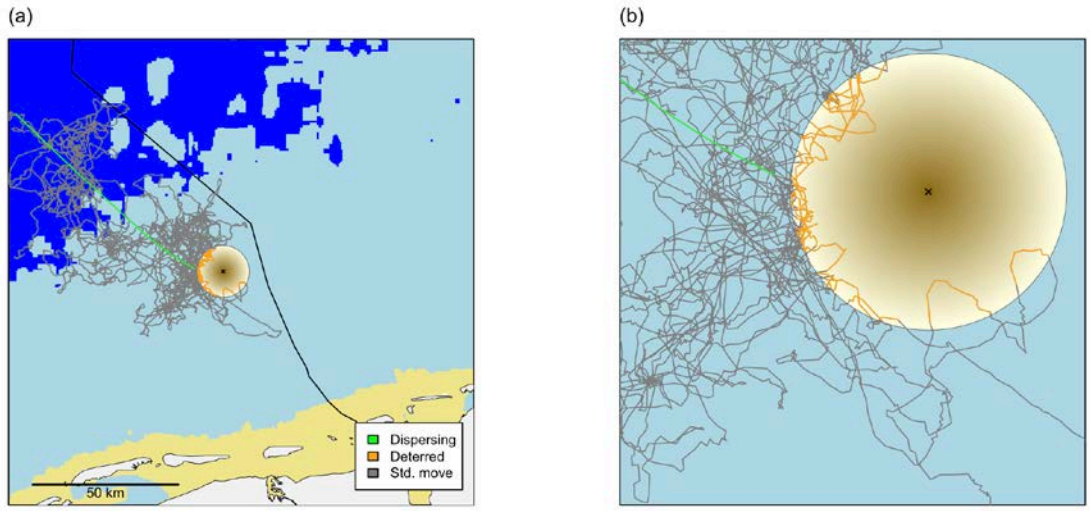


Figure 15. Porpoise movement tracks in the presence of continuous pile-driving noise. The yellow circle indicates the area where porpoises react to noise when the model is parameterized based on data from the Gemini wind farm.

## 5.2 Testing the dispersal model

The persistent spatial memory (PSM) dispersal behavior was developed exclusively in Repast/Java. It differs from the dispersal model described by Nabe-Nielsen et al. (2014), which was specific to the inner Danish waters. We tested that the dispersal model produced the desired output by plotting and analyzing the movement tracks for dispersing porpoise agents. This was done using the parameter "trackedPorpoiseCount" and the trackedporpoise.txt file that records movements (coordinates) of random agents after each

time step. We plotted how the turning angles following each dispersal step changed as the simulated animals approached their dispersal targets (Figure 7) and by monitoring variations in step lengths and energy levels. Further, we conducted stress tests of the PSM dispersal by analyzing simulated tracks for extreme values of $d_{disp,}$ *PSM_angle*, *PSM_dist*, *PSM_log* and *PSM_tol*.

### 5.3 Testing population dynamics

The population model (Nabe-Nielsen et al. 2014) was tested by inspecting how porpoise agent movements were influenced by their energetic status and by analyzing relationships between their average energetic status of porpoises and food patches. The inspection of individual porpoise agents was done using the built-in inspector in NetLogo as well as custom made code for writing out the track, food consumption, energy use and fate of individual porpoises. Population dynamics were inspected using the built-in functionality for creating dynamic plots in NetLogo and by close inspection of generated output.

## 6 Model output verification

**This TRACE element provides supporting information on**: (1) how well model output matches observations and (2) how much calibration and effects of environmental drivers were involved in obtaining good fits of model output and data.

**Summary:**

**The DEPONS model was able to reproduce the fine-scale movement patterns and dispersal patterns observed for porpoises in nature. It was also able to reproduce the relative animal densities observed at different distances from a wind farm during construction. These three types of output were parameterized using pattern-oriented modeling. Emergent patterns related to variations in population size could not be compared to observations due to lack of field data.**

### 6.1 Types of model output

The DEPONS model writes out three data files after each simulation. (1) The first file (.csv) reports the change in population size over time. By default it produces one line of output per 30-min time step, but the reporting interval can be changed in the graphical user interface (GUI). (2) Data on the distribution of porpoise agents (.csv) among 'blocks' in the simulation landscape (defined in a raster file, see the section 'Input data'), which is by default recorded for each 30-min step. (3) Data on the movements (.csv) of individual porpoise agents during the simulation, measured and recorded by default for each 30-min step. By default, one porpoise is tracked, but multiple agents can be tracked using the parameter trackedPorpoiseCount.

In the GUI version of the model an additional data set is written out: Data on number of animals per age class in the population and number of animals that have died in the preceding year in that age class. When running simulations in batch mode only the first three files are produced, but in addition the associated parameter input values used during the simulation are written to a separate file. The data files are written out to the working directory when

simulations are run in the GUI while output from the batch procedure is written out to the output folder within the working directory. Each output file has a date and time stamp in the title, which reflects when the simulation finished.

### 6.2 Comparison of model output and observations

Only animal movement patterns and recovery of local population densities after pile-driving could be compared to corresponding field data recorded in the North Sea. The emergent population dynamics could not be compared to field data, as the available data on variations in population densities are either unavailable for the North Sea, or available on a very rough temporal and spatial resolution (Hammond et al. 2013). In the inner Danish waters, the predecessor of the DEPONS model was, however, capable of reproducing the spatial distribution observed for porpoises using acoustic survey data (Figure 7 in Nabe-Nielsen et al. 2011). The age class distribution observed for simulated animals that died each year corresponded to the one observed for stranded animals along the Danish shores (Nabe-Nielsen et al. 2014).

The fine-scale movement model enabled animals to develop a range of track characteristics observed for animals in the inner Danish waters (Nabe-Nielsen et al. 2013b). In version 1.1 of the DEPONS model, the correlated random walk component of the fine-scale movement model was calibrated to ensure a close match with field data (by iteratively calibrating the parameters $a$, $b$, $m$, $R_1$, $R_2$ and $R_3$ as described in the appendix of Nabe-Nielsen et al. 2013b; see Table 2 for description of parameters). Subsequently the parameters $r_R$ and $r_S$ were calibrated using pattern-oriented modeling (POM) to ensure that animal home range sizes and residence times (Barraquand & Benhamou 2008) closely resembled those observed for satellite-tracked animals (see details on POM). Here residence time is a measure of how long animals have spent in the neighborhood of each position in a track, which is often interpreted as a measure of how suitable the area is for foraging. Although fine-scale movements may depend on various types of environmental variation in nature (e.g. bathymetry, salinity and distance to coast), these did not have a direct impact on the distance animals moved per step or on turning angles in DEPONS model version 1.1. The reason was that there was no data available to parameterize such variations. We consistently used the simplest possible model (i.e. the model that involved the smallest number of parameters) if there was no data to support the use of a more complex relationship in the model.

The recovery of relative porpoise densities after the pile-driving ended resembled those observed at different distances from the Gemini wind farm during construction (Figure 12). The recovery resulted from the simulated animals' tendency to move back to known food patches after deterrence stops.

The simulated dispersal patterns matched those observed for satellite-tracked animals in the north-eastern part of the North Sea after calibrating parameters related to persistent spatial memory (see details on POM).

# 7 Model analysis

**This TRACE element provides supporting information on**: (1) how sensitive model output is to changes in model parameters (sensitivity analysis), and (2) how well the emergence of model output has been understood.

**Summary:**

**A sensitivity analysis was performed to explore how the equilibrium population size changed in response to variations in each of the parameters in the model. The emergent equilibrium population size was most sensitive to variations in food replenishment rate and to parameters related to animal energetics, but relatively insensitive to changes in the parameters related to animal movements. It is discussed to what extent the realism of the patterns that emerge from the model have been tested against field data.**

## 7.1 Sensitivity analysis

### *7.1.1 Sensitivity – parameters related to general porpoise behavior*

We conducted a sensitivity analysis to explore how the equilibrium population size changed when varying parameters related to life history, energetics, fine-scale movements and dispersal in simulations without noise (Figure 16). Parameters were changed one at a time to produce a local sensitivity analysis (cf. Bar Massada & Carmel 2008). In this study parameters were increased or decreased by 20% relative to their default values and the corresponding impact on equilibrium population size was calculated as the mean daily population size for 8 replicate simulations. For the sensitivity analyses we used 40-year simulations, but calculated the equilibrium population size based on the last 20 years only (a 20-year burn-in period was always sufficient to ensure that the population had stabilized).

The equilibrium population size was most sensitive to variations in parameters related to energetics (2nd group of parameters in Figure 16), and variations in the food replenishment rate, $r_U$ were particularly important. The default value for this parameter caused food to replenish after approximately 48 hours (see appendix of Nabe-Nielsen *et al.* 2013b). When increasing $r_U$ by 20% relative to its default value (see Table 1) food replenished faster, leading to generally higher food availability and a larger population size. The equilibrium population size is nearly equally sensitive to parameters that influence the individual animals' energy consumption per time step, $E_{use}$, their increased energy use while lactating, $E_{lact}$, and increased energy use in periods with warm water, $E_{warm}$. It is, however, insensitive to variations in the survival probability constant $\beta$, which determines the exact relationship between the animals' energetic status and their survival probability.

Equilibrium population size was less sensitive to variations in parameters related to animal life history (1st group in Figure 16), fine-scale movement (3rd group) and dispersal (4th group). One exception is the maximum distance moved during a fine-scale move, $d_{maxmove}$. When decreasing this parameter by 20% relative to its default value (provided in Table 2) it caused the mean population size to decrease by 16.5%, suggesting that the distance animals move while using fine-scale movements is important for their ability to rapidly return to previously visited patches when they do not find much food using a correlated random walk. For $R_1$ and $R_3$, which control distance moved and turning angles during fine-scale movements, respectively, only the parameter means were varied (standard deviation components were kept constant).

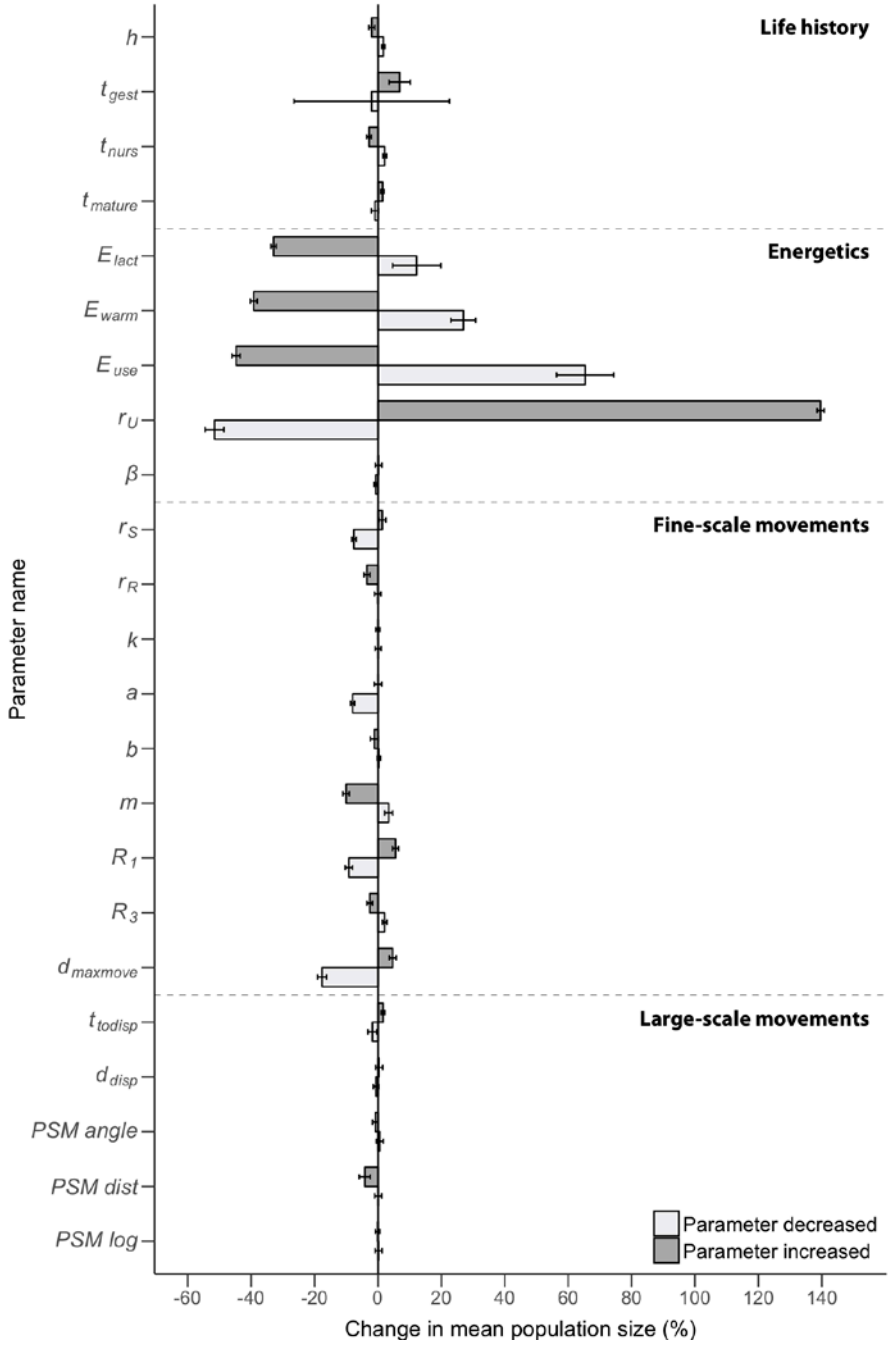


Figure 16. Sensitivity analysis for parameters related to animal life history, energetics, fine-scale movements and large-scale movements/dispersal. Bars show changes in equilibrium population size when increasing or decreasing each parameter by 20% relative to its default value. Error bars show confidence intervals based on 8 replicate simulations.

The relatively low sensitivity for most parameters related to animal movements, as compared to parameters related to energetics, does not indicate that population dynamics are unaffected by animal movements. Inclusion of, e.g., novel types of dispersal might result in changes in the equilibrium population size that exceed those observed with the current dispersal model for any parameter combinations.

Only parameters that could potentially influence the behavior of all animals, and where an adjustment of ±20% made sense, were included in the sensitivity analysis. The sensitivity to

the life history/energetics parameters $t_{maxage}$, $E_{init}$, $t_{mating}$, $U_{min}$ was not studied. The $t_{maxage}$ only influenced the few, old animals. $E_{init}$ was only important during the burn-in period. For $t_{mating}$ it did not make sense adjusting by ±20%. The same was the case for $R_2$ (turning angle between consecutive fine-scale moves), which had a mean of 0. $U_{min}$ affects the time it takes food in patches to replenish, which could be adequately analyzed by adjusting $r_U$. *PSM_tol* presumably mostly affected animals while they gathered information about potential areas to disperse to (i.e. during the burn-in phase). The parameters $w_{disp}$, $w_{min}$ influenced only the relatively few animals that were close to land, and varying these parameters by ±20% therefore inevitably has small impact on overall population dynamics.

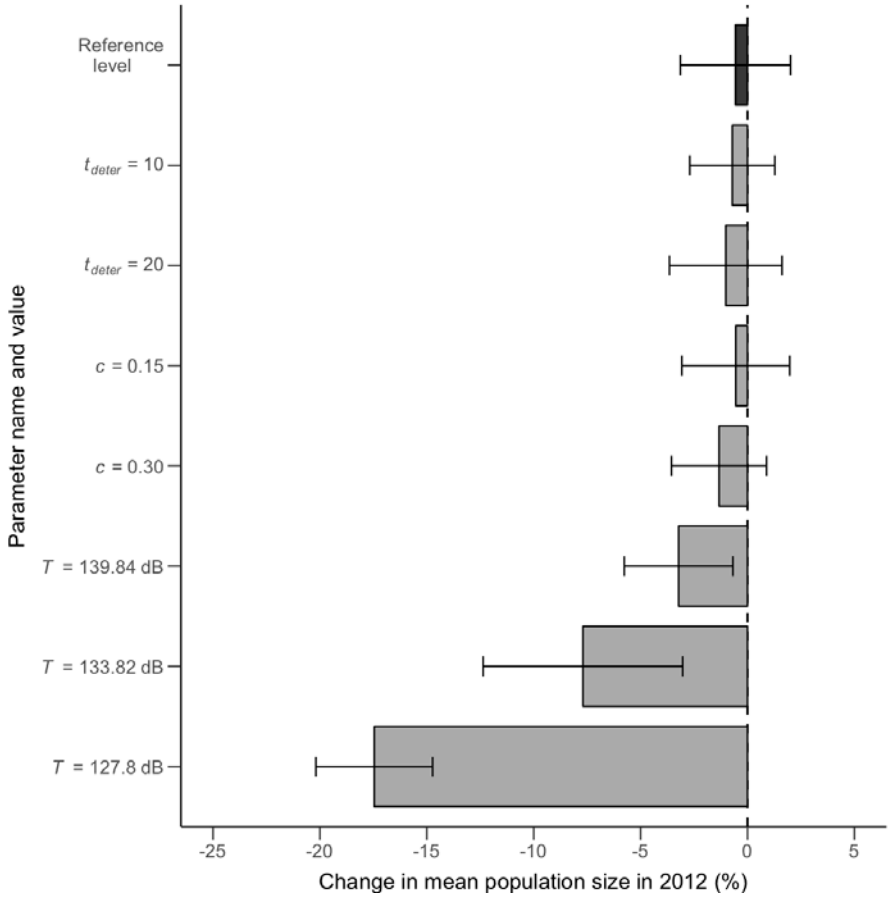


Figure 17. Sensitivity analysis for parameters related to noise, i.e. residual deterrence time $t_{deter}$, deterrence coefficient $c$, and response threshold $T$. $T$ equal to 139.8 dB, 133.8 dB and 127.8 dB cause simulated animals to respond to distances of 51.3 km, 102 km and 204 km, respectively. Error bars show 95% confidence intervals based on 8 simulations.

### *7.1.2 Sensitivity – parameters related to impacts of noise*

To assess the model's sensitivity to variations in parameters influencing individual animals' response to noise, we measured the population size in the year where it was most affected by noise. This happened in the second year of the 10-y wind farm construction period in Scenario 1 (i.e. in year 2012 in the 'Random, slow' scenario; Figure 3 in main text). The population effect of noise was measured after increasing or decreasing the noise parameters by 20%, one at a time, and recording the corresponding mean population size in eight replicate simulations. The same was done for the default parameter values, which yielded the 'reference level', where animals responded up to 8.9 km from the noise source.

When decreasing the noise parameter $T$ to 139.8 dB, 133.8 dB and 127.8 dB (causing simulated animals to react to noise out to distances of 51.3 km, 102 km and 204 km from the noise source, respectively) it resulted in a much larger decrease in the mean population size than the one observed when using default parameter values (Figure 17). There was, however, a large variation in mean population size among simulations. When increasing $c$ to either 0.15 or 0.30, which caused individual animals to respond much more strongly to noise than observed during construction of the Gemini wind farm (Figure 13), it did not significantly influence the population impact of noise, i.e. the confidence intervals overlapped with the reference level. Increasing the residual deterrence time, $t_{deter}$, to either 10 or 20 did not cause the population impact to differ from the reference level either. Here 20 corresponds to a residual deterrence of 10 hours, which is the highest likely value of $t_{deter}$ as based on field data; van Beest et al. (2018). The sensitivity of $\psi_{deter}$ was not investigated as it was closely related to $t_{deter}$, and that of $d_{max\_deter}$ was not relevant with the default parameter settings. The simulated population effect of noise was therefore only influenced by decreasing $T$, which also caused the population size to drop below the equilibrium level.

### *7.1.3 Sensitivity – impact of energetics parameters on response to noise*

To test if the population impact of noise was sensitive to the choice of energetics parameters, which were the parameters with the largest influence on equilibrium population size (Figure 16), we increased or decreased these parameters one at a time in simulations including noise. This is equivalent to testing for interactions between $T$ and each of the energetics parameters. The reference population size was obtained as the daily mean population size during the second year of the 10-y wind farm construction period in scenario 1 (i.e. in 2012; mean of 8 simulations). It was based on default parameter values, except that $T$ was decreased to 127.8 dB SEL (causing animals to react up to 204 km from the pilings). The population impact of noise was considered sensitive to an energetics parameter when either increasing or decreasing the parameter by 20% resulted in a change in the population size relative to the reference population size.

The population impact of noise was sensitive to $E_{lact}$, $E_{warm}$ and $r_U$, as changing either of these parameters caused the population size during the second year of the wind farm construction period to differ from the reference population size (i.e. the confidence intervals did not overlap with the reference value; Figure 18). When reducing $E_{lact}$ or $E_{warm}$ by 20%, wind farm construction noise no longer had a significant impact on the population, even when letting animals be deterred up to 204 km from the piling. The population impact of noise was not sensitive to changes in $E_{use}$ or $\beta$, but a 20% decrease in $E_{use}$ caused the impact of noise to be non-significant. Only an increase in $E_{warm}$ caused noise to have a larger impact on the population, but only slightly so. Although improved estimates of the noise parameters could potentially result in more accurate estimates of the population impacts of noise, it is unlikely that larger population effects would be predicted with moderately altered energetics parameters.

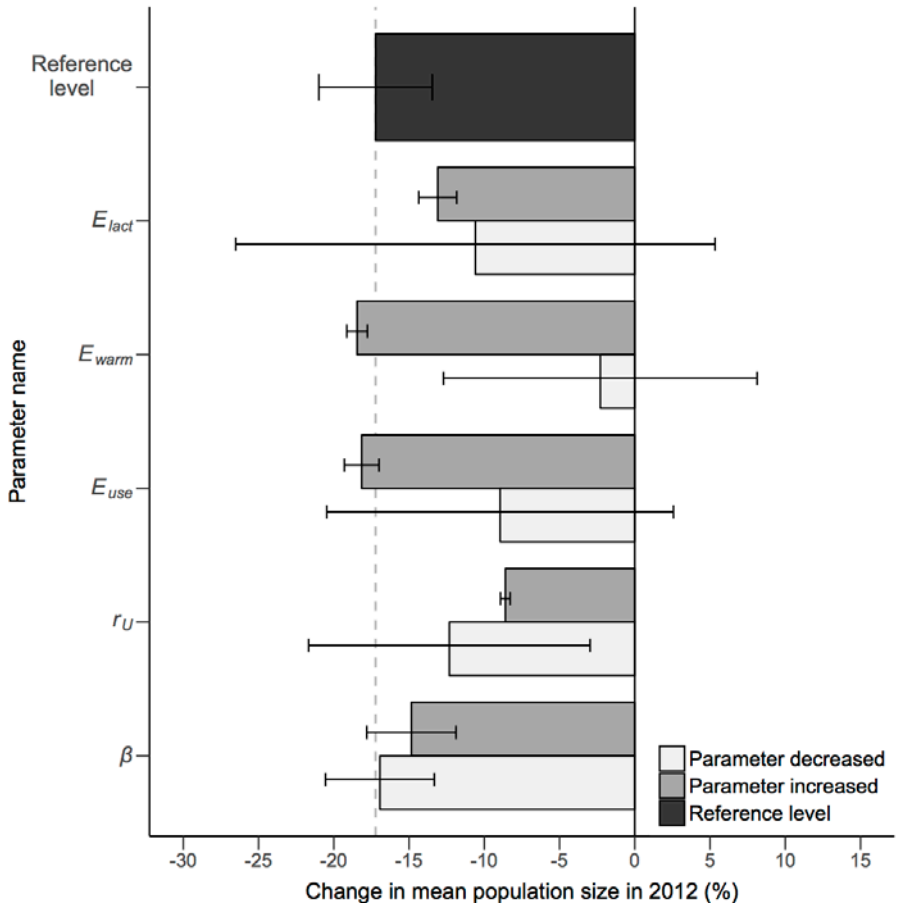


Figure 18. Sensitivity of population effect of noise to parameters related to energetics. Bars show mean population sizes during the second year of the wind farm construction period, when increasing or decreasing parameters by 20% relative to their default values. Error bars show 95% confidence intervals. Simulations were based on $T$=127 dB, assuming that animals reacted up to 204 km from pilings.

## 7.2 Tests of emergence

The model produces four different emergent patterns: (1) population size, (2) spatial distribution of animals, (3) their age class distribution, and (4) local recovery of populations after exposure to pile-driving noise (see ‘Design concepts’). All four patterns emerge from ubiquitously valid mechanisms derived from ‘first principles’ (Nathan et al. 2008; Sibly et al. 2013), including use of energy for maintenance and movement and acquisition of food by actively searching for optimal foraging areas. Such models where population and community-level patterns emerge from adaptive traits related to general evolutionary and physiological principles are more likely to maintain their predictive power across a wide range of environmental conditions than other models (Stillman et al. 2015).

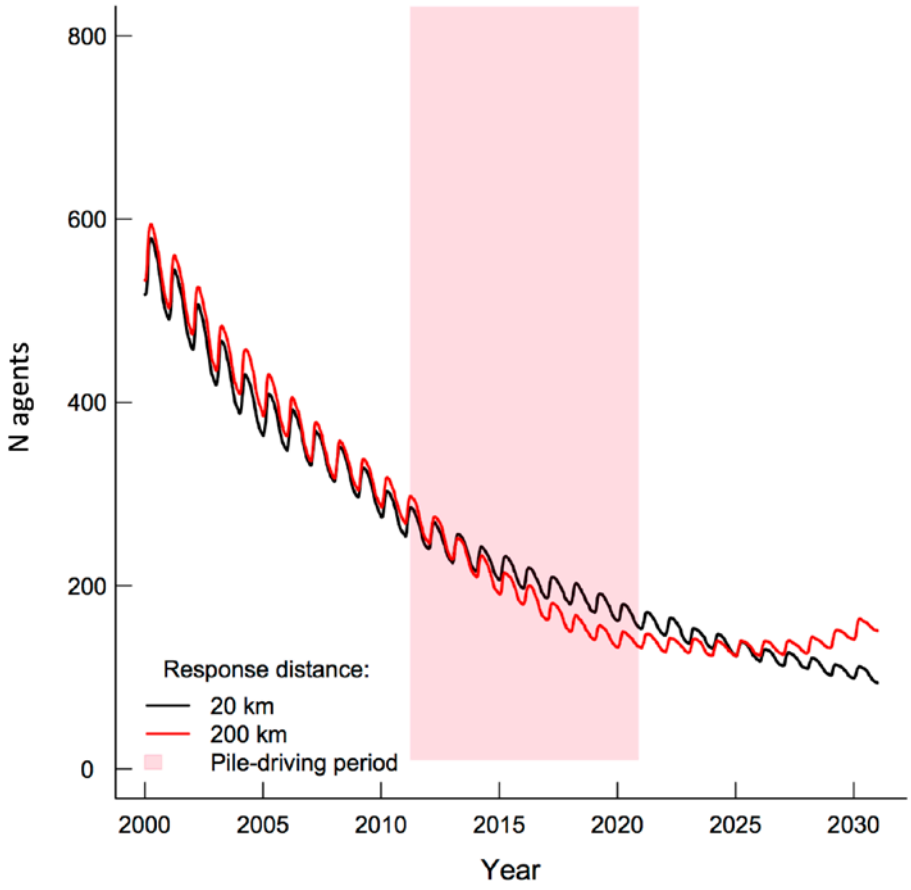


Figure 19. Population dynamics in model without dispersal. Impacts of noise are illustrated for the 'Random, slow' scenario.

In order to test which elements of the model were responsible for the observed emergent patterns, we gradually refined the model until reaching the level of complexity present in the current version of the DEPONS model. While increasing model complexity we monitored the changes in population size and spatial distribution of animals and in the animal movement patterns. The simplest model, where animal movements were simulated using a correlated random walk model without spatial memory of previously visited patches did not allow realistic fine scale space-use patterns to emerge. This suggested that the model was too simple to represent real animals (see Table A1 in Nabe-Nielsen et al. 2013b for details on the relationship between animal space use and spatial memory). Inclusion of a mechanism that allowed animals to return to previously visited food patches (see 'Fine-scale movement') allowed simulated animals to develop space-use patterns that closely resembled those of satellite-tracked animals by balancing their tendency to move at random (i.e. following a correlated random walk) and their tendency to return to previously visited food patches (Nabe-Nielsen et al. 2013b). This also enabled simulated animals to forage optimally, thereby facilitating fitness-maximization. Although this suggested that the inclusion of spatial memory in the model was required to faithfully simulate the movements and energetics of real animals, it did not permit the simulated animals to develop long-term home ranges that resembled those observed for satellite-tracked animals. It is essential that simulated animals have home ranges of a realistic size in order to ensure that they have access to the same amount of food resources as real animals have. Only in that case will the decreased food intake that they experience when being scared away from a wind-farm construction site result

in a realistic decrease in in the population size. The model was only able to simulate home ranges that resembled those of satellite-tracked animals after including a dispersal mechanism that allowed individuals to return to the area where they had previously experienced the highest energy intake rate (Figure 10 illustrates how animals that disperse less, i.e. with smaller *PSM_dist*, have unrealistically small home ranges). The inclusion of this dispersal mechanism in the model caused the equilibrium population size to increase (relative to a model without dispersal; Figure 19). It also resulted in the emergence of realistic movement patterns at multiple spatial and temporal scales (see TRACE Appendix A), and in the emergence of realistic local population densities. This suggests that the mechanisms that control animal foraging and food acquisition in the current version of the DEPONS model are sufficiently realistic for the purpose of the model. It also suggests that the model cannot be simplified without compromising its realism.

# 8 Model output corroboration

**This TRACE element provides supporting information on**: How model predictions compare to independent data and patterns that were not used, and preferably not even known, while the model was developed, parameterized, and verified. By documenting model output corroboration, model users learn about evidence, which, in addition to model output verification, indicates that the model is structurally realistic so that its predictions can be trusted to some degree.

**Summary:**

**The model's ability to faithfully predict population effects of wind farm construction noise cannot be corroborated using independent data, as harbor porpoise population estimates based on field data are scarce and inherently imprecise. The simulated effects of noise on local population densities have not been compared with independent data due to the scarcity of data from comparable wind farm construction sites.**

Only some of the model predictions can be directly compared to independent data due to the scarcity of harbor porpoise survey data from the North Sea and due to the large variability associated with such data. Four different patterns emerged from the model: (1) variations in total population size in time; (2) spatial distribution of animals, (3) their age class distribution, and (4) local recovery of populations after exposure to pile-driving noise (see 'Design concepts'). In the following we discuss to what extent each of these patterns can be corroborated using independent data and which types of independent data that should be collected to further evaluate the realism of the model predictions.

A direct comparison of the predicted porpoise population size with population estimates based on survey data (e.g. those collected during SCANS surveys; SCANS II 2008) is unlikely to be informative for two reasons: (i) The North Sea population estimates based on SCANS data are associated with considerable variation, making it relatively easy for the simulation model to produce population estimates within the confidence limits of these estimates. (ii) The SCANS surveys are conducted relatively infrequently, making them unsuited for validation of the fine-scale temporal population dynamics produced by the DEPONS model. The robustness of

the model predictions regarding variations in population sizes in space and time is therefore only ensured by the generality of the mechanisms responsible for producing this emergent pattern.

The predicted spatial distribution of animals could, in principle, be compared to independent data, but although alternative porpoise distribution maps exist (e.g. Reid et al. 2003) they are partly based on the same underlying data as the study by Gilles et al. (2016), so they are not truly independent. The spatial distribution patterns produced by the predecessor of the DEPONS model in the inner Danish waters, did, however, closely match those obtained from acoustic survey data that were not used for designing or calibrating the model (see page 23 in Nabe-Nielsen et al. 2011; monthly average densities per 40 km x 40 km block). These simulations of the inner Danish waters population did not include wind-farm construction scenarios. The model's ability to reproduce the porpoise distributions observed in nature is reassuring, as this causes a realistic proportion of the simulated porpoises to get exposed to noise during wind farm construction scenarios.

The age class distribution of the simulated animals can be directly compared to the age class distribution of stranded and by-caught animals. This comparison has already been conducted in the inner Danish waters (Nabe-Nielsen et al. 2014). Here the age class distribution that emerged from the model corresponded closely to that in the field data.

Recovery of local population densities following the construction of individual wind turbine foundations was studied in the Gemini wind farm during construction. This data set was the only one available providing both noise measurements and relative porpoise population densities at different distances from the mono-pile pilings, and where no noise mitigation was used. This data set was used for simultaneously calibrating deterrence and local population recovery (Figures 11 and 12). As the only available data set was used for model calibration, there are no data available for model output corroboration.

In addition to using already collected data for model output corroboration, the collection of local population densities around other wind farm construction sites would help us obtaining a better understanding of the structural realism of the DEPONS model and of the generality of the model predictions. This would also make it possible to verify that the sound propagation model employed is realistic for the sound frequencies that porpoises react to. In such field studies it is essential to measure how porpoise densities change during and after pile-driving at large distances from the wind farm construction sites in order to determine whether model predictions are realistic at these distances.

It is possible that the animals' tendency to return to areas they have been deterred from depends on the food availability in that area, in nature as well as in the model. Animals are more likely to return to profitable areas. The model's ability to faithfully simulate local population recovery in areas with different levels of food availability could be corroborated using long-term data collected with CPODS in areas where wind farms are constructed. This would provide an independent measure of local food availability as well as local population recovery.

# 9 Literature cited


Austin, D., Bowen, W.D. & McMillan, J.I. (2004). Intraspecific variation in movement patterns: modeling individual behaviour in a large marine predator. *Oikos*, 105, 15–30.

Bar Massada, A. & Carmel, Y. (2008). Incorporating output variance in local sensitivity analysis for stochastic models. *Ecol. Modell.*, 213, 463–467.

Barraquand, F. & Benhamou, S. (2008). Animal movements in heterogeneous landscapes: identifying profitable places and homogeneous movement bouts. *Ecology*, 89, 3336–48.

van Beest, F.M., Kindt-Larsen, L., Bastardie, F., Bartolino, V. & Nabe-Nielsen, J. (2017). Predicting the population-level impact of mitigating harbor porpoise bycatch with pingers and time-area fishing closures. *Ecosphere*, 8, e01785.

van Beest, F.M., Teilmann, J., Hermannsen, L., Galatius, A., Mikkelsen, L., Sveegaard, S., Balle, J.D., Dietz, R. & Nabe-Nielsen, J. (2018). Fine-scale movement responses of free-ranging harbour porpoises to capture, tagging and short-term noise pulses from a single airgun. *R. Soc. Open Sci.*, 5, 170110.

Bejder, L., Samuels, A., Whitehead, H., Gales, N., Mann, J., Connor, R., Heithaus, M., Watson, Capps, J., Flaherty, C. & Krutzen, M. (2006). Decline in relative abundance of bottlenose dolphins exposed to long-term disturbance. *Conserv. Biol.*, 20, 1791–1798.

Berger-Tal, O. & Bar-David, S. (2015). Recursive movement patterns: review and synthesis across species. *Ecosphere*, 6, art149.

Brandt, M.J., Diederichs, A., Betke, K. & Nehls, G. (2011). Responses of harbour porpoises to pile driving at the Horns Rev II offshore wind farm in the Danish North Sea. *Mar. Ecol. Prog. Ser.*, 421, 205–216.

Brandt, M.J., Diederichs, A., Betke, K. & Nehls, G. (2012). *The Effects of Noise on Aquatic Life*. *Adv. Exp. Med. Biol.*, Advances in Experimental Medicine and Biology. Springer New York, New York, NY.

Dähne, M., Gilles, A., Lucke, K., Peschko, V., Adler, S., Krügel, K., Sundermeyer, J. & Siebert, U. (2013). Effects of pile-driving on harbour porpoises (*Phocoena phocoena*) the first offshore wind farm in Germany. *Environ. Res. Lett.*, 8, 25002.

DeRuiter, S.L., Southall, B.L., Calambokidis, J., Zimmer, W.M.X., Sadykova, D., Falcone, E.A., Friedlaender, A.S., Joseph, J.E., Moretti, D.J., Schorr, G.S., Thomas, L. & Tyack, P.L. (2013). First direct measurements of behavioural responses by Cuvier's beaked whales to mid-frequency active sonar. *Biol. Lett.*, 9, 20130223.

Diederichs, A., Brandt, M.J. & Nehls, G. (2009). *Auswirkungen des Baus des Umspannwerks am Offshore-Testfeld „alpha ventus" auf Schweinswale - Untersuchungen zu Schweinswalen mit T-PODs*. BioConsult SH, Husum.

EU. (1992). *Council Directive 92/43/EEC on the Conservation of natural habitats and of wild fauna and flora*.

EU. (2009). *Directive 2009/28/EC of the European Parliament and of the Council of 23 April 2009 on the promotion of the use of energy from renewable sources and amending and subsequently repealing Directives 2001/77/EC and 2003/30/EC (Text with EEA relevance)*.

EU Marine Strategy Framework Directive. (2008). *Directive 2008/56/EC of the European Parliament and of the Council of 17 June 2008 establishing a framework for community action in the field of marine environmental policy (Marine Strategy Framework Directive). Official Journal of the European Union L 16*.

Fagan, W.F., Lewis, M.A., Auger-Méthé, M., Avgar, T., Benhamou, S., Breed, G., Ladage, L., Schlägel, U.E., Tang, W., Papastamatiou, Y.P., Forester, J. & Mueller, T. (2013). Spatial memory and animal movement. *Ecol. Lett.*, 16, n/a-n/a.

Gilles, A., Viquerat, S., Becker, E.A., Forney, K.A., Geelhoed, S.C. V., Haelters, J., Nabe-Nielsen, J., Scheidat, M., Siebert, U., Sveegaard, S., van Beest, F.M., van Bemmelen, R. & Aarts, G. (2016). Seasonal habitat-based density models for a marine top predator, the harbor porpoise, in a dynamic environment. *Ecosphere*, 7, e01367.

Goss-Custard, J.D., Burton, N.H.K., Clark, N.A., Ferns, P.N., McGrorty, S., Reading, C.J., Rehfisch, M.M., Stillman, R.A., Townend, I., West, A.D. & Worrall, D.H. (2006). Test of a behavior-based individual-based model: response of shorebird mortality to habitat loss. *Ecol. Appl.*, 16, 2215–22.

Grimm, V., Berger, U., DeAngelis, D.L., Polhill, G., Giske, J. & Railsback, S.F. (2010). The ODD protocol: A review and first update. *Ecol. Modell.*, 221, 2760–2768.

Grimm, V. & Railsback, S.F. (2005). *Individual-based modeling and ecology*. Princeton University Press.

Grimm, V. & Railsback, S.F. (2012). Pattern-oriented modelling: a "multi-scope" for predictive systems ecology. *Philos. Trans. R. Soc. B-Biological Sci.*, 367, 298–310.

Grimm, V., Revilla, E., Berger, U., Jeltsch, F., Mooij, W.M., Railsback, S.F., Thulke, H.-H., Weiner, J., Wiegand, T. & DeAngelis, D.L. (2005). Pattern-oriented modeling of agent-based complex systems: lessons from ecology. *Science*, 310, 987–91.

Hammond, P.S., Macleod, K., Berggren, P., Borchers, D.L., Burt, L., Cañadas, A., Desportes, G., Donovan, G.P., Gilles, A., Gillespie, D., Gordon, J., Hiby, L., Kuklik, I., Leaper, R., Lehnert, K., Leopold, M., Lovell, P., Øien, N., Paxton, C.G.M., Ridoux, V., Rogan, E., Samarra, F., Scheidat, M., Sequeira, M., Siebert, U., Skov, H., Swift, R., Tasker, M.L., Teilmann, J., Van Canneyt, O. & Vázquez, J.A. (2013). Cetacean abundance and distribution in European Atlantic shelf waters to inform conservation and management. *Biol. Conserv.*, 164, 107–122.

Kastelein, R.A., van der Sijs, S.J., Staal, C. & Nieuwstraten, S.H. (1997). Blubber thickness in harbour porpoises (*Phocoena phocoena*). In: *Biol. Harb. porpoise* (eds. Read, A.J., Wiepkema, P.R. & Nachtigall, P.E.). De Spil Publishers. Learmonth, Woerden, The Netherlands, pp. 179–199.

Kramer-Schadt, S., Revilla, E., Wiegand, T. & Grimm, V. (2007). Patterns for parameters in simulation models. *Ecol. Modell.*, 204, 553–556.

Lockyer, C. (2003). Harbour porpoises (*Phocoena phocoena*) in the North Atlantic: biological parameters. *Harb. porpoises North Atl.*, 5, 71–91.

Lockyer, C., Desportes, G., Hansen, K., Labberté, S. & Siebert, U. (2003). Monitoring growth and energy utilization of the harbour porpoise (<i>Phocoena phocoena<\i>) in human care. *Harb. porpoises North Atl.*, 5, 107–120.

Lockyer, C. & Kinze, C. (2003). Status, ecology and life history of harbour porpoise (*Phocoena phocoena*), in Danish waters. In: *Harb. porpoises North Atl.* (eds. Haug, T., Desportes, G., Víkingsson, G.A. & Witting, L.). The North Atlantic Marine Mammal Commission, Tromsø, pp. 143–175.

Miller, P.J.O., Kvadsheim, P.H., Lam, F.P.A., Tyack, P.L., Cure, C., DeRuiter, S.L., Kleivane, L., Sivle, L.D., van IJsselmuide, S.P., Visser, F., Wensveen, P.J., von Benda-Beckmann, a. M., Martin Lopez, L.M., Narazaki, T. & Hooker, S.K. (2015). First indications that northern bottlenose whales are sensitive to behavioural disturbance from anthropogenic noise. *R. Soc. Open Sci.*, 2, 140484–140484.

Nabe-Nielsen, J., Sibly, R.M., Tougaard, J., Teilmann, J. & Sveegaard, S. (2014). Effects of noise and by-catch on a Danish harbour porpoise population. *Ecol. Modell.*, 272, 242–251.

Nabe-Nielsen, J., Teilmann, J. & Tougaard, J. (2013a). Effects of wind farms on porpoise population dynamics. In: *Danish Offshore Wind. Key Environ. Issues – a Follow.* The Environmental Group: The Danish Energy Agency, The Danish Nature Agency, DONG Energy and Vattenfall, Copenhagen, Denmark, pp. 61–68.

Nabe-Nielsen, J., Tougaard, J., Teilmann, J., Lucke, K. & Forchhammer, M.C. (2013b). How a simple adaptive foraging strategy can lead to emergent home ranges and increased food intake. *Oikos*, 122, 1307–1316.

Nabe-Nielsen, J., Tougaard, J., Teilmann, J. & Sveegaard, S. (2011). *Effects of wind farms on harbour porpoise behavior and population dynamics*. Danish Centre for Environment and Energy, Aarhus University.

Nathan, R., Getz, W.M., Revilla, E., Holyoak, M., Kadmon, R., Saltz, D. & Smouse, P.E. (2008). A movement ecology paradigm for unifying organismal movement research. *Proc. Natl. Acad. Sci.*, 105, 19052–19059.

Nowacek, D.P., Clark, C.W., Mann, D., Miller, P.J.O., Rosenbaum, H.C., Golden, J.S., Jasny, M., Kraska, J. & Southall, B.L. (2015). Marine seismic surveys and ocean noise: time for coordinated and prudent planning. *Front. Ecol. Environ.*, 13, 378–386.

Nowacek, D.P., Thorne, L.H., Johnston, D.W. & Tyack, P.L. (2007). Responses of cetaceans to anthropogenic noise. *Mamm. Rev.*, 37, 81–115.

Pinheiro, J., Bates, D., DebRoy, S., Sarkar, D. & R Core Team. (2016). nlme: Linear and non-linear mixed effects models.

R Development Core Team. (2016). *R: A language and environment for statistical computing*. *R Found. Stat. Comput.*, R Foundation for Statistical Computing. R Foundation for Statistical Computing, http://www.R-project.org, Vienna, Austria.

Read, A.J. (1990). Age at sexual maturity and pregnancy rates of harbour porpoises, *Phocoena phocoena*, from the Bay of Fundy. *Can. J. Fish. Aquat. Sci.*, 47, 561–565.

Read, A.J., Drinker, P. & Northridge, S.P. (2006). Bycatch of Marine Mammals in U.S. and Global Fisheries. *Conserv. Biol.*, 20, 163–169.

Read, A.J. & Hohn, A.A. (1995). Life in the fast lane: The life history of harbor porpoises from the Gulf of Maine. *Mar. Mammal Sci.*, 11, 423–440.

Reid, J.B., Evans, P.G.H. & Northridge, S.P. (2003). *Atlas of Cetacean distribution in north-west European waters*. Joint Nature Conservation Committee.

Richardson, W.J. & Würsig, B. (1997). Influences of man-made noise and other human actions on cetacean behaviour. *Mar. Freshw. Behav. Physiol.*, 29, 183–209.

SCANS II. (2008). *Small cetaceans in the European Atlantic and North Sea (SCANS-II). Final report to the European Commission under project LIFE04NAT/GB/000245*. University of St Andrews, Fife, Scotland, U.K.

Scheffer, M., Baveco, J.M., DeAngelis, D.L., Rose, K.A. & van Nes, E.H. (1995). Super-individuals a simple solution for modelling large populations on an individual basis. *Ecol. Modell.*, 80, 161–170.

Sibly, R.M., Grimm, V., Martin, B.T., Johnston, A.S.A., Kułakowska, K., Topping, C.J., Calow, P., Nabe-Nielsen, J., Thorbek, P. & DeAngelis, D.L. (2013). Representing the acquisition and use of energy by individuals in agent-based models of animal populations. *Methods Ecol. Evol.*, 4, 151–161.

Sinclair, A.R.E. (2003). Mammal population regulation, keystone processes and ecosystem dynamics. *Philos. Trans. R. Soc. London. Ser. B Biol. Sci.*, 358, 1729–1740.

Slabbekoorn, H., Bouton, N., van Opzeeland, I., Coers, A., ten Cate, C. & Popper, A.N. (2010). A noisy spring: the impact of globally rising underwater sound levels on fish. *Trends Ecol. Evol.*, 25, 419–427.

Stillman, R.A., Railsback, S.F., Giske, J., Berger, U. & Grimm, V. (2015). Making predictions in a changing world: The benefits of individual-based ecology. *Bioscience*, 65, 140–150.

Tougaard, J., Carstensen, J., Teilmann, J., Skov, H. & Rasmussen, P. (2009). Pile driving zone of responsiveness extends beyond 20 km for harbor porpoises (*Phocoena phocoena* (L.)) (L). *J. Acoust. Soc. Am.*, 126, 11–14.

Turchin, P. (1998). *Quantitative analysis of movement*. Sinauer Associates, Inc., Sunderland, MA.

Tyack, P.L. (2008). Implications for marine mammals of large-scale changes in the marine acoustic environment. *J. Mammal.*, 89, 549–558.

Urick, R.J. (1983). *Principles of underwater sound*. 3rd edn. McGraw-Hill, New York.

White House Executive Order. (2010). *U.S. national policy for the stewardship of the ocean, our coasts, and the Great Lakes. Executive order 13547 (19 July)*.

Wilson, R.P., Liebsch, N., Davies, I.M., Quintana, F., Weimerskirch, H., Storch, S., Lucke, K., Siebert, U., Zankl, S., Müller, G., Zimmer, I., Scolaro, A., Campagna, C., Plötzg, J., Bornemann, H., Teilmann, J., McMahon, C.R., Plötz, J., Bornemann, H., Teilmann, J. & McMahon, C.R. (2007). All at sea with animal tracks; methodological and analytical solutions for the resolution of movement. *Deep Sea Res. Part II Top. Stud. Oceanogr.*, 54, 193–210.

Wisniewska, D.M., Johnson, M., Teilmann, J., Rojano-Doñate, L., Shearer, J., Sveegaard, S., Miller, L.A., Siebert, U. & Madsen, P.T. (2016). Ultra-high foraging rates of harbor porpoises make them vulnerable to anthropogenic disturbance. *Curr. Biol.*, 1–6.

# TRACE Appendix A – Calibration of dispersal behavior

**This appendix provides supporting information on**: How porpoise movement tracks were analyzed to make it possible to calibrate animal dispersal using pattern-oriented modeling. The appendix is not part of the standard TRACE documentation.

**Summary:**

**This appendix provides information on the procedure used for calibrate the simulated porpoises' dispersal behavior using pattern-oriented modeling. The animal dispersal patterns obtained from animals equipped with Argos satellite tags and from the DEPONS model were analyzed using non-linear mixed effects models. This yielded estimates of the asymptotic home range sizes for each movement track. We here demonstrate that the median asymptotic values for simulated animals resembled those of satellite-tracked animals.**

## Analysis of porpoise dispersal patterns

To ensure that the simulated dispersal movements resembled those of satellite-tracked animals as closely as possible, we calibrated the parameters controlling dispersal, i.e. $d_{\text{disp}}$ (distance moved per dispersal step), *PSM_angle* (maximum turning angle after each step) and *PSM_dist* (see section 3.2.2 for details). To do so we used three different statistics for comparing simulated tracks to those of satellite-tracked animals: (1) home range size ($km^2$), (2) home range length (km) and (3) cumulative distance moved. These statistics characterize complementary aspects of the animals' space use. As all three statistics are sensitive to the number of positions in the movement track, i.e. the number of days from the beginning till the end of the track, we decided to compare the statistics for day 150 of each tracks. All tracks were based on 3-year simulations with 2-years burn in period. Not all tracks lasted 150 days (because the satellite tags stopped working), so the first step in the analysis was to fit a function that enabled us to extract the values for day 150 of the tracks.

The temporal change in home range size and length was modeled using non-linear mixed models for both simulated and satellite-tracked animals. These were fitted using a negative exponential function (i.e. asymptotic regression function through the origin)

$$x = Asym \times (1 - \exp(-\exp(lrc) \times t) \quad \text{Eqn. A14}$$

where $x$ is the track statistic, *Asym* is the horizontal asymptote, *lrc* is the rate constant and $t$ is time since the start of the track (unit: days) (Pinheiro et al. 2016). Both *Asym* and *lrc* were fitted as fixed and random effects to capture individual variation in the large-scale movements. Temporal autocorrelation in the residuals was reduced by fitting a continuous autocorrelation structure to $t$ (corCAR1 class). Homogeneity of residuals was ensured by incorporating a power variance weights structure to $t$.

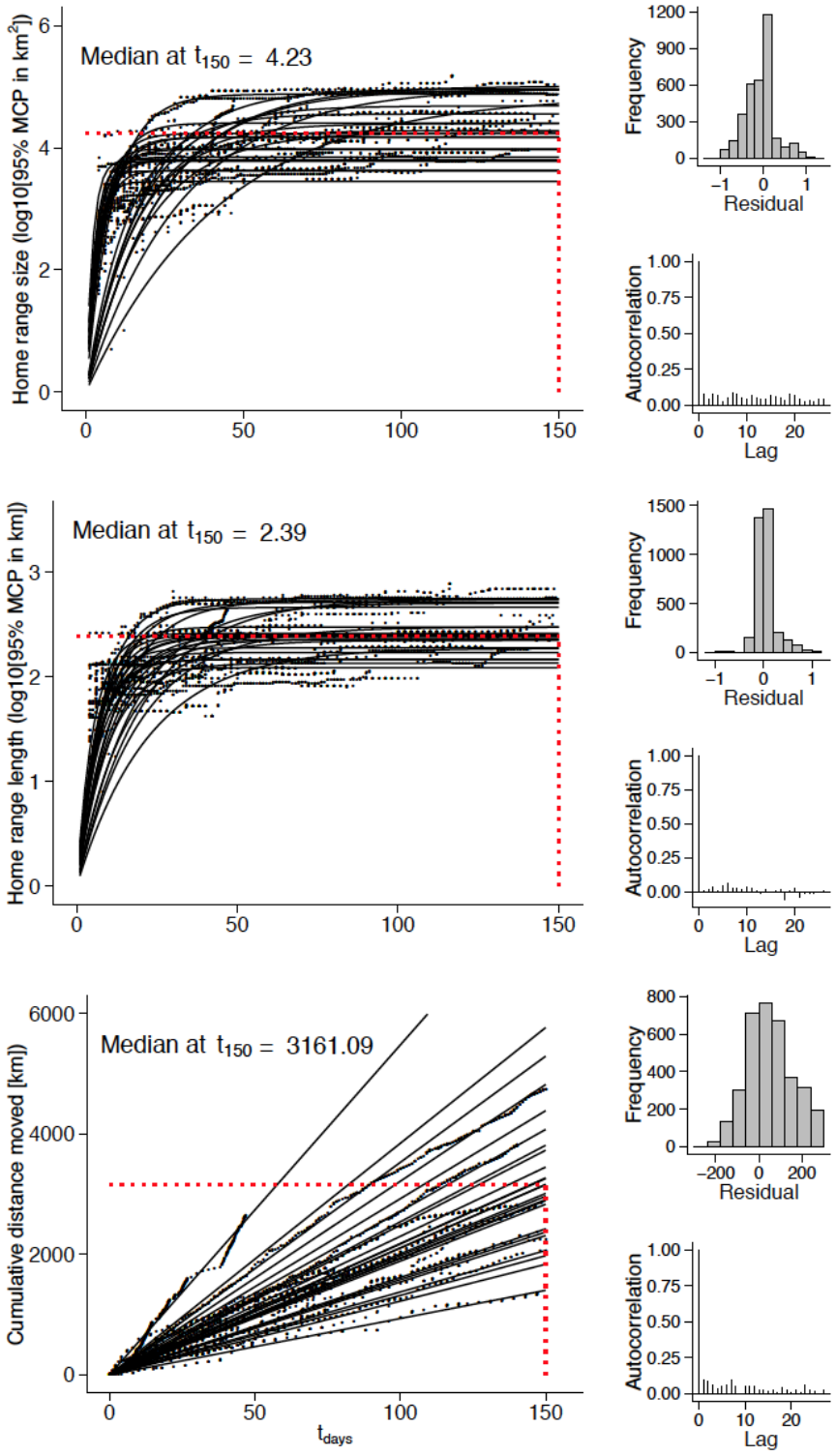


Figure 20. Median home range size, home range length and distance moved after 150 days for 25 free-ranging porpoises equipped with satellite tags.

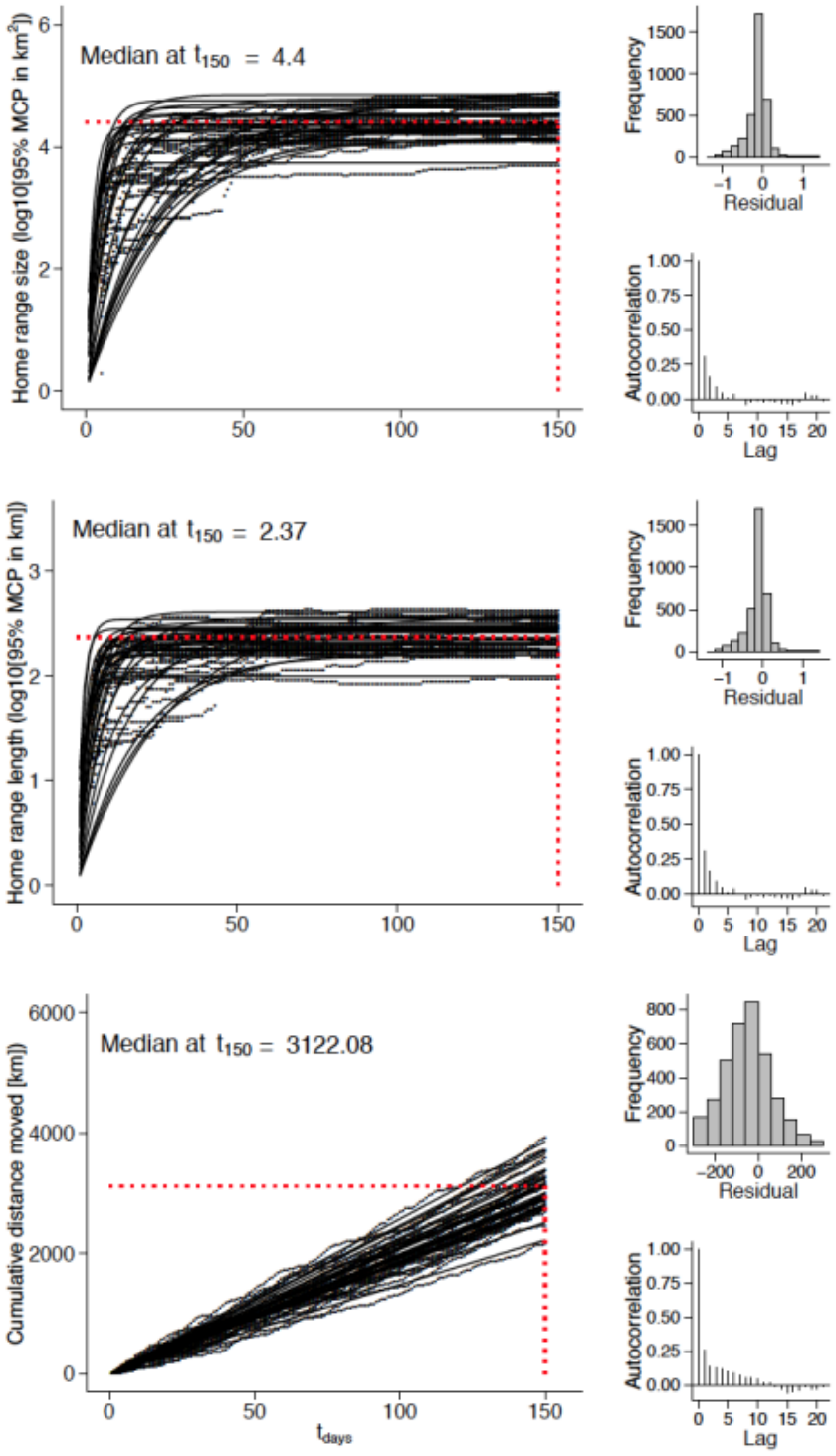


Figure 21. Median home range size, home range length and distance moved after 150 days for 25 porpoise agents. Simulations were based on parameter values provided in Table 2.

Cumulative distance moved over time was quantified with a linear mixed model forced through the origin. Here *t* was both a fixed and random effect and porpoise ID was included as an additional random effect. Again, we included the corCAR1 autocorrelation function and the power variance weights structure to $t_d$ to ensure the validity of the model residuals. All

statistical analyses were performed in the package nlme (Pinheiro et al. 2016) within R (R Development Core Team 2016).

For each of the three statistical models, we extracted the median predicted value at day 150 ($t_{150}$; Figure 20), which were set as the target values in the POM procedure. This procedure consisted on running simulations corresponding to all different combinations of the parameters $d_{\text{disp}}$, *PSM_angle* and *PSM_dist* and calculating home range size, home range length and distance moved after day 150 for each combination. Figure 21 shows the value of these statistics for the best fitting combination of the three parameters (correspondence between statistic based on simulated and satellite-tracked animals shown in Figure 10).

## List of figures

# TRACE document

This is a TRACE document ("TRAnsparent and Comprehensive model Evaludation") which provides supporting evidence that our model presented in:

> **Ayllón, D., Railsback, S.F., Vincenzi, S., Groeneveld, J., Almodóvar, A., Grimm, V., 2016. InSTREAM-Gen: modelling eco-evolutionary dynamics of trout populations under anthropogenic environmental change. Ecological Modelling 326: 36-53.**

was thoughtfully designed, correctly implemented, thoroughly tested, well understood, and appropriately used for its intended purpose.

The rationale of this document follows:

> Schmolke A, Thorbek P, DeAngelis DL, Grimm V. 2010. Ecological modelling supporting environmental decision making: a strategy for the future. *Trends in Ecology and Evolution* 25: 479-486.

and uses the updated standard terminology and document structure in:

> Grimm V, Augusiak J, Focks A, Frank B, Gabsi F, Johnston ASA, Liu C, Martin BT, Meli M, Radchuk V, Thorbek P, Railsback SF. 2014. Towards better modelling and decision support: documenting model development, testing, and analysis using TRACE. *Ecological Modelling* 280: 129-139.

and

> Augusiak J, Van den Brink PJ, Grimm V. 2014. Merging validation and evaluation of ecological models to 'evaludation': a review of terminology and a practical approach. *Ecological Modelling* 280: 117-128.

If this document include **hyperlinks**, navigation back and forth along previously chosen links works via "ALT" + "←" or "ALT" + "→".

# Contents



## 1 Problem formulation

**This TRACE element provides supporting information on**: The decision-making context in which the model will be used; the types of model clients or stakeholders addressed; a precise specification of the question(s) that should be answered with the model, including a specification of necessary model outputs; and a statement of the domain of applicability of the model, including the extent of acceptable extrapolations.

**Summary:**

**Climate change and other anthropogenic pressures are key drivers and accelerators of the short-term dynamic feedbacks resulting from ecological and evolutionary interactions. Consequently, understanding how rapid anthropogenic-driven evolutionary and adaptive processes can influence ecological dynamics is crucial for defining ecosystem conservation and management strategies under ongoing global change. This is particularly relevant in freshwater ecosystems, where the impacts of climate change on ecosystem functioning pose additional complex difficulties to management and threaten the implementation of several environmental directives, conventions and protocols, especially the European Water Framework Directive. InSTREAM-Gen was**

**developed to simulate the eco-evolutionary consequences of river management decisions on trout river systems under a climate change context.**

InSTREAM-Gen was designed to understand how environmental conditions and anthropogenic disturbances drive the evolution of demographics and life-history strategies of stream-dwelling trout populations. Therefore, it is particularly suited to simulate the eco-evolutionary consequences of river management decisions under a climate change context.

Recent human-induced species extinction rates are likely a thousand times higher than the background rate of extinction (Pimm et al. 2014), while current rates of population extirpation are at least three orders of magnitude higher than species extinction rates (Hughes et al. 1997). Human growth and increasing per capita consumption together with associated anthropogenic climate disruption are main drivers of population extirpations and finally species extinctions (Parmesan 2006, Pimm et al. 2014). As the climate changes, species might undergo adaptation, migration or extinction depending largely on their life history and dispersal traits in relation to habitat fragmentation and the rate of environmental change (Woodward et al. 2010). Since habitat fragmentation potentially constrains range shifts to track the optimal environment, populations of many species will have to locally adapt to the changing environment to avoid extinction, particularly when demographic rescue from neighbouring populations is unlikely or impossible (Reed et al. 2011, Vedder et al. 2013). In this case, evolution over short-term must reverse demographic threats due to altered or novel selection pressures to prevent otherwise inevitable extirpation (i.e., evolutionary rescue). However, there is concern that the rate of environmental change is currently exceeding the capacity of populations to adapt (Bell and Gonzalez 2011). This is the case of resident freshwater fish populations, which are responding to climate change at higher extirpation rates than terrestrial organism as shifts in range toward higher elevation or latitude are not keeping pace with the rate of warming in streams and rivers (Comte and Grenouillet 2013). However, most assessments of population extinction risk due to climate change are based on statistical approaches (e.g., climate envelope models) that neglect accounting for a population's capacity to adapt to changing environmental conditions. In contrast, mechanistic eco-genetic modelling is an integrative approach for studying life-history evolution, in particular at contemporary timescales and in realistically complex ecological settings (Dunlop et al. 2009).

InSTREAM-Gen is an individual-based model (IBM) developed with an eco-genetic structure, whose ecological structure is a replicate of a previous IBM, inSTREAM (Railsback et al. 2009). Aside from fundamentals applications to ecological research, inSTREAM was intended to support **environmental impact assessment** on trout systems, as it was developed to address critical river management issues such as instream flow assessment, effects of channel modification or restoration, or analysis of cumulative effects of multiple stressors (e.g., modification of instream habitat and/or channel morphology, changes in environmental and/or ecological conditions). InSTREAM, and thus inSTREAM-Gen, were consequently designed in a way that their predictions could easily be coupled with socio-economic models, or models for decision analysis, in the wider context of river management. InSTREAM-Gen would be thus framed within **evolutionary impact assessment** (Jørgensen et al. 2007), whose goal (in a wide sense) is to predict how alternative management options change the impacts of human-induced evolution on utility metrics, so that management decisions can provide for the greatest long-term benefit to ecosystems and society (Dunlop et al. 2009, Palkovacs and Hendry 2010). Bringing together socio-economic, climatic, eco-hydrological, eco-hydraulic, genetic, life-history and demographic aspects allows the development of a general modelling and conservation framework to support decision-making under the current climate change context, especially regarding the **implementation of the European Water Framework**

**Directive** (Directive, 2000/60/EC; WFD) in Mediterranean salmonid systems. The WFD emphasises a whole-basin approach and requires both the determination and restoration of ecological quality rather than simply water quality. It is underpinned by the concept of baseline conditions or reference systems, defined as those unaltered or only negligibly altered by human activity. As climate change will have an effect on the status of both impacted water bodies as well as sites used for reference, it will affect the characterisation of water bodies, and the definition of reference conditions and the ecological thresholds currently used to set the targets on which river basin management plans are based (see Battarbee et al. 2008, Laaser et al. 2009). Likewise, climate change will affect ecosystem recovery trajectories by shifting baselines (or, more accurately, targets), adding uncertainty to the success of river restoration plans (Verdonschot et al. 2012). One of inSTREAM-Gen's main purposes is to simulate the long-term dynamics of biological reference conditions, ecological thresholds and targets, and system recovery trajectories of Mediterranean mountain trout rivers under different climate change and river basin management scenarios at multiple temporal and spatial scales.

InSTREAM-Gen can only be used to model populations of stream-dwelling trout. Clearly, InSTREAM-Gen is not appropriate (or extrapolations must be considered with caution) for study sites or problems where trout population dynamics are strongly dependent on processes that are not represented, or represented only coarsely, in the model. Therefore, inSTREAM-Gen might not be suitable to model sites where: 1) other fish species are significant competitors for food or habitat; 2) water quality elements other than temperature have strong effects or are the management issues of interest; 3) the effects of ice are important. (See Section "Conceptual model evaluation" of the present TRACE document for further details on the matter.)

# 2 Model description

**This TRACE element provides supporting information on**: The model. Provide a detailed written model description. For individual/agent-based and other simulation models, the ODD protocol is recommended as standard format. For complex submodels it should include concise explanations of the underlying rationale. Model users should learn what the model is, how it works, and what guided its design.

**Summary:**

**We present the complete model description following the ODD (Overview, Design concepts, Details) protocol for describing individual-based models (Grimm et al. 2006, 2010). The model was implemented in NetLogo 5.0.4 (Wilensky 1999), a free software platform for implementing individual-based models. The NetLogo code has been made available in the Supplementary Material of Ayllón et al. (2015).**

Section content

## 2.1 Purpose

InSTREAM-Gen was designed to understand how environmental conditions and anthropogenic disturbances drive the evolution of demographics and life-history strategies of stream-dwelling trout populations. Therefore, it is particularly suited to simulate the eco-evolutionary consequences of river management decisions under a climate change context.

## 2.2 Entities, state variables, and scales

*Spatial scales*: The entire model is represented by one spatially-explicit stream reach of a length defined by the user, but never longer than 300 meters nor wider than 50 meters. The stream habitat within the reach is depicted as a grid of cells of variable size.

*Temporal scale*: The model includes a temporal scaling factor which allows the user to set the time step (never less than one day), so that it is user-specified. At any case, there are three trout actions (habitat selection, feeding and growth, and survival) which are always performed on a daily basis irrespective of the time step defined. The extent (duration) of the simulation is also defined by the user through the length of the environmental and habitat time-series.

*Entities*: This IBM includes three types of entities: Cells, trout and redds. Cells are objects that represent patches of relatively uniform habitat within a reach. Trout are modelled as individuals. Redds are spawning nests made by trout that are modelled as individual objects.

*State variables*: The global (reach) environment is characterized by its environmental and biological conditions. Each cell is characterized both by its physical habitat, and also by its production rate of two different kinds of food, drift and search (stationary) food. Each trout has 21 state variables, while redds' state is described through 18 variables. All state variables of agents are described in Table A1.

**Table A1.** Agents included in inSTREAM-Gen with their state variables and units of measurement.

| Agent | Variable | Description | Unit |
|---|---|---|---|
| Cells | cellArea* | Area of the cell | $cm^2$ |
| | CellAreaCover* | Area of the cell with cover | $cm^2$ |
| | cellAreaShelter* | Area of the cell with velocity shelters | $cm^2$ |
| | cellDepth | Value of depth at specific time | cm |
| | cellDistanceToHide | Average distance from hiding cover from the cell's center | cm |
| | cellFracCover* | Fraction of the cell with cover | Unitless (0-1) |
| | cellFracGravel* | Fraction of the cell with spawning gravel | Unitless (0-1) |
| | cellFracShelter* | Fraction of the cell with velocity shelters | Unitless (0-1) |
| | cellFracSpawn* | Fraction of the cell with spawning gravel | Unitless (0-1) |
| | cellNumber* | Number of the cell | number |
| | cellVelocity | Value of velocity at specific time | cm $s^{-1}$ |
| | driftHourlyCellTotal | Production rate of drift food items | g $h^{-1}$ |
| | my-adjacentCells* | Adjacent cells | agents |
| | my-patches* | Patches composing the cell | agents |
| | searchHourlyCellTotal | Production rate of search food items | g $h^{-1}$ |
| | Transect* | Transect where the cell is located | number |
| Redds | creationDate* | Date when the redd is created | date |

| | | | |
|---|---|---|---|
| | days-after-hatch | Number of days since emergence starts in the redd | days |
| | eggsLostToDewateringTot | Total number of eggs lost due to scouring | eggs |
| | eggsLostToHighTempTot | Total number of eggs lost due to high water temperatures | eggs |
| | eggsLostToLowTempTot | Total number of eggs lost due to low water temperatures | eggs |
| | eggsLostToScourTot | Total number of eggs lost due to dewatering | eggs |
| | eggsLostToSuperimpTot | Total number of eggs lost due to superimposition of redds | eggs |
| | fracDeveloped | Developmental status of a redd's eggs | Unitless (0-1) |
| | my-cell* | Cell where the redd is located | cell-id |
| | numberOfEggs | Number of eggs in the redd | eggs |
| | numberOfHatchedEggs | Number of eggs hatched (creating a new trout) | eggs |
| | reddFathersgenNeutralTrait* | Genotypic values of neutral trait of fathers | User-specific |
| | reddFathersgenNewlength* | Genotypic length at emergence of fathers | cm |
| | reddFathersgenSpawnMinLength* | Genotypic minimum length to spawn of fathers | cm |
| | ReddID * | Identity number of the redd | id |
| | reddMothergenNeutralTrait* | Genotypic value of neutral trait of the mother | User-specific |
| | reddMothergenNewlength* | Genotypic length at emergence of the mother | cm |
| | reddMothergenSpawnMinLength* | Genotypic minimum length to spawn of the mother | cm |
| Trout | age | Number of days since the fish was born | days |
| | age-class | Age class | Age0-Age5Plus |
| | CauseOfDeath* | Mortality source by which the fish is dead | 8 sources |
| | cMax | Physiological maximum daily intake | g $d^{-1}$ |
| | energyAvailableforGrowth | Net energy gain in my-cell during the time step | J $d^{-1}$ |
| | fishCondition | Condition factor | Unitless (0-1) |
| | fishLength | Body length | cm |
| | fishMaxSwimSpeed | Maximum sustainable swimming speed | cm $s^{-1}$ |
| | fishNeutralTrait* | Phenotypic value of the neutral trait | User-specific |
| | fishNewLength* | Phenotypic length at emergence | cm |
| | fishSpawnMinLength* | Minimum length to spawn | cm |
| | fishWeight | Body weight | g |
| | genNeutralTrait* | Genotypic value of the neutral trait | User-specific |
| | genNewLength* | Genotypic length at emergence | cm |
| | genSpawnMinLength* | Genotypic minimum length to spawn | cm |
| | is-sheltered? | Access to a velocity shelter | True/False |
| | maturityStatus | Maturity status | mature/non-mature |
| | my-cell | Cell where the fish is located | cell-id |
| | sex* | Sex | M/F |
| | spawnedThisSeason? | Spawned this spawning season | true/false |
| | status | Status | alive/dead |

* Fixed state variables.

### 2.3 Process overview and scheduling

*Processes*: The model is developed to cover the whole life-cycle of a stream-dwelling trout species. It is structured in nine processes: one related to the reach and cells (update of environmental and habitat conditions), five concerning trout (habitat selection, feeding and growth, survival, reproduction, and ageing) and three performed by redds (development, survival, and hatching of eggs and genetic transmission of traits to new trout).

The reach and cells update their state variables every time step over the whole simulation; trout perform each process every time step of the simulation, but for reproduction, which only occurs during the spawning season (every time step), and angling and hooking mortality, which is restricted to the angling season (every time step); trout age every time step but change their age-class once a year (the Julian day they were born); redd's development and survival processes occur on a time-step basis since redd creation until all eggs have hatched; transmission of heritable traits occurs just when the egg hatches and the new trout is created.

*Schedule*: The simulation starts at an initial date set by the user through the input parameter *initial-date*. Environmental and habitat updates are scheduled first because subsequent trout and redd actions depend on the time step's environmental and habitat conditions. Trout actions occur before redd's because one trout action (reproduction) can cause redd mortality via superimposition. Reproduction is the first trout action because spawning can be assumed the primary activity of a fish on the day it spawns. Spawning also affects habitat selection because 1) spawners move to the spawning habitat when a redd is created and fertilized, and 2) spawners incur on weight, and thus body condition, loss after spawning, which affects their choice of habitat. Habitat selection is the second trout action each time step because it is the way that trout adapt to the new habitat conditions; habitat selection strongly affects both growth and survival. Feeding and growth precedes survival because changes in a trout's length or condition factor affect its probability of survival. Survival has its own sub-schedule because the order in which survival probabilities for the different mortality sources are evaluated strongly affects the number of trout killed by each mortality source. Widespread, less random mortality sources are scheduled first: 1) high temperature, 2) high water velocity, 3) stranding, 4) poor condition, 5) predation by terrestrial animals, 6) predation by piscivorous fish, and 7) angling and hooking. The user has the possibility of choosing which mortality sources can kill trout during the simulation and which ones are not taken into account. Redd actions occur after cell and most trout actions because redds do not affect either habitat or fish, with the exception of creating new trout, which do not execute therefore their first actions until the day after their emergence. Redd survival is the first redd action to be executed. It includes five separate egg mortality sources that follow their own sub-schedule, from least to most random: 1) low temperature, 2) high temperature, 3) scouring, 4) dewatering, 5) superimposition. Trout emergence and genetic transmission of heritable traits is the last redd action. Since survival is scheduled before emergence, trout within redds are subject to redd mortality on the day they emerge (but not to trout mortality). Trout ageing is the last agent's executed action each time step so that both pre-existent and new created trout can increase their age. Finally, observer actions (plotting graphs and writing output files) take place at the end of the time step. All actions occur in the same predetermined order:

1. Reach updates environmental and biological conditions. Cells update depth and velocity as a function of flow, and drift/search food production rate.

2. Trout reproduce:

    2.1. Trout become spawners.

    2.2. Trout spawn and create redds.

3. Trout select habitat.

4. Trout feed and grow: update length, weight and body condition factor.

5. Trout survive or die.

6. Redds' eggs survive or die.

7. Redds' eggs develop.

8. Redds' eggs hatch, new trout are created and heritable traits are transmitted.

9. Trout age.

10. Observer plots model graphical outputs and write model output files.

### 2.4 Design concepts

Learning and Collectives concepts do not apply to this IBM.

*Basic principles*: The model was designed with an eco-genetic structure to analyze both ecological and genetic effects on population dynamics and life-history evolution on contemporary timescales. Accounting for inheritance of quantitative genetic traits allows the study of the eco-evolutionary responses of populations to changing environmental conditions, extreme climate events and strong anthropogenic selection pressures. InSTREAM-Gen is therefore a spatial dynamics model, which integrates the demographic, genetic and spatial dimensions of individual variability through its underlying spatially explicit bioenergetics model and its quantitative genetic model of inheritance of genetic traits.

InSTREAM-Gen is underpinned by "State and prediction-based theory", a new approach that combines existing trade-off methods with routine updating: individuals make a prediction of the future growth and risk conditions over an entire time horizon under different alternative behaviours, but each time they update their decision by considering how their internal state and external conditions have changed, so that they can select the alternative optimizing a fitness measure (see review by Railsback and Harvey 2013).

In inSTREAM-Gen, population abundance and structure can be influenced by density-dependent or density-independent processes. Direct density dependence is only represented through the aquatic predation mortality function, which partly depends on density of piscivorous fish in the reach. Indirect density-dependent mortality occurs during the spawning season, since increasing number of spawners increases the probability of redds dying by superimposition. Density-independent mortality factors include terrestrial predation, flow and temperature extreme events and recreational fishing.

*Emergence*: Dynamics of population demographics (abundance, biomass, production, age- and size-structure) and genetics (evolutionary changes in life-history traits such as size-at-emergence, size maturity threshold, age-at-first-reproduction, time of spawning and emergence) emerge from the growth, survival, and reproduction of individuals, individual-level processes which are driven by complex interactions between individuals and their spatio-temporally heterogeneous habitat. Likewise, other population-level responses, like density-dependent mortality and growth, and habitat selection patterns, are emergent properties of the modelled systems.

*Adaptation*: Habitat selection (i.e., the decision of which cell to occupy each time step) is the primary adaptive trait of trout, strongly driving trout growth and survival. Other adaptive trait is the selection of the feeding strategy (drift-feeding vs. search-feeding) a fish uses each time

step, since it directly affects growth and, indirectly, survival. Trout are able to adapt some of their reproductive behaviors to environmental conditions and their own state: The decision by female spawners of when and where to spawn affects offspring production as well as recruitment survival and growth; selection of male spawners by female spawners is based on the male's body condition factor, and offspring's genotypic body size and size maturity threshold are inherited from their parents.

*Objectives*: Habitat selection is modelled as a fitness-seeking process, by which trout select the cell that maximizes "Expected Reproductive Maturity", a fitness measure developed by Railsback et al. (1999) that represents the expected probability of surviving and reaching reproductive size over a future time horizon.

*Prediction*: Trout are able to predict the probability of both surviving starvation and other mortality sources (except fishing mortality), and approaching maturity size over a future time horizon defined by the user.

*Sensing*: Trout sense water temperature, which influences growth and survival, and consequently, habitat selection. Redds sense water temperature too, affecting survival, development and the timing of hatching. Trout perceive the cell's habitat conditions, both hydraulic conditions and structural features (cover and substrate). This is a main driver of habitat selection. In the case of redds, they also sense their hydraulic environment, which determines the probability of survival of eggs. Trout are aware of all mortality sources in the model and are able to estimate the risk posed by each of them (but for fishing mortality, whose risk is not sensed).

*Interaction*: Competition for food and feeding habitat (velocity shelters) are modelled explicitly, at the cell scale, according to a size-based dominance hierarchy. Each habitat cell contains a limited daily food supply and a fixed area of velocity shelter, so that the food consumed and the sheltered area once used by larger trout are not available for smaller fish. Sexual selection is simulated by indirect interactions of males through their relative weight and condition factor.

*Stochasticity*: InSTREAM-Gen is not a highly stochastic model. The most important process represented as stochastic is trout and redd mortality. While mortality is modelled by calculating the daily probability of each individual agent's survival through deterministic logistic functions, whether the agent actually lives or dies is a stochastic event. Stochasticity is also used in the reproduction process for setting the timing of redd creation, and for the selection of the number and identity of males fertilizing the eggs of a redd, as well as of the identity of the male spawner transmitting its genetic inheritance to each egg. The genotypic and phenotypic values of heritable traits of new created trout are drawn from empirical probability distributions. Likewise, position, sex, age (in days), body size, as well as the genotypic value and its phenotypic expression of heritable life-history traits of trout at initialization are stochastic (drawn from probabilistic functions).

*Observation*: The model produces both graphical displays and output files.

The model provides a graphical display of habitat cells and the location of fish and redds as the model executes. In addition, the model provides several graphical displays of model outputs: population structure updated on a tick basis; fish numbers and biomass, dead fish numbers broken out by mortality source, and total number of eggs in the reach, all updated on a tick basis; yearly demographic outputs (written on the Julian date set by *OutputDate* parameter) including fish numbers and biomass, dead fish numbers broken out by mortality source, number of breeders, and number of initial eggs and fry hatched; yearly life-history outputs including minimum, mean and maximum values of length-at-age, length and age at

spawning broken out by sex, spawning date, emergence date, and age at death; yearly genetic outputs including minimum, mean and maximum values of genotypic length at emergence, neutral trait and length maturity threshold, the latter broken out by sex.

The following demographic and genetic outputs can be recorded at the population level to follow the changes through time of the population ecogenetic structure: 1) Summary population statistics (*LiveFishOutput* file): These statistics include abundance, abundance of mature fish, total fish biomass, and mean and variability (standard deviation) of fish length, weight, and phenotypic values of length maturity threshold, length at emergence and neutral trait, broken out by age-class; 2) Summary breeder population statistics (*BreedersPopOutput* file): These statistics include abundance, and mean, minimum value and variability (standard deviation) of age and fish length at spawning, all broken out by sex. It includes also both phenotypic and genotypic values of length at emergence, neutral trait and length maturity threshold, the latter broken out by sex. Finally, the output file records the mean, minimum value and standard deviation of spawning date and date of emergence of the offspring; 3) Fish mortality (*DeadFishOutput* file): It records the number of fish that have died of each mortality source during a time step, broken out by age class; 4) Redd status and mortality (*ReddOutput* file): It reports when a redd was created, how many viable eggs were created, and when the redd was removed from the model because all its eggs had died or emerged, together with the number of eggs died from each redd mortality source and the number of emerged new trout.

The model also allows the possibility of recording life-history features of breeders at the individual level (*BreedersIndOutput* file): It records the trout and fertilized redd's IDs, the sex, age-class, age, length and weight at spawning, as well as both the phenotypic and genotypic values of length maturity threshold, length at emergence and neutral trait. Habitat use and availability can be recorded through the *HabSelecOutput* file: It reports, for every cell, its area, depth, velocity, fraction with velocity shelters, fraction with cover from predation, average distance to hiding cover, and food availability (drift and search food production rates, as well as the number of trout in the cell broken out by age-class. The output file also provides the flow, temperature and total trout abundance in the reach.

Both demographic fish output files (*LiveFishOutput* and *DeadFishOutput*) can be either written on a yearly or tick basis (set through the *AnnualFishOutput?* global parameter). When written on a tick basis, the parameter *fileOutputFreq* sets the frequency. The *OutputDate* parameter defines the Julian date when the yearly population outputs are written, but for the *ReddOutput* file, which is updated every time a redd is dead or emptied.

### 2.5 Initialization

At initializing a model run, the user must specify the initial date of simulation and the duration of a time step. State of reach's environmental variables, as well as cells' hydraulic and habitat variables are input data. Trout population numbers, age-structure and length-distribution are input data. Population-level distributions of heritable traits are also input data.

Each individual's state variable (sex, age, length, and genotypic and phenotypic values of heritable traits) is initialized by drawing from probability distributions describing their variability. Length and genotypic values of heritable traits are truncated at 4 standard deviations from the center of the probability distributions. Length of 0+ trout cannot be lower than a minimum user-defined value *fishMinNewLength*. Trout weight is calculated as a function of length:

$$fishWeight = fishWeightParamA \times (fishLength)^{fishWeightParamB} \quad (1)$$

and condition factor is subsequently calculated as a function of body length and weight. The condition factor variable used in the model (*fishCondition*) can be considered the fraction of "healthy" weight a fish is, given its length (approach adopted from Van Winkle et al. 1996). The value of *fishCondition* is 1.0 when a fish has a "healthy" weight for its length, according to the length-weight relationship. Trout maximum sustainable swimming speed is a function of the fish's length and water temperature. It is modelled as a two-term function, where the first term represents how it varies linearly with fish length, while the second modifies maximum swimming speed with a non-linear function of temperature:

(2)

$$fishMaxSwimSpeed\ [\text{cm s}^{-1}] = [fishMaxSwimParamA \times fishLength + fishMaxSwimParamB] \times [fishMaxSwimParamC \times (temp)^2 + fishMaxSwimParamD \times temp + fishMaxSwimParamE)]$$

Status is set to "alive". Maturity status is set to either "mature" or "non-mature" depending on whether trout's initial length is over or under the phenotypic value of the length maturity threshold (*fishSpawnMinLength*). The *spawnedThisSeason?* variable is set to "NO".

Each trout's location is assigned stochastically while avoiding extremely risky habitat. The model limits the random distribution of trout to cells where the trout are not immediately at high risk of mortality due to high velocity or stranding. Therefore, each trout is located in a random wetted cell (*cellDepth* > 0) with a ratio of cell velocity to the trout's maximum swimming speed (*cellVelocity* / *fishMaxSwimSpeed*) lower than the parameter *mortFishVelocityV9*, the value at which the probability of surviving high velocity mortality equals 0.9 (see 2.7 Submodels Section 5).

### 2.6 Input data

Times series of three reach environmental variables (temperature, flow and Julian date) are input data. Temporal series of cells' hydraulics (water depth and velocity) are input data too. Fixed physical habitat features of cells (spatial location, and fraction of the cell's area having velocity shelters, elements providing cover from predators and gravels) are specified by means of input files.

### 2.7 Submodels

Since the demographic structure of inSTREAM-Gen is a replicate of inSTREAM IBM, the formulation of all its submodels follows the approaches and equations originally developed by and described in Railsback et al. (2009), unless it is otherwise explicitly stated.

*2.7.1. Environmental and habitat conditions update*:

2.7.1.1. Reach updates temperature and flow from input time series. Day length is calculated and updated:

$$dayLength = 24 - 2\left[\left(\frac{12}{\pi}\right)\arccos\left\{\tan\left(\frac{\pi \times siteLatitude}{180}\right)\tan\delta\right\}\right] \quad (3)$$

where $$\delta = \left[\left(\frac{23.45}{180}\right)\pi\cos\left\{\left(\frac{2\pi}{365}\right)(173 - julianDate)\right\}\right] \quad (4)$$

2.7.1.2. Cells update hydraulics (depth and velocity) from input time series. *wettedArea* and *cellDistanceToHide* are calculated accordingly. *wettedArea* is simply the sum of the area of all cells with *cellDepth* > 0. *cellDistanceToHide* represents the average distance a fish located in the cell would need to move to find hiding cover. While in inSTREAM, *cellDistanceToHide* is fixed along time, in inSTREAM-Gen it dynamically changes its value

every time step. Importantly, cover is only available if the covered cell is not dry; in a cell with cover, it is the average distance within the area with cover (0 meters) plus the average distance within the area without cover (represented as a circumference); in a cell without cover, it is the sum of the distance to the closest covered cell plus the average distance within the area without cover of the closest covered cell.

2.7.1.3. Production rates of both drift and search (stationary) food in the cell are updated. Importantly, the trout feeding submodel uses hourly food production and consumption rates because the number of feeding hours per day varies.

Drift food production rate is calculated from hydraulic data, being modelled as the rate at which prey items flow into the cell from upstream, plus the rate at which consumed prey are regenerated within the cell:

$$driftHourlyCellTotal\ [g\ h^{-1}] = 3600\ [s\ h^{-1}] \times cellDepth\ [cm] \times cellVelocity\ [cm\ s^{-1}] \times cellArea\ [cm^2] \times habDriftConc\ [g\ cm^{-3}] / habDriftRegenDist\ [cm] \quad (5)$$

where *habDriftConc* and *habDriftRegenDist* are reach parameters representing the drift food density in the reach and the drift regeneration distance, respectively.

The rate at which search food is produced in a cell is simply the cell area multiplied by a reach parameter defining the search food density rate:

$$searchHourlyCellTotal\ [g\ h^{-1}] = habSearchProd\ [g\ cm^{-2}\ h^{-1}] \times cellArea\ [cm^2] \quad (6)$$

2.7.1.4. The density of piscivorous fish (*PiscivFishDens*) is calculated as the number of trout with a fish length greater than the reach parameter *fishPiscivoryLength* divided by the reach's wetted area (*wettedArea*). The value of the temperature function of the trout's physiological maximum daily food consumption (*cmaxTempFunction*) is updated as a function of updated water temperature.

*2.7.2. Trout Reproduction and Redd creation*:

It is scheduled in two main actions:

2.7.2.1. Trout become spawners:

Every day, each female trout determines whether to spawn based on whether it meets all of the following fish- and habitat-based spawning criteria:

- Trout only spawn within a spawning date window (spawning season) defined by the global parameters *fishSpawnStartDate* and *fishSpawnEndDate*.

- Trout have to be sexually mature (maturity is attained when the trout reaches an age and length equal to *fishSpawnMinAge* and *fishSpawnMinLength*, respectively) and have enough energy reserves to spawn (its condition factor must exceed the minimum condition factor parameter *fishSpawnMinCond*).

- Female trout are assumed not to spawn more than once per annual spawning season. At the start of the first day of the spawning season the Boolean variable *spawnedThisSeason?* is set to NO for all trout. Once a female trout spawns, the variable is set to YES so that the trout is not allowed to spawn again during the rest of the spawning season.

- Trout only spawn within a temperature range defined by parameters for maximum and minimum temperatures for spawning (*fishSpawnMaxTemp* and *fishSpawnMinTemp*, respectively).

- Trout cannot spawn if the flow in the reach is higher than a maximum threshold defined by the reach habitat parameter *habMaxSpawnFlow*.

- Trout are assumed not to spawn when flows are unsteady. Therefore, if the fractional change in flow from the previous day is greater than the value of the parameter *fishSpawnMaxFlowChange* then spawning is not allowed. This fractional change in flow is evaluated as:

$$fracFlowChange = \text{abs}(todaysFlow - yesterdaysFlow)/todaysFlow \quad (7)$$

Finally, on the time-steps when all the spawning criteria are met for a female, then whether it actually spawns is determined stochastically. The probability of spawning on any such day is the parameter *fishSpawnProb* (unitless).

A male trout becomes spawner, only within the spawning season, when it is sexually mature (its age and length are equal or greater than *fishSpawnMinAge* and *fishSpawnMinLength*, respectively) and has a body condition over *fishSpawnMinCond*. Males are able to spawn multiple times over the spawning season, as it is typically described in the literature (Jonsson and Jonsson 2011).

2.7.2.2. Redd creation and fertilization:

This action assumes a size-based dominance hierarchy for spawning, so that the following steps are carried out in descending order of fish length.

2.7.2.2.1. Selection of the spawning cell.

Female spawners select the cell in which they then build a redd. The first step in identifying the location for a new redd is identifying all the cells that are potential spawning sites. It follows the same method used by trout to identify potential destinations during habitat selection (2.7 Submodels Section 3). Afterwards, potential spawning cells are rated by the spawner to identify the cell with the highest value of variable *spawnQuality*:

$$spawnQuality = spawnDepthSuit \times spawnVelocitySuit \times spawnGravelArea \quad (8)$$

where variables *spawnDepthSuit* and *spawnVelocitySuit* are unitless habitat suitability factors, whose values are interpolated linearly from suitability functions provided as parameters. The value of *spawnGravelArea* is the cell area times its fraction with spawning gravel (*cellArea* × *cellFracGravel*). If *spawnGravelArea* is 0 then the female trout moves to the cell that maximizes (*spawnDepthSuit* × *spawnVelocitySuit*).

The female trout moves then to the selected spawning cell to create a redd.

2.7.2.2.2. Selection of male spawners.

InSTREAM-Gen allows for both monogamy (each cross involving two parents) and polygamy (each cross involving one female and several satellite males) mating strategies. Both monogamous and polygamous matings have been commonly observed in trout breeding systems (García-Vázquez et al. 2001, Serbezov et al. 2010a). The number of males per female (*number-males*) is randomly drawn from a uniform distribution from 1 to *max-n-males-per-female* (a global parameter). Following Piou and Prévost (2012), the probability of a male spawner *j* of being selected to fertilize a redd depends on its weight:

$$P(\text{selected} \mid fishWeight_j) = (fishWeight_j / \sum fishWeight_l) \quad (9)$$

where *l* is the number of available male spawners. The largest male is always selected. The rest of *number-males* males are then randomly selected among a list containing the *n* male spawners having the highest probability (*candidate-spawners*). This number *n* is stochastically chosen. If the number of selected spawners is lower than *number-males*, then additional males are randomly selected (if possible) among the remaining male spawners until *number-males* is reached. If no male meets the criteria as a spawner, or there are no more

male spawners available, there is no effect on the female or redd and the female still produces a fertile redd, so that transmission of heritable traits depends only on the mother's genotypic values.

Contrarily to inSTREAM, male spawners move to the spawning cell selected by the female.

2.7.2.2.3. Redd creation and fertilization.

- When a female spawner has selected a spawning cell, it creates a redd in the cell. The number of eggs in the redd depends on the spawner's fecundity (a function of length) and losses during spawning:

$$numberOfEggs = (eggsize\text{-}fecund\text{-}tradeoff \times fishFecundParamA \times fishLength^{fishFecundParamB}) \times EggViability \quad (10)$$

Since trout length at emergence is a heritable trait in the model and it is typically correlated to egg size (see references in reviews by Klemetsen et al. 2003, and Jonsson and Jonsson 2011), we introduced the term *eggsize-fecund-tradeoff* to deal with the fact that in salmonids the number of eggs in a redd is traded-off with egg size (see again Klemetsen et al. 2003, Jonsson and Jonsson 2011). It was modelled as the relationship between the number of eggs that would be created by the trout if the offspring had the population mean length at emergence and such number if the offspring had the female spawner's genetic length at emergence, which is mathematically expressed as:

$$eggsize\text{-}fecund\text{-}tradeoff = (fishNewLengthMean / genNewLength)^{fishWeightParamB} \quad (11)$$

The parameter *fishSpawnEggViability* is the fraction of eggs that are successfully fertilized and placed in the redd.

- After the redd is created by the female trout, it is fertilized by the selected male spawners. That means that the genotypic value of heritable traits of both the mother and all fathers are stored in the genetic trait map of the redd (*reddMothergenSpawnMinLength*, *reddMotherNewLength*, *reddMotherNeutralTrait; reddFathersgenSpawnMinLength*, *reddFathersNewLength*, *reddFathersNeutralTrait*).

2.7.2.2.4. Incur weight loss.

Both female spawner and all males contributing to the redd incur on weight loss. Their weight is reduced according to the parameter *fishSpawnWtLossFraction*, so that *fishWeight* is multiplied by (1- *fishSpawnWtLossFraction*). In consequence, the body condition factor is accordingly reduced, which can significantly affect subsequent habitat selection and survival.

*2.7.3. Trout Habitat selection*:

The habitat selection trait is modelled as follows: every time step, each trout moves to the habitat cell that (1) is close enough that the fish can be assumed to be aware of conditions in it, and (2) offers the highest "expected fitness", where expected fitness is approximated as the expected probability of surviving and reaching reproductive size over a future time horizon.

The habitat selection trait assumes a size-based dominance hierarchy: trout can only use resources (food and velocity shelters) that have not been consumed by larger trout. The number of trout feeding in a cell is limited by its daily food production. Each trout using a drift-feeding strategy can use a maximum velocity shelter area ($cm^2$) equal to $(fishLength)^2$.

2.7.3.1. Identify potential destination cells:

When each individual trout begins its habitat selection procedure, its first action is to identify the cells that are potential movement destinations. Distance and depth can limit potential destination cells, but the number of fish already in a cell does not limit its availability as a destination.

Only wetted (*cellDepth* > 0) habitat cells within a certain distance are included as potential destinations. This maximum movement distance should be considered the distance over which a fish is likely to know its habitat well enough to be aware when desirable destinations are available, over the time step. It is an exponential function of fish length (Diana et al. 2004):

$$maxMoveDistance \text{ (cm)} = fishMoveDistParamA \times (fishLength)^{fishMoveDistParamB} \quad (12)$$

However, as discussed by Railsback et al. (2009), for small fish, it is possible that no cells other than the current one are within this *maxMoveDistance*, which poses an artificial barrier to movement, an artifact of the model's spatial resolution. Consequently, a fish's potential destinations always include the cells adjacent to the fish's current cell.

2.7.3.2. Evaluate potential destination cells:

A trout evaluates each potential destination cell to determine the fitness it would provide, using the "Expected Reproductive Maturity" fitness measure of Railsback et al. (1999), where:

$$expectedMaturity = nonstarvSurvival \times starvSurvival \times fracMature \quad (13)$$

*nonstarvSurvival* is the probability of survival for all mortality sources except starvation and angling and hooking over the fitness horizon (see Submodels Section 5); its formulation implicitly assumes that trout consider all mortality sources in their habitat selection decision. This means that the trout are assumed to be aware of all the kinds of mortality in the model and are able to estimate the risk posed by each, except for fishing mortality:

$$nonstarvSurvival = (S_{hightemp} \times S_{highvel} \times S_{strand} \times S_{terrpred} \times S_{aqpred})^{fishFitnessHorizon} \quad (14)$$

*starvSurvival* represents the probability of surviving starvation over the fitness horizon; the method assumes that trout evaluate expected maturity using the simple prediction that the current time-step's growth rate would persist over the time horizon. It is implemented following the next steps:

First, determine the foraging strategy, food intake, and growth for the trout and habitat cell in question, for the current time step, using the methods described in Section 2.7.4.

Second, project the fish's weight, length, and condition factor that would result if the current day's growth persisted over the fitness time horizon specified by *fishFitnessHorizon*.

Third, approximate the probability of surviving starvation over the fitness horizon, estimated as the first moment of the logistic function of poor condition survival vs. condition factor:

$$starvSurvival = \left[\frac{\left(\frac{1}{b}\right)\ln\left(\frac{1+e^{(a+b\times K_{t+T})}}{1+e^{(a+b\times K_t)}}\right)}{(K_{t+T}-K_t)}\right]^T \quad (15)$$

where $K_t$ is the fish's value of *fishCondition* at the current time-step and $K_{t+T}$ is the projected condition factor at the end of the fitness horizon, $T$ is equal to *fishFitnessHorizon*, and $a$ and $b$ are the *logistA* and *logistB* variables of the logistic function of poor condition survival [described in Section 2.7.5, equation (42)].

This equation can cause significant computational errors when $K_{t+T}$ is extremely close to $K_t$ (and a divide-by-zero error when they have the same value). To avoid it, *starvSurvival* is set

equal to the daily survival probability for *Kt*, raised to the power *fishFitnessHorizon*, whenever ($K_{t+T}$ - $K_t$) is less than 0.001.

*fracMature* represents how close to the size of sexual maturity a fish would be at the end of the fitness time horizon. It is simply the ratio between (a) the length the fish is projected to be at the end of the time horizon, and (b) the parameter *fishSpawnMinLength* (see Section 2.7.2), limited to a maximum of 1.0.

*2.7.4. Trout Feeding and Growth*:

In the model, trout can use either of two feeding strategies, drift or active search feeding. The feeding and growth methods calculate the potential food intake and metabolic costs a fish would experience in a cell, for both drift and search feeding. Standard bioenergetics approaches are used to calculate net energy intake (the difference between energy intake from food and metabolic energy cost) for each feeding strategy (following Hanson et al. 1997). The fish then selects the strategy that provides the highest net energy intake. Daily growth is proportional to net energy intake. A fish's length and condition factor at the end of the time-step are updated from its daily growth. The following steps describe the process used by a trout to determine the feeding strategy it would use, and the resulting food intake and growth it would obtain, for a particular habitat cell.

2.7.4.1. Feeding:

1. Determine the **potential daily drift intake** that would be obtained in the absence of more dominant fish in the cell. This *dailyPotentialDriftFood* is determined from the hourly intake rates and hours spent feeding:

*dailyPotentialDriftFood* [g $d^{-1}$] = *driftIntake* [g $h^{-1}$] × *feedTime* [h $d^{-1}$] (16)

Hours spent feeding is the day length plus one hour before sunrise and one after sunset:

*feedTime* = *dayLength* + 2

A fish's intake rate is calculated as the mass of prey passing through the capture area times the capture success:

*driftIntake* [g $h^{-1}$] = *habDriftConc* [g $cm^{-3}$] × *cellVelocity* [cm $s^{-1}$] × *captureArea* [$cm^2$] (17)

× 3600 [s $h^{-1}$] × *captureSuccess* [unitless]

The capture area models the area over which drift-feeding trout can detect prey and is depicted as a rectangular area perpendicular to the current, whose dimensions ultimately depend on fish size through the detection distance. Fish are assumed able to detect all drift that comes within the detection distance to their left and right, while the height of the capture area is the minimum of the reactive distance and the depth (which often is lower):

(18)

*captureArea* [$cm^2$] = [2 × *detectDistance* [cm]] × [min (*detectDistance*, *cellDepth*) [cm]]

Detection distance is defined as the distance over which fish can see and attack - but not necessarily capture - prey. Detection distance is primarily a function of the size of the fish:

(19)

*detectDistance* (cm) = *fishDetectDistParamA* + *fishDetectDistParamB* × *fishLength* [cm]

Railsback et al. (2009) developed this model based on empirical data from the study of Schmidt and O'Brien (1982) for arctic grayling, whose results had been used successfully as the basis of the previous drift feeding models of Hughes (1992a) and Hughes et al. (2003). The linear model is not, however, a regression fit to those data, but rather it was derived from pre-calibration of the growth model. In fact, an exponential model provided a better fit to the data, but the linear model, nevertheless, was able to capture a series of qualitative patterns the exponential formulation was not (see Railsback et al. 2009 or the "Data evaluation" element of the present TRACE document for further details).

Capture success represents what fraction of detected prey is actually caught. Capture success is largely a function of water velocity but also of the fish's maximum sustainable swimming speed:

*captureSuccess* ~ logistic (*cellVelocity* / *fishMaxSwimSpeed*) (20)

Maximum sustainable swimming speed is a component of not only the drift feeding trait but also of high velocity mortality (Submodels Section 5.2), and strongly affects the relationship between a cell's velocity and habitat quality for various size trout. The maximum swim speed used for both drift-feeding and high velocity mortality must be a speed that fish can swim for hours, not a burst or short-term maximum speed. It is a function of a fish's length and water temperature, as described in equation (2).

2. Determine the **daily drift intake available** after more dominant fish in the cell have consumed their intake:

$dailyAvailableDriftFood$ [g $d^{-1}$] = $driftHourlyCellAvail$ [g $h^{-1}$] × $feedTime$ [h $d^{-1}$] (21)

The drift food production rate in a cell *driftHourlyCellTotal* is updated every time a trout moves to that cell, so that the drift food available in a cell for a trout is the drift food production rate in the cell at the beginning of the time-step minus the *driftIntake* of all larger trout using a drift-feeding strategy that already occupy the cell. Therefore, hierarchical competition for food is implemented via the food availability rates.

$driftHourlyCellAvail$ [g $h^{-1}$] = $driftHourlyCellTotal - \sum driftIntake$ (22)

3. Determine the **physiological maximum daily consumption (*cMax*)**:

Maximum daily consumption (*cMax*) represents the maximum rate of food consumption if a fish is limited only by its physiology. The equation for *cMax* includes (a) an allometric function, relating *cMax* to fish size; and (b) a temperature function (Hanson et al. 1997), which is represented as a set of seven points used to interpolate a value of *cmaxTempFunction* from the reach's temperature:

$cMax$ (g $d^{-1}$) = $fishCmaxParamA \times (fishWeight)^{(1 + fishCmaxParamB)} \times cmaxTempFunction$ (23)

4. Calculate the actual **daily drift food intake**, considering whether it is limited by actual food availability or the physiological maximum intake:

(24)

$dailyDriftFoodIntake$ [g $d^{-1}$] = min($dailyPotentialDriftFood$, $dailyAvailableDriftFood$, $cMax$)

5. Convert daily drift intake in grams of food to joules of **energy** by means of the *Prey energy density* reach parameter:

(25)

*dailyDriftEnergyIntake* [j $d^{-1}$] = *dailyDriftFoodIntake* [g $d^{-1}$] × *habPreyEnergyDensity* [j $g^{-1}$]

6. Conduct the bioenergetics energy balance to get **net energy intake for drift feeding**:

*dailyDriftNetEnergy* [j $d^{-1}$] = *dailyDriftEnergyIntake* [j $d^{-1}$] - *respTotal* [j $d^{-1}$] (26)

The model uses the Wisconsin Model equation 1 for respiration (Hanson et al. 1997), as modified by Van Winkle et al. (1996) to apply the activity respiration rate only during active feeding hours. Respiration is therefore modelled as the energetic cost of metabolism and swimming, including then (a) standard respiration that is independent of the fish's activity, and (b) an additional activity respiration that increases with the daily swimming speed.

Drift-feeding fish are assumed to swim at a speed (*swimSpeed*, cm $s^{-1}$) equal to their habitat cell's water velocity unless they have access to velocity shelter. If a drift-feeding fish has access to velocity shelter, then its *swimSpeed* is assumed equal to a constant fraction of its habitat cell's mean water velocity, defined by the reach parameter *habShelterSpeedFrac*. A fish has access to velocity shelter in a cell only if the sum of shelter areas occupied by larger drift-feeding fish in the cell (each drift-feeding fish is assumed to use up an area of velocity shelter equal to the square of its length) is less than the cell's total shelter area.

*respTotal* [j $d^{-1}$] =*respStandard* [j $d^{-1}$] + *respActivity* [j $d^{-1}$] (27)

$$respStandard = (fishRespParamA \times (fishWeight)^{\text{fishRespParamB}}) \times e^{(fishRespParamC \times \text{temp})} \quad (28)$$

$$respActivity = (feedTime / 24) \times (e^{(\text{fishRespParamD} \times \text{swimmSpeed})} - 1) \times respStandard \quad (29)$$

7. Determine the **potential daily search feeding intake** that would be obtained in the absence of more dominant fish in the cell:

*dailyPotentialSearchFood* [g $d^{-1}$] = *searchIntake* [g $h^{-1}$] × time feeding [h $d^{-1}$] (30)

The model assumes that the rate of search food intake is proportional to the rate at which search food becomes available: every fish searches for food at about the same rate, so intake increases linearly with food production. Search feeding intake is also assumed to decrease linearly to zero as water velocity increases to the fish's maximum sustainable swim speed. This velocity function represents how the ability of a fish to see and search for food decreases with velocity. The rate of search food intake is formulated as follows:

*searchIntake* [g $h^{-1}$] = *habSearchProd* [g $cm^{-2}$ $h^{-1}$] × *fishSearchArea* [$cm^2$] (31)

× max([(*fishMaxSwimSpeed – cellVelocity*) / *fishMaxSwimSpeed*], 0)

where *habSearchProd* is the rate at which search food is produced, *fishMaxSwimSpeed* is the fish's maximum sustainable swimming speed, and *cellVelocity* is the velocity of the fish's cell. The proportionality constant *fishSearchArea* can be loosely interpreted as the area over which the production of stationary (non-drifting) food is consumed by one fish.

8. Determine the **daily search intake available** after more dominant fish have consumed their intake:

*dailyAvailableSearchFood* [g $d^{-1}$] = *searchHourlyCellAvail* [g $h^{-1}$] × *feedTime* [h $d^{-1}$] (32)

In the same way that drift feeding is modelled, search food available in a cell for a trout is calculated as the search food production rate in the cell at the beginning of the time-step minus the *searchIntake* of all larger trout using a search-feeding strategy that already occupy the cell. Again, hierarchical competition for food is implemented via the food availability rates.

*searchHourlyCellAvail* [g $h^{-1}$] = *searchHourlyCellTotal* – ∑ *searchIntake* (33)

9. Calculate the actual **daily search intake** considering whether it is limited by food availability or maximum daily intake:

(34)

*dailySearchFoodIntake* [g $h^{-1}$] = min(*dailyPotentialSearchFood, dailyAvailableSearchFood, cMax*)

10. Convert daily search intake in grams of food to joules of **energy** by means of the *Prey energy density* reach parameter:

(35)

*dailySearchEnergyIntake* [j $d^{-1}$] = *dailySearchFoodIntake* [g $d^{-1}$] × *habPreyEnergyDensity* [j $g^{-1}$]

11. Conduct the bioenergetics energy balance to get net energy intake for search feeding:

*dailySearchNetEnergy* [j $d^{-1}$] = *dailySearchEnergyIntake* [j $d^{-1}$] – *respTotal* [j $d^{-1}$] (36)

Respiration costs for fish using a search feeding strategy are calculated in the same way than for drift-feeding fish. However, fish using the search feeding strategy are assumed to swim at a speed equal to their cell's mean water velocity. There is no reduction in *swimSpeed* due to velocity shelters.

12. Select the most profitable feeding strategy by comparing *dailyDriftNetEnergy* to *dailySearchNetEnergy*; and determine the **energy intake for the best strategy**:

*bestNetEnergy* [j $d^{-1}$] = max(*dailyDriftNetEnergy*, *dailySearchNetEnergy*) (37)

2.7.4.2. Growth:

13. Convert net energy intake to **daily growth** by means of the *Fish energy density* reach parameter:

*dailyGrowth* [g $d^{-1}$] = *bestNetEnergy* [j $d^{-1}$] / *fishEnergyDensity* [g $j^{-1}$] (38)

14. Update the fish's **weight** at the end of the time-step:

*FishWeight* [g] = *fishWeight* [g] + *dailyGrowth* [g $d^{-1}$] × *timestep-scale* [d] (39)

15. Update the fish's **length** at the end of the time-step:

Fish length is then the maximum length between current length and potential length (*fishWannabeLength*; the length the fish would be if its condition factor were 1.0). This potential length is calculated with the fish's new weight and the inverted length-weight relation for healthy fish:

$$fishWannabeLength\ [\text{cm}] = (fishWeight\ /\ fishWeightParamA)^{(1\ /\ fishWeightParamB)} \quad (40)$$

If the fish's current length is less than *fishWannabeLength* (indicating that the fish is not underweight), then its new length is set to *fishWannabeLength*. Otherwise, its length is not changed.

16. Update the fish's **condition factor** at the end of the time-step:

The new value of *fishCondition* is equal to the fish's new weight divided by the "healthy" weight for a fish given its length:

$$fishCondition = fishWeight / \left(fishWeightParamA \times (fishLength)^{fishWeightParamB}\right) \quad (41)$$

*2.7.5. Trout Survival*:

Survival simulations determine, each day, which fish die from what causes. Mortality sources are represented separately because the probability of surviving each varies differently with fish state and habitat conditions. Mortality sources are represented as survival probabilities: the daily probability of not being killed by one specific mortality source. Survival probabilities are used (1) during habitat selection (Section 2.7.3) as a major input trout use in deciding which habitat cell to occupy, and (2) to model mortality: when and why each fish actually dies. The same methods are therefore used to determine survival probabilities in modelling both habitat selection and mortality.

On every simulated time step, each fish determines whether it dies of each mortality source following a two-step process: first is calculating the daily survival probability from the current state of the fish and its cell and project it over the time extent defined by *timestep-scale*; second is determining, stochastically, whether the fish actually dies by comparing a random number drawn from a uniform distribution between zero and one to the projected survival probability. If the random number is greater than the survival probability, then the fish dies as a result of the mortality source and no further mortality sources are evaluated for the fish. If the fish does not die, then the next mortality source is evaluated. The user has the option to select the mortality sources that can actually kill the trout.

The survival probabilities are modelled through logistic functions, so that their values increase from zero to one, or decrease from one to zero, along the range of the predictor used as a proxy for the evaluated mortality source. In the model, logistic functions are defined via parameters that specify the predictor values at which the survival probability value equals 0.1 and 0.9. The logistic functions are defined as:

$$S = e^Z / (1 + e^Z) \quad (42)$$

where

$Z = LogistA + (LogistB \times habitatVariable)$,

$LogistA = LogistC - (LogistB \times habVarAtS01)$,

$LogistB = (LogistC - LogistD) / (habVarAtS01 - habVarAtS09)$,

$LogistC = \ln(0.1/0.9)$, and

$LogistD = \ln(0.9/0.1)$.

While death due to each mortality source is treated independently, the order in which mortality sources are evaluated can have a (usually very small) effect on how many fish die of each kind of mortality. They are scheduled in the following order:

2.7.5.1. High temperature:

This mortality source represents the breakdown of physiological processes at high temperatures. It does not represent the effect of high temperatures on bioenergetics (reduced growth at high temperature). The survival probability is based on the daily mean water temperature.

2.7.5.2 High velocity:

The high velocity survival function represents the potential for trout to suffer fatigue or lose their ability to hold position in a cell with high velocity. This function is included not because trout often die due to high velocity, but because it strongly affects habitat selection: mortality due to high velocities is not observed in nature because fish avoid it by moving. The survival probability is based on the ratio of the swimming speed a fish uses in a cell to the fish's maximum sustainable swim speed (described in Section 2.7.4.1).

2.7.5.3. Stranding:

Stranding mortality represents the death of fish that are unable to move out of cells that become extremely shallow or dry as flow decreases. Survival of stranding is modelled as an increasing logistic function of depth divided by fish length in order to scale how the risks of low depths vary with fish size.

2.7.5.4. Poor condition:

Fish in poor condition (low value of the condition factor, weight in relation to length) are at risk of starvation, disease, and excess vulnerability to predators. These risks are combined in the poor condition survival probability. Poor condition can have a strong effect on habitat selection as well as mortality. As commented, the survival probability is based on the fish's condition factor.

2.7.5.5. Terrestrial predation:

The formulation of this mortality source assumes a minimum survival probability *mortFishTerrPredMin* that applies when fish are most vulnerable to terrestrial predation, and a number of "survival increase functions" that can increase the probability of survival above this minimum. Survival increase functions are described as logistic functions that have values between zero and one, with higher values for greater protection from predation. The survival increase functions are assumed to act independently. Therefore, the terrestrial predation survival probability is obtained by increasing the minimum survival (decreasing the difference between minimum survival and 1.0) by the maximum of the independent survival increase functions. This assumption is expressed mathematically as:

(43)

$$terrPredSurv = mortFishTerrPredMin + [(1 - mortFishTerrPredMin) \times \max(terrPredDepthF, terrPredLengthF, terrPredFeedTimeF, terrPredVelF, terrPredCoverF)]$$

where *terrPredDepthF* is the value of the survival increase function for **depth**. The depth survival increase function is an increasing logistic curve: survival increases as depth increases; *terrPredLengthF* is the value of the survival increase function for **fish length**. Survival of terrestrial predation is assumed to decrease with fish length; *terrPredFeedTimeF* is the value of the survival increase function for **feeding time**. The survival increase function is modelled as a decreasing function of *feedTime* (h), the hours spent feeding per day; *terrPredVelF* is the value of the survival increase function for **water velocity**. The survival increase function is an increasing logistic curve: survival increases with velocity; *terrPredCoverF* is the value of the survival increase function for **distance to hiding cover**. Hiding cover is represented with a survival increase function that increases as distance to hiding cover (*cellDistanceToHide*, cm) decreases.

2.7.5.6. Aquatic predation:

The aquatic predation formulation represents mortality due to predation by fish. By adjusting parameter values, the formulation can be made to apply both to sites where the modelled trout are the only piscivorous fish and sites where non-trout fish, not otherwise represented in the model, are a significant risk. The formulation can represent the effect of adult trout density on aquatic predation survival, making this survival probability the only component of the model with direct density dependence. It allows a type of feedback that is potentially important in regulating trout populations: when adult abundance is greatly reduced, juveniles can safely use a wider range of habitat and, hence, have greater growth and survival to adulthood.

As with terrestrial predation, the formulation uses a minimum survival probability *mortFishAqPredMin* that applies when fish are most vulnerable to aquatic predation, and a number of survival increase functions:

(44)

$$aqPredSurv = mortFishAqPredMin + [(1 - mortFishAqPredMin) \times \max(aqPredDensF, aqPredDepthF, aqPredLengthF, aqPredFeedTimeF, aqPredTempF)]$$

where *aqPredDensF* is the value of the survival increase function for **piscivorous trout density**. This function represents only the effect of trout included in the model and not of other piscivorous fish that may be present in the reach. Any trout with length greater than the parameter *fishPiscivoryLength* (cm) is assumed to be a piscivorous trout. Predation is represented at the reach spatial scale (as opposed to the cell scale) because large, piscivorous trout are likely to foray and attack fish in other cells. The predator density survival increase function causes the survival increase function to increase as the density of piscivorous trout decreases; *aqPredDepthF* is the value of the survival increase function for **depth**. The depth survival increase function is a decreasing logistic function; *aqPredLengthF* is the value of the survival increase function for **fish length**. Survival of aquatic predation is increases with fish length; *aqPredFeedTimeF* is the value of the survival increase function for **feeding time**. The survival increase function is modelled as a decreasing function of the hours spent feeding per day; *aqPredTempF* is the value of the survival increase function for **water temperature**. This survival increase function reflects how low temperatures reduce the metabolic demands and, therefore, feeding activity of piscivorous fish. The survival increase function is therefore a decreasing logistic curve.

2.7.5.7. Angling and hooking:

This mortality component follows the models implemented in inSTREAM-SD (Railsback et al. 2013).

The angler mortality model includes three separate components: fishing pressure, capture rate, and survival probability. **Survival of angling mortality** depends on how many times a trout is hooked (the rate at which trout are caught being a function of fishing pressure) and whether it is kept vs. released each time hooked. **Hooking mortality** (the subsequent death of fish caught and released by anglers) is modelled as a separate but related mortality source.

The fundamental assumption of the angler mortality formulation is that the risk to an individual fish of being hooked by anglers is a function of fishing pressure and not directly a function of trout abundance. The model also assumes that an individual trout can be caught more than once in a day. We assume that the trout are not aware of angling mortality risk and how it varies with habitat, and therefore we do not include angling among the risks that trout consider when selecting their habitat.

The angler model is executed as follows:

1. The **daily capture rate** is calculated from the fishing pressure and the trout's length.

**Fishing pressure** (variable *anglerPressure*) is evaluated as angler hours per day per km of stream. **Capture rate** is represented as the average number of times a fish is hooked per day. This capture rate is assumed to be a linear function of fishing pressure, with the proportionality constant being the parameter *mortFishAngleSuccess*. This parameter represents fishing success as the fraction of catchable fish hooked per angler hour. Capture rate is also assumed to be a logistic function of trout size. The capture probability model is:

(45)

*captureRate* (trout caught per trout catchable per day) = *mortFishAngleSuccess* [trout caught per trout catchable per angler-hr] × *anglePressure* [angler-hr $km^{-1}$ $day^{-1}$] × *reachLength* [cm] × $10^{-5}$ [km $cm^{-1}$] × logistic(*fishLength*)

where the logistic function of fish length is defined by two trout parameters *mortFishAngleL1* and *mortFishAngleL9*.

2. The **number of times a trout is hooked** during a time-step (variable *timesHooked*) is drawn from a Poisson distribution parameterized with the capture rate (average captures per day) and time step size (number of days defined by *timestep-scale* parameter). If *timesHooked* is zero, the survival probability is 1.0 for angling and hooking mortality.

3. If *timesHooked* is one or more, the model first determines whether it is **legal to keep the trout** according to a "slot limit": it is legal to keep trout that have length greater than the value of the parameter *mortFishAngleSlotLower* (cm) or less than the value of *mortFishAngleSlotUpper* (cm).

4. The following steps are conducted once for each time the trout is hooked.

5. If the trout is of legal size to keep, a random draw is applied to the parameter *mortFishAngleFracKeptLegal* to **determine whether the trout is kept**. If the trout is not of legal size, a random draw and the parameter *mortFishAngleFracKeptIllegal* determine whether the trout is kept. If the trout is kept, the survival probability is 0.0. Hooked fish that are kept by anglers are considered dead by a mortality source called "angling". Fish that die of angling mortality are not subject to hooking mortality.

6. If **the trout is released** (not kept), the survival probability for angling is 1.0, but the fish is then subject to the hooking mortality source. The probability of surviving hooking mortality is defined by the parameter *mortFishAngleHookSurvRate*. Trout that do not survive are considered dead by the mortality source called "hooking".

*2.7.6. Redd Survival*:

Eggs incubating in a redd are subject to five mortality sources: low and high temperatures, scouring by high flows, dewatering, and superimposition (having another redd laid on top of an existing one). Redd survival is modeled using redd "survival functions", which determine, for each redd on each day, the probability of each egg surviving one particular kind of mortality. Then, a random draw is made on a binomial distribution to determine how many eggs survive each redd mortality source. The binomial distribution returns a randomly drawn number of eggs that die each day, given the number of live eggs in the redd and the per-egg

mortality probability (one minus the survival function value). (The alternative approach of multiplying the mortality probability by the number of live eggs introduces a number of numerical difficulties when the number of live eggs is small.) The number of eggs dying over the whole time step is calculated as the number of eggs that die each day multiplied by the parameter *timestep-scale* (it only applies to low and high temperature as well as dewatering mortality sources, since superimposition mortality only occurs once per time step and scouring results in mortality of all eggs in the redd).

The separate redd mortality sources are executed sequentially: the eggs killed by one source are subtracted from the number alive before the next source is processed. The order in which redd survival functions are evaluated is as follows:

2.7.6.1. Low temperature:

The daily fraction of eggs surviving low temperatures is modeled as an increasing logistic function of temperature.

2.7.6.2. High temperature:

The fraction of eggs surviving high temperatures is modeled as a decreasing logistic function of temperature.

2.7.6.3. Scouring and deposition:

Scouring and deposition mortality results from high flows disturbing the gravel containing a redd. The model assumes that the probability of a redd being destroyed is equal to the proportion of the stream reach scouring or filling to depths greater than the value of the fish parameter *mortReddScourDepth* (cm). Consequently, the probability of a redd not being destroyed (*scourSurvival*) is equal to the proportion of the stream scouring or filling to a depth less than the value of *mortReddScourDepth*. This scour survival probability is estimated from the exponential distribution model of Haschenburger (1999); the proportion of the stream scouring to less than a given depth is the integral of the exponential distribution between zero and the depth:

$$scourSurvival = 1 - e^{-(scourParam \times mortReddScourDepth)} \quad (46)$$

The value of *scourSurvival* is set to 1.0 if (*scourParam* × *mortReddScourDepth*) is greater than 100. The value of *scourParam* was modeled by Haschenburger (1999) empirically:

$$scourParam = 3.33 \times e^{-1.52\ (shearStress\ /\ 0.045)} \quad (47)$$

where *shearStress* is the peak Shields stress (measured at a reach scale) occurring during the high-flow event. Shields stress is a dimensionless indicator of scour potential often used in modeling sediment transport, described in the sediment transport literature. Shields stress increases with flow, a relationship represented in the model by the equation:

$$shearStress = habShearParamA \times (flow)^{habShearParamB} \quad (48)$$

where *habShearParamA* (s $m^{-3}$) and *habShearParamB* (unitless) are habitat reach parameters. Since *scourSurvival* is 1.0 when (*scourParam* × *mortReddScourDepth*) is greater than 100, this allows users to effectively turn scouring and deposition mortality off by using a very large value of *mortReddScourDepth*, e.g., 10,000 cm.

2.7.6.4. Dewatering:

Dewatering mortality occurs when flow decreases until a redd is no longer submerged. The dewatering survival function is simply that if depth is zero then the daily fraction of eggs surviving is equal to the fish parameter *mortReddDewaterSurv*.

2.7.6.5. Superimposition:

Superimposition redd mortality can occur when a new redd is laid over an existing one. Importantly, superimposition only occurs when the redds are laid in gravel. Otherwise, it is assumed that they cannot be disturbed by another spawner. Therefore, in the event that *cellFracGravel* is zero, there is no risk of superimposition. Otherwise, superimposition redd mortality is modelled as a function of the area disturbed in creating the new redd and the area of spawning gravel available. The following steps are used for each redd, for each time step:

1. Determining if one or more new redds were created in the same cell on the current time step. If not, then superimposition survival is 1.0.

2. If one or more redds were created in the same cell, the probability of each new redd causing superimposition (*reddSuperImpRisk*, unitless) is equal to the area of a redd (*reddSize*, $cm^2$) divided by the area of spawning gravel in the redd.

$$reddSuperImpRisk = reddSize / (cellArea \times cellFracGravel) \quad (49)$$

3. A random number is drawn from a uniform distribution between zero and one; if it is less than *reddSuperImpRisk*, then superimposition mortality occurs.

4. If superimposition mortality occurs, then the fraction of eggs surviving is the value of another random number drawn from a uniform distribution between zero and one.

5. Steps 2-4 are executed once for each new redd placed in the cell on the current time-step.

*2.7.7. Redd Development*:

To predict the timing of emergence, the developmental status of a redd's eggs is updated daily. We used the fractional development approach of Van Winkle et al. (1996) which is based on accumulated degree-days. Model redds accumulate the fractional development that occurs each day (*reddDailyDevel*), a function of temperature. This means the redd has a state variable *fracDeveloped* that starts at zero when the redd is created and is increased each day by the value of *reddDailyDevel*. When *fracDeveloped* reaches 1.0, then the eggs are ready to emerge. The daily value of *reddDailyDevel* is determined using this second-order polynomial equation:

$$reddDailyDevel = reddDevelParamA + (reddDevelParamB \times temp) + (reddDevelParamC \times temp^2) \quad (50)$$

The fractional development that occurs over the whole time step is then calculated as the daily development multiplied by the parameter *timestep-scale*.

*2.7.8. Emergence from the redds and Transmission of traits*:

2.7.8.1. Emergence:

"Emergence" is the conversion of each surviving egg into a new trout agent. Emergence begins on the day when *fracDeveloped* reaches 1.0, and then the new fish emerge over a period of several days. As a simple way to spread emergence over several days, the emergence model assumes that 10% of the redd's eggs emerge on the first day of emergence; 20% of the redd's remaining eggs emerge on the next day; 30% of the remaining eggs emerge on the third day; etc, until 100% of remaining eggs emerge. The time at which all eggs have emerged depends on the time step defined by the user through the parameter *timestep-scale*. As emergence proceeds, the eggs remaining in a redd remain susceptible to egg mortality.

2.7.8.2. Transmission of heritable traits:

For modelling the transmission of heritable traits, we followed the approach of Vincenzi et al. (2012). Only length at emergence and the size threshold value for maturation are considered genetically coded and heritable. We additionally included a neutral trait (not affecting the fitness of individuals) to assess whether potential changes along time in the genotypic values of heritable traits are actually due to directional selection and not by genetic drift. We assume that each egg is fertilized by just one male spawner. Therefore, each new trout emerging from the redd inherits its traits from a father randomly assigned from the *number-males* males contributing to the redd (see Section 2.7.2.2).

As commonly modelled (Lynch and Walsh 1998), the phenotype z of an individual *i*, $z_i$, is defined in our model as the sum of its genotypic (also called breeding) value $a_i$ (representing additive genetic variance) randomly drawn from a normal distribution N($\mu_G$, $\sigma_G^2$), and a statistically independent random environmental effect from N($\mu_E$, $\sigma_E^2$):

$$z_i = a_i + e_i \quad (51)$$

where the narrow-sense heritability $h^2 = \sigma_G^2 / \sigma_Z^2$ indicates how much of the phenotypic variance $\sigma_Z^2$ present in the population is explained by the additive genetic variance $\sigma_G^2$.

In our model, a genotypic value *genTraitZ* of the heritable traits is set at initialization of the individuals following a normal distribution around the mean phenotypic value at the population level (*fishTraitZMean*; input parameter) and with an additive genetic variance computed as:

$$additivevarTraitZ = h^2_{TraitZ} \times fishTraitZVar \quad (52)$$

where *fishTraitZVar* is the phenotypic variance of the trait at the population level and $h^2_{TraitZ}$ is the narrow-sense heritability of the trait. Both *fishTraitZVar* and $h^2_{TraitZ}$ are input parameters to the model.

The phenotypic expression of the trait (*fishTraitZ*) for each individual at initialization is then calculated as *genTraitZ* plus the environmental effect drawn from a normal distribution with mean 0 and an environmental variance $\sigma_E^2$ equal to (1 - $h^2_{TraitZ}$) × *fishTraitZVar*. The environmental variance is maintained constant along the whole simulation.

Inheritance rules are based on the infinitesimal model of quantitative genetics theory. Each offspring's *genTraitZ* value for a trait *z* under selection is drawn from a normal distribution centered on the arithmetic mean of the two parental values, while the variance of this distribution is equal to half the total additive genetic variance for the trait at the population level (i.e., the within-family additive variance remains constant).

In an idealized population with no input of new variation from mutation or migration, the additive variance generated from the initial variation in the base population eventually declines. Ultimately, a selection limit or plateau is reached, and as the genetic variation in the base population becomes exhausted, the effects of new mutations become increasingly important for continued response (Johnson and Barton 2005). In our model, the user has the option to choose whether the total additive genetic variance fixed at initialization remains constant across generations or it changes otherwise, being then computed as the variance of the breeding genotypic values. The inheritance model is a modified version of the inheritance model of the infinitesimal model of quantitative genetics theory, adapted to account for new input of variation from mutation. Offspring then inherit the trait *genTraitZ* from a normal distribution centered on the arithmetic mean of the two parental values and with the variance

$\sigma^2_{G,off}$ of the distribution equal to half the mean of population additive genetic variance (*additivevarTraitZ*) plus the mutational variance $\sigma^2_m$ multiplied by a factor *M* defining the amplitude of mutation:

$$\sigma^2_{G,off} = \frac{1}{2}(additivevarTraitZ + M\sigma^2_m) \quad (53)$$

In our model, the mutational variance $\sigma^2_m$ (variance introduced by mutation per generation) at the population level is computed as (*mutationalVarParam* × $\sigma^2_E$), where *mutationalVarParam* is in the order of $10^{-3}$ to $10^{-2}$, as suggested by reviews of empirical data (Lynch and Walsh 1998, Johnson and Barton 2005). Variation from mutation can be turned off by the user by setting the amplitude of mutation factor *M* to 0.

The environmental $e_i$ component of the trait is drawn from a normal distribution of mean 0 and variance equal to the environmental variance $\sigma^2_E$ fixed at initialization. Offspring phenotypes are then formulated as $fishTraitZ = genTraitZ + e_i$.

The model allows the possibility of defining different maturation thresholds for males and females. Therefore, the way this trait is transmitted is slightly different from the other two heritable traits. We used a standard transformation for this purpose. The parental genotypic values of the trait are standard transformed as follows:

(54)

$$StdParentgenSpawnMinLength = \frac{ParentgenSpawnMinLength - SexPopMeangenSpawnMinLength}{\sqrt{\frac{1}{2}(additivevarSpawnMinLength + M\sigma^2_m)}},$$

where *StdParentgenSpawnMinLength* is the standard transformed of the genotypic value of either the father or the mother (*ParentgenSpawnMinLength*), *SexPopMeanSpawnMinLength* is the mean genotypic value of either males or females at the population level (depending on the sex of the new trout and equal to *SpawnMinLengthMean* if additive variance is fixed across generations or computed as the mean genotypic value of either male or female breeder population otherwise), *additivevarSpawnMinLength* is the additive genetic variance for the trait and $M\sigma^2_m$ represents the mutational variance. The two parental standardized values are then averaged (*stdMean*) and a random number (*randStd*) is drawn from a normal distribution N(*stdMean*, 1). Finally, the genotypic value of the maturity threshold for the new trout is calculated by transforming back as follows:

*genSpawnMinLength* = *SexPopMeanSpawnMinLength*
(55)

$$+ randStd \times \sqrt{\frac{1}{2}(additivevarSpawnMinLength + M\sigma^2_m)}$$

Both the genotypic value and the environmental component of the heritable traits are truncated at 4 standard deviations from the centers of the normal distributions from which they are drawn.

*2.7.9. Trout Ageing*:

Trout update every time step their state variable *age*, which track the number of days since a trout was born. Trout update their *age-class* state variable the Julian date where they were

born. When new trout are born, then all trout from the older cohorts update their age-class to avoid that some fish could have the same age-class while belonging to different cohorts. The same action happens likewise when the first fish of older cohorts updates its age-class and new recruits have not been born yet.

# 3 Data evaluation

**This TRACE element provides supporting information on**: The quality and sources of numerical and qualitative data used to parameterize the model, both directly and inversely via calibration, and of the observed patterns that were used to design the overall model structure. This critical evaluation will allow model users to assess the scope and the uncertainty of the data and knowledge on which the model is based.

**Summary:**

**There are a total of 203 global parameters in inSTREAM-Gen. Thirty-four of them are user-specified parameters by which the user sets the spatio-temporal resolution of the simulations, selects among different options regarding the mortality and genetic models, and chooses the desired graphical and file outputs. There are 47 site-specific parameters; although the values of 20 of them could be potentially borrowed from existing studies in the case they are not available for the simulated population. T33here are 114 parameters whose values are typically derived from the literature. Finally, there are six parameters that are specially suited for calibration since they are pretty uncertain and model results are highly sensitive to them. They were calibrated following a pattern-oriented modelling approach, using site-specific quantitative demographic and life-history patterns.**

Section content



In inSTREAM-Gen there are a grand total of 203 global parameters. In outline, they can be grouped in four main categories based on their nature and data source: 1) user-specified, 2) site-specific, 3) values borrowed from the literature, and 4) calibrated.

## 3.1. User-specified parameters

Sixteen out of the 203 global parameters are related to the observer actions, and represent the choices the user has to make to obtain the desired graphical and file outputs from the model. Those parameters are therefore only involved in the *plot-modelOutputs* and *write-modelOutputs* procedures. There are 15 Boolean parameters which allow the user to select the mortality models for trout agents to be deployed in the *move* and *survive-or-die* procedures during the simulation. There are five additional parameters that are user-specified too: the *spatial-scale* and *timestep-scale* parameters define the spatial (the width of a NetLogo patch) and temporal (the extent of a time step) resolution of the model during the simulation; *initial-date* sets the date when the simulation starts (it is necessary to specify this parameter in order to create the LogoTime object that will link the current date of each time step to the native time tracking mechanism in NetLogo); with the *GeneticTransmission?* Boolean parameter,

the user indicates whether genetic transmission of heritable traits must be simulated during the model's run, while *FixedAdditiveVar?* permits the user to choose whether the total additive genetic variance of heritable traits fixed at initialization must be considered constant across generations or must be otherwise computed each generation as the variance of the breeding genotypic values.

### 3.2. Site-specific parameters

There are 27 parameters that are inherently site-specific and whose values cannot be borrowed from the literature. *siteLatitude* and *reachLength* are geographic and physical attributes of the simulated reach. There are 20 parameters used to define the abundance, as well as the age- and size-structure of the population at initialization. Five parameters involved in the angler mortality model are site-specific since they characterize the legal restrictions to recreational fishing in the simulated reach: *startAnglingSeason*, *endAnglingSeason*, *anglePressure*, *mortFishAngleSlotLower* and *mortFishAngleSlotUpper*.

In addition, there are 20 population parameters which are highly site-specific, but although their values are typically obtained from on-site field studies, they can be also borrowed from the literature in the case they are not available for the simulated population. Most of them are involved in the reproduction process, being either connected to the size maturity threshold (*fishSpawnMinLengthMeanM*, *fishSpawnMinLengthMeanF*, *fishSpawnMinLengthVarM*, *fishSpawnMinLengthVarF*) and the other criteria mature trout must meet to spawn (*habMaxSpawnFlow*, *fishSpawnMinAge*), to define the time window for spawning (*fishSpawnStartDate*, *fishSpawnEndDate*), or related to the fecundity relationship (*fishFecundParamA*, *fishFecundParamB*). The parameters describing the central tendency and dispersion of phenotypic values of heritable traits (*fishNewLengthMean*, *fishNewLengthVar*, *fishNeutralTraitMean*, *fishNeutralTraitVar*) as well as those defining the weight-length relationship (*fishWeightParamA*, *fishWeightParamB*) are typically highly variable across populations. Prey energy density (*habPreyEnergyDensity*) depends on the kind of prey dominating the system's trophic web, so it is variable across sites. Likewise, the size at which trout can predate on smaller trout (*fishPiscivoryLength*) is site-specific. Finally, it is important to notice that the habitat parameters *habShearParamA* and *habShearParamB* included in the equation to calculate the Shield stress (indicator of the flow scour potential, which affects redds survival), are highly reach specific.

For the case study presented in Ayllón et al. (2015), which simulates brown trout (*Salmo trutta*) population dynamics in the Belagua river (Northern Spain), we used the site-specific parameter values shown in Table A2. They were derived from a comprehensive four-year research project carried out during 2003-2006 and funded by the Government of Navarra. In the study, 58 sampling sites were monitored, sites being selected to cover both environmental and human disturbance gradients. Based on long-term time series (12 years) of ecological data previously collected by the staff of the Government of Navarra, and new ecological and environmental data collected during the study, stream-dwelling brown trout populations were fully characterized, including spatio-temporal patterns of: 1) population dynamics (abundance, biomass and production, as well as recruitment and mortality rates); 2) life history strategies (size-at-age, growth rates, reproductive traits); 3) carrying capacity dynamics; 4) habitat selection and territorial behavior; 5) inter- and intra-population genetic variability and levels of genetic introgression; 6) incidence of recreational fishing and other human drivers and stressors; 7) ecological and genetic conservation status of populations. Complete results from this study are reported in Almodóvar et al. (2006), though the main

results have been published in peer reviewed journals, providing insights within a wide range of topics, including spatial and temporal patterns of population abundance (Ayllón et al. 2013), carrying capacity dynamics (Ayllón et al. 2012a), individual growth (Parra et al. 2010, 2011, 2012) and other life history traits (Parra et al. 2014), habitat selection (Ayllón et al. 2009, 2010a) and territorial behavior (Ayllón et al. 2010b), as well as analyses of the effects of global warming (Almodóvar et al. 2012) and other anthropogenic drivers and stressors (Ayllón et al. 2012b) on the conservation status of these resident brown trout populations.

**Table A2.** Example values for site-specific parameters, indicating the data source (* Almodóvar et al. 2006; ** Parra et al. 2014).

| Parameter | Definition (units) | Value |
|---|---|---|
| **Initial population** | | |
| *init-N* | Initial number of fish in the simulation | 696* |
| *prop-Age0* | Proportion of age-0 fish within the population | 0.73* |
| *prop-Age1* | Proportion of age-1 fish within the population | 0.19* |
| *prop-Age2* | Proportion of age-2 fish within the population | 0.06* |
| *prop-Age3* | Proportion of age-3 fish within the population | 0.008* |
| *prop-Age4* | Proportion of age-4 fish within the population | 0.009* |
| *prop-Age5Plus* | Proportion of age-5 and older fish within the population | 0.003* |
| *fishLengthMeanAge0* | Mean length of age-0 fish (cm) | 6.5* |
| *fishLengthSdAge0* | Standard deviation of age-0 fish length (cm) | 0.7* |
| *fishLengthMeanAge1* | Mean length of age-1 fish (cm) | 13.4* |
| *fishLengthSdAge1* | Standard deviation of age-1 fish length (cm) | 1.2* |
| *fishLengthMeanAge2* | Mean length of age-2 fish (cm) | 17.1 |
| *fishLengthSdAge2* | Standard deviation of age-2 fish length (cm) | 1.2* |
| *fishLengthMeanAge3* | Mean length of age-3 fish (cm) | 22.5* |
| *fishLengthSdAge3* | Standard deviation of age-3 fish length (cm) | 1.4* |
| *fishLengthMeanAge4* | Mean length of age-4 fish (cm) | 27.5* |
| *fishLengthSdAge4* | Standard deviation of age-4 fish length (cm) | 1.7* |
| *fishLengthMeanAge5Plus* | Mean length of age-5 and older fish (cm) | 36.5* |
| *fishLengthSdAge5Plus* | Standard deviation of age-5 and older fish length (cm) | 1.6* |
| *fishEmergenceDateMean* | Population mean date of emergence (Julian date) | 91* |
| **Reproduction** | | |
| *fishSpawnStartDate*, | Starting date of the spawning window (Julian date) | 305* |
| *fishSpawnEndDate* | Ending date of the spawning window (Julian date) | 366* |
| *fishSpawnMinAge* | Minimum age to spawn (days) | 366** |
| *fishFecundParamA* | Multiplier of the female length-number of eggs | 0.038* |

| | | |
|---|---|---|
| | relationship (eggs per redd) | |
| *fishFecundParamB* | Exponent of the female length-number of eggs relationship (unitless) | 3.01* |
| **Feeding and growth** | | |
| *fishWeightParamA* | Multiplier of the weight-length relationship for healthy fish (g $cm^{-1}$) | 0.01057* |
| *fishWeightParamB* | Exponent of the weight-length relationship for healthy fish (unitless) | 3.021* |
| **Angler mortality** | | |
| *startAnglingSeason* | Start of the angling season (Julian date) | 94* |
| *endAnglingSeason* | End of the angling season (Julian date) | 276* |
| *anglePressure* | Angling pressure (angler-h $km^{-1}$ $d^{-1}$) | 0.22* |
| *mortFishAngleSlotLower* | Lower end of the length range in which fish are legal to keep (cm) | 21* |
| *mortFishAngleSlotUpper* | Upper end of the length range in which fish are legal to keep (cm) | 100* |
| **Genetic transmission** | | |
| *fishSpawnMinLengthMeanM* | Population mean length maturity threshold for males (cm) | 16.7** |
| *fishSpawnMinLengthVarM* | Population variance of length maturity threshold for males (unitless) | 1.5** |
| *fishSpawnMinLengthMeanF* | Population mean length maturity threshold for females (cm) | 16.7** |
| *fishSpawnMinLengthVarF* | Population variance of length maturity threshold for females (unitless) | 1.5** |
| *fishNewLengthMean* | Population mean of length at emergence (cm) | 2.3* |
| *fishNewLengthVar* | Population variance of length at emergence (unitless) | 0.023* |
| *fishNeutralTraitMean* | Population mean value of neutral trait | 0.7* |
| *fishNeutralTraitVar* | Population variance of neutral trait | 0.05* |

Since we did not have an estimate of the value of the flow limit for spawning (***habMaxSpawnFlow***) in our study population, we estimated it by using the scarce available data in the literature. Frank and Baret (2013) described a mean centered value of 6.85 $m^3$ $s^{-1}$ for a log-normal distribution for a brown trout population in Belgium. However, the rivers described in Frank and Baret's study are of a larger size than the model stream used in our study. Ayllón et al. (2012a) found a significant negative relationship between extreme flow conditions at different times of the hydrologic cycle (including extreme flow events during spawning period) and the summer density/carrying capacity ratio of age-0 trout in the rivers and streams of our study area. Using the statistical models presented by Ayllón and coauthors, we estimated that a weighted maximum flow during seven consecutive days of 16.75 over the

spawning season (that is, a flow 16.75 times higher than the historical median flow, maintained during 7 consecutive days) would cause zero recruitment next year (when the values of the rest of significant covariates are fixed to their average value). Using flow time series statistical analyses to correlate different time spans, we estimated that a weighted maximum flow during the whole spawning season (60 days) of 5.95 would cause zero recruitment next year. That value translates into an absolute flow value of 3.98 $m^3$ $s^{-1}$. However, Gortázar et al. (2007) observed that brown trout spawning activity did not completely cease during strong spates (flows ca. 4 $m^3$ $s^{-1}$) in highly unpredictable Iberian mountain streams with conditions similar to ours. Therefore, we decided to set a value of 4.5 $m^3$ $s^{-1}$ for *habMaxSpawnFlow*.

The value of prey energy density (the habitat parameter ***habPreyEnergyDensity***, j $g^{-1}$) can be derived from the literature too. This parameter is used to convert grams of prey eaten to joules of energy intake and it applies to both drift and search food. Values of *habPreyEnergyDensity* are provided for various prey types by Hanson et al. (1997). A value of 2500 j $g^{-1}$ is reasonable for streams where drift prey is dominated by aquatic insect larvae; a value of 4000 j $g^{-1}$ is appropriate for streams where drift is dominated by higher-energy prey such as amphipods. Values can be higher when diet is only comprised by high-energy prey. Since we did not have these data for our study site, we chose to calibrate this parameter.

There were no available data about the size at which trout can predate on smaller trout (***fishPiscivoryLength***) in our study population. Therefore, the value for the parameter was derived from the existing literature. In freshwaters, brown trout may start fish feeding from a body length of 15cm (Klemetsen et al. 2003). In general, considering observed predator-prey size ratios for salmonids (collected and reviewed by Keeley and Grant 2001), values in the range of 15-30 cm are reasonable for *fishPiscivoryLength*. However, salmonids begin to feed on fish at a smaller size in oceans and in lakes than in streams; on average salmonids in streams only begin eating fish when 27 cm long (Keeley and Grant 2001). In fact, piscivorous behaviour is most frequent in large stream-dwelling brown trout, and studies show that it occurs in older individuals with a size of 20-30 cm, but rarely in smaller size classes (e.g, Jensen et al. 2004, Sánchez-Hernández and Cobo 2012). For Little Jones Creek, Railsback et al. (2009) set the value of *fishPiscivoryLength* to 15 cm because cutthroat trout (*Oncorhynchus clarkii*) rarely grow much larger than this size there and appear to eat only very small trout. For our study population, we set *fishPiscivoryLength* to the average length age-2 individuals attain during summer, 17 cm.

The parameters *habShearParamA* and *habShearParamB* can be evaluated by means of an equation commonly used to estimate Shields stress in rivers:

$$shearStress = \frac{\rho \cdot R \cdot S}{(\rho_s - \rho)D}$$

where $\rho$ is the density of water (1.0 g $cm^{-3}$); *R* is the reach-average hydraulic radius (cm); *S* is the reach-scale energy slope (dimensionless); $\rho s$ is the density of sediment, approximated as 2.7 g $cm^{-3}$; and *D* is the mean substrate particle diameter (cm). The hydraulic radius *R* can be approximated as the average depth and *S* can be approximated as the average water surface slope, using data collected for hydraulic model calibration at several different flows. Then logarithmic regression of *shearStress* vs. flow produces the values of *habShearParamA* and *habShearParamB*. Following this procedure, we estimated for our study reach values for the shear stress parameters of *habShearParamA* = 0.006 and *habShearParamB* = 0.683 ($p<0.0001$, $R^2=0.9992$).

### 3.3. Parameters with values borrowed from the literature

There are 114 parameters in inSTREAM-Gen whose values are not reach- or population-specific so that they can be derived from the literature. They are described below grouped by the processes they are involved in.

- *Trout reproduction*:

Railsback et al. (2009) considered a value of 0.04 reasonable for ***fishSpawnProb*** (probability of spawning on any such day). This value causes an average of 25% of ready fish to spawn in the first week of suitable conditions and 68% to spawn within 28 days of suitable conditions. It must be taken into account that if the inverse of *fishSpawnProb* is large compared to the number of days in the spawning period, then it is likely that some potential spawners will not spawn. We selected however a higher value (0.1) for the present case study.

Regarding the criteria mature trout must meet to be ready to spawn, Railsback et al. (2009) recommended that the value of ***fishSpawnMinCond*** (minimum condition factor to spawn) should be slightly less than 1.0 (typical applications of inSTREAM use a value of 0.98). Van Winkle et al. (1996) and Railsback and Harvey (2001) estimated 0.20 as a reasonable value for ***fishSpawnMaxFlowChange***. Finally, Van Winkle et al. (1996) estimated that spawning can only occur when water temperature falls within a range of 4 (***fishSpawnMinTemp***) and 10ºC (***fishSpawnMaxTemp***) for brown trout or 8-13ºC for rainbow trout (*Oncorhynchus mykiss*). This agrees with the common belief that spawning activity of brown trout ceases when temperature falls below 5 ºC (Jonsson and Jonsson 2011). For the present application of inSTREAM-Gen, we chose a value of 12 ºC for *fishSpawnMaxTemp* because of potential thermal adaptations to higher temperatures at Southern latitudes.

The suitability of the hydraulic conditions of a cell for a female spawner to create a redd is evaluated in inSTREAM-Gen by means of **spawning suitability functions**. Typical applications of inSTREAM use the functions developed by PG&E (1994) for brown trout and rainbow trout (Table A3). However, there are other spawning suitability functions available in the literature for brown trout (e.g., Raleigh et al. 1986, Grost et al. 1990, Louhi et al. 2008, Gortázar et al. 2012).

**Table A3.** Parameter values for spawning depth and velocity suitability for brown trout (from PG&E 1994).

| Parameter | Parameter value | Parameter | Suitability value |
|---|---|---|---|
| | Depth (cm) | | (unitless) |
| *fishSpawnDSuitD1* | 0 | *fishSpawnDSuitS1* | 0 |
| *fishSpawnDSuitD2* | 5 | *fishSpawnDSuitS2* | 0 |
| *fishSpawnDSuitD3* | 50 | *fishSpawnDSuitS3* | 1 |
| *fishSpawnDSuitD4* | 100 | *fishSpawnDSuitS4* | 1 |
| *fishSpawnDSuitD5* | 1000 | *fishSpawnDSuitS5* | 0 |
| | Velocity (cm $s^{-1}$) | | |
| *fishSpawnVSuitV1* | 0 | *fishSpawnVSuitS1* | 0 |
| *fishSpawnVSuitV2* | 10 | *fishSpawnVSuitS2* | 0 |
| *fishSpawnVSuitV3* | 20 | *fishSpawnVSuitS3* | 1 |

| | | | |
|---|---|---|---|
| *fishSpawnVSuitV4* | 75 | *fishSpawnVSuitS4* | 1 |
| *fishSpawnVSuitV5* | 100 | *fishSpawnVSuitS5* | 0 |
| *fishSpawnVSuitV6* | 1000 | *fishSpawnVSuitS6* | 0 |

After selecting a spawning cell, female spawners create redds. The number of eggs in the redd depends on the spawner's fecundity (a function of length) and losses during spawning (defined through the parameter ***fishSpawnEggViability***). There is little published literature to support consistent values of *fishSpawnEggViability* for stream salmonids. Despite the fact that the number of viable eggs in a redd can be considerably less than the female's fecundity if some eggs are washed away by high current velocities, incompletely buried, eaten by other fish during redd creation, or if some are not fertilized, some studies evidence that in general losses are low (e.g., Healy 1991). Based on these grounds, Railsback et al. (2009) recommended a value of 0.2.

When a female spawns, male spawners are selected to fertilize the eggs in the redd. The maximum number of males that can be involved in the mating is set through the parameter ***max-n-males-per-female***. While in inSTREAM only one male is selected to mate with a female spawner, inSTREAM-Gen allows for both monogamy and polygamy mating strategies. This is because both monogamous and polygamous matings have been observed in brown trout breeding systems (e.g., Serbezov et al. 2010a). Further, Frank and Baret (2013) found that when they included in their *DemGenTrout* IBM a polygamous mating mode (with a *max-n-males-per-female* equal to 4), it yielded better fit to observed demographic and genetic brown trout population patterns than the alternative model implementing monogamy.

After spawning, both female and male spawners incur on mass loss. In consequence, their weight is reduced according to the parameter ***fishSpawnWtLossFraction***. Mean mass losses from spawning for brown trout can be up to 22% in females and 15% in males (Lien 1978). It suggests a value of 0.2 for *fishSpawnWtLossFraction*. However, higher values could be justified as proportional energy loss substantially exceeds mass loss (Lien 1978). Railsback et al. (2009) estimated that a 20% loss of body weight during spawning reduces the probability of surviving starvation and disease for 90 days by about 10 to 15%, while a 30% weight loss reduces survival by about 40%. The authors found these values similar to the spawning survival ranges suggested by Stearley (1992) for resident trout.

- *Trout habitat selection*:

During habitat selection (*move* procedure), every trout assess each potential destination cell to determine the fitness it would provide, using the "Expected Reproductive Maturity" (ERM) fitness measure of Railsback et al. (1999). ERM depends on three elements: *nonstarvSurvival* (probability of survival for all mortality sources except poor condition over a specified time horizon), *starvSurvival* (probability of surviving the risk of poor condition over the specified fitness time horizon), and *fracMature* (how close to the size of sexual maturity a trout would be at the end of the fitness time horizon). Therefore, it is clear this action includes nearly all parameters involved in the feeding and growth, and survival processes (*feed-and-grow* and *survive-or-die* procedures, respectively). Those will be treated separately, however.

There are only three parameters that are not involved in either feeding or survival procedures. Two of them are the parameters included in the exponential function used to quantify the maximum movement distance within which fish evaluate the ERM of cells (this local variable is also used in the reproduction process to define the potential cells which female spawners can spawn in). This maximum movement distance should be considered the distance over which a fish is likely to be aware of habitat conditions over a daily time step, and not the

maximum distance a fish could swim or migrate in a day. It is an exponential function of fish length. Based on literature data (June 1981, Harvey et al. 1999, Diana et al. 2004), Railsback et al. (2009) estimated a value of 20 for ***fishMoveDistParamA*** and of 2 for ***fishMoveDistParamB*** for stream-dwelling trout. However, these parameters can be potentially site-specific.

The other one is the time horizon parameter ***fishFitnessHorizon***, used in the expected maturity fitness measure equation, which represents the time horizon over which fish evaluate the tradeoffs between food intake and mortality risks to maximize their probability of surviving and reproducing. It is an important parameter and, as such, its theoretical foundations and implications of its value are discussed in detail in Railsback et al. (2009). As a general rule, longer time horizons better reflect how an individual's fitness depends on how well it makes decisions throughout its reproductive life, while smaller values of *fishFitnessHorizon* place less emphasis on feeding and avoiding starvation in habitat selection. Railsback et al. (2009) observed that values of *fishFitnessHorizon* of 5 to 10 days cause ERM to vary almost exclusively with *nonstarvation* survival (mortality risks other than starvation), meanwhile values in the range of 100 days cause ERM to depend almost exclusively on growth rates when growth is less than the minimum needed to maintain a condition factor of 1.0. If according to literature, fish are able to anticipate seasonal changes in habitat conditions and their life stage, it makes sense to assume they use a habitat selection time horizon of several months. Consequently, most applications of inSTREAM to date have used a value of 90 days.

- *Trout feeding and growth*:

A fish's drift intake rate is calculated as the mass of prey passing through the capture area times the capture success. Capture area is dependent on the detection distance. In InSTREAM-Gen, **detection distance** depends linearly on the size of the fish (parameter values in Table A4). This linear formulation contrasts to the exponential formulation of Hughes and Dill (1990), which has been used in different bioenergetics models (for e.g., Rosenfeld and Taylor 2009, Jenkins and Keeley 2010). Railsback et al. (2009) developed this linear model based on empirical data from the study of Schmidt and O'Brien (1982) for arctic grayling (*Thymallus arcticus*), whose results had been used successfully as the basis of the previous drift feeding models of Hughes (1992) and Hughes et al. (2003). The linear model is not, however, a regression fit to those data, but rather it was derived from pre-calibration of the growth model. In fact, a logarithmic model provided a better fit to the data, but the linear model, nevertheless, was able to capture a series of qualitative patterns the logarithmic formulation was not. First, it captures the fact that very small trout cannot use as wide a range of prey sizes as larger trout can, a process not otherwise represented in the feeding model of inSTREAM and inSTREAM-Gen. Second, a logarithmic fit to these data predicts negative detection distances for trout lengths less than 2 cm and does not reproduce the observations of Hughes et al. (2003) that detection distance continues to increase to over 100 cm for very large trout. Finally, the pre-calibration analysis indicated that the growth rates of very small trout are very sensitive to the intercept. An intercept of 4.0 was found to provide growth of very small trout that was realistic at the same drift food availability values that produce realistic growth rates in larger trout.

**Capture success** is largely a function of water velocity and the swimming capacity of the fish. In consequence, Railsback and colleagues developed a logistic function of the ratio of water velocity to maximum sustainable swimming speed of the fish based on observations from Hill and Grossman (1993) for rainbow trout to estimate capture success (parameter

values in Table 4). Maximum sustainable swimming speed (***fishMaxSwimSpeed***) is a function of fish length and water temperature. Because inSTREAM-Gen uses time steps of at least one day, the maximum sustainable swimming must be a speed that fish can swim for hours, not a burst or short-term maximum speed. Railsback et al. (2009) used literature values from "critical swimming speed" laboratory tests for different species of salmonids (Schneider and Connors 1982, Butler et al. 1992, Hawkins and Quinn 1996, Taylor et al. 1996, Alsop and Wood 1997, Myrick and Cech 2000, 2003, MacNutt et al. 2004) to develop a two-term function for modelling *fishMaxSwimSpeed*. The first term represents how *fishMaxSwimSpeed* varies linearly with fish length, while the second modifies *fishMaxSwimSpeed* with temperature, following a second-order polynomial function (parameter values in Table A4).

**Table A4.** Parameter values for detection distance, capture success and maximum sustainable swimming speed (from Railsback et al. 2009).

| Parameter | Definition (units) | Value |
|---|---|---|
| *fishDetectDistParamA* | Intercept in equation for detection distance (cm) | 4 |
| *fishDetectDistParamB* | Slope in equation for detection distance (unitless) | 2 |
| *fishCaptureParam9* | Ratio of cell velocity to fish's maximum swim speed at which capture success is 0.9 (unitless) | 0.5 |
| *fishCaptureParam1* | Ratio of cell velocity to fish's maximum swim speed at which capture success is 0.1 (unitless) | 1.6 |
| *fishMaxSwimParamA* | Length coefficient in maximum swim speed equation ($s^{-1}$) | 2.8 |
| *fishMaxSwimParamB* | Constant in maximum swim speed length term (cm $s^{-1}$) | 21.0 |
| *fishMaxSwimParamC* | Temperature squared coefficient in maximum swim speed equation ($°C^{-2}$) | -0.0029 |
| *fishMaxSwimParamD* | Temperature coefficient in maximum swim speed equation ($°C^{-1}$) | 0.084 |
| *fishMaxSwimParamE* | Constant in maximum swim speed temperature term (unitless) | 0.37 |

As part of the net energy intake calculations, calculated food intake from drift or search feeding is checked to make sure it does not exceed the physiological maximum daily intake (***cMax***). Unfortunately, *cMax* is poorly defined and difficult to measure, largely because it varies with factors such as the fish's exercise condition, food type, and feeding conditions in the laboratory. However, there are a number of published equations for *cMax* that include an allometric function relating *cMax* to fish size, and a temperature function. InSTREAM-Gen follows this formulation, which is widely used with the parameters developed by Rand et al. (1993) for rainbow trout (Table A5) for modelling *cMax* of salmonids in general (e.g., Van Winkle et al. 1996, Railsback and Rose 1999, Booker et al. 2004).

The *cMax* temperature function used in inSTREAM-Gen (developed by Railsback et al. 2009) is based in part on laboratory studies on rainbow trout by Myrick (1998) and Myrick and Cech (2000). These studies focused on higher temperatures, measuring cMax at 10, 14, 19, 22, and 25ºC. Previous models of *cMax* for salmonids (Rand et al. 1993) used temperature functions based on the laboratory studies of From and Rasmussen (1984), who studied

rainbow trout at temperatures of 5-22ºC; and of Elliott (1982) who studied brown trout. Instead of an equation, the *cMax* temperature function is a set of seven points used to interpolate a value of ***cmaxTempFunction*** from the temperature of a fish's habitat reach (Table A6).

**Table A5.** Parameter values for the allometric function of physiological maximum consumption (from Rand et al. 1993).

| Parameter | Definition (units) | Value |
|---|---|---|
| *fishCmaxParamA* | Allometric constant in *cMax* equation (unitless) | 0.628 |
| *fishCmaxParamB* | Allometric exponent in *cMax* equation (unitless) | -0.30 |

**Table A6.** Parameter values for temperature function of physiological maximum consumption (from Railsback et al. 2009).

| Parameter | Temperature (ºC) | Parameter | Temperature Function value (unitless) |
|---|---|---|---|
| *fishCmaxTempT1* | 0 | *fishCmaxTempF1* | 0.05 |
| *fishCmaxTempT2* | 2 | *fishCmaxTempF2* | 0.05 |
| *fishCmaxTempT3* | 10 | *fishCmaxTempF3* | 0.5 |
| *fishCmaxTempT4* | 22 | *fishCmaxTempF4* | 1.0 |
| *fishCmaxTempT5* | 23 | *fishCmaxTempF5* | 0.8 |
| *fishCmaxTempT6* | 25 | *fishCmaxTempF6* | 0 |
| *fishCmaxTempT7* | 100 | *fishCmaxTempF7* | 0 |

InSTREAM-Gen's bioenergetics modelling approach models respiration as the energetic cost of metabolism and swimming. In its formulation, drift-feeding fish are assumed to swim at a speed equal to their habitat cell's water velocity unless they have access to velocity shelter. If they do, then its swimming speed is assumed equal to a constant fraction of its habitat cell's mean water velocity. This fraction is defined by the parameter ***fishShelterSpeedFrac***. A number of studies have shown that "focal" water velocities (the velocity measured as closely as possible to the spot where a fish was drift-feeding) are related to, but less than, the depth-averaged velocity at the same location (e.g., Baltz and Moyle 1984, Baltz et al. 1987, Moyle and Baltz 1985). However, as argued by Railsback et al. (2009), relations between focal and depth-averaged velocities observed in these studies are not directly applicable to this formulation because *fishShelterSpeedFrac* approximates the difference between cell average water velocity and the swimming speed of a fish using velocity shelter. The best value of this parameter will vary with the kind of velocity shelter being used and could easily be estimated in the field. For a small, hydraulically complex stream with velocity shelter due to boulders

and logs, Railsback and Harvey (2001) used a value of 0.3 for *fishShelterSpeedFrac*. Railsback et al. (2006) used a value of 0.5 for a river where substrates are relatively small and embedded.

For modelling **respiration costs**, inSTREAM-Gen uses the Wisconsin Model equation 1 for respiration (Hanson et al. 1997), as modified by Van Winkle et al. (1996) to apply the activity respiration rate only during active feeding hours. The parameters that Rand et al. (1993) developed for steelhead trout (*Oncorhynchus mykiss*; converted from calories to joules; Table A7) are widely used and appear to be the best available for stream trout in general.

**Table A7.** Parameter values for the respiration model (from Rand et al. 1993).

| Parameter | Definition (units) | Value |
|---|---|---|
| *fishRespParamA* | Allometric constant in standard respiration equation * | 30 |
| *fishRespParamB* | Allometric exponent in standard respiration equation (none) | 0.784 |
| *fishRespParamC* | Temperature coefficient in standard respiration equation ($°C^{-1}$) | 0.0693 |
| *fishRespParamD* | Velocity coefficient in activity respiration equation (s $cm^{-1}$) | 0.03 |

*This is an empirical parameter with units that depend on *fishRespParamB*.

The energy density of fish (fish parameter ***fishEnergyDensity***, j $g^{-1}$) is used to convert a fish's net energy intake to growth in weight. The energy density of salmonids actually varies through their life cycle (typically higher in adults, especially during gonad development prior to spawning), but this variation is ignored in inSTREAM-Gen. The literature summarized by Hanson et al. (1997) indicates that 5900 j $g^{-1}$is a reasonable value for all stream trout.

- *Trout survival*:

Mortality sources are represented in inSTREAM-Gen as survival probabilities: the daily probability of not being killed by one specific mortality source. Death of fish is modelled stochastically by comparing pseudo-random numbers to the survival probabilities. The survival probabilities are modelled by means of logistic functions, which are useful for depicting many functions that vary between 0 and 1 in a nonlinear way. The Y value of a logistic function (daily survival probability, in this case) increases from zero to one, or decreases from one to zero, as the X value (the habitat variable, in this case) increases over any range. In inSTREAM-Gen, logistic functions are defined via parameters that specify two points: the X values at which the Y value equals 0.1 and 0.9 (*habVarAtS01* and *habVarAtS09*, respectively). The parameters *habVarAtS01* and *habVarAtS09* are therefore the values of the habitat variable at which survival is defined to be 0.1 and 0.9, respectively. The value of these two parameters must not be equal.

As highlighted by Railsback et al. (2009), it is important to understand that seemingly high daily survival probabilities can result in low survival over time. For example, a daily survival probability of 0.99 results in mortality of 26% of fish within 30 days ($0.99^{30} = 0.74$). Survival probabilities should be well above 0.99 if they are not to cause substantial mortality over time.

It is often helpful to translate daily survival values into the probability of surviving for 30 days and think about monthly survival.

There are six different mortality sources, which are represented separately because the probability of surviving each varies differently with fish state and habitat conditions:

Mortality owing to **high temperature** represents the breakdown of physiological processes at high temperatures. It does not represent the effect of high temperatures on bioenergetics (reduced growth at high temperature). The high temperature survival function is based on laboratory data collected from (presumably) disease-free fish, so it does not represent the effect of disease even though fish are probably more susceptible to disease at high temperatures. Instead, disease is modelled as part of poor condition mortality; a fish able to maintain its weight at sublethal temperatures is assumed to remain healthy.

High temperature mortality has been addressed by numerous laboratory studies, but models of this mortality remain variable and uncertain because mortality varies with laboratory conditions and techniques and the endpoints used to define mortality; varies between laboratory and field conditions; and undoubtedly varies among individuals. In fact, any differences in measured lethal temperatures among trout species are not clearly distinguishable from uncertainty and variability in the measurements. Recent laboratory data showed approximately 60% survival of golden trout (*Oncorhynchus mykiss*) juveniles over a 30-day period at a constant 24°C (Myrick 1998), equivalent to a daily survival of 0.98. Dickerson and Vinyard (1999) measured survival of Lahontan cutthroat trout (*Oncorhynchus clarkii*) for 7 days at high temperatures, finding zero survival at 28°C, 40% survival at 26° (equivalent to daily survival of 0.88), and 100% survival at 24°C. This literature indicates that high temperature mortality can be modelled well as a logistic function. The parameter values in Table A8 appear suitable for sites with relatively low diurnal variation in temperature; they produce survival of 0.98 at 24°C, 0.88 at 26°C, and < 0.5 at 28°C.

The **high velocity** survival function represents the potential for trout to suffer fatigue or lose their ability to hold position in a cell with high velocity. This function is included not because trout often die due to high velocity, but because it strongly affects habitat selection: mortality due to high velocities is not observed in nature because fish avoid it by moving. Velocities posing mortality risk can be widespread at high flows, but can also occur (especially for small fish) at normal flows.

The survival probability is based on the ratio of the swimming speed a fish uses in a cell to the fish's maximum sustainable swim speed. The swimming speed used in a cell is determined when calculating respiration energy costs: fish are assumed to swim at the cell's water velocity unless they are drift-feeding with access to velocity shelters. Fish using velocity shelters are assumed to swim at a speed equal to the cell's velocity times the parameter *fishShelterSpeedFrac*. A decreasing logistic function relates survival probability to the fish's swimming speed in its habitat cell divided by the fish's value of *fishMaxSwimSpeed*. The parameters for this function (Table 8) are chosen so that high velocity mortality is negligible at swimming speeds less than *fishMaxSwimSpeed*, reflecting that (a) the laboratory equipment for measuring swim speeds does not provide the kinds of turbulence and fine-scale velocity breaks that trout can often use to reduce swimming effort in natural conditions, and (b) stream fish are likely to be in better condition than laboratory fish.

**Stranding** mortality represents the death of fish that are unable to move out of cells that become extremely shallow or dry as flow decreases. Survival of stranding is modelled as an increasing logistic function of depth divided by fish length (Table A8). Because the terrestrial predation function does not represent the greatly increased likelihood of predation when depth

is extremely low (e.g., when fish are trapped in isolated pools; Harvey and Stewart 1991), this risk is included as part of stranding mortality. The stranding survival function does not distinguish whether fish in very low or zero depths die from lack of water or from predation. The stranding parameters do not cause survival to reach zero when depth is zero, reflecting that real habitat (as opposed to the model's cells) has variation in bottom elevation- some water could remain even if a cell's simulated depth becomes zero. Depth is divided by fish length to scale how the risks of low depths vary with fish size: shallow habitat that may be very valuable for small fish (protecting them from aquatic predation) may pose a stranding risk for large fish.

Fish in **poor condition** (low value of the condition factor *K*, weight in relation to length) are at risk of starvation, disease, and excess vulnerability to predators. These risks are combined in the poor condition survival probability. Simpkins et al. (2003a, b) studied starvation mortality in large juvenile trout, finding that: 1) trout can survive for long periods (over 147 days, in some cases) with no food intake; 2) survival is lower at higher swimming activity and temperature (which both increase metabolism); 3) relative weight (equivalent to *K*) decreased linearly over time during starvation; but 4) mortality was predicted better by an index of lipid content than by *K* (one reason is that lipids are replaced by water as energy stores are depleted).

Unfortunately, modelling how body lipids are depleted and replaced by water and related processes would add considerable complexity and uncertainty to inSTREAM-Gen, as they are not well understood. Instead, poor condition survival probability is represented as an increasing logistic function of *K* with parameter values estimated to provide reasonable survival probabilities over several days and weeks (Table A8). The parameters produce a survival probability less than 100% even when *K* is at its maximum of 1.0, because disease can occur (though is less likely) when condition is relatively good. Poor condition is a unique mortality source in that fish can never increase their survival probability immediately by selecting different habitat. Fish in poor condition have a strong incentive to select habitat that provides rapid growth so their condition increases; however, sufficient growth to recover high condition takes a number of days. Even apparently high daily survival probabilities for this mortality source (e.g., 0.90) result in a low probability of surviving until normal weight can be regained. Railsback and coauthors (2009) estimated that the probability of surviving for extended periods becomes quite low when *K* falls below 0.8.

Railsback et al. (2009) advise that before modifying the parameters for poor condition, one should be aware that poor condition mortality can have a strong effect on habitat selection as well as mortality. Consequently, changes in parameter values are likely to have widespread, complex, and unexpected effects. For example, one might assume that increasing the survival probability (e.g., by decreasing *mortFishConditionK9* from 0.6 to 0.7) would result in less mortality due to poor condition. However, because fish select habitat using a trade-off between poor condition and other (primarily, predation) mortality sources, this change in parameters could result in fish selecting different habitat that has lower growth and lower predation risk, at least partially offsetting the expected reduction in poor condition mortality.

Predation by terrestrial animals is a dominant source of mortality to trout, especially adults (Alexander 1979, Harvey and Marti 1993, Valdimarsson et al. 1997, Metcalfe et al. 1999, Quinn and Buck 2001, Harvey and Nakamoto 2013). The **terrestrial predation** formulation represents predation by a mix of such predators that lead to these generalizations about terrestrial predation: 1) big trout are vulnerable, often more vulnerable than small trout; 2) risks are year-round because warm-blooded predators feed as much or more in winter (except those that hibernate or migrate); and 3) trout are more at risk when more visible from the air.

The formulation assumes a minimum survival probability (*mortFishTerrPredMin*) that applies when fish are most vulnerable to terrestrial predation, and a number of "survival increase functions" that can increase the probability of survival above this minimum. Survival increase functions have values between zero and one, with higher values for greater protection from predation. The survival increase functions are assumed to act independently. Using this approach, the probability of surviving terrestrial predation does not vary with how many survival increase functions there are, but instead is only limited by one function at a time. Survival increase functions can be added, removed, or revised without re-calibrating the overall predation survival rate.

The value of *mortFishTerrPredMin* is assumed to be the daily probability of surviving terrestrial predation under conditions where the survival increase functions are minimal (offering no reduction in risk). Field data for estimating this minimum survival are unlikely to be available, so it is best estimated by calibrating the model to observed abundance and habitat use patterns (see next section about parameters needing calibration). It is important to note that results from inSTREAM-Gen can be quite sensitive to the parameters that define how terrestrial predation risk depends on habitat variables, which is not surprising, considering that terrestrial predation is normally the only mortality source that adult trout are routinely vulnerable to. If those parameters are set in such a way that the survival increase function is very close to 1.0 in several or many cells, then trout occupying those cells can be almost immune to mortality.

The following survival increase functions are included (suggested parameter values are provided at Table A8):

- **Depth**. Fish are more vulnerable to terrestrial predators when in shallow water, where they are easier for predators to locate and catch. The depth survival increase function is an increasing logistic curve: survival increases as depth increases. Power (1987) indicates that predation by birds is low at depths above 20 cm, and Hodgens et al. (2004) report that 85% of successful strikes by herons were at depths less than 20 cm but some were at depths up to 50 cm. However, predators that are larger or better swimmers (mergansers, otters) are effective at greater depths, especially in clear water. (Note that the very high risk of terrestrial predation that occurs when fish are in near-zero depths is included in stranding mortality.) Railsback et al. (2009) warn based on experience that appropriate values for the depth survival increase function parameters can differ among sites. Parameters useful in relatively small streams of coastal California (Railsback and Harvey 2001) provide high relative survival in depths > 1 m. However, these parameters were not useful for the much larger Green River in Utah, where depths can be several meters and otters are prevalent; so Railback et al. (2005) developed separate parameters for the Green River site.
- **Fish length**. Small fish are less vulnerable to terrestrial predation, presumably because they are less visible (Power 1987), less desirable, and possibly more difficult to capture, than larger fish. Therefore, survival of terrestrial predation is assumed to decrease with fish length, but only fish less than 4 cm in length are relatively protected. These parameter values should be reconsidered for sites where predation is dominated by larger mammals (otters, bears) that strongly prefer large fish.
- **Feeding time**. Fish are much more vulnerable to predation when they are actively feeding during the day instead of resting and hiding at night (Metcalfe et al. 1999). The survival increase function is modeled as a decreasing function of *feedTime* (h), the hours spent feeding per day. Parameters are chosen so survival decreases nearly linearly with *feedTime*.

- **Water velocity**. Water velocity is assumed capable of increasing terrestrial predation survival because (1) velocity-caused turbulence makes fish harder to see, and (2) some predators are poorer swimmers than trout so they are expected to be less able capture fish in faster water. The survival increase function is therefore an increasing logistic curve that provides sharply increasing protection from terrestrial predators at velocities above 50 cm $s^{-1}$. As with the depth survival increase function, useful parameter values for the velocity function may differ between small and large streams. In small streams, high velocities combine with high turbulence and obstacles to make swimming difficult. In large rivers, however, there can be run habitat where velocities are high while turbulence is low, so good swimmers such as mergansers and otters may perform quite well.
- **Distance to hiding cover**. Fish can avoid mortality by hiding when predators are detected. The success of this tactic depends on the presence of hiding cover and the distance the fish must travel to reach it. Hiding cover is represented with a survival increase function that increases as distance to hiding cover decreases. Distance to cover (*cellDistanceToHide*, cm) is an input for each habitat cell, estimated as the average distance a fish in the cell would need to move to hide from a predator. The effect of distance to hiding cover is modelled as a decreasing logistic function of *cellDistanceToHide* because very short distances to hiding cover (< 100 cm) provide nearly complete protection from some predators, but do not protect fish from predators that strike very quickly (e.g., some birds) or that could be able to extract trout from hiding (e.g., otters); while cover several meters away is still valuable for escaping from terrestrial predators that have been detected.

The **aquatic predation** formulation represents mortality due to predation by fish. In many but not all trout populations, the dominant source of aquatic predation is cannibalism by large trout. By adjusting parameter values, the formulation can be made to apply both to sites where the modelled trout are the only piscivorous fish and sites where non-trout fish, not otherwise represented in inSTREAM-Gen, are a significant risk.

As with terrestrial predation, the formulation uses a minimum survival probability (*mortFishAqPredMin*) that applies when fish are most vulnerable to aquatic predation, and a number of survival increase functions. Data for directly estimating aquatic risks are again unlikely to be available, so it is recommended that *mortFishAqPredMin* be estimated by calibrating the model to observed patterns of abundance and habitat selection by juvenile fish (see next section about parameters needing calibration).

Especially at sites where trout rarely get larger than 20-30 cm, cannibalism by trout is often rare; e.g., at the Little Jones Creek site fewer than 1% of adult fish contained juveniles (Railsback and Harvey 2001). However, the risk of predation appears to be an important factor driving habitat selection (e.g., Brown and Moyle 1991): avoiding predation is likely a key reason why small fish prefer shallow water. If aquatic predation rarely occurs, it is likely because small fish avoid it with some success by avoiding risky habitat. Also, there have been anecdotal reports of very high cannibalism rates during fry emergence in some salmonids.

There is no survival increase function for distance to hiding cover in the aquatic predation formulation because only small trout are usually vulnerable to aquatic predators, and small trout are capable of hiding in many places that do not offer refuge to adult trout (e.g., between relatively small cobbles).

The following survival increase functions are included (suggested parameter values are provided at Table A8):

- **Predator density**. This function represents how survival of aquatic predation depends on the density of trout predators. It is important to understand that this function represents only the effect of trout included in the model; it does not represent non-trout piscivorous fish. The predator density survival increase function causes the survival increase function to increase as predator density decreases. Parameters for this logistic function depend on whether the modelled trout are the only piscivorous fish. The parameters shown in Table A8 represent a site where there are no non-trout fish predators. The parameters reflect (a) near-zero risk when there are no piscivorous trout, and (b) a steep decline in survival as predator density exceeds one piscivorous trout per 25 $m^2$ (250,000 $cm^2$) of reach area. Post et al. (1998) measured the mortality of tethered juvenile trout due to predation by adult trout in lakes. This study showed the risk to increase exponentially with adult trout density, rising very sharply between 8 and 10 predators per 1000 $m^3$. This result supports a logistic-like relation between adult trout density and juvenile trout survival probability. However, Railsback et al. (2009) reasoned that the exact relation is not directly applicable to inSTREAM, and hence to inSTREAM-Gen, because (a) it was obtained in lakes where cover and other habitat complexities may mediate the effect of predator density, and (b) risks were evaluated over 1 hour periods, whereas inSTREAM model uses a daily time step. For sites where fish other than the trout represented in the model pose a piscivory risk, parameter values should be adjusted to reflect the reduced importance of trout to survival of aquatic predation. For example, if a site has a dense population of piscivorous fish, then trout density may have little effect on survival. In that case, the predator density function should be low and relatively flat (e.g., *mortFishAqPredP9* = -1.0; *mortFishAqPredP1* = 0.001).
- **Depth**. Aquatic predation survival is assumed to be high in water shallow enough to physically exclude large fish, or shallow enough to place large fish at high risk of terrestrial predation. The depth survival increase function is therefore a decreasing logistic function, with high survival at depths less than 5 cm.
- **Fish length**. As fish grow, they become better able to out-swim piscivorous fish and fewer piscivorous fish are big enough to swallow them. The length survival increase function is therefore an increasing logistic function, the parameters for which depend on the size of the piscivorous fish. Keeley and Grant (2001) provide an empirical relation between the size of piscivorous stream trout and the size of their fish prey. Table A8 illustrates parameters for sites where the only predator fish are trout of 25-30 cm in length. For sites with larger predator fish, the curve should be shifted to the right. For sites such as Little Jones Creek where adult trout are rarely more than 20 cm, survival is likely quite high when length is greater than 8 cm.
- **Feeding time**. This survival increase function is the same for aquatic predation as it is for terrestrial predation. The survival increase is a decreasing logistic function of feedTime, the number of hours per day spent foraging. Separate parameters control the feeding time function for aquatic vs. terrestrial predation, but the values recommended above for terrestrial predation are also recommended for aquatic predation.
- **Low temperature**. This survival increase function reflects how low temperatures reduce the metabolic demands and, therefore, feeding activity of piscivorous fish. The function is based on the bioenergetics of the trout predators, using a decreasing logistic function that approximates the decline in maximum food consumption (*cMax*) with declining temperature.

**Table A8.** Parameter values for different mortality sources (from Railsback et al. 2009).

| Parameter | Definition (units) | Value |
|---|---|---|
| *mortFishHiTT9* | Daily mean temperature at which high temperature survival is 90% (°C) | 25.8 |
| *mortFishHiTT1* | Daily mean temperature at which high temperature survival is 10% (°C) | 30 |
| *mortFishVelocityV9* | Ratio of fish swimming speed to maximum swim speed at which high velocity survival is 90% (unitless) | 1.4 |
| *mortFishVelocityV1* | Ratio of fish swimming speed to maximum swim speed at which high velocity survival is 10% (unitless) | 1.8 |
| *mortFishStrandD9* | Ratio of depth to fish length at which stranding survival is 90% (unitless) | 0.3 |
| *mortFishStrandD1* | Ratio of depth to fish length at which stranding survival is 10% (unitless) | -0.3 |
| *mortFishConditionK9* | Fish condition factor *K* at which survival is 90% (unitless) | 0.6 |
| *mortFishConditionK1* | Fish condition factor *K* at which survival is 10% (unitless) | 0.3 |
| *mortFishTerrPredD9* | Depth at which survival increase function is 90% of maximum (cm) | Small streams: 150<br>Large rivers: 300 |
| *mortFishTerrPredD1* | Depth at which survival increase function is 10% of maximum (cm) | Small streams: 5<br>Large rivers: 50 |
| *mortFishTerrPredL9* | Fish length at which survival increase function is 90% of maximum (cm) | 3 |
| *mortFishTerrPredL1* | Fish length at which survival increase function is 10% of maximum (cm) | 6 |
| *mortFishTerrPredF9* | Feeding time at which survival increase function is 90% of maximum (h) | 0 |
| *mortFishTerrPredF1* | Feeding time at which survival increase function is 10% of maximum (h) | 18 |
| *mortFishTerrPredV9* | Velocity at which survival increase function is 90% of maximum (cm $s^{-1}$) | Small streams: 100<br>Large rivers: 300 |
| *mortFishTerrPredV1* | Velocity at which survival increase function is 10% of maximum (cm $s^{-1}$) | Small streams: 20<br>Large rivers: 20 |
| *mortFishTerrPredH9* | Distance to hiding cover at which survival increase function is 90% of maximum (cm) | -100 |
| *mortFishTerrPredH1* | Distance to hiding cover at which survival | 500 |

| | | |
|---|---|---|
| | increase function is 10% of maximum (cm) | |
| *mortFishAqPredP9* | Predator density at which survival increase function is 90 % of maximum ($cm^{-2}$) | $2\times10^{-6}$ |
| *mortFishAqPredP1* | Predator density at which survival increase function is 10 % of maximum ($cm^{-2}$) | $1\times10^{-5}$ |
| *mortFishAqPredD9* | Depth at which survival increase function is 90% of maximum (cm) | 5 |
| *mortFishAqPredD1* | Depth at which survival increase function is 10% of maximum (cm) | 20 |
| *mortFishAqPredL1* | Fish length at which survival increase function is 10% of maximum (cm) | 4 |
| *mortFishAqPredL9* | Fish length at which survival increase function is 90% of maximum (cm) | 8 |
| *mortFishAqPredF9* | Feeding time at which survival increase function is 90% of maximum (h) | 0 |
| *mortFishAqPredF1* | Feeding time at which survival increase function is 10% of maximum (h) | 18 |
| *mortFishAqPredT9* | Temperature at which survival increase function is 90% of maximum (°C) | 2 |
| *mortFishAqPredT1* | Temperature at which survival increase function is 10% of maximum (°C) | 6 |

Angling and hooking mortality resulting from recreational fishing are two additional sources of trout mortality, which are not considered in the habitat selection process, but only on the survival action. The reason is that we assume that the trout are not aware of angling mortality risk and how it varies with habitat. Together with the five parameters that are site-specific, there are six additional parameters involved in the angler mortality model (suggested values are shown in Table A9). The parameter *mortFishAngleSuccess*, used to calculate capture rate, represents fishing success as the fraction of catchable fish hooked per angler hour. The value of this parameter can vary among species (e.g., between species that are and are not stocked) to reflect differences in vulnerability to angler harvest. Capture rate is also assumed to be a logistic function of trout size. The size dependency reflects the success of anglers in selecting for larger trout by (a) using tackle more attractive to larger fish and (b) fishing in habitat better for large trout. The logistic function of fish length is defined by the parameters *mortFishAngleL1* and *mortFishAngleL9*.

Survival of angling mortality depends on how many times a trout is hooked (*timesHooked*) and whether it is kept vs. released each time hooked. Separate probabilities of keeping hooked fish are applied to fish that are and are not within the legal length ranges. The probability of keeping trout that are of legal length is defined by the parameter *mortFishAngleFracKeptLegal*, and the probability of keeping trout of illegal length is the parameter *mortFishAngleFracKeptIllegal*. The values for these parameters should be selected considering that the fraction kept is the fraction of all fish hooked that are landed and kept, not the fraction of landed fish that are kept: trout that shake the hook before being netted are considered as captured but released.

The survival probability for hooking is evaluated separately, using *timesHooked* as its basis. If *timesHooked* is zero, this survival probability is 1.0. If *timesHooked* is greater than zero (and the fish did not die of angling mortality), the hooking survival probability is equal to the parameter *mortFishAngleHookSurvRate* raised to the power *timesHooked*.

**Table A9.** Parameter values for angling and hooking mortality (from Railsback et al. 2006).

| Parameter | Definition (units) | Value |
|---|---|---|
| *mortFishAngleSuccess* | Multiplier to determine capture probability from fishing pressure (angler-h)$^{-1}$ | 0.003 |
| *mortFishAngleL9* | Length at which hooking risk is 90% of maximum (cm) | 20 |
| *mortFishAngleL1* | Length at which hooking risk is 10% of maximum (cm) | 10 |
| *mortFishAngleFracKeptLegal* | Probability of fish of legal length being kept by anglers (unitless) | 0.2 |
| *mortFishAngleFracKeptIllegal* | Probability of fish not of legal length being kept by anglers (unitless) | 0.05 |
| *mortFishAngleHook-SurvRate* | Survival probability for released trout (or trout that shake the hook) (unitless) | 0.8 |

- *Redds survival and development*:

There are 10 parameters concerned with redds survival and development processes. In InSTREAM-Gen, eggs incubating in a redd are subject to five mortality sources: low and high temperatures, scouring by high flows, dewatering, and superimposition (having another redd laid on top of an existing one). Redd survival is modelled using redd "survival functions", which determine, for each redd on each day, the probability of each egg surviving one particular kind of mortality.

The daily fraction of eggs surviving **low temperatures** is modelled as an increasing logistic function of temperature. Parameter values appear to differ among trout species, with differences especially likely between species that spawn in the fall v. spring. In developing parameter values from published data on egg survival, it is important to remember that eggs incubate slowly at low temperatures, so even apparently high daily survival rates can result in low egg survival over the entire incubation period.

Parameter values for spring-spawning rainbow trout and fall-spawning brown trout (Table A10) have been determined from data compiled by Brown (1974); Railsback and Harvey (2001) also used the rainbow trout parameters for cutthroat trout. The data compiled by Brown (1974) indicate that rainbow trout spawn at temperatures as low as 3 - 5°C and eggs have a 90% survival rate over a 100-d incubation period at 3°C (daily egg survival = 0.999). Railsback et al. (2009) assumed a daily survival rate of 0.9 (very low long-term survival) for 0°C, and logistics parameters that reproduce these two points were determined. Similarly, Brown (1974) cited data indicating that brown trout egg incubation can take over 150 days at

very low temperatures. Parameter values for brown trout were estimated by Railsback and coauthors by assuming 90% egg survival over 150 days at 1ºC (daily survival of 0.9993) and daily survival of 0.9 at 0°C.

**High temperatures** can induce direct mortality in trout eggs, and also promote fungus and disease. The fraction of eggs surviving high temperatures is modelled as a decreasing logistic function of temperature. Parameter values for rainbow trout (also used for cutthroat trout by Railsback and Harvey 2001) are based on interim results of laboratory studies conducted by the University of California at Davis (Myrick 1998). These data showed daily survival rates declining from about 0.9998 at 11°C to about 0.985 at 19°. The resulting parameter values (Table A10) appear to indicate high survival at high temperatures, but in fact cause low survival if temperatures are elevated for long periods. Fall spawning trout are likely to be less-well adapted to high incubation temperatures. Parameter values for brown trout in Table A10 were arbitrarily set by Railsback et al. (2009) to 5º less than the rainbow trout values and should not be considered reliable.

**Table A10.** Parameter values for low and high temperature mortality (from Railsback et al. 2009).

| Parameter | Definition (units) | Value |
|---|---|---|
| *mortReddLoTT9* | Temperature at which low temperature survival is 90% (°C) | Rainbow trout: 0<br>Brown trout: 0 |
| *mortReddLoTT1* | Temperature at which low temperature survival is 10% (°C) | Rainbow trout: -3<br>Brown trout: -0.8 |
| *mortReddHiTT9* | Temperature at which high temperature survival is 90% (°C) | Rainbow trout: 21<br>Brown trout: 16 |
| *mortReddHiTT1* | Temperature at which high temperature survival is 10% (°C) | Rainbow trout: 30<br>Brown trout: 25 |

**Scouring and deposition** mortality results from high flows disturbing the gravel containing a redd. InSTREAM-Gen assumes that the probability of a redd being destroyed is equal to the proportion of the stream reach scouring or filling to depths greater than the value of the fish parameter *mortReddScourDepth* (cm). Consequently, the probability of a redd not being destroyed is equal to the proportion of the stream scouring or filling to a depth less than the value of *mortReddScourDepth*. This parameter can be evaluated as the egg burial depth, the distance down from the gravel surface to the top of a redd's egg pocket. Scour to this depth is almost certain to flush eggs out of the redd. Deposition of new material to this distance would double the egg pocket's depth, likely to severely reduce the survival and emergence of its eggs. DeVries (1997) reviews egg burial depths for stream trout. Values of 5-10 cm are reasonable for small trout using relatively small gravel; field observations at the Little Jones Creek site found eggs buried as little as 5 cm. The average depths at which salmonid eggs are buried appear to vary from 0.4 body lengths for a 20 cm female, to 0.3 body lengths for a 70 cm fish, and 15.2 cm deep seems to be a reasonable average value for brown trout (see references in review by Armstrong et al. 2003). Due to the formulation of scouring survival, users can effectively turn scouring and deposition mortality off by using a very large value of *mortReddScourDepth*, e.g., 10,000 cm.

**Dewatering** mortality occurs when flow decreases until a redd is no longer submerged; eggs can be killed by dessication or the buildup of waste products that are no longer flushed away. Reiser and White (1983) did not observe significant mortality of eggs when water levels were reduced to 10 cm below the egg pocket for several weeks. However, they also cited literature indicating high mortality when eggs and alevins are only slightly submerged (which may yield poorer chemical conditions than being dewatered), and high mortality for dewatered alevins. Because inSTREAM-Gen does not distinguish between eggs and alevins, these processes are not modelled mechanistically or in detail. The dewatering survival function is simply that if depth is zero then the daily fraction of eggs surviving is equal to the fish parameter *mortReddDewaterSurv*. Railsback et al. (2009) indicated a suggested value of 0.9, which reflects the variability in dewatering effects. Egg survival may be high when a redd is first dewatered, so *mortReddDewaterSurv* should not be too low.

**Superimposition** redd mortality can occur when a new redd is laid over an existing one; females digging new redds can disturb existing redds and cause egg mortality through mechanical damage or by displacing eggs from the redd environment. If one or more redds are created in the same cell, the probability of each new redd causing superimposition is equal to the area of a redd (*reddSize*, $cm^2$, a global parameter that can be species-specific) divided by the area of spawning gravel in the redd. Because of how the parameter *reddSize* is used in this formulation, it is defined as the area a spawner disturbs in creating a new redd. Railsback et al. (2009) reports that field observations at the Little Jones Creek site suggest a *reddSize* value of 1200 $cm^2$ (the area of a circle with a diameter of 35 cm) for relatively small trout.

To predict the timing of emergence, the **developmental status** of a redd's eggs is updated daily. The fractional development approach of Van Winkle et al. (1996) is used; this approach is based on accumulated degree-days, a common technique for modelling incubation. Model redds accumulate the fractional development that occurs each day, a non-linear function of temperature. The parameters for this equation should be considered likely to vary among species, and among populations that spawn at different times of year. Hatchery management data or literature can sometimes be used to develop or test parameter values. Parameter values for spring-spawning rainbow trout and fall-spawning brown trout were developed by Van Winkle et al. (1996) (Table A11). Railsback and Harvey (2001) found the rainbow trout parameter values reasonable for a cutthroat trout population in coastal California.

**Table A11.** Parameter values for egg development rates (from Van Winkle et al. 1996).

| Parameter | Definition (units) | Rainbow, cutthroat trout (spring spawning) | Brown trout (fall spawning) |
|---|---|---|---|
| *reddDevelParamA* | Constant in daily redd development equation (unitless) | -0.000253 | 0.00313 |
| *reddDevelParamB* | Temperature coefficient in daily redd development equation ($°C^{-1}$) | 0.00134 | 0.0000307 |
| *reddDevelParamC* | Temperature squared coefficient in daily redd development equation ($°C^{-2}$) | 0.0000321 | 0.0000934 |

- *Trout emergence and transmission of heritable traits*:

Quantitative genetic parameters are difficult to estimate, especially for wild populations. These parameters are most often measured on populations that are reared in experimental settings, like hatcheries, where the environment can be controlled and/or measured on captive-bred broodstock (derived from farmed or hatchery populations), which are often the subject of intentional artificial selection on important fitness-related traits. However, Carlson and Seamons (2008) showed in their extensive review that estimates of genetic parameters are influenced by the environment in which parents and offspring are reared, yet estimates generated on wild-reared populations are exceedingly rare. Indeed, estimates of the narrow-sense heritability $h^2$ from wild fish that were reared in the wild comprised only 2% of the total number of $h^2$ estimates Carlson and Seamons collected from the literature. Importantly, the authors found that $h^2$ estimates for a given trait differed among species, life history stages, and life history types. This fact suggests that parameter estimates for one group may not be representative of those from another, so caution must be paid when borrowing values from previous studies and across trait types.

Serbezov et al. (2010b) estimated a value of length heritability (***fishNewLengthHeritability***) of 0.18 for age-0 stream-living brown trout of a Norwegian brook. Frank and Baret (2013) successfully used this value for predicting the genetic structure of a stream-dwelling brown trout population in Belgium. This value is also within the ranges reported by Blanc (2005) for hatchery-reared age-0 brown trout. Hence this value of 0.18 seems reasonable for stream-dwelling brown trout populations. Values reported in the literature (Aulstad et al. 1972, McKay et al. 1986, Fishback et al. 2002, Henryon et al. 2002) for farmed rainbow trout are pretty much more variable, ranging from 0.09 to 0.66, but heritability of length at the first weeks of life seems to be low.

The length of new recruits can never be lower than a minimum value set by the parameter ***fishMinNewLength***. When they first start to feed, the fry of many marine and freshwater fish species are less than 1 cm long (Miller et al. 1988). However, this is not the case for the larger anadromous salmonids like Atlantic salmon and sea trout, whose newly-emerged fry are rarely less than 2.5 cm (Elliott 1994). Besides, Elliott (1994) found trout emerging from a redd to vary in size only slightly; the author observed a coefficient of variation of 0.07 in length at emergence for brown trout at several sites. Converting this value to the standard deviation in length (with a coefficient of variation of 0.07 and a mean length of 2.5 cm) and truncating potential length of new recruits to 4 SD of such mean length, it rarely would be lower than 1.8 cm. However, accounting for potential variations in mean and variability of length at emergence across species and populations [for e.g., alevins of stream-dwelling brown trout typically swim up from the gravel with a length ca. 2 cm (Klemetsen et al. 2003)], we set a conservative value of 1 cm for this parameter.

We are not aware of any study reporting heritability values of length-at-maturity (***fishSpawnMinLengthHeritability***) for stream-dwelling trout species. Regarding iteroparous anadromous salmonids, Gjerde and Gjedrem (1984) estimated a $h^2$ value of 0.16 for farmed steelhead trout and of 0.35 for farmed Atlantic salmon (*Salmo salar*). Piou and Prévost (2012, 2013) used an initial value of 0.4 (based on Gjerde et al. 1994) when initializing simulations of their IBASAM individual-based model meant to predict the evolutionary consequences of climate change on French Atlantic salmon populations. Regarding semelparous anadromous salmonids, $h^2$ values found in the literature for pink salmon (*Oncorhynchus gorbuscha*) ranged from non-significance in wild populations (Dickerson et al. 2005) up to 0.45 in sea-ranched conditions (Smoker et al. 1994, Funk et al. 2005). Taken into account the uncertainty

in this parameter, we selected a conservative value of 0.2, in the order of magnitude of what commonly observed for life-history traits (Lynch and Walsh 1998).

The heritability of the neutral trait (***fishNeutralTraitHeritability***) depends obviously on the trait selected by the user. Studies available in the literature can be checked in the thorough review of Carlson and Seamons (2008).

In the model for genetic transmission of heritable traits, we modified the inheritance model of the infinitesimal model of quantitative genetics theory to account for new input of variation from mutation. This is accomplished by adding to the additive genetic variance the mutational variance $\sigma_m^2$ multiplied by a factor *M* defining the amplitude of mutation. The mutational variance (variance introduced by mutation per generation) at the population level is computed as (*mutationalVarParam* × $\sigma_E^2$), where ***mutationalVarParam*** is in the order of $10^{-3}$ to $10^{-2}$, as suggested by reviews of empirical data (Lynch and Walsh 1998, Johnson and Barton 2005). Following Vincenzi et al. (2012), we used a value of $10^{-3}$ in our simulations. Using a similar quantitative genetic model, Vincenzi et al. (2012) explored the evolution of a fitness-related trait in a population and its effects on population dynamics with a gradual increase in mean and variance of a climate variable determining the optimum for the trait under selection. To do this, the authors used simulations with variations in trend (i.e., directional change) and stochasticity (i.e., increase in variance) of a climate variable defining a phenotypic optimum, and various hypotheses on mutational variance and strength of selection on a phenotypic fitness-related trait. Specifically, the authors varied the **mutation factor (*M*)** over a range of 1 to 100. According to their results, the probability of population persistence does not increase with increasing mutation, in particular when variability of the optimum is too high, although higher mutation generally increases the probability of tracking a moving optimum. Accordingly, in our simulations we used a value of 1.

### 3.4. Calibrated parameters

The parameters most suitable for calibration are those to which model results are highly sensitive and for which there is little basis, other than calibration, for selecting values. There are only six parameters that are especially suited for calibration in inSTREAM-Gen. Four of them are involved in the bioenergetics model and are easily calibrated using observed individual growth and survival rates. The other two parameters, *mortFishAqPredMin* and *mortFishTerrPredMin*, define the daily probability of surviving aquatic and terrestrial predation under the most vulnerable conditions.

- Food production parameters:

As discussed by Railsback et al. (2009), the processes influencing food availability for stream salmonids are complex and not well understood, and there is little information available on how food availability varies over time and space at scales relevant to individual-based models. Modelling food production is also complicated by the multiple sources of food available to trout. Therefore, the parameters describing production of both kinds of food (*habDriftConc* and *habSearchProd*) in inSTREAM-Gen are highly uncertain. While *habDriftConc* strongly affects growth rates of all age-classes, *habSearchProd* mainly affects growth of juveniles because they are the only trout that consistently use search feeding. This search food parameter is therefore useful for calibrating differences in growth between juveniles and larger trout. Notwithstanding the fact that the key food parameter, *habDriftConc*, can indeed be measured in the field instead of calibrated, Railsback and colleagues discouraged attempting to use measured drift concentrations. This is mainly

because this parameter captures many of the uncertainties resulting from model simplifications (such as ignoring variation in prey size and spatial and seasonal variation in drift production or assuming fish feed only during daytime), and therefore, accurately measured drift concentrations may not produce accurate model results. Thus, it is recommended the calibration of growth rates by adjusting the parameters for food production, since they not only affect the amount of food in a cell but also the food capture rates of feeding fish.

The parameter *habDriftRegenDist* should theoretically have a value approximating the distance over which drift depleted by foraging fish is regenerated. This parameter affects the total availability of drift food per cell, which can limit how many trout can occupy each high-quality cell. Smaller values of *habDriftRegenDist* provide then higher production of food in a cell. As highlighted by Railsback et al. (2009), this parameter can be used to calibrate habitat selection and starvation survival because varying it changes drift food availability without changing the amount that a drift-feeding fish captures. It could be calibrated by attempting to match observed densities of trout in high-quality habitat.

Finally, the parameter *fishSearchArea*, which can be interpreted as the area over which the production of stationary food is consumed by one fish, is a highly uncertain one. However, because *habSearchProd* and *fishSearchArea* have the same effect on search intake and both would be very difficult to measure, either would be suited to use for calibration, but it is not necessary calibrating both.

Railsback et al. (2009) performed several thorough calibration analyses to identify ranges of values for food production that produce reasonable feeding and growth rates under simplified conditions in inSTREAM. Those ranges are a good starting point for the calibration process. According to their study, reasonable values for the drift-food parameter *habDriftConc* were identified as the range producing food intake (g $d^{-1}$) of 20 to 50% of *cMax* in the adult trout for 15-cm trout using near optimal velocities and velocity shelter. This range is $5 \cdot 10^{-10}$ to $12 \cdot 10^{-10}$ g $cm^{-3}$. Within this range of *habDriftConc*, modelled adult trout growth ranged 0.5 to 2.5% body weight per day. For 5-cm juvenile trout, this range of *habDriftConc* produced food intake between 50 and 100% of *cMax* and growth in the range of 5 to 15% per day; the lower ends of these ranges are consistent with rates observed in field studies and laboratory growth data (see references in Railsback et al. 2009).

Railsback and colleagues estimated that for 15-cm adult trout feeding in optimal feeding positions, where all drift food production is consumed by the trout so that each individual achieves a drift intake equal to 30% of *cMax*, then with *habDriftConc* in the range of $5 \cdot 10^{-10}$ to $7 \cdot 10^{-10}$ g $cm^{-3}$, the value of *habDriftRegenDist* must be approximately 300 to 500 cm.

Assuming that a search feeding fish consumes the production of 2 $m^2$ (i.e., the value of *fishSearchArea* is 20,000 $cm^2$), Railsback et al. (2009) calculated that the range of *habSearchProd* values providing a 5-cm juvenile trout feeding at optimal search feeding conditions with a daily growth rate ranging between 0 and 2% body weight is $2 \cdot 10^{-7}$ to $5 \cdot 10^{-7}$ g $cm^{-2}$ $h^{-1}$. This estimate appeared reasonable compared to the values of trout-food production rates reported by the scarce number of available field studies (see references in Railsback et al. 2009).

- Survival probability parameters:

The values of *mortFishTerrPredMin* and *mortFishAqPredMin* represent the daily probability of surviving terrestrial and aquatic predation, respectively, under conditions where the survival increase functions offer no reduction in risk. However, field data for estimating actual predation rates are unlikely to be available. On one hand, terrestrial predation is

typically a dominant source of mortality for all but the smallest trout, hence it is best estimated by calibrating the model to observed abundance and habitat use patterns of age 1+ and older trout. Railsback et al. (2009) recommend starting with a value of 0.99 until fit via calibration. On the other hand, small juvenile trout are highly vulnerable to predation by other fish, so this parameter is particularly appropriate for calibrating the abundance of juveniles. It is advisable to begin with a value of 0.90. At any rate, as warned by Railsback et al. (2009), survival probabilities are not the only processes affecting mortality rates in the modelled trout populations since the number of fish that die is also a function of food production and density of fish competing for food. As a consequence, mortality parameter values cannot be estimated well except by calibrating the full model.

- Parameters not typically calibrated but suited for calibration if necessary:

Although initial population parameters are highly site-specific, the initial number of fish in the simulation (*init-N*) as well as the proportion of individuals of each age-class (*prop-AgeX*) can be calibrated if a short "warm-up" time is set.

It is worth noting that although some studies (e.g., Hanson et al. 1997) provide values of prey energy density (*habPreyEnergyDensity*) for various prey types, this parameter may be a good parameter to use for calibrating growth when there is no available information regarding the composition of trout-prey in the simulated reach. Varying this parameter changes the net energy gain of fish without altering either the food production rates of the cell or the food intake of individuals.

Parameters defining the criteria mature trout must meet to spawn (*fishSpawnMinCond, fishSpawnMaxFlowChange, fishSpawnMinTemp, fishSpawnMaxTemp, habMaxSpawnFlow*), as well as the stochastic probability of spawning when they are met (*fishSpawnProb)*, can be used to calibrate population fecundity (total production of eggs), and thus recruitment, pattern. However, the user must take into account that regulating the number and features of breeders may have potential effects on the evolution of heritable traits, since these model outputs are highly sensitive to spawning parameters.

# 4 Conceptual model evaluation

**This TRACE element provides supporting information on**: The simplifying assumptions underlying a model's design, both with regard to empirical knowledge and general, basic principles. This critical evaluation allows model users to understand that model design was not ad hoc but based on carefully scrutinized considerations.

**Summary:**

**InSTREAM-Gen's demographic structure builds on an existing rather complex model, inSTREAM, whose model concepts make however quite some simplifying assumptions. We discuss all the simplifying assumptions of the different demographic sub-models in detail. We further added a genetic dimension to the demographic and spatial dimensions of inSTREAM by including a quantitative genetic model of inheritance. Reasons for selecting a quantitative genetics approach instead of an allelic model are discussed.**

As remarked by Railsback et al. (2009), the first question a potential user of any model must address is whether the model is an appropriate tool for the research problem to be faced. Clearly, inSTREAM-Gen is not appropriate for study sites or problems where the model's fundamental assumptions are not met or where trout population dynamics are strongly

dependent on processes that are not represented, or represented only coarsely, in the model. Some examples of sites or problems where inSTREAM-Gen may not be appropriate (without modification) are: 1) sites where non-salmonid species are significant competitors for food or habitat; 2) sites where water quality elements other than temperature have strong effects or are the management issues of interest. Dissolved oxygen, for example, is not considered, nor the effects of fine sediment on egg incubation; 3) sites where the effects of ice are important. Ice can cause direct mortality, alter or exclude habitat, reduce invertebrate food production via scouring, and provide protection from predation. None of these processes are now included in inSTREAM-Gen, in part because they are difficult to model; even the presence of ice is difficult to predict, and how it will change under global warming is even more uncertain.

In addition to those limitations inherited from inSTREAM, inSTREAM-Gen was simplified in relation to inSTREAM by restricting simulations to only one modelled reach and one trout species. Therefore, the effects of river fragmentation or interspecific competition in sympatric salmonid populations cannot be simulated with the current version of inSTREAM-Gen. Furthermore, one environmental variable, water turbidity, is not taken into account in inSTREAM-Gen. Turbidity can have both positive and negative effects: increasing turbidity reduces the risk of predation on trout but reduces their ability to feed. Unfortunately, time series of water turbidity are not typically available in most river systems.

We describe below the main simplifying assumptions underlying the design of the different processes represented in the model:

- *Reproduction*:

Spawning is included in inSTREAM-Gen because the model's objectives require simulation of the full life cycle and multiple trout generations, and of the effects of flow and temperature on reproduction. Salmonids are clearly capable of adapting some of their reproductive behaviours to environmental conditions and their own state, especially by deciding whether or when to spawn each year considering their current size and condition and habitat conditions (e.g., Nelson et al. 1987). However, inSTREAM-Gen's objectives do not entirely justify a detailed representation of such processes as the bioenergetics of spawning or the adaptive decision of whether to spawn each year considering the fish's current state and expected growth and mortality risks. Instead, inSTREAM-Gen's spawning methods simply force model trout to reproduce general spawning behaviours observed in real trout. Behaviours are included only if they appear important for simulating flow and temperature effects on reproduction or for representing the consequences of spawning on the adult spawners.

In inSTREAM-Gen, each day, each female trout decides whether to spawn or not. To do this, each female trout determines whether it meets all of the fish- and habitat-based spawning criteria. The criteria for readiness to spawn, however, do not include a requirement that good spawning habitat be available; it is assumed that trout will spawn whether or not ideal gravel spawning habitat is present. This assumption is supported by observations reported by Magee et al. (1996).

While selection of habitat for foraging is modelled very mechanistically, selection of spawning habitat is modelled in a simple, empirical way, with spawning cells chosen using preferences for depth, velocity, and substrate observed in real trout. This decision was made because a detailed, mechanistic representation of spawning habitat selection would require considerable additional complexity: modelling processes such as intergravel flow and water quality, which are extremely data-intensive and uncertain. This additional complexity is not necessary to meet inSTREAM-Gen's objectives, but we do need a simple representation of

how flow affects where redds are placed because a redd's location affects its survival of dewatering.

When a female spawns, it attempts to select a (user-specified) number of males to fertilize the eggs. However, if no male meets the criteria as a spawner, there is no effect on the female or redd. The female still produces a fertile redd and incurs weight loss due to spawning. This assumption is made because spawning failure due to absence of males is considered too rare and unpredictable to include in the model.

- *Habitat selection*:

One element of competition for food or space is not included in inSTREAM-Gen. Some literature indicates that individuals have an inherent tendency to stay in one location ("site fidelity") and that prior residence of a site increases the ability of a trout to defend the site from larger competitors (Cutts et al. 1999, Johnsson et al. 1999, Johnsson and Forser 2002). However, prior residence effects on dominance are not clearly universal; and it is possible for them to be reproduced in an IBM without being hardwired in. For example, large trout may appear to exhibit site fidelity simply because their habitat offers very high fitness under a wide range of flows and temperatures, so they rarely have incentive to move. This element of competition is not explicitly included in inSTREAM-Gen because it is not clearly important and because doing so would require assumptions and parameters for which there is little basis.

- *Feeding and growth*:

Food production is modelled using the simple assumption that both the concentration of food items in the drift and the production of search food items are constant over time and space. Therefore, these two variables are input as habitat parameters. How food is produced in specific habitats such as riffles, and depleted by fish as it travels downstream, has been simulated in other models (e.g., Hughes 1992b). However, the model of Hughes (1992b) shows that simulating drift production and depletion over space would require a major increase in the complexity, while the simpler approach used in inSTREAM-Gen appears to generally capture the important dynamics of food competition.

Fish in inSTREAM-Gen are assumed to always feed during daylight hours and never at night, a major simplifying assumption. While trout have long been thought of as feeding visually and therefore during day, recent literature shows that night feeding is not unusual and under some conditions is more common than daytime feeding (e.g., Fraser and Metcalfe 1997, Metcalfe et al. 1999, Bradford and Higgens 2001). Whether an individual trout feeds during day or night (or neither) appears to emerge from how mortality risk and food intake vary between day and night, which can in turn vary with fish size, competition, and many habitat variables (Railsback et al. 2005). Modelling this requires a major increase in the model's complexity, which does not appear justified by the objectives of inSTREAM-Gen. While the assumption that trout feed during daytime only is clearly not always realistic, it is useful for the purposes that inSTREAM-Gen is intended for.

InSTREAM-Gen does not specify the exact kinds of food consumed by fish, but its feeding formulation and parameters generally represent invertebrate food. Even though the model assumes small fish are vulnerable to predation by adult trout, fish generally do not make up a large part of the diet of stream trout. Therefore, piscivory is not represented in the feeding methods, but only in the mortality submodel.

In inSTREAM-Gen, a fish updates its length and condition factor based on its daily weight growth. How an organism allocates its energy intake to growth (increase in length), storage (increase in weight or fat reserves but not length), or gonads is in reality a complex, adaptive decision. For example, a juvenile fish may reduce its risk of predation most by increasing in length as rapidly as possible, but allocating all energy intake to growth instead of storage increases the risk of starvation during periods of reduced intake. However, inSTREAM-Gen does not model energy allocation as an adaptive trait. Instead it uses the approach of Van Winkle et al. (1996) that simply forces fish to maintain a standard relation between length and weight during periods of positive growth.

The method for calculating daily change in length adopted from Van Winkle et al. (1996) uses their nonstandard definition of a condition factor. The condition factor variable used in inSTREAM-Gen (*fishCondition*) can be considered the fraction of "healthy" weight a fish is, given its length, according to a length-weight relation input to the model. Consequently, the value of *fishCondition* is 1.0 when a fish has a "healthy" weight for its length. Fish grow in length whenever they gain weight while their value of *fishCondition* is 1.0. Condition factors less than 1.0 indicate that the fish has lost weight, but in this formulation, values of *fishCondition* cannot be greater than 1.0 (contrarily to the standard condition factor used in fisheries science, which is a unitless index of a fish's weight relative to its length). This formulation is simple and succeeds in producing reasonably realistic patterns of trout growth under many conditions. However, as noted by Railsback et al. (2009), the formulation has several noteworthy limitations as well: 1) fish cannot store a high-energy-reserve condition. Fish will have a condition of 1.0 only on those days when daily growth is positive. Even if a fish has eaten well for many days in succession, its *fishCondition* can only be as high as 1.0 and one day of negative net energy intake causes condition to fall below 1.0. This could be important under conditions of highly variable food intake because survival is assumed to decrease with condition; 2) this weight-based condition factor is not the best predictor of starvation mortality. Simpkins et al. (2003a,b) found that mortality was predicted better by an index of lipid content than by the condition factor; 3) this formulation locks in a length-weight relationship for growing fish. Calibration of growth to situations where this relationship is valid will be automatic, but calibration to situations where the relationship is not valid will be impossible. For example, the model cannot predict the existence of unusually fat fish; 4) as previously highlighted, the energetics of reproduction are not considered. While inSTREAM-Gen does simulate weight loss due to spawning, it does not model storage of energy for gonad development and how gonad production affects length and weight.

These limitations could be eliminated only by making inSTREAM-Gen considerably more complex. In their individual-based Atlantic salmon model (IBASAM), Piou and Prévost (2012) represented energy allocation more realistically by diverting a portion of weight growth to fat reserves. Then, they successfully implemented the approach of Thorpe et al. (1998) in which maturation is modelled based on a time window evaluation of the rate of change in lipid content and a comparison of a projected lipid content at a given time horizon with a set threshold. The authors additionally considered genetic variability of maturation thresholds. In inSTREAM-Gen the maturation threshold is also variable across individuals and sexes and heritable, but size-based (defined by a minimum length to spawn). We considered that Piou and Prévost's approach, although more realistic, would exponentially increase not only the complexity of inSTREAM-Gen but also the uncertainty in its growth and reproduction processes due to the lack of available data for stream-dwelling trout regarding the high number of parameters involved in such representation. The current formulation appears adequate and appropriate for inSTREAM-Gen's objectives.

Unlike some previous models of drift feeding, inSTREAM-Gen neglects prey size as a variable. Prey size is naturally variable and unpredictable, and its effects could not be easily be distinguished from those of other factors. Actively searching for benthic or drop-in food is an alternative to the drift-feeding strategy. Unlike drift feeding, there are no established models for search feeding by trout. An optimal foraging approach would be to assume fish search for food at a rate that maximizes the difference between energy intake from feeding and energy cost of swimming. To avoid the complexity of such an approach, inSTREAM-Gen simply assumes that the rate of search food intake is proportional to the rate at which search food becomes available: every fish searches for food at about the same rate, so intake increases linearly with food production.

A major simplification on inSTREAM-Gen's bioenergetics formulation is that it does not include terms for energy losses due to egestion, excretion, and specific dynamic action. These terms are not included in inSTREAM-Gen because their effects are small compared to the uncertainties and variability in food availability and in the feeding and growth formulation (Bartell et al. 1986). These terms may be important at extremely low or high temperatures when the ability to digest food can limit growth; instead, inSTREAM-Gen uses the *cMax* function to limit food consumption at extreme temperatures.

The energy density of fish (*fishEnergyDensity*) is used to convert a fish's net energy intake to growth in weight. The energy density of salmonids actually varies through their life cycle (typically higher in adults, especially during gonad development prior to spawning), but this variation is ignored in inSTREAM-Gen.

- *Fish survival*:

Fish in poor condition are at risk of starvation, disease, and excess vulnerability to predators. These risks are combined in the poor condition survival probability, which is a function of the trout's condition factor. But as commented before, previous studies indicate that mortality is predicted better by an index of lipid content than by the condition factor, partly because water replaces lipids as energy stores are depleted. Unfortunately, modelling how body lipids are depleted and replaced by water and related processes would add considerable complexity and uncertainty to inSTREAM-Gen, as they are not well understood. Representing poor condition survival probability as an increasing logistic function of the condition factor instead, provides a reasonable and successful alternative.

Regarding terrestrial predation, it is necessary to clarify that no temperature-based survival increase function is included in inSTREAM-Gen because there are no clear mechanisms that would cause terrestrial predation pressure (unlike fish predation) to change with temperature. As discussed by Railsback et al. (2009), there is not a good basis for assuming predator activity is lower in winter; most important terrestrial predators are warm-blooded and many do not hibernate. In fact, such predators need additional food to maintain their metabolic needs in winter. The reduced swimming ability of trout at low temperatures can also offset any decreased activity by predators by reducing the ability of trout to escape (Metcalfe et al. 1999). Terrestrial predation can be greatly reduced when rivers freeze over, but ice is not represented in the model.

There is no survival increase function for distance to hiding cover in the aquatic predation formulation. This decision was made because only small trout are usually vulnerable to aquatic predators, and small trout are capable of hiding in many places that do not offer refuge to adult trout (e.g., between relatively small cobbles).

Two assumptions are needed to implement the predator density survival increase function within the aquatic predation survival formulation. First, a definition of piscivorous trout must be assumed. Any trout with length greater than the parameter *fishPiscivoryLength* is assumed to be a potential predator on smaller trout. This is a simplification, because in reality the larger a fish becomes, the larger prey fish it potentially can consume. The second assumption is choosing the spatial scale over which trout predation is represented. Predator density could be represented in inSTREAM-Gen at the cell or reach scales. The reach scale was chosen because large, piscivorous trout are likely to foray and attack fish in other cells.

- *Redd survival and development*:

Because of its objectives as a management-oriented model, inSTREAM-Gen models redds with relatively little biological detail but with substantial detail in how stream flow and temperature affect egg incubation and survival. The following are among the processes that can affect salmonid spawning success (see, e.g., Groot and Margolis 1991) that are not considered explicitly in inSTREAM-Gen: 1) some eggs may be diseased, unspawned, unfertilized, or washed out of the redd during its construction; 2) eggs can be killed by a variety of predators and parasites; 3) gravel size, fine sediment, and water quality can affect egg survival and development rates. In particular, low flow of water through the redd can allow metabolic wastes to accumulate and kill eggs. Deposition of fine sediment can prevent newly hatched fish from emerging; 3) salmonids go through several life stage transformations while in their redds. The most important of these is the transformation from eggs into alevins, which have respiratory and movement capabilities.

Importantly, inSTREAM-Gen adopts an approach for predicting the probability of redd scouring or deposition from the empirical, reach-scale work of Haschenburger (1999). This approach was developed for gravel-bed channels and may not be appropriate for sites where spawning gravels occur mainly in pockets behind obstructions (where scouring is likely even less predictable). InSTREAM-Gen should be considered more uncertain for sites where populations are strongly limited by redd scouring, especially if spawning is limited to pocket gravels (but all models of trout populations or habitat are likely less useful at such sites).

With regard to mortality due to superimposition, for simplicity, inSTREAM-Gen currently assumes that superimposition is accidental with no bias for or against spawning over existing redds. The study by Essington et al. (1998) indicates that stream trout may indeed intentionally superimpose their redds over existing ones. The submodel's formulation could be modified to represent intentional superimposition and the complex effects that it might have, but there is currently little known about what factors (e.g., sediment quality, spawner density) might encourage intentional superimposition.

- *Emergence and genetic transmission of traits*:

In trout, egg size is strongly correlated with size of the offspring (Elliott 1984, Einum and Fleming 1999, Olsen and Vøllestad 2001). Larger offspring have improved competitive ability and higher survival relative to offspring from smaller eggs (Elliott 1984, Hutchings 1991, Wootton 1998). Variation among individuals in length at emergence was hence represented in inSTREAM because habitat selection (and, consequently, growth and survival) is modelled using a length-based hierarchy. In inSTREAM-Gen, length at emergence, aside from varying across individuals as in inSTREAM, is a heritable trait (as shown by genetic studies; see Carlson and Seamons 2008). Therefore, females with higher genotypic values of

length at emergence produce offspring with higher values too (though its phenotypic expression depends also on environmental variance). There is a trade-off, however, between egg size and fecundity as females have limited energy resources available for egg production and limited body cavity for accommodation of the eggs (reviewed by Klemetsen et al. 2003 and Jonsson and Jonsson 2011). In inSTREAM-Gen, this trade-off is simplistically modelled through the variable *eggsize-fecund-tradeoff*, defined as the relationship between the number of eggs that would be created by the trout if the offspring had the population mean length at emergence and such number if the offspring had the mother's genetic length at emergence. Egg size, and thus size at emergence, increases also with the size of the mother at spawning and water temperature (Klemetsen et al. 2003, Jonsson and Jonsson 2011), but those mechanisms are not represented in inSTREAM-Gen as there is no easy way to model them in a mechanistic way.

In inSTREAM-Gen, the inheritance rules for the transmission of heritable traits are based on a modified version of the infinitesimal model of quantitative genetics (Lynch and Walsh 1998). When mutation is not taken into account, each offspring's genotypic value for the two traits under selection in our model is drawn from a normal distribution centered on the arithmetic mean of the two parental values, while the variance of this distribution is equal to half the total additive genetic variance for the trait at the population level (i.e., the within-family additive variance remains constant). That is, the genetic model used here is not really following the genetic map of individuals since at some points the model draws certain values from population probabilistic distributions. The most commonly considered alternative model of inheritance is the allelic model, in which individual alleles are modelled as being passed on directly from parents to offspring. The advantages of this kind of model are that no assumptions are made about the offspring trait distribution, and it also permits specification of haploid vs. diploid inheritance of loci and the inclusion of nonadditive effects such as dominance and epistasis (see Dunlop et al. 2009). There are examples of effective implementation of a bi-allelic multilocus system for modelling the genetic coding of heritable traits in fish IBMs (e.g., Piou and Prévost 2012, Vincenzi 2014). As argued by Piou and Prévost (2012), this type of genetic coding has been shown to be a good trade-off between a purely quantitative approach and the detailed multi-allelic multilocus reality (Kopp and Gavrilets 2006). However, a quantitative genetics approach is typically used in eco-genetic models because most life-history traits are regarded as polygenic quantitative characters, which are assumed to be affected by a large number of genetic loci, each with small effects (see Dunlop et al. 2009 and references therein). The infinitesimal model of quantitative genetics, which accurately predicts evolutionary responses of polygenic traits to selection over timescales of tens of generations (Falconer and Mackay 1996), has been successfully used within an individual-based framework to model the evolutionary dynamics of life history traits of salmonid populations under environmental change (e.g., Reed et al. 2011).

# 5 Implementation verification

**This TRACE element provides supporting information on**: (1) whether the computer code for implementing the model has been thoroughly tested for programming errors and (2) whether the implemented model performs as indicated by the model description.

**Summary:**

**We followed a wise risk-management strategy, by which testing occurred continually as the code was being developed so that all parts of the software were tested before the model was put to use. These tests included syntax checking of**

**the code, visual testing through NetLogo interface, print statements, spot tests with agent monitors, stress tests with extreme parameters values, test procedures and test programs, and code reviews. The most important verification technique was, however, testing all submodels against independent versions re-implemented in a different platform. Finally, the ecological structure of the model was tested against inSTREAM IBM under the same simulation conditions.**

Since we considered software verification (i.e., verifying that the software accurately implements the model formulation) as a pervasive part of model programming, we followed a wise risk-management strategy, by which testing occurred continually as the code was being developed so that all parts of the software were tested before the model was put to use. We started building the most basic submodel (creation of cells, uploading of environmental and hydraulic time series, and update of cell and global variables dependent on these time series). After checking that it performed correctly, the next submodel was implemented, building on the already tested first submodel. We proceeded along the process of code development in the same way, sequentially implementing new submodels on the already tested assembled model. This practice made mistakes easier to identify and isolate. There were, of course, some logic and formulation errors that became apparent in a subsequent stage after a submodel had been already tested, since some procedures required the fully formulation of a later submodel to be accurately tested, but those errors were still easy to isolate.

We used all the techniques recommended by Railsback and Grimm (2012) for code debugging and testing. The tests executed to verify the implementation of the model ranged from very simple checks using the tools provided by the software platform NetLogo, to complex analyses. Tests included:

- *Syntax checking*:

The syntax of the code was frequently checked through the NetLogo syntax checker. Aside from checking for syntax errors, immediately after writing a full procedure or a complex statement, the program would be run to check for run-time errors.

- *Visual testing through NetLogo interface*:

Visual testing was continuously used to look for errors that may be readily visible from the display while being unlikely to be detected soon, if ever, via other methods. That ranged from simple procedures, as checking that cells correctly defined their adjacent cells, to more complex ones, like observing that trout agents performed some actions (e.g., movement) on a daily basis irrespective of the simulation being run with longer time steps.

- *Print statements*:

We programmed the model to print the value of some variables at different times to check that the model was behaving in the expected way. Basic examples are: asking the cells to write the value of the environmental and hydraulic variables to check that they match the expected value of that time step; asking the observer to output population and global parameter values after the setup to check that they are correctly initialized; or simply writing the number of trout agents at every time step to check that they are actually dying and leaving the model. The model was also programmed to print error statements when impossible results were yielded, such as a trout agent having either a negative length, weight or body condition after performing the feeding and growing action. Finally, the NetLogo extension “Time profiler” was used to monitor the time every procedure and reporter took to execute, as well as the number of times they were called at each time step, in order to isolate excessively time-consuming ones for streamlining purposes.

- *Spot tests with Agent Monitors*:

The agent monitors were used for quickly seeing agent state variable values and testing key calculations for obvious errors (e.g, drift-feeding trout failing to reduce their swimming speed when using velocity shelters, or trout failing to update their age-class at due time).

- *Stress tests*:

Tests using extreme parameter values were performed to expose errors that would have been hidden under normal conditions. Again, this technique ranged from soft to extreme tests. Soft tests included, for instance, using parameter values that would effectively turn off (or directly turning them off) some functions in order to check that model outputs actually give expected logical results (e.g., after turning off the genetic transmission model, genotypic values of heritable traits must be constant across generations), or using parameter values that should either let the population live forever or, on the contrary, make it quickly go to extinction (e.g., setting very low values of minimum survival probability from terrestrial and aquatic predation, which should lead the population to quickly become extinct). Under this stress testing, we verified, for instance, that without a correct defensive programming, survival functions may yield a run-time error under certain conditions. The most extreme tests were carried out during the global sensitivity analyses, when the model was tested against the simultaneous combination of extreme values from several key parameters. We observed that despite the fact that certain parameter combinations (simultaneous negligible terrestrial and aquatic mortality, over-availability of both kinds of food, extremely high fecundity) caused the model to have a number of trout agents over 250,000 (the maximum numbers recorded under normal conditions was around 6,000 agents), simulations were extremely slow (5 days against 30 minutes under normal conditions) but never caused the model to crash.

- *Test procedures*:

This technique consisted of the addition of new procedures to the code just to produce intermediate output, used only for testing. It was rarely used during model development.

- *Test programs*:

At some cases, it was convenient to write a separate short program under simplified conditions that served only to test a particular algorithm or procedure. For instance, the bioenergetics model underlying the feeding and growth submodel was first developed and implemented into the habitat selection procedure under simplified movement rules and no mortality. Only when it was already tested, the feeding and growth submodel was integrated with a fully developed version of the mortality submodel into a realistic habitat selection framework.

- *Simulation experiments*:

Several controlled simulation experiments were performed, in which the model or its parts were simplified so that the outcome of each experiment could be predicted and verified.

- *Code reviews*:

The code was peer-reviewed, i.e., it was thoroughly compared with the written formulation of the model by four other scientists (Drs V. Grimm, S. Railsback, J. Groeneveld, S. Vincenzi).

- *Independent reimplementation of submodels*:

This was the most important testing technique used during implementation verification. It was the way by which almost all critical implementation errors were detected. Along model development, all submodels were independently tested against a version re-implemented in

excel. To test each submodel, we added statements to the NetLogo code that write to a file the input to, and results from, the submodel. Then we imported that output file to an Excel spreadsheet, and reprogramed the submodel in the same spreadsheet. We finally compared the results produced by the Excel spreadsheet code to the results produced by the NetLogo code. Tests were performed under different testing conditions, varying the resolution (duration) of the time steps, initial numbers or conditions at initialization. The span of the simulation test depended on the submodel being tested. Table A12 summarizes all tests performed during model development. Likewise, all submodels were tested again after being assembled in the final version of the model (see Table A13). That helped finding some minor errors, which could only be noticed when all submodels were working altogether with their fully developed formulation. Final tests cover at least a cycle comprising the key processes (spawning, redd development, and emergence and transmission of traits). All Excel files containing the re-implemented codes and tests can be downloaded from here.

- InSTREAM-Gen *vs* inSTREAM - the final test:

InSTREAM-Gen is an IBM developed with an eco-genetic structure, whose ecological structure is a replicate of a previous IBM, inSTREAM (Railsback et al. 2009). Apart from the addition of a genetic architecture (a quantitative model of genetic transmission of two fitness-related heritable traits), the ecological structure of inSTREAM-Gen presents some simplifications and minor modifications in relation to inSTREAM. InSTREAM-Gen was simplified by restricting simulations to only one modelled reach and one trout species. In addition, one environmental variable, water turbidity, and thus all its derived effects on trout feeding and survival, are not taken into account in inSTREAM-Gen. On the other side of the track, we added to inSTREAM-Gen the angler mortality model, which was replicated from a recent version of inSTREAM (inSTREAM-SD V6.0) but it's not included in its regular version. There are also minor modifications, mainly concerning the reproduction process: 1) inSTREAM-Gen allows for both monogamous and polygamous mating systems, 2) male spawners can mate several times during the same spawning season and 3) they move to the cell where the female spawner creates the redd to fertilize it; besides, 4) the algorithm used by female spawners to select the spawning cell differs between both models. Another difference is that the cell state variable defining the distance from hiding cover (*cellDistanceToHide*) is dynamically updated every time step as a function of hydraulic conditions in inSTREAM-Gen while fixed in inSTREAM. The addition of the inheritance model allows for the genetic transmission of genotypic values of length at emergence and minimum length to spawn. Therefore, these two variables are no longer global parameters but state variables of trout. Since trout length at emergence is a heritable trait in the model and it is typically correlated to egg size, inSTREAM-Gen introduces the term *eggsize-fecund-tradeoff* to model the fact that in salmonids the number of eggs in a redd is traded-off with egg size. Contrarily to inSTREAM, minimum length to spawn can be variable across individuals (even if the genetic model is turned off) and sexes.

In short, since the ecological structure inSTREAM-Gen is a replicate of inSTREAM, both models should yield not significantly different results when the genetic transmission model of inSTREAM-Gen is turned off and both models are parameterized with the same parameter values. InSTREAM has been thoroughly tested and used in ecological research for more than 15 years. Therefore, we considered that the robustness of the ecological structure of inSTREAM-Gen would be proved if it behaved the same way as inSTREAM under the same simulation conditions and scenarios.

To test it, we ran in both models a 40 year-long simulation scenario using the parameter values described in the section "Data evaluation" of the present document. Values for calibrated parameters are described in the section "Model output verification". To make both models comparable, we tuned inSTREAM-Gen in the following way: the models for genetic transmission and angler mortality were turned off; the maximum number of males that can mate with a female spawner (*max-n-males-per-female*) was set to 1, and thus the largest available male spawner was always selected; the length maturity threshold (*fishSpawnMinLengthMean*) had the same value for males and females and their variance (*fishSpawnMinLengthVar*) was set to 0, so that all individuals in the system had the same length maturity threshold. On the other hand, we set a value of 0 for turbidity at every simulated day, so that this environmental variable did not have any influence on inSTREAM's simulations. Both models were initialized in the same way, but we did not force them to have the same values for stochastic elements, so the initial position as well as size and sex distribution of individuals differed across models at initialization.

**Table A12.** Re-implementation tests performed for independent submodel verification.

| Excel output file | NetLogo file | date | Test name | Conditions | Purpose |
|---|---|---|---|---|---|
| Testing Environment | Testcells_nopatches_array_headings_Outputtest_Time | 14/8/2013 | TestInicellsTime | 573 ticks * | Check that habitat and identity features are assigned correctly from the input files to the cells (using Time extension) |
| | | | TestSimcellsTime | | Check that habitat features are correctly updated during the simulation (using Time extension) |
| | | | TestEnvironTime | | Check that environmental features are correctly updated during the simulation (using Time extension) |
| Testing feeding hierarchy | Cells_feeding_growth | 19/8/2013 | cellEnergetics/Trout | 10 trout 60 ticks * | Check that feeding hierarchy is correctly implemented |
| Testing growth | | 22/8/2013 | Size before-after | 10 trout 573 ticks * | Check that trout's body size variables are correctly updated |
| | | 23/8/2013 | EnergeticsBeforeSelection | 1 trout 573 ticks * | Check that bioenergetics local variables are correctly calculated and updated for trout of different size |
| | | | bestEnergyIntake/TestOutputTroutBefore | | Check that trout actually select the cell with the highest best energy intake |
| | | | TestOutputTroutBefore | | Check that trout's body size variables are correctly updated and Trout actually select the cell with the highest best energy intake |
| | | | TestOutputTrout/Pivot table | 5000 trout 573 ticks * | Check that model doesn´t crash and feeding hierarchy correctly implemented (CV size variables must increase with time) |
| Testing mortality functions | Cells_mortality | 19/11/2013 | Mortality functions | 100 trout 100 ticks * | Check that survival probability is correctly calculated and that trout die when random number is higher than mortality probability |
| | cells-mortality_fishing_Testoutput | 25/11/2013 | Angling | 100 trout 150 ticks * | Check that angling and hooking mortality is correctly calculated and trout die when they must |
| Testing habitat selection | Cells_growth_mortality_habselection_switches | 3/12/2013 | HabitatSelection | 50 trout 30 ticks * | Check that starvSurvival, nonstarvSurvival and expected maturity are correctly calculated |
| Testing Spawning | Cells_growth_mortality_habselection_spawning_OUTPUT | 28/1/2014 | BecomeSpawner | 250 trout 573 ticks * | Check that trout only get the status of spawner if, and only if, they meet the required criteria |
| | | | CellsSpawningQuality | | Check that the spawning quality of cells is correctly calculated |

| | | | | | |
|---|---|---|---|---|---|
| | | | MaleSpawnersSelection | | Check that candidate spawners are correctly discriminated from non-candidate ones based on their probability of selection |
| | | | MaleSpawnerSelection2 | | Check that the number of selected male spawners is never higher than the maximum number of male spawners per female to be selected |
| | | | MaleSpawnerSelection2 | | Check that spawners from the non-candidate spawners agentset are correctly selected when needed |
| | | | MaleSpawnersAfterSelection | | Check that all trout which have spawned update their body condition and effectively change their "spawned this season?" status to "True" |
| | | | Redds | | Check that the number of eggs calculated is correct |
| | | 2/3/2014 | Redds2 | | Check that genetic length at emergence and minimum length for spawning are correctly transmitted from "fathers"to the redd |
| Testing Redd Survival | Cells_growth_mortality_habselection_spawning_redddev_OUTPUT | 12/2/2014 | Bernoulli | 250 trout 35 redds 65 ticks * | Calculate the number of lost eggs due to different mortality sources when it cannot be aproximated by the product of number of inicial eggs times the probability of survival of an egg |
| | | | Superimposition | | Calculate the number of lost eggs due to superimposition |
| | | | Redd Surv | | Check that the number of eggs lost by different mortality sources and so the final number of eggs surviving in the redd are correctly calculated |
| Testing Emergence & Transmission Sex | Cells_growth_mortality_habselection_spawning_redddev_emergence_sexmaturity_OUTPUT | 20/3/2014 | HatchingEggs | 350 trout 124 redds 573 ticks * | Check that the number of eggs hatching every time step and the eggs remaining in the redd are calculated correctly |
| | | | Breeders | | Check that the variance of the trait's genotypic values from breeders are calculated correctly by the hatching procedure |
| | | | redds | | Check that the genetic info is transmitted correctly from the redds to new trout |
| | | | Transmission | | Check that genetic state and local variables are calculated correctly |
| Testing habitat selection UPSCALING | Cells_growth_mortality_habselection_spawning_redddev_emergence_sexmaturity_upscaling4b_OUTPUT | 24/3/2014 | HabitatSelection | 350 trout 2 ticks * | Check that expected maturity is correctly calculated after upscaling and optimizing the code |
| Testing | Cells_growth_mortality_habsel | 3/4/2014 | Transmission | 250 trout | Check that genetic state and local variables are calculated correctly after |

| | | | | |
|---|---|---|---|---|
| TransmissionSexUPSCALING | ection_spawning_redddev_emergence_sexmaturity_upscaling_genetics2_OUTPUT | | 573 ticks * | upscaling and optimizing the code |
| | | Breeders | | Check that the variance of the trait's genotypic values from breeders are calculated correctly by the hatching procedure after upscaling and optimizing the code |

* Each tick corresponded to a weekly time step

**Table A13.** Re-implementation tests performed for submodel verification in the final model version.

| Excel output file | NetLogo file | date | Test name | Conditions | Purpose |
|---|---|---|---|---|---|
| 0.Testing cellsFood whole time series | 12_Whole model Test | 3/6/2014 | FoodTest | 150 trout * 4070 ticks ** | Check that available drift and search food are correctly updated after being consumed |
| 1.Testing habitat selection | 12_Whole model Test | 19/6/2014 | HabitatSelection | 150 trout * 365 ticks ** | Check that starvSurvival, nonstarvSurvival and expected maturity are correctly calculated |
| 1.Testing habitat selection debugged | 12_Whole model Test Debugged | 21/7/2014 | HabitatSelection | 150 trout * 365 ticks ** | Check that starvSurvival, nonstarvSurvival and expected maturity are correctly calculated |
| 2.TestAdjacentCells | | | Pivot/TestAdjacentCells | 140 cells 4070 ticks * | Check that the number of adjacent cells and their identity are the same each tick for each cell |
| 3.TestDestinationCells | | | | 100 trout * 4070 ticks ** | Check that all potential destination cells are really within the max distance or are adjacent cells |
| 2.Testing growth | 12_Whole model Test | 19/6/2014 | Size before-after | 150 trout * 365 ticks ** | Check that trout's body size variables are correctly updated after feeding and growing |
| | | | Comp | | Trout actually select the cell with the highest expected maturity |
| 3.Testing mortality | 12_Whole model Test | 19/6/2014 | Mortality functions | 150 trout * 474 ticks *** | Check that survival probability is correctly calculated and that trout die when random number is higher than mortality probability |
| 3. Testing Angling mortality | | 20/6/2014 | Angling | 150 trout * 2195 ticks *** | Check that angling and hooking mortality is correctly calculated and trout die when they must |
| 4.Testing Become Spawner (spawning season over 2 nat yr) | 12_Whole model Reproduction Test | 20/6/2014 | BecomeSpawner | 350 trout * 1948 ticks ** | Check that trout only get the status of spawner if, and only if, they meet the required criteria, when the spawning season covers two natural years (from December year x to January year x+1) |
| 4.Testing Spawning | 12_Whole model Reproduction Test WO Redd outputs | 20/6/2014 | CellsSpawningQuality | 350 trout * 2190 ticks ** | Check that the spawning quality of cells is correctly calculated |
| | | | MaleSpawnersSelection | | Check that candidate spawners are correctly discriminated from non-candidate ones based on their probability of selection |
| | | | MaleSpawnerSelection2 | | Check that the number of selected male spawners is never higher than the maximum number of male spawners per female to be selected |

| | | | | | |
|---|---|---|---|---|---|
| | | | MaleSpawnerSelection2 | | Check that spawners from the non-candidate spawners agentset are correctly selected when needed |
| | 12_Whole model Reproduction Test WO Redd outputs_NewMaleSelAlgorithm | 18/08/2014 | MaleSpawnerSelection3 | 350 trout * 2190 ticks ** | Check that 1) the largest male spawner is always selected to fertilize the eggs, 2) the number of selected male spawners is never higher than the maximum number of male spawners per female to be selected, and 3) spawners from the non-candidate spawners agentset are correctly selected when needed |
| | | | MaleSpawnerSelection3(2) | 350 trout * 4070 ticks ** | Check that 1) the largest male spawner is always selected to fertilize the eggs, 2) the number of selected male spawners is never higher than the maximum number of male spawners per female to be selected, and 3) spawners from the non-candidate spawners agentset are correctly selected when needed |
| 5.Testing Redd Survival | 12_Whole model Reproduction Test | 19/6/2014 | Bernoulli | 350 trout * 1948 ticks ** | Calculate the number of lost eggs due to different mortality sources when it cannot be aproximated by the product of number of inicial eggs times the probability of survival of an egg |
| | | | Superimposition | | Calculate the number of lost eggs due to superimposition |
| | | | Redd Surv | | Check that the number of eggs lost by different mortality sources and so the final number of eggs surviving in the redd are correctly calculated |
| 6.Testing Transmission | 12_Whole model Reproduction Test WO Redd outputs | 20/6/2014 | Breeders | 350 trout * 2032 ticks ** | Check that the variance of the trait's genotypic values from breeders are calculated correctly by the hatching procedure |
| | | | Transmission Fixed Var | | Check that genetic state and local variables are calculated correctly when additive variance is fixed across generations |
| | | | Transmission Not Fixed Var | | Check that genetic state and local variables are calculated correctly when additive variance is NOT fixed across generations |

* Number of trout agents at initialization; ** Each tick corresponded to a daily time step.

We generated time series for water temperature, flow and cells' hydraulic conditions (water depth and velocity) for the 1993-2033 time period. We used the real data collected by the closest meteorological (Urzainqui, AEMET) and gauging (Isaba, Navarra Government) stations to generate the water temperature and flow time series for the 1993-2011 period. Time series for the 2012-2033 period were thus projected. Water temperatures were projected using the air temperature projections developed by the AEMET (Spanish National Meteorological Agency) for the Urzainqui meteorological station under the B2 SRES emission scenario (Brunet et al. 2009). We used the regional air temperature projections derived through statistical downscaling techniques based on the ECHAM4 Global Climate Model data (see Brunet et al. 2009). Since there is too much uncertainty about whether and how flow patterns may change in our study area due to future climate change, we used historical flow data to develop the projected flow time series. That is, we did not simulate changes in flow regime induced by climate change. We analyzed the available historical flow time series (1992-2011) by means of the IHA v7.1 software (The Nature Conservancy) to estimate the probability that a hydrological year presented extreme low flows (0.158), small floods (0.368), large floods (0.053), and extreme low flows together with large floods (0.053). Thus the probability of a hydrological year having only low flows was 0.368. Each year of the 1992-2011 time series was assigned to one of these five categories. We then randomly selected the flow regime from one of those initial years every year for the 2012-2033 time period, the probability of selection depending on the probability of occurrence of the environmental flow event (extreme low flows, low flows, small floods, large floods, and extreme low flows together with large floods). That is, the 2012-2033 flow time series is a probabilistic randomized version of the 1992-2011 series. Hydraulics time series were calculated using the projected flow time series by means of the depth-flow and velocity-flow relationships generated by the PHABSIM v.1.5.1 software (Milhous and Waddle 2012).

We compared across models 17 model outputs: time series of 12 demographic patterns (abundance, length-at-age and biomass of four age-classes), and 5 reproduction patterns (mean length of female spawners, number of redds created, initial number of viable eggs, number of hatched eggs and proportion of hatched eggs).

This test was fundamental for the development of the model as it allowed for the detection of a few minor but also one serious bug in the code. First simulations showed significant discrepancies in the numbers and biomass of age-0 trout because of differences in the mortality rates owing to starvation. After thorough review of the code and exhaustive new testing, which resulted in a long delay in model development, we detected a critical bug in the procedure defining potential destination cells during the habitat selection action. This error in the code led to reduced dispersal of new emerged trout and thus increased competion and higher mortality owing to low body condition.

After all bugs were fixed, we repeated the simulations to compare both models. The simulated time series of the 12 demographic patterns were pretty similar, almost identical, across models (Table A13; Figs. A1-3).

**Table A13.** Mean values and 95% confidence intervals for the mean of 12 demographic model outputs (abundance, length-at-age and biomass time series, broken out by 4 age-classes) over 40-year simulations (1993-2033) and 10 replicates from inSTREAM and inSTREAM-Gen IBMs.

| | Abundance (trout) | | Length (cm) | | Biomass (g) | |
|---|---|---|---|---|---|---|
| | *inSTREAM* | *inSTREAM-Gen* | *inSTREAM* | *inSTREAM-Gen* | *inSTREAM* | *inSTREAM-Gen* |
| Age-0 | 223.1 | 222.5 | 7.48 | 7.62 | 1131.8 | 1195.1 |
| | (218.7-227.5) | (218.1-226.8) | (7.45-7.52) | (7.59-7.66) | (1107.6-1156.0) | (1171.5-1218.8) |
| Age-1 | 60.0 | 58.8 | 12.13 | 12.14 | 1134.2 | 1111.8 |
| | (58.8-61.2) | (57.7-60.0) | (12.09-12.17) | (12.10-12.18) | (1108.0-1160.4) | (1086.1-1137.6) |
| Age-2 | 19.2 | 18.6 | 17.36 | 17.41 | 1078.5 | 1047.0 |
| | (18.7-19.8) | (18.1-19.1) | (17.29-17.43) | (17.34-17.48) | (1046.0-1111.0) | (1015.4-1078.6) |
| Age-3Plus | 12.8 | 12.6 | 23.97 | 24.10 | 2081.5 | 2102.6 |
| | (12.4-13.2) | (12.2-13.0) | (23.86-24.08) | (23.98-24.21) | (2007.4-2155.7) | (2026.5-218.8) |

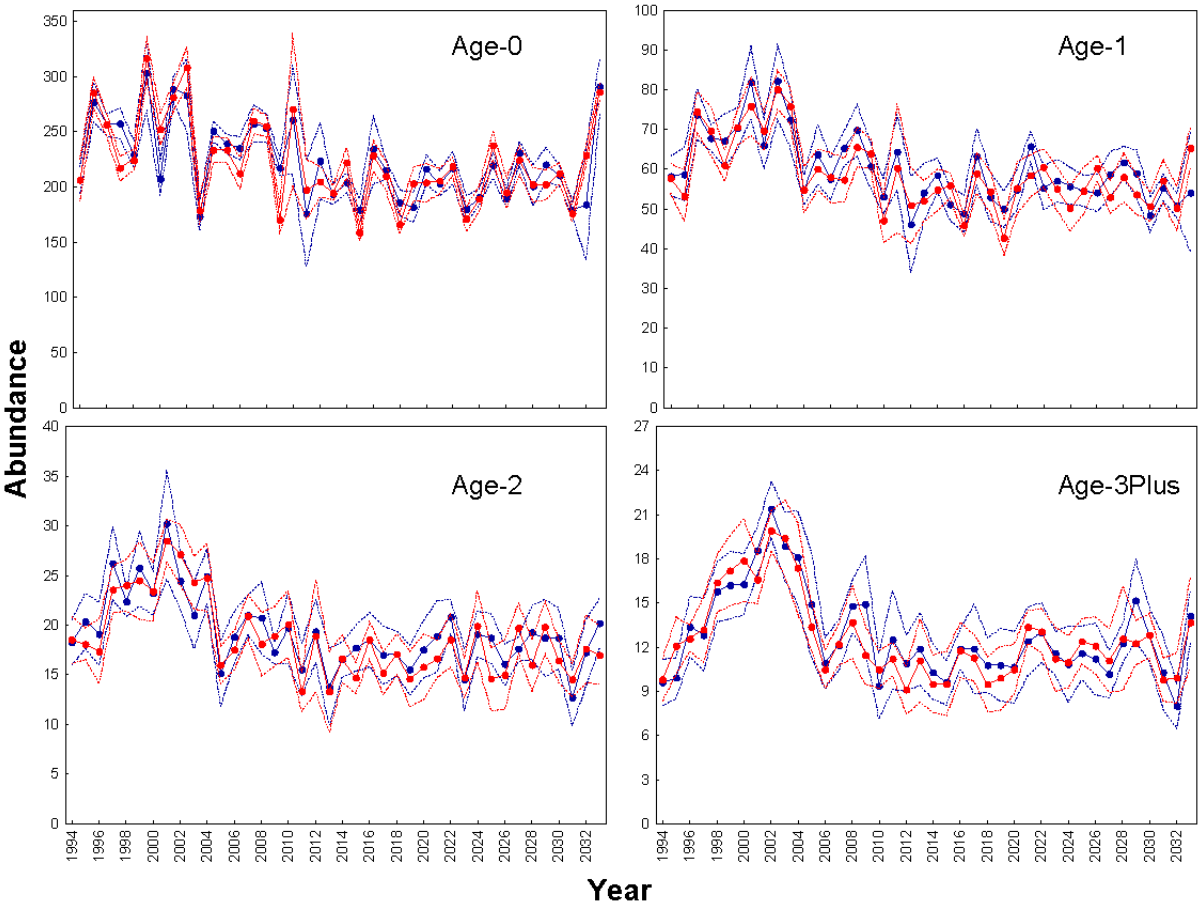


**Figure A1.** Mean values and 95% confidence intervals for the mean of simulated abundances of 4 age-classes over 40-year simulations (1993-2033) and 10 replicates from inSTREAM (blue line) and inSTREAM-Gen (red line) IBMs.

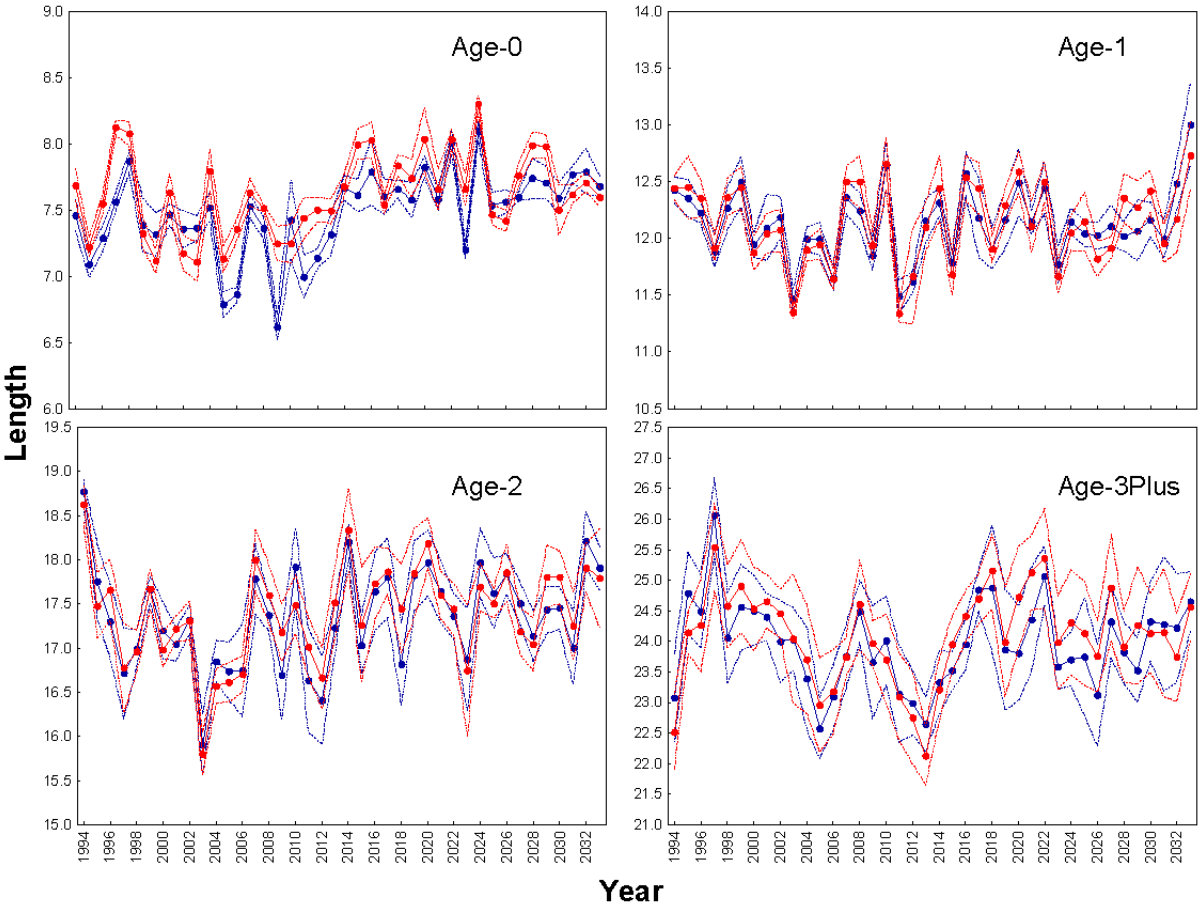


**Figure A2.** Mean values and 95% confidence intervals for the mean of simulated length-at-age of 4 age-classes over 40-year simulations (1993-2033) and 10 replicates from inSTREAM (blue line) and inSTREAM-Gen (red line) IBMs.

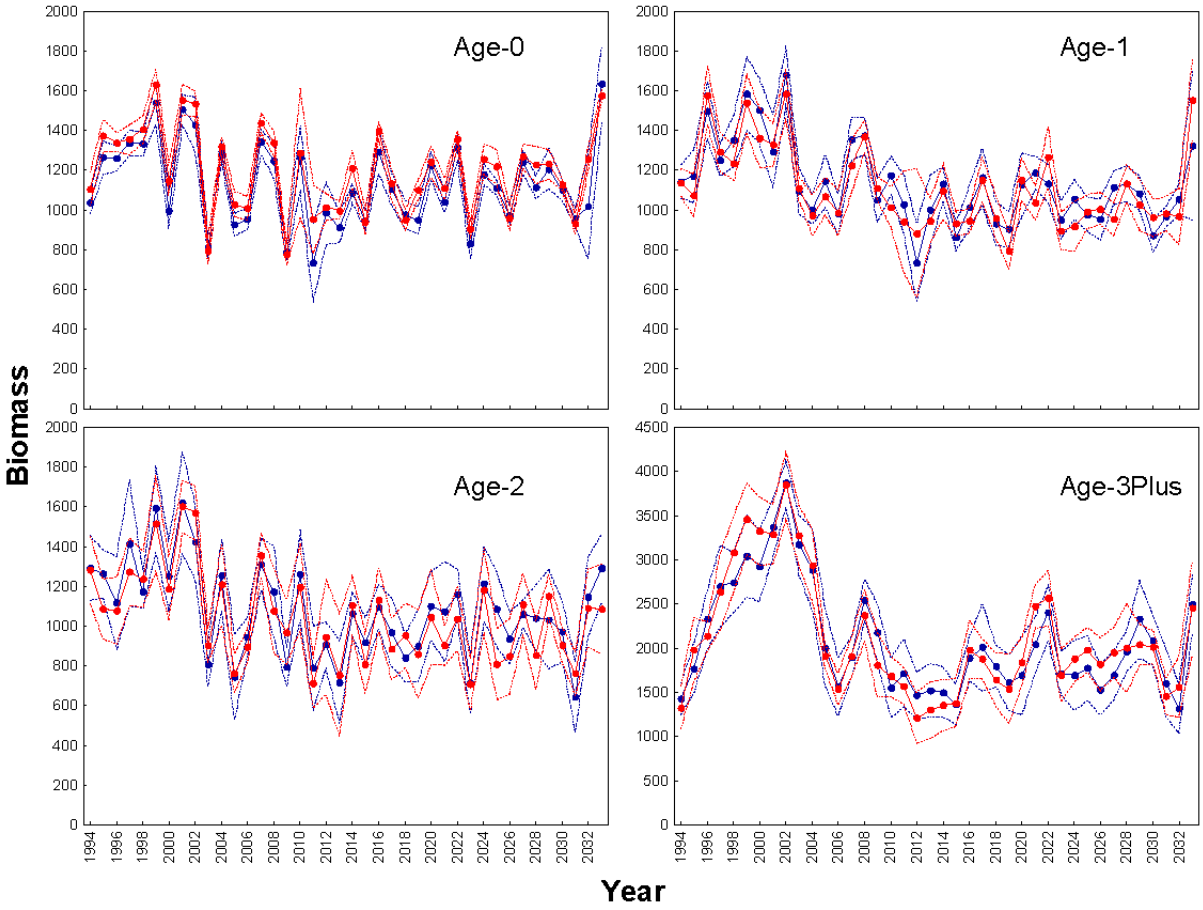


**Figure A3.** Mean values and 95% confidence intervals for the mean of simulated biomasses of 4 age-classes over 40-year simulations (1993-2033) and 10 replicates from inSTREAM (blue line) and inSTREAM-Gen (red line) IBMs.

The interannual variations in all 12 demographic outputs predicted by both models were highly and significantly correlated (Table A14). We only detected significant differences between models in the means of simulated length-at-age of age-0 trout, and consequently in age-0 biomass too (Table A15). InSTREAM-Gen predicted slightly (but significantly) higher fork lengths for age-0 trout. Nevertheless, the discrepancy in the mean predicted value of length-at-age of age-0 trout over time between both models was only 1.5% (Table A13). This small discrepancy is probably due to a slight difference in the number of emerged fry.

**Table A14.** Correlation coefficients and their probabilities (*** P<0.001) from time series cross-correlation analyses of 12 demographic model outputs (abundance, length-at-age and biomass time series, broken out by 4 age-classes) averaged over 10 replicates between inSTREAM and inSTREAM-Gen models.

| **Pattern\Age-class** | Age-0 | Age-1 | Age-2 | Age-3Plus |
|---|---|---|---|---|
| Abundance | 0.88 *** | 0.87 *** | 0.89 *** | 0.92 *** |
| Length | 0.58 *** | 0.65 *** | 0.75 *** | 0.86 *** |
| Biomass | 0.96 *** | 0.90 *** | 0.90 *** | 0.95 *** |

**Table A15.** Summary of comparison of 12 demographic model outputs (abundance, length-at-age and biomass time series, broken out by 4 age-classes) across models (inSTREAM *vs* inSTREAM-Gen), replicates (10 replicates) and its interaction (model x replicate), using factorial analysis of variance (ANOVA).

| **Pattern** | Model | | Replicate | | Model x Replicate | |
|---|---|---|---|---|---|---|
| | *F* | *P* | *F* | *P* | *F* | *P* |
| Age-0 | | | | | | |
| *Abundance* | 0.04 | 0.84 | 0.15 | 1.0 | 0.25 | 0.99 |
| *Length* | 33.0 | <0.001 | 0.30 | 0.96 | 0.20 | 0.99 |
| *Biomass* | 13.3 | <0.001 | 0.06 | 1.0 | 0.11 | 1.0 |
| Age-1 | | | | | | |
| *Abundance* | 1.91 | 0.17 | 0.27 | 0.98 | 0.25 | 0.99 |
| *Length* | 0.10 | 0.72 | 0.80 | 0.62 | 0.60 | 0.76 |
| *Biomass* | 1.41 | 0.24 | 0.19 | 1.0 | 0.18 | 1.0 |
| Age-2 | | | | | | |
| *Abundance* | 2.92 | 0.10 | 0.13 | 1.0 | 0.34 | 0.96 |
| *Length* | 0.90 | 0.35 | 0.60 | 0.82 | 0.50 | 0.90 |
| *Biomass* | 1.85 | 0.17 | 0.28 | 0.98 | 0.50 | 0.88 |
| Age-3Plus | | | | | | |
| *Abundance* | 0.74 | 0.39 | 0.45 | 0.91 | 0.50 | 0.87 |
| *Length* | 2.50 | 0.11 | 0.70 | 0.70 | 1.00 | 0.40 |
| *Biomass* | 0.16 | 0.69 | 0.43 | 0.92 | 0.30 | 0.98 |

The simulated time series of the five reproduction patterns were again nearly identical across models (Tables 16-18). The interannual variations in the five reproduction outputs predicted by both models were highly and significantly correlated (Table A17).

**Table A16.** Mean values and 95% confidence intervals for the mean of 5 reproduction model outputs over 40-year simulations (1993-2033) and 10 replicates from inSTREAM and inSTREAM-Gen IBMs.

| | *inSTREAM* | *inSTREAM-Gen* |
|---|---|---|
| Mean length female spawners (cm) | 21.1 (21.0-21.2) | 21.1 (20.9-21.2) |
| Number of redds | 9.8 (9.5-10.2) | 9.6 (9.2-9.9) |
| Initial number of viable eggs | 3273.8 (3121.3-3424.4) | 3179.2 (3030.0-3328.4) |
| Number of hatched eggs | 2563.7 (2442.9-2684.5) | 2618.0 (2493.3-2742.8) |
| Ratio hatched eggs/number eggs (%) | 78.3 (77.8-78.8) | 82.5 (82.0-83.1) |

**Table A17.** Correlation coefficients and their probabilities (*** P<0.001) from time series cross-correlation analyses of 5 reproduction model outputs averaged over 10 replicates between inSTREAM and inSTREAM-Gen models.

| **Pattern** | **Correlation** |
|---|---|
| Mean length female spawners (cm) | 0.93 *** |
| Number of redds | 0.78 *** |
| Initial number of viable eggs | 0.95 *** |
| Number of hatched eggs | 0.95 *** |
| Ratio hatched eggs/number eggs (%) | 0.90 *** |

We detected, however, significant differences in the mean ratio of hatched eggs to initial number of viable eggs (Table A18), because the algorithm used to model the selection of the spawning cell by female spawners differs between inSTREAM and inSTREAM-Gen. The algorithm used by inSTREAM results in a higher density of redds laid in fewer spawning cells, so that the number of dead eggs owing to superimposition is higher, and consequently the number of surviving eggs is lower than in inSTREAM-Gen. Therefore, the number of fry emerged is slightly, but not significantly, higher in inSTREAM-Gen. As a result, mortality owing to starvation during the critical period (see Elliott 1994) is higher in inSTREAM-Gen, simulated numbers of age-0 trout after this period being hence lower (below the cohort's thinning-line). Due to the operation of emergent density dependence, age-0 trout simulated by inSTREAM-Gen would have higher growth rates during the time lag between the end of the critical period and the moment when the cohort reaches again the thinning-line. We suggest that could be the reason why simulated length-at-age of age-0 trout differs across models.

**Table A18.** Summary of comparison of 5 reproduction model outputs (mean length of female spawners, number of redds created, initial number of viable eggs, number of hatched eggs and ratio of hatched eggs) across models (inSTREAM *vs* inSTREAM-Gen), replicates (10 replicates) and its interaction (model x replicate), using factorial analysis of variance (ANOVA).

| **Pattern** | Model | | Replicate | | Model x Replicate | |
|---|---|---|---|---|---|---|
| | *F* | *P* | *F* | *P* | *F* | *P* |
| Spawner length | 0.40 | 0.54 | 0.80 | 0.64 | 1.40 | 0.17 |
| N redds | 1.10 | 0.30 | 0.92 | 0.51 | 1.19 | 0.30 |
| N eggs | 0.77 | 0.38 | 0.93 | 0.50 | 1.27 | 0.25 |
| N hatched eggs | 0.38 | 0.54 | 0.88 | 0.54 | 1.20 | 0.29 |
| Ratio hatched eggs | 132.3 | <0.001 | 0.90 | 0.51 | 0.30 | 0.98 |

On the grounds of all these results, we believe that inSTREAM-Gen and inSTREAM show the same modelling behaviour when run under the same initials conditions and simulation scenarios. All the tests carried out during the model development and testing phases indicate that the model performs as indicated by the model description.

# 6 Model output verification

**This TRACE element provides supporting information on**: (1) how well model output matches observations and (2) how much calibration and effects of environmental drivers were involved in obtaining good fits of model output and data.

**Summary:**

**Based on previous sensitivity analyses, a set of six parameters were selected for inclusion in the pattern-oriented parameterization described in this section. We used six time series demographic patterns of field observations to determine those six parameters following an inverse modelling approach. After its calibration, the model was additionally tested against two extra time series demographic field patterns. Results of the 10 replicates run with the final parameterization indicate that inSTREAM-Gen was able to reproduce relatively well both the range of values and the interannual variations of the eight time series taken as validation patterns.**

We performed a global sensitivity analysis to identify those parameters having the strongest effect on both demographic and genetic model outputs (described in the next section of the present TRACE document). Based on that analysis, we selected a set of six parameters for inclusion in the pattern-oriented parameterization described in this section. Such parameters (*habDriftRegenDist*, *habDriftConc*, *habSearchProd*, *habPreyEnergyDensity*, *mortFishAqPredMin*, and *mortFishTerrPredMin*) were selected because (1) all tested model outputs were highly sensitive to their variations, (2) they are typically unknown and highly uncertain, and (3) they are usually site-specific.

InSTREAM-Gen was parameterized within the pattern-oriented framework (Grimm et al. 2005). We used different patterns of field observations to determine the aforementioned unknown parameters using an inverse modelling approach. The central idea of pattern-oriented parameterization is to make the model reproduce multiple observed patterns simultaneously, so that the structural realism of the model is increased and thus its sensitivity to parameter uncertainty is decreased. To validate the model, we used 12 years (1993-2004) of data from the Belagua River (Spain; Almodóvar et al. 2006). We focused on the reproduction of six time series patterns: length-at-age of age-1 trout (L1), age-2 trout (L2), and age-3 and older trout (age-3Plus; L3), as well as abundances of the same age-classes (age-1, -2 and -3Plus; A1-3). After its calibration, the model was tested against two extra time series field patterns: biomass of age-1 trout (B1) and age-2 and older trout (age-2Plus; B2). We did not focus on numbers or biomass of age-0 trout since they are more variable and difficult to quantify in the field, so that these figures are not usually taken into account for population management.

For the simulations aiming at reproducing those eight patterns, parameters were set to the values described in the "Data evaluation" section of the present document. The starting date of simulations was the 1st of October of 1993. The population was initialized using the real data observed in the field that year (see "Data evaluation" section). We used real site-specific time series of water temperature, flow and hydraulic conditions as model inputs. We subsequently used a Latin hyper-cube sampling design (Iványi et al. 1979), optimizing the sample with a genetic type algorithm, by means of the *lhs* package V0.10 (Carnell 2012) to draw 2000 parameter sets from the entire parameter space defined by the six parameters selected for calibration. Following Frank and Baret (2013), we used the sum of standardized squared errors (SSSE) to evaluate the agreement between the observed and predicted patterns. This quantitative measure is computed as the sum of standardized squared errors between the

observed and simulated values: $\sum_i \frac{(\mathrm{sim}_i - \mathrm{obs}_i)^2}{\mathrm{obs}_i}$. We next followed a Monte Carlo Filtering approach, by which tested patterns are applied as filters to separate good from bad sets of parameter values (Wiegand et al. 2003, Grimm and Railsback 2005). To do this, quantitative criteria for the agreement between observed and simulated patterns were developed. The first patterns used as filters were length-at-age's: first, we only retained the parameter sets reproducing patterns of length-at-age of age-3Plus trout; second, from this reduced set, we separated those parameter combinations reproducing patterns of length-at-age of age-2 trout; finally, we repeated the same procedure, retaining those parameter sets mimicking patterns of length-at-age of age-1 trout. We considered an observed field length-at-age pattern to be accurately reproduced by a model simulation when SSSE was equal to or less than the sum of yearly deviations corresponding to a maximum of 10% of the observed annual value. The remaining parameter sets were then filtered by means of the abundance patterns, following the same order (first, abundance of age-3Plus trout, then age-2, and finally age-1 trout). We only retained parameter sets producing a median SSSE lower than a value equal to a yearly deviation of 30% of the observed value. We selected the parameter set having the overall lowest SSSE values for tested abundance patterns.

Using again a Latin-hypercube sampling design, we drew 2000 additional parameter sets around the final parameterization to verify possible parameterizations that would reproduce the six field patterns better than the "final parameter set" found according to the previous description. Therefore, we repeated the procedure explained above, using as well trial and error by-hand adjustment on all six parameters to find the final parameter set. We considered we had the final parameter set when concurrently the goodness-of-fit measure (SSSE) of the six patterns could not be improved by small changes of any of the parameters, and all analysis of variance tests of the comparison between observed and 10 replicates of simulated trout length-at-age and abundance distributions for the three age-classes were non-significant.

The final parameter set, after using the six length-at-age and abundance patterns as filters, was: *habDriftRegenDist* = 600 cm, *habDriftConc* = 2.1E-10 g $cm^{-3}$, *habSearchProd* = 4.8E-7 g $cm^{-2}$ $h^{-1}$, *habPreyEnergyDensity* = 5200 j $g^{-1}$, *mortFishAqPredMin* = 0.984, and *mortFishTerrPredMin* = 0.996. While the calibrated value of *habSearchProd* falls well within the range reported by Railsback et al. (2009) for typical inSTREAM applications, the combined values of *habDriftConc* and *habDriftRegenDist* would produce a lower food productivity than previously reported. Nevertheless, the value of *habPreyEnergyDensity* is twice as much as the one reported by Railsback et al. (2009) for Little Jones Creek (2500 j $g^{-1}$), which indicates a great difference in trout diet composition. Studies of diet composition in rivers within our study area showed that brown trout mainly consumed high-energy prey, age-0 fish consuming mainly *ephemenoptera* larvae while adult preying on amphipods (Oscoz et al. 2000, 2005). Therefore, the obtained parameter value seems to be in agreement with previous field observations.

Results of the 10 replicates with the selected parameterization indicate that the model was able to reproduce relatively well both the range of values and the interannual variations of the eight time series taken as validation patterns (Figs. A4 and A5). Although some points of field observations lay outside the ranges of the replicates, the mean values and interannual variations observed in the Belagua population were reasonably well reproduced by inSTREAM-Gen for the sizes and numbers of individuals.

Regarding pattern A1, we observed small discrepancies for years 1997 (16% of the SSSE for this pattern) and 2004 (13%), and a significantly higher one in 2001 (49%). As a consequence, the highest discrepancies for pattern A2 were found on years 1998 (30%) and

2002 (26%). This latter year was also problematic for A3 along with year 2000, since they contributed to the SSSE computed for this pattern in an amount of 32 and 22%, respectively. For L1, the fit between observed and simulated values was pretty good over almost all years but for years 2001 (due to the extremely high discrepancy in numbers of age-1 trout that year) and 1994, whose contribution to the SSSE was as high as a 51 and 22%, respectively. Considering L2, most of the SSSE was attributed to years 2001 (44%) and 2003 (27%). Regarding L3, the bulk of SSSE fell on years 1995 (14%), 1996 (24%) and 2003 (35%).

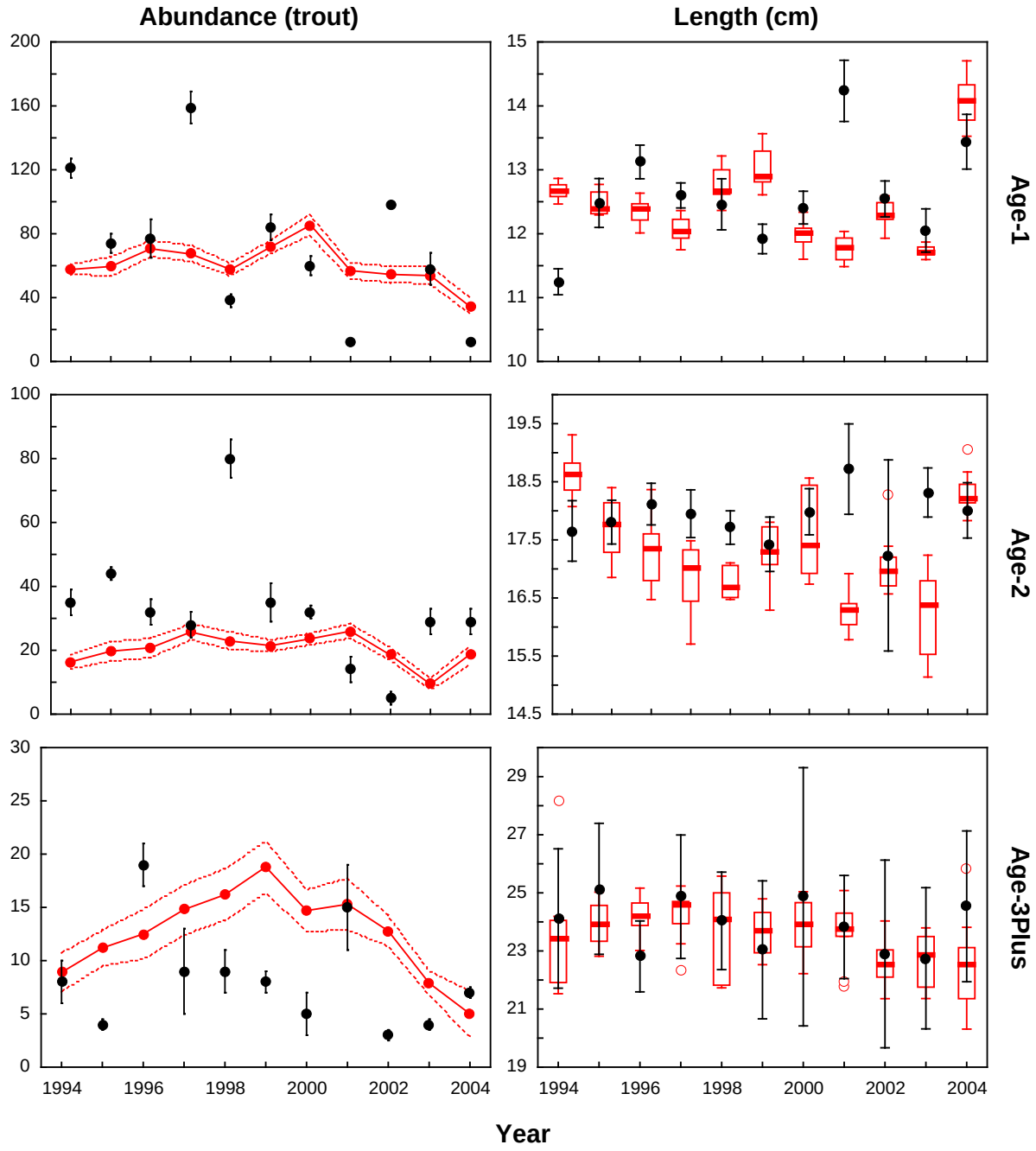


**Figure A4.** Simulation results of 10 replicates with the final parameterization (red) compared to field observations from the Belagua River (black). Graphs on the left column show the number of individuals of three age-classes. Graphs on the right column show the time series of mean length-at-age of individuals at three age-classes. Box-plots are the corresponding distribution of simulation replicates.

Biomass time series, which were not used as filters for parameterization, were used as extra validation patterns. There were no significant differences in the mean values between observed and simulated patterns (ANOVA, P> 0.35). The observed temporal distribution of discrepancies between observed and simulated values regarding abundance and length-at-age patterns, resulted in years 2004 and 2001 having the highest contribution to SSSE of pattern B1 (40 and 20%, respectively), while almost all SSSE of pattern B2 came from years 2002 (60%), 1999 and 2000 (both 12%).

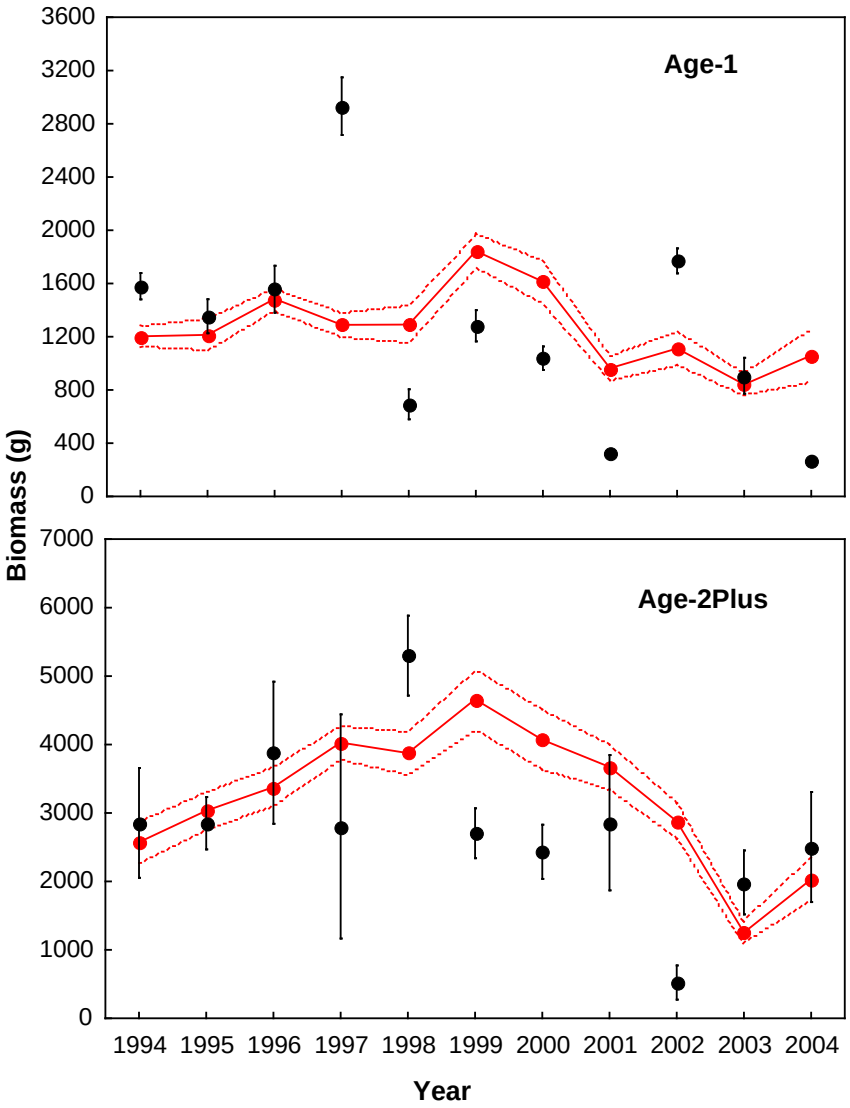


**Figure A5.** Simulation results of 10 replicates with the final parameterization (red) compared to field observations from the Belagua River (black). Graphs show the biomass of two age-classes, which were used as additional validation patterns.

# 7 Model analysis

**This TRACE element provides supporting information on**: (1) how sensitive model output is to changes in model parameters (sensitivity analysis), and (2) how well the emergence of model output has been understood.

**Summary:**

**A global sensitivity analysis was performed to explore the behavior of the model in response to variations in the values of the 72 parameters regarded as potentially most relevant. Four demographic (abundance and biomass of both young-of-the-year and older individuals), as well as three genetic (genotypic values of length at emergence and length maturity threshold of male and female breeders) model outputs were deployed in this sensitivity analysis. We first used the Morris method to screen the most influential parameters in the model. Based on obtained results, we subsequently used the Sobol method to decompose the model outputs' variance into variances attributable to each of the most influential parameters. We repeated the same analyses but using a different input temperature profile (daily temperatures increased by 3 °C), because parameters controlling effects of high temperature on reproduction, survival or metabolism may have little effect under conditions where temperatures are never extreme but the same parameters could be very important when temperatures are limiting.**

Section content



We conducted a global sensitivity analysis in order to (1) screen non-influential and influential parameters in the model, and (2) among the most influential parameters, identify those that would lead to the greatest reduction in the output variance when fixed to their reference values. In both cases, we used the sensitivity R package (Pujol et al. 2013) to both generate the design of experiments and estimate the sensitivity measures. We analysed parameter sensitivity under two temperature scenarios because parameters controlling effects of high temperature on reproduction, survival or metabolism may have little effect under current conditions when temperatures are never extreme but could have strong effects at projected higher temperatures. The sensitivity analysis examined seven model outputs: mean total abundance and biomass of both young-of-the-year (YOY; age 0) and older (age 1 and older) trout, as well as the mean genotypic values of length at emergence and length maturity threshold (for both males and females) of breeders over a 12-year period. One measure of each model output was obtained for each year (near September 1) and used to compute a mean for the entire model run.

As detailed in the section 3 of this TRACE document, there are a total of 203 parameters in inSTREAM-Gen. There are 36 user-specified and 22 site-specific parameters not suited for this kind of analysis. As a result, we had a grand total of 145 parameters to explore. We then proceeded to identify a subset of this total parameter set in order to make the task affordable. The parameters omitted from the sensitivity analysis were the following:

- The entire *Cmax* temperature function, encompassing 14 parameters, was eliminated due to concerns over redefining its shape. These parameters define a piecewise function that cannot easily be varied using global sensitivity analysis techniques. Likewise, the set of parameters

used to define the spawning suitability functions regarding depth and velocity was also removed from further study. Those parameters are: *fishSpawnDSuitD1* through *D5*, *fishSpawnDSuitS1-S5*, *fishSpawnVSuitS1-S5*, and *fishSpawnVSuitV1-V5*.

- The ending date of the spawning time window (*fishSpawnEndDate*) is impossible to model for brown trout since the parameter's units is Julian date. It would have not been possible to simulate a range of variation of a spawning season spanning over two natural years (for e.g., from 15$^{th}$ November to 15$^{th}$ January). In consequence, it made no sense to include *fishSpawnStartDate*.

- Simulating realistic slot size limits for angling would not have been possible either, as both parameters (*mortFishAngleSlotLower* and *mortFishAngleSlotUpper*) are interconnected.

- We regarded the parameters defining the beginning and the end of the angling season (*startAnglingSeason* and *endAnglingSeason*) as irrelevant.

- We took into consideration the results from the local sensitivity analyses performed by Cunningham (2007) on inSTREAM (see Railsback et al. 2009 for further details). Cunningham (2007) ranked 90 parameters of inSTREAM based on the sensitivity of adult biomass to their values. Since sensitivity values and ranking are expected to differ substantially among sites, we only eliminated from the analysis the parameters whose sensitivity index (as a percentage of the maximum sensitivity index value) was less than 3%. Those parameters are: *fishCmaxParamA*, *fishCmaxParamB*, *habMaxSpawnFlow*, *fishSpawnMaxFlowChange*, *fishSpawnEggViability*, and all redd global parameters but redd size (*mortReddDewaterSurv*, *habShearParamA*, *habShearParamB*, *mortReddScourDepth*, *mortReddLoTT1*, *mortReddLoTT9*, *mortReddHiTT1*¸ *mortReddHiTT9*, *reddDevelParamA*, *reddDevelParamB*, and *reddDevelParamC*).

- We additionally performed a pre-sensitivity analysis by which we tested the effects of all the trout survival and increasing survival probability functions on both YOY and older trout biomass. We compared results from a normal run against a run with a survival function turned off (one function at a time, 5 replicates). The parameters governing a survival probability function were not used in the global sensitivity analysis if (1) results of the comparison did not significantly differ, and (2) their sensitivity index (as a percentage of the maximum sensitivity index value) in Cunningham's study was less than 5%. Those parameters are: *mortFishHiTT1*, *mortFishHiTT9*, *mortFishStrandD1*, *mortFishStrandD9*, *mortFishTerrPredF1*, *mortFishTerrPredF9*, *mortFishAqPredD1*, *mortFishAqPredD9*, *mortFishAqPredF1*, *mortFishAqPredF9*, *mortFishAqPredT1*, and *mortFishAqPredT9*.

### 7.1. Screening of influential parameters under observed-temperature scenario

After performing this parameter selection, we retained a total of 72 parameters to conduct the global sensitivity analysis. First, we used an improved version of the Morris's elementary effects screening method (Morris 1991; Campolongo et al. 2007) to identify the parameters to which inSTREAM-Gen was particularly insensitive or sensitive. This method appears to be the most suited screening method for IBMs (Thiele et al. 2014). Based on individually randomised one-factor-at-a-time designs, it estimates the effects of changes in the input factor levels, i.e., the parameter values, which are called elementary effects (EEs). The EEs are then statistically analysed to measure their relative importance. We used the estimate of the mean of the distribution of the absolute values of the elementary effects, $\mu^*$, as a sensitivity measure to establish the relative influence of each parameter. It can be considered as a proxy of the total sensitivity index, which itself is a measure of the overall effect of a parameter on the output, including interactions with the rest of the model (Saltelli et al. 2008). All 72 selected parameters ($K$) were varied over five levels according to predefined ranges, the central value

being the value used to calibrate the model (Table A19). We used several methods to determine the range of parameter values analyzed, but the maximal range of variation hardly ever exceeded the 50% of the central value. The number of tested settings is given by $r \times (k + 1)$, where $r$ is the number of EEs computed per parameter. As we chose 50 EEs, this led to $50 \times (72 + 1) = 3650$ model runs.

**Table A19.** Range of parameter values used to conduct the global sensitivity analysis. Parameters are displayed by alphabetical order.

| Parameter | Lower extreme | Lower median | Central | Upper median | Upper extreme |
|---|---|---|---|---|---|
| *anglePressure* | 0 | 0.5 | 2 | 5 | 15 |
| *fishCaptureParam1* | 1.2 | 1.4 | 1.6 | 1.8 | 2 |
| *fishCaptureParam9* | 0.375 | 0.437 | 0.5 | 0.563 | 0.625 |
| *fishDetectDistParamA* | 3.2 | 3.6 | 4.0 | 4.4 | 4.8 |
| *fishDetectDistParamB* | 1.6 | 1.8 | 2.0 | 2.2 | 2.4 |
| *fishEnergyDensity* | 3900 | 4900 | 5900 | 6900 | 7900 |
| *fishFecundParamA* | 0.038 | 0.1 | 0.2 | 0.5 | 1 |
| *fishFecundParamB* | 1.7 | 2 | 2.6 | 3 | 3.3 |
| *fishFitnessHorizon* | 22 | 55 | 90 | 125 | 158 |
| *fishMaxSwimParamA* | 0.95 | 1.47 | 1.90 | 2.35 | 2.85 |
| *fishMaxSwimParamB* | 15.0 | 22.5 | 30.0 | 37.5 | 45.0 |
| *fishMaxSwimParamC* | -0.00375 | -0.00310 | -0.00250 | -0.0019 | -0.00125 |
| *fishMaxSwimParamD* | 0.036 | 0.054 | 0.072 | 0.09 | 0.108 |
| *fishMaxSwimParamE* | 0.250 | 0.375 | 0.500 | 0.625 | 0.750 |
| *fishMoveDistParamA* | 5 | 12.5 | 20 | 27.5 | 35 |
| *fishMoveDistParamB* | 1.5 | 1.75 | 2 | 2.25 | 2.5 |
| *fishNewLengthHeritability* | 0 | 0.1 | 0.18 | 0.3 | 0.4 |
| *fishNewLengthMean* | 2 | 2.25 | 2.5 | 2.75 | 3 |
| *fishNewLengthVar* | 0.005 | 0.02 | 0.04 | 0.06 | 0.08 |
| *fishPiscivoryLength* | 13 | 15 | 17 | 19 | 22 |
| *fishRespParamA* | 18 | 24 | 30 | 36 | 42 |
| *fishRespParamB* | 0.627 | 0.710 | 0.784 | 0.86 | 0.940 |

| | | | | | |
|---|---|---|---|---|---|
| *fishRespParamC* | 0.0415 | 0.0550 | 0.0693 | 0.0830 | 0.0970 |
| *fishRespParamD* | 0.018 | 0.024 | 0.03 | 0.036 | 0.042 |
| *fishSearchArea* | 10000 | 15000 | 20000 | 25000 | 30000 |
| *fishShelterSpeedFrac* | 0.15 | 0.225 | 0.3 | 0.375 | 0.45 |
| *fishSpawnMaxTemp* | 7 | 8.5 | 10 | 11.5 | 13 |
| *fishSpawnMinAge* | 365 | 547 | 730 | 912 | 1095 |
| *fishSpawnMinCond* | 0.9 | 0.925 | 0.95 | 0.975 | 1 |
| *fishSpawnMinLengthHeritability* | 0 | 0.1 | 0.18 | 0.3 | 0.4 |
| *fishSpawnMinLengthMeanF* | 14.5 | 15.5 | 16.5 | 17.5 | 18.5 |
| *fishSpawnMinLengthMeanM* | 16.5 | 17.5 | 18.5 | 19.5 | 20.5 |
| *fishSpawnMinLengthVarF* | 0.5 | 1 | 1.5 | 2 | 2.5 |
| *fishSpawnMinLengthVarM* | 0.75 | 1.5 | 2 | 2.5 | 3 |
| *fishSpawnMinTemp* | 2 | 3 | 4 | 5 | 6 |
| *fishSpawnProb* | 0.01 | 0.04 | 0.1 | 0.15 | 0.2 |
| *fishSpawnWtLossFraction* | 0.1 | 0.15 | 0.2 | 0.3 | 0.4 |
| *fishWeightParamA* | 0.00668 | 0.00770 | 0.00879 | 0.01135 | 0.01390 |
| *fishWeightParamB* | 2.949 | 3.022 | 3.098 | 3.155 | 3.212 |
| *habDriftConc* | 2.00E-10 | 4.00E-10 | 6.00E-10 | 8.00E-10 | 1.00E-09 |
| *habDriftRegenDist* | 100 | 300 | 500 | 700 | 900 |
| *habPreyEnergyDensity* | 1600 | 2000 | 2500 | 3500 | 5000 |
| *habSearchProd* | 1.3E-07 | 3.00E-07 | 5.00E-07 | 7.00E-07 | 8.8E-07 |
| *max-n-males-per-female* | 1 | 2 | 3 | 4 | 5 |
| *mortFishAngleFracKeptIllegal* | 0 | 0.025 | 0.05 | 0.1 | 0.2 |
| *mortFishAngleFracKeptLegal* | 0 | 0.1 | 0.2 | 0.3 | 0.4 |
| *mortFishAngleHookSurvRate* | 0.6 | 0.7 | 0.8 | 0.9 | 1 |
| *mortFishAngleL1* | 7 | 8.5 | 10 | 11.5 | 13 |
| *mortFishAngleL9* | 14 | 17 | 20 | 23 | 26 |
| *mortFishAngleSlotLower* | 17 | 19 | 21 | 23 | 25 |
| *mortFishAngleSuccess* | 0.0001 | 0.0015 | 0.003 | 0.006 | 0.03 |

| | | | | | |
|---|---|---|---|---|---|
| *mortFishAqPredL1* | 2.5 | 3.25 | 4 | 4.5 | 5 |
| *mortFishAqPredL9* | 5.1 | 6.5 | 8 | 9.5 | 11 |
| *mortFishAqPredMin* | 0.91 | 0.93 | 0.95 | 0.97 | 0.99 |
| *mortFishAqPredP1* | 0.000005 | 0.0000075 | 0.00001 | 0.0000125 | 0.000015 |
| *mortFishAqPredP9* | 0.000001 | 0.0000015 | 0.000002 | 0.0000025 | 0.000003 |
| *mortFishConditionK1* | 0.21 | 0.24 | 0.3 | 0.36 | 0.4 |
| *mortFishConditionK9* | 0.42 | 0.48 | 0.6 | 0.72 | 0.8 |
| *mortFishTerrPredD1* | 2.5 | 3.75 | 5 | 6.25 | 7.5 |
| *mortFishTerrPredD9* | 50 | 85 | 125 | 165 | 200 |
| *mortFishTerrPredH1* | 250 | 375 | 500 | 625 | 750 |
| *mortFishTerrPredH9* | -150 | -125 | -100 | -75 | -50 |
| *mortFishTerrPredL1* | 4.1 | 5 | 6 | 7.5 | 9 |
| *mortFishTerrPredL9* | 1.5 | 2.25 | 3 | 3.5 | 4 |
| *mortFishTerrPredMin* | 0.98 | 0.984 | 0.988 | 0.992 | 0.996 |
| *mortFishTerrPredV1* | 10 | 15 | 20 | 25 | 30 |
| *mortFishTerrPredV9* | 50 | 75 | 100 | 125 | 150 |
| *mortFishVelocityV1* | 1.6 | 1.7 | 1.8 | 2 | 2.2 |
| *mortFishVelocityV9* | 1 | 1.2 | 1.4 | 1.49 | 1.58 |
| *mutationalVarParam* | 0.0005 | 0.001 | 0.005 | 0.01 | 0.02 |
| *mutationFactor* | 0 | 1 | 5 | 50 | 100 |
| *reddSize* | 600 | 900 | 1200 | 1500 | 1800 |

The complete results from the screening analysis (Table A20) show that the vast majority of parameters had little effect under the simulated conditions - but any of these parameters could have strong effects under other conditions. The parameters to which inSTREAM-Gen's demographic and genetic outputs were determined to be most sensitive are shown in Tables 21 and 22. Comments in Tables 23 and 24 explain why the model is sensitive to the parameters, how uncertain the parameters are, and therefore how the parameter should be treated in parameterizing and calibrating inSTREAM-Gen. A parameter may not be of special concern if its value is well known, even if the model is highly sensitive to it. On the other hand, the parameters in Tables 23 and 24 that also do not have well-known values or that represent inherently variable and uncertain processes deserve special attention.

**Table A20.** Complete sensitivity results conducted on inSTREAM-Gen for Belagua River (Morris method), as a percentage of the maximum sensitivity (computed as the $\mu^*$ index). Parameters are displayed by alphabetical order. The sensitivity index was computed for seven model outputs: number and biomass of trout of age 0 and older (Count Age0, Count Age1Plus, Biomass Age0, Biomass Age1Plus), mean genotypic value of length maturity threshold for male (Males GMSL) and females (Females GMSL) breeders, and mean genotypic value of length at emergence of breeders (Emergence Length). Sensitivity values over 50% of the maximum are highlighted in bold.

| Parameter | Count Age0 | Count Age1Plus | Biomass Age0 | Biomass Age1Plus | Males GMSL | Females GMSL | Emergence Length |
|---|---|---|---|---|---|---|---|
| *anglePressure* | 16.2 | 19.8 | 20.3 | 19.1 | 20.9 | 23.7 | 24.7 |
| *fishCaptureParam1* | 19.8 | 15.8 | 18.6 | 8.7 | 30.0 | 28.2 | 29.2 |
| *fishCaptureParam9* | 20.7 | 14.5 | 21.9 | 9.2 | 24.0 | 33.8 | 36.2 |
| *fishDetectDistParamA* | 20.2 | 17.0 | 7.3 | 3.7 | 25.5 | 24.5 | 24.8 |
| *fishDetectDistParamB* | 31.0 | 13.0 | 10.8 | 4.9 | 31.2 | 33.1 | 33.2 |
| *fishEnergyDensity* | 35.6 | 24.4 | 13.9 | 6.8 | 29.4 | 26.7 | 26.9 |
| *fishFecundParamA* | **72.3** | 28.7 | 20.7 | 14.4 | 34.1 | 28.6 | 28.6 |
| *fishFecundParamB* | **98.3** | 33.4 | **55.4** | 21.6 | 38.3 | 27.6 | 30.6 |
| *fishFitnessHorizon* | 33.4 | 25.8 | 33.5 | 14.7 | 35.1 | 35.9 | 35.0 |
| *fishMaxSwimParamA* | 19.2 | 12.1 | 22.8 | 8.7 | 30.0 | 29.0 | 28.5 |
| *fishMaxSwimParamB* | 28.5 | 20.2 | 35.1 | 18.3 | 38.0 | 32.2 | 33.8 |
| *fishMaxSwimParamC* | 25.5 | 29.2 | 29.1 | 15.3 | 28.9 | 24.1 | 23.1 |
| *fishMaxSwimParamD* | 33.5 | 15.3 | 21.4 | 14.3 | 41.8 | 36.5 | 35.3 |
| *fishMaxSwimParamE* | 20.9 | 18.1 | 19.6 | 9.9 | 23.5 | 34.4 | 34.8 |
| *fishMoveDistParamA* | 27.6 | 34.9 | 27.2 | 29.7 | 34.0 | 33.4 | 36.7 |
| *fishMoveDistParamB* | 11.4 | 8.8 | 8.2 | 6.1 | 18.0 | 18.9 | 18.0 |
| *fishNewLengthHeritability* | 24.2 | 17.2 | 10.9 | 5.8 | 22.0 | 24.2 | 24.1 |
| *fishNewLengthMean* | 26.2 | 9.4 | 9.9 | 4.4 | 16.4 | 22.9 | 29.5 |
| *fishNewLengthVar* | 26.3 | 8.8 | 17.7 | 5.3 | 22.9 | 26.3 | 27.9 |
| *fishPiscivoryLength* | 23.0 | 13.7 | 8.3 | 4.8 | 22.3 | 26.2 | 28.6 |
| *fishRespParamA* | 35.5 | 22.9 | 15.0 | 11.5 | 46.6 | 33.3 | 34.4 |
| *fishRespParamB* | **50.2** | **66.2** | **56.2** | **57.3** | **83.1** | **70.0** | **69.5** |
| *fishRespParamC* | 35.5 | 29.4 | 42.6 | 24.5 | 44.1 | 31.6 | 32.9 |
| *fishRespParamD* | 14.8 | 7.6 | 11.3 | 7.2 | 20.5 | 19.0 | 17.7 |
| *fishSearchArea* | 23.1 | 10.9 | 14.8 | 6.0 | 15.7 | 25.3 | 26.4 |
| *fishShelterSpeedFrac* | 13.3 | 12.3 | 9.5 | 5.7 | 25.5 | 18.6 | 19.4 |
| *fishSpawnMaxTemp* | 26.9 | 17.5 | 20.4 | 8.7 | 31.9 | 29.1 | 31.8 |
| *fishSpawnMinAge* | 39.4 | 20.1 | 12.9 | 7.2 | 49.8 | 38.3 | 37.0 |
| *fishSpawnMinCond* | 22.6 | 14.7 | 16.4 | 15.0 | 33.7 | 33.9 | 35.4 |
| *fishSpawnMinLengthHeritability* | 14.9 | 10.2 | 13.6 | 10.2 | 17.3 | 22.5 | 23.5 |
| *fishSpawnMinLengthMeanF* | 25.6 | 20.9 | 23.5 | 14.1 | 22.7 | 26.9 | 21.3 |
| *fishSpawnMinLengthMeanM* | 18.7 | 9.2 | 11.1 | 4.0 | 21.3 | 25.6 | 25.4 |
| *fishSpawnMinLengthVarF* | 20.7 | 15.1 | 19.0 | 8.0 | 20.9 | 20.6 | 20.6 |
| *fishSpawnMinLengthVarM* | 9.9 | 11.2 | 7.8 | 6.4 | 18.5 | 17.6 | 18.1 |

| | | | | | | | |
|---|---|---|---|---|---|---|---|
| *fishSpawnMinTemp* | 24.3 | 14.0 | 17.7 | 7.4 | 29.8 | 33.5 | 33.6 |
| *fishSpawnProb* | 33.2 | 24.8 | 23.6 | 9.6 | 49.7 | 46.3 | 46.8 |
| *fishSpawnWtLossFraction* | 14.3 | 9.6 | 13.8 | 9.4 | 19.5 | 17.6 | 17.6 |
| *fishWeightParamA* | 22.2 | 18.2 | 21.2 | 8.6 | **50.6** | 40.9 | 40.3 |
| *fishWeightParamB* | 27.4 | 22.8 | 20.8 | 8.2 | 35.3 | 31.8 | 35.2 |
| *habDriftConc* | 36.2 | 23.9 | **53.2** | 28.6 | **63.6** | **59.9** | **57.5** |
| *habDriftRegenDist* | **100.0** | **100.0** | **100.0** | **64.6** | 38.7 | 34.0 | 35.9 |
| *habPreyEnergyDensity* | 30.2 | 49.1 | **56.9** | **69.8** | 36.6 | 33.1 | 38.3 |
| *habSearchProd* | 37.5 | 33.0 | 21.2 | 11.8 | 29.2 | 30.3 | 31.0 |
| *max-n-males-per-female* | 23.6 | 9.9 | 16.5 | 4.4 | 22.7 | 25.6 | 26.2 |
| *mortFishAngleFracKeptIllegal* | 20.4 | 7.8 | 13.4 | 5.8 | 20.6 | 23.4 | 26.0 |
| *mortFishAngleFracKeptLegal* | 17.9 | 12.1 | 11.4 | 7.3 | 26.3 | 19.8 | 21.7 |
| *mortFishAngleHookSurvRate* | 22.8 | 16.5 | 21.1 | 21.0 | 22.6 | 21.6 | 23.6 |
| *mortFishAngleL1* | 19.4 | 14.9 | 14.6 | 7.1 | 20.8 | 19.4 | 20.0 |
| *mortFishAngleL9* | 26.0 | 11.8 | 23.5 | 8.1 | 18.2 | 19.6 | 20.6 |
| *mortFishAngleSlotLower* | 18.4 | 11.5 | 20.1 | 9.8 | 31.4 | 33.6 | 35.2 |
| *mortFishAngleSuccess* | 32.5 | 16.7 | 34.8 | 21.4 | 33.2 | 28.6 | 27.3 |
| *mortFishAqPredL1* | 29.4 | 19.9 | 26.0 | 8.2 | 36.8 | 38.2 | 37.4 |
| *mortFishAqPredL9* | 22.2 | 17.6 | 9.1 | 6.8 | 16.0 | 21.3 | 23.6 |
| *mortFishAqPredMin* | 32.4 | 29.2 | 18.2 | 9.3 | 17.8 | 23.1 | 23.2 |
| *mortFishAqPredP1* | 15.0 | 7.8 | 12.8 | 4.1 | 23.7 | 20.3 | 19.9 |
| *mortFishAqPredP9* | 23.8 | 14.8 | 10.4 | 5.1 | 19.8 | 17.7 | 17.8 |
| *mortFishConditionK1* | 23.0 | 31.7 | 11.6 | 12.2 | 32.0 | 26.4 | 25.6 |
| *mortFishConditionK9* | **89.1** | **90.4** | **52.1** | **100.0** | **100.0** | **100.0** | **100.0** |
| *mortFishTerrPredD1* | 17.4 | 11.8 | 8.9 | 5.8 | 32.5 | 26.4 | 27.0 |
| *mortFishTerrPredD9* | 19.8 | 10.2 | 21.9 | 14.9 | 19.5 | 31.1 | 31.1 |
| *mortFishTerrPredH1* | 29.5 | 29.1 | 23.6 | 24.2 | 26.0 | 21.0 | 24.3 |
| *mortFishTerrPredH9* | 23.9 | 14.0 | 12.6 | 7.0 | 33.4 | 30.8 | 30.2 |
| *mortFishTerrPredL1* | 23.4 | 7.9 | 17.7 | 5.9 | 32.4 | 22.3 | 24.4 |
| *mortFishTerrPredL9* | 20.1 | 9.2 | 13.4 | 4.3 | 27.9 | 33.5 | 35.4 |
| *mortFishTerrPredMin* | 41.8 | **72.1** | 36.5 | 46.6 | 48.9 | 33.5 | 34.0 |
| *mortFishTerrPredV1* | 13.3 | 9.8 | 12.2 | 5.7 | 25.2 | 20.6 | 20.4 |
| *mortFishTerrPredV9* | 27.7 | 17.5 | 34.1 | 28.4 | 41.1 | 35.4 | 38.1 |
| *mortFishVelocityV1* | 8.2 | 11.7 | 10.2 | 7.3 | 20.0 | 23.0 | 23.6 |
| *mortFishVelocityV9* | 25.2 | 17.7 | 11.6 | 6.1 | 30.6 | 27.0 | 26.5 |
| *mutationalVarParam* | 15.9 | 11.0 | 11.1 | 4.8 | 20.2 | 26.0 | 28.3 |
| *mutationFactor* | 22.5 | 13.2 | 22.5 | 6.9 | 29.8 | 21.8 | 24.5 |
| *reddSize* | 22.3 | 12.1 | 12.1 | 6.2 | 25.8 | 19.0 | 19.8 |

The parameter *mortFishConditionK9* appeared to be extremely important. This parameter controls the probability of surviving poor condition but it is highly interconnected to many different processes, so that it can have a strong effect not only on mortality (controlling population numbers) but also on habitat selection and thus on growth (affecting biomass). As a consequence, changes in parameter values are likely to have widespread, complex, and unexpected effects, as revealed by the fact, that this parameter has a pervasive influence on genetic traits. It drives the number of potential spawners: lowering its value diminishes mortality, increasing then the number of adults while diminishing their body condition factor through increased competition, so that the potential number of spawners decreases as mature trout do not meet the minimum body condition to reproduce. Therefore, *mortFishConditionK9* affects genotypic values of genetic traits by filtering the number and quality of spawners.

The three habitat parameters, *habDriftRegenDist*, *habDriftConc* and *habPreyEnergyDensity* all had strong effects on model outputs, especially on demographic ones. They control the energy flux through the population, affecting both numbers and growth, and hence biomass. The parameter *habSearchProd* was only relatively important for setting numbers of recruits, and consequently of older trout (through downstream cohort effects). There was also a high degree of uncertainty in these parameters, as each one reflects a constant function intended to represent a variable one, which introduces many simplifications. Besides, their values are quite site-specific and rarely well-known, so they are best estimated via calibration.

All model outputs were very sensitive to the three respiration parameters but especially to *fishRespParamB*. They strongly affect energy costs and growth, and thus survival.

Fecundity parameters, *fishFecundParamA* and *B*, were very important to control young-of-the-year trout numbers and biomass, and thus, relatively important for older trout dynamics, though their effects are somehow diluted along ontogeny.

All model outputs were very sensitive to the parameter *mortFishTerrPredMin*, its strongest effects being on numbers and biomass of adult trout. Terrestrial predation is normally the most important mortality source for older trout. Therefore, abundance of old trout is highly dependent on this parameter, affecting the number of spawners, and consequently having strong effects on heritable traits and number of new recruits. Its values are highly uncertain and variable, so they are best estimated via calibration to observed survival and abundance. On the contrary, *mortFishAqPredMin* was only relatively important to control population abundance, not having a strong effect on other model outputs. Among all parameters controlling the survival probability functions and the increasing survival functions for terrestrial and aquatic predation, the ones the model showed more sensitivity to were (ranked by global importance): *mortFishTerrPredV9*, *mortFishAqPredL1*¸ *mortFishTerrPredH1* and *mortFishConditionK1*. Cunningham (2007) found *mortFishTerrPredD9* to be highly influential on inSTREAM's adult biomass output, while the effect of *mortFishTerrPredV9* was negligible. We found quite the contrary, probably because the physical habitat of the Belagua River has more high-velocity area than deep area, the opposite occurring in Little Jones Creek.

The *fishFitnessHorizon* ranked among the 24 most influential parameters to all assessed outputs. The biological meaning of this parameter is the time horizon over which fish evaluate the tradeoffs between food intake and mortality risks to maximize their probability of surviving and reproducing. Therefore, it is understandable that it exerts a great influence on both demographic and genetic outputs. However, Cunningham (2007) found very little response from insSTREAM to this parameter, perhaps because the response was nonlinear and peaked right at 90 days (value used for calibration).

Parameters defining the maximum swimming speed for fish, above all *fishMaxSwimParamB*, had a relative influence on demographic outputs, since maximum swimming speed affects both growth and survival. Likewise, the parameter *fishMoveDistParamA* showed great effect on demographic outputs since it affects the potential destination cells during habitat selection, and therefore, growth and survival.

Three parameters involved in the angler model (*anglePressure*, *mortFishAngleSuccess* and *mortFishAngleHookSurvRate*) affected biomass of older trout, due to their effects on mortality, those effects being both quantitative (number of trout removed from the system) and qualitative (size of trout removed from the system).

There were a few parameters that had strong influence on genetic traits but not on demographic outputs. They were the parameters defining the criteria trout must meet to become spawners (*fishSpawnMinAge* and *fishSpawnMinCond*), and also the probability of spawning once all spawning criteria are met, *fishSpawnProb*. The parameters governing the length-weight relationship for healthy fish, predominantly *fishWeightParamA*, were revealed as particularly influential on heritable traits. These two parameters strongly define how much energy a trout needs to grow in length (via growth in weight), so variations in their values modify the strength for selection towards higher length at emergence (favoring monopolization of resources due to the length-based dominance hierarchy ruling habitat selection and feeding) and lower length maturity thresholds (by increasing probability of reproducing at least once).

**Table A21.** Ranking and sensitivity values (as a percentage of the maximum sensitivity) of the 24 parameters to which demographic outputs are most sensitive.

| Parameter | Count Age0 | Parameter | Count Age1Plus | Parameter | Biomass Age0 | Parameter | Biomass Age1Plus |
|---|---|---|---|---|---|---|---|
| *habDriftRegenDist* | 100.0 | *habDriftRegenDist* | 100.0 | *habDriftRegenDist* | 100.0 | *mortFishConditionK9* | 100.0 |
| *fishFecundParamB* | 98.3 | *mortFishConditionK9* | 90.4 | *habPreyEnergyDensity* | 56.9 | *habPreyEnergyDensity* | 69.8 |
| *mortFishConditionK9* | 89.1 | *mortFishTerrPredMin* | 72.1 | *fishRespParamB* | 56.2 | *habDriftRegenDist* | 64.6 |
| *fishFecundParamA* | 72.3 | *fishRespParamB* | 66.2 | *fishFecundParamB* | 55.4 | *fishRespParamB* | 57.3 |
| *fishRespParamB* | 50.2 | *habPreyEnergyDensity* | 49.1 | *habDriftConc* | 53.2 | *mortFishTerrPredMin* | 46.6 |
| *mortFishTerrPredMin* | 41.8 | *fishMoveDistParamA* | 34.9 | *mortFishConditionK9* | 52.1 | *fishMoveDistParamA* | 29.7 |
| *fishSpawnMinAge* | 39.4 | *fishFecundParamB* | 33.4 | *fishRespParamC* | 42.6 | *habDriftConc* | 28.6 |
| *habSearchProd* | 37.5 | *habSearchProd* | 33.0 | *mortFishTerrPredMin* | 36.5 | *mortFishTerrPredV9* | 28.4 |
| *habDriftConc* | 36.2 | *mortFishConditionK1* | 31.7 | *fishMaxSwimParamB* | 35.1 | *fishRespParamC* | 24.5 |
| *fishEnergyDensity* | 35.6 | *fishRespParamC* | 29.4 | *mortFishAngleSuccess* | 34.8 | *mortFishTerrPredH1* | 24.2 |
| *fishRespParamC* | 35.5 | *fishMaxSwimParamC* | 29.2 | *mortFishTerrPredV9* | 34.1 | *fishFecundParamB* | 21.6 |
| *fishRespParamA* | 35.5 | *mortFishAqPredMin* | 29.2 | *fishFitnessHorizon* | 33.5 | *mortFishAngleSuccess* | 21.4 |
| *fishMaxSwimParamD* | 33.5 | *mortFishTerrPredH1* | 29.1 | *fishMaxSwimParamC* | 29.1 | *mortFishAngleHookSurvRate* | 21.0 |
| *fishFitnessHorizon* | 33.4 | *fishFecundParamA* | 28.7 | *fishMoveDistParamA* | 27.2 | *anglePressure* | 19.1 |
| *fishSpawnProb* | 33.2 | *fishFitnessHorizon* | 25.8 | *mortFishAqPredL1* | 26.0 | *fishMaxSwimParamB* | 18.3 |
| *mortFishAngleSuccess* | 32.5 | *fishSpawnProb* | 24.8 | *mortFishTerrPredH1* | 23.6 | *fishMaxSwimParamC* | 15.3 |
| *mortFishAqPredMin* | 32.4 | *fishEnergyDensity* | 24.4 | *fishSpawnProb* | 23.6 | *fishSpawnMinCond* | 15.0 |
| *fishDetectDistParamB* | 31.0 | *habDriftConc* | 23.9 | *mortFishAngleL9* | 23.5 | *mortFishTerrPredD9* | 14.9 |
| *habPreyEnergyDensity* | 30.2 | *fishRespParamA* | 22.9 | *fishSpawnMinLengthMeanF* | 23.5 | *fishFitnessHorizon* | 14.7 |
| *mortFishTerrPredH1* | 29.5 | *fishWeightParamB* | 22.8 | *fishMaxSwimParamA* | 22.8 | *fishFecundParamA* | 14.4 |
| *mortFishAqPredL1* | 29.4 | *fishSpawnMinLengthMeanF* | 20.9 | *mutationFactor* | 22.5 | *fishMaxSwimParamD* | 14.3 |
| *fishMaxSwimParamB* | 28.5 | *fishMaxSwimParamB* | 20.2 | *fishCaptureParam9* | 21.9 | *fishSpawnMinLengthMeanF* | 14.1 |
| *mortFishTerrPredV9* | 27.7 | *fishSpawnMinAge* | 20.1 | *mortFishTerrPredD9* | 21.9 | *mortFishConditionK1* | 12.2 |
| *fishMoveDistParamA* | 27.6 | *mortFishAqPredL1* | 19.9 | *fishMaxSwimParamD* | 21.4 | *habSearchProd* | 11.8 |

**Table A22.** Ranking and sensitivity values (as a percentage of the maximum sensitivity) of the 24 parameters to which genotypic outputs are most sensitive.

| Parameter | Males GMSL | Parameter | Females GMSL | Parameter | Emergence Length |
|---|---|---|---|---|---|
| *mortFishConditionK9* | 100.0 | *mortFishConditionK9* | 100.0 | *mortFishConditionK9* | 100.0 |
| *fishRespParamB* | 83.1 | *fishRespParamB* | 70.0 | *fishRespParamB* | 69.5 |
| *habDriftConc* | 63.6 | *habDriftConc* | 59.9 | *habDriftConc* | 57.5 |
| *fishWeightParamA* | 50.6 | *fishSpawnProb* | 46.3 | *fishSpawnProb* | 46.8 |
| *fishSpawnMinAge* | 49.8 | *fishWeightParamA* | 40.9 | *fishWeightParamA* | 40.3 |
| *fishSpawnProb* | 49.7 | *fishSpawnMinAge* | 38.3 | *habPreyEnergyDensity* | 38.3 |
| *mortFishTerrPredMin* | 48.9 | *mortFishAqPredL1* | 38.2 | *mortFishTerrPredV9* | 38.1 |
| *fishRespParamA* | 46.6 | *fishMaxSwimParamD* | 36.5 | *mortFishAqPredL1* | 37.4 |
| *fishRespParamC* | 44.1 | *fishFitnessHorizon* | 35.9 | *fishSpawnMinAge* | 37.0 |
| *fishMaxSwimParamD* | 41.8 | *mortFishTerrPredV9* | 35.4 | *fishMoveDistParamA* | 36.7 |
| *mortFishTerrPredV9* | 41.1 | *fishMaxSwimParamE* | 34.4 | *fishCaptureParam9* | 36.2 |
| *habDriftRegenDist* | 38.7 | *habDriftRegenDist* | 34.0 | *habDriftRegenDist* | 35.9 |
| *fishFecundParamB* | 38.3 | *fishSpawnMinCond* | 33.9 | *mortFishTerrPredL9* | 35.4 |
| *fishMaxSwimParamB* | 38.0 | *fishCaptureParam9* | 33.8 | *fishSpawnMinCond* | 35.4 |
| *mortFishAqPredL1* | 36.8 | *mortFishAngleSlotLower* | 33.6 | *fishMaxSwimParamD* | 35.3 |
| *habPreyEnergyDensity* | 36.6 | *fishSpawnMinTemp* | 33.5 | *fishWeightParamB* | 35.2 |
| *fishWeightParamB* | 35.3 | *mortFishTerrPredMin* | 33.5 | *mortFishAngleSlotLower* | 35.2 |
| *fishFitnessHorizon* | 35.1 | *mortFishTerrPredL9* | 33.5 | *fishFitnessHorizon* | 35.0 |
| *fishFecundParamA* | 34.1 | *fishMoveDistParamA* | 33.4 | *fishMaxSwimParamE* | 34.8 |
| *fishMoveDistParamA* | 34.0 | *fishRespParamA* | 33.3 | *fishRespParamA* | 34.4 |
| *fishSpawnMinCond* | 33.7 | *fishDetectDistParamB* | 33.1 | *mortFishTerrPredMin* | 34.0 |
| *mortFishTerrPredH9* | 33.4 | *habPreyEnergyDensity* | 33.1 | *fishMaxSwimParamB* | 33.8 |
| *mortFishAngleSuccess* | 33.2 | *fishMaxSwimParamB* | 32.2 | *fishSpawnMinTemp* | 33.6 |
| *mortFishTerrPredD1* | 32.5 | *fishWeightParamB* | 31.8 | *fishDetectDistParamB* | 33.2 |

**Table A23.** Parameters to which inSTREAM-Gen's assessed demographic outputs were found most sensitive in the global sensitivity analysis, in order of decreasing sensitivity.

| Parameter | Sensitivity considerations |
|---|---|
| *habDriftRegenDist* | This parameter controls total food availability in a cell.<br><br>Values are highly uncertain, as this single parameter represents a highly variable process that is difficult to measure. Values are best obtained via calibration of fish density in high-quality cells. |
| *mortFishConditionK9* | This parameter controls the probability of surviving poor condition but it is highly interconnected to many different processes, so that it can have a strong effect not only on mortality but also on habitat selection and thus on growth.<br><br>Values are not well known and changes in them are likely to have widespread, complex, and unexpected effects. |
| *fishRespParamB*<br>*fishRespParamC*<br>*fishRespParamA* | Respiration parameters strongly affect energy costs and growth.<br><br>Values are relatively well-known from laboratory studies, and typically should not be changed. |
| *fishFecundParamB*<br>*fishFecundParamA* | Fecundity parameters control the number of eggs laid by the spawner in the redd as a function of its length.<br><br>It is a highly site-specific population parameter. Values should be known for the study population before calibration. |
| *habPreyEnergyDensity* | Trout energy intake increases linearly with this parameter, and is not limited by the maximum daily intake (*Cmax*).<br><br>Energy density of invertebrate prey can vary seasonally as prey types change, but the range of reasonable values is well-known. Values should be selected for a study site before calibration. |
| *mortFishTerrPredMin* | Terrestrial predation is normally the most important mortality source for trout more than a few cm in length.<br><br>Values are highly uncertain and variable, so are best estimated via calibration to observed survival and abundance. |
| *habDriftConc* | Energy intake increases linearly with this parameter, until intake is limited by *Cmax*.<br><br>Values are site-specific, rarely well-known, and this parameter also represents a variety of simplifications and uncertainties in food availability, so there is no guarantee that measured values will produce useful model results. This parameter is best evaluated via calibration to observed growth or size. |
| *fishMoveDistParamA* | Multiplier for the maximum movement distance. It limits potential destinations during habitat selection. It affects small trout above all, influencing the intensity of competition by limiting dispersal.<br><br>Parameter values are based on literature observations. There are some uncertainties in its values because observed movement distances generally show how far fish actually move, not the distance over which they evaluate habitat. |

| | |
|---|---|
| *fishFitnessHorizon* | This parameter represents the number of days over which the terms of the expected maturity fitness measure equation are evaluated.<br><br>Values are not completely well-known as only a few studies have addressed the issue of fitness time horizons. Assuming that fish anticipate seasonal changes in habitat conditions and their life stage, it makes sense to assume they use a habitat selection time horizon of several months. |
| *mortFishTerrPredV9* | If this parameter is set to a low velocity (or close to *mortFishTerrPredV1*), velocity offers very high protection and terrestrial predation becomes negligible in many cells. The parameter is expected to have much less effect when set to higher values.<br><br>Values are not well known and can vary with predator types and the size of the stream. Normally, the value should be set so no habitat is routinely immune to terrestrial predation. Values should be selected for each study site, before calibration. |
| *habSearchProd* | Search-feeding energy intake increases linearly with this parameter, until intake is limited by *Cmax*. It mainly affects young-of-the-year trout growth and survival.<br><br>Values are site-specific and rarely well-known. This parameter is best evaluated via calibration to observed growth rates. |
| *fishMaxSwimParamB*<br>*fishMaxSwimParamC* | These affect both food intake (how capture success varies with velocity) and velocity mortality. Consequently, they strongly affect how many cells offer positive growth and high survival.<br><br>Values are from laboratory studies, but are moderately uncertain due to variability among individuals and measurement difficulties. Values should typically not be changed. |

**Table A24.** Parameters to which inSTREAM-Gen's assessed genetic outputs were found most sensitive in the global sensitivity analysis, in order of decreasing sensitivity.

| Parameter | Sensitivity considerations |
|---|---|
| *mortFishConditionK9* | See Table A23 |
| *fishRespParamB* | See Table A23 |
| *fishRespParamC* | |
| *fishRespParamA* | |
| *habDriftConc* | See Table A23 |
| *fishSpawnProb* | It defines the probability of spawning on the days when all the spawning criteria are met for a female. It gives the model user some control over what percent of spawning-sized fish actually spawn.<br>Values are uncertain and really not well-known. |
| *fishWeightParamA*<br>*fishWeightParamB* | Seemingly small changes can greatly affect the growth in length that results from growth in weight.<br>Values can vary among sites; using values from field data or literature will prevent significant error. |
| *fishSpawnMinAge* | It defines the minimum age a fish must have to be able to spawn.<br>Values can vary considerably among sites and can often be estimated from site-specific census data. Values should be selected for each study site, before calibration. |
| *mortFishTerrPredMin* | See Table A23 |
| *mortFishTerrPredV9* | See Table A23 |
| *fishMaxSwimParamD* | See Table A23 |
| *fishMaxSwimParamB* | |
| *habPreyEnergyDensity* | See Table A23 |
| *habDriftRegenDist* | See Table A23 |
| *fishFitnessHorizon* | See Table A23 |
| *fishSpawnMinCond* | It defines the minimum condition factor a fish must have to be able to spawn.<br>Values are uncertain, but considering the non-standard definition of condition factor, that the growth formulation makes it impossible that condition is equal to 1.0 on any days when fish did not obtain at least as much energy as expended for respiration, and that the bioenergetics of reproduction are not explicitly represented and fish have no incentive to put on weight in anticipation of spawning, its value is recommended to be slightly less than 1.0. |

### 7.2. Prioritization of parameters under observed-temperature scenario

As a second step, after determining the most influential parameters using the Morris method, we applied the variance decomposition technique of Sobol (1993) on the same seven model outputs. The rationale of performing such analysis was to decompose the model outputs' variance into variances attributable to each parameter. In practice, for a first order analysis each parameter was fixed one at a time across a selected matrix of parameter sets. Sobol first order sensitivity indices measure the effect of varying a focus parameter alone, but averaged over variations in other input parameters, providing thus information on the average reduction of output variance when the parameter is fixed. The sensitivity R package (Pujol et al. 2013) implements the Monte Carlo estimation of the Sobol's indices using the improved formulas of Sobol et al. (2007) and Saltelli et al. (2010). The number of tested settings was given by $m \times (p + 2)$, where $m$ is the size of the Monte Carlo sample matrix and $p$ is the number of parameters to analyze. We selected the eight parameters identified as most influential on both demographic and genetic outputs by the Morris method. Each parameter was varied over the following ranges: *habDriftConc* (2E-09-1E-09), *habDriftRegenDist* (100-900), *habPreyEnergyDensity* (1600-5500), *fishSpawnProb* (0.01-0.2), *fishFecundParamB* (1.7-3.3), *fishRespParamB* (0.627-0.94), *mortFishConditionK9* (0.42-0.8), and *mortFishTerrPredMin* (0.98-0.998). We chose a sample matrix of size 400, and Sobol first-order indices were computed for each parameter from a total number of runs of $400 \times (8 + 2) = 4000$.

For trout abundance, results indicated that *fishFecundParamB* and *mortFishConditionK9* had the greatest contribution to the variance of numbers of age-0 trout, while *mortFishConditionK9* and *mortFishTerrPredMin* had the highest mean Sobol indices for numbers of older trout. In consequence, *mortFishConditionK9* was the most important parameter for biomass of both age-0 and older trout. The parameter *mortFishConditionK9* explained the bulk (more than 40%) of all three genetic outputs variance (Table A25).

**Table A25.** Sobol first-order indices of sensitivity for the eight parameters of inSTREAM-Gen identified as the most influential by the Morris method influencing seven demographic and genetic outputs. Mean estimates and standard errors from 1000 bootstrap iterations are shown.

| Parameter | Count Age0 | Count Age1Plus | Biomass Age0 | Biomass Age1Plus | Males GMSL | Females GMSL | Emergence Length |
|---|---|---|---|---|---|---|---|
| *habDriftConc* | 0.056 | 0.001 | 0.074 | **0.135** | **0.142** | **0.163** | **0.157** |
| | (0.034) | (0.016) | (0.070) | (0.091) | (0.061) | (0.065) | (0.065) |
| *habDriftRegenDist* | 0.037 | 0.028 | 0.013 | 0.042 | 0.004 | 0.001 | -0.004 |
| | (0.039) | (0.065) | (0.057) | (0.084) | (0.041) | (0.041) | (0.040) |
| *habPreyEnergyDensity* | 0.034 | 0.015 | 0.090 | 0.059 | 0.063 | **0.119** | **0.116** |
| | (0.030) | (0.026) | (0.063) | (0.075) | (0.017) | (0.058) | (0.057) |
| *fishSpawnProb* | 0.005 | -0.007 | -0.018 | -0.008 | 0.017 | 0.036 | 0.030 |
| | (0.012) | (0.009) | (0.026) | (0.007) | (0.030) | (0.034) | (0.034) |
| *fishFecundParamB* | **0.232** | 0.021 | 0.010 | -0.004 | 0.026 | 0.041 | 0.035 |
| | (0.100) | (0.034) | (0.071) | (0.025) | (0.040) | (0.044) | (0.044) |
| *fishRespParamB* | 0.019 | -0.011 | 0.034 | 0.045 | 0.047 | 0.089 | 0.088 |
| | (0.025) | (0.018) | (0.034) | (0.058) | (0.046) | (0.051) | (0.049) |
| *mortFishConditionK9* | **0.205** | **0.231** | **0.142** | **0.368** | **0.417** | **0.467** | **0.466** |

| | | | | | | | |
|---|---|---|---|---|---|---|---|
| | (0.094) | (0.286) | (0.116) | (0.243) | (0.092) | (0.099) | (0.103) |
| *mortFishTerrPredMin* | 0.065 | **0.124** | 0.053 | **0.165** | 0.048 | 0.041 | 0.039 |
| | (0.043) | (0.149) | (0.084) | (0.154) | (0.045) | (0.049) | (0.047) |

However, ranking the analyzed parameters based on their first order sensitivity indices may be not enough in this case as their sum is well below 1. This is an indication that interactions among parameters are playing an important role, their combined effects being strongly non-additive. In this case, it is more informative to assess the total-effect indices, which measure the contribution to the output variance of the focus parameter, including all variance caused by its interactions, of any order, with any other input parameters.

Results showed that *fishFecundParamB* and *mortFishConditionK9* were the most important parameters in the estimation of abundance and biomass of age-0 trout (Table A26). The parameter *habDriftRegenDist* had also a relatively high contribution to the variance of biomass of age-0 trout through interactions with other parameters. Numbers and biomass of trout older than one year were highly sensitive to *mortFishConditionK9* and *mortFishTerrPredMin*. The analysis showed that the interaction of parameters *fishFecundParamB* and *fishRespParamB* with the rest of parameters highly driven variations in numbers of trout older than one year. For the three genetic outputs, *mortFishConditionK9* was clearly the parameter that could reduce most of the variance when fixed to its true value.

**Table A26.** Sobol total-effect indices of sensitivity for the eight parameters of inSTREAM-Gen identified as the most influential by the Morris method influencing seven demographic and genetic outputs. Mean estimates and standard errors from 1000 bootstrap iterations are shown.

| **Parameter** | **Count Age0** | **Count Age1Plus** | **Biomass Age0** | **Biomass Age1Plus** | **Males GMSL** | **Females GMSL** | **Emergence Length** |
|---|---|---|---|---|---|---|---|
| *habDriftConc* | 0.222 | 0.266 | 0.307 | 0.272 | 0.314 | 0.310 | 0.316 |
| | (0.080) | (0.132) | (0.117) | (0.173) | (0.067) | (0.069) | (0.069) |
| *habDriftRegenDist* | 0.288 | 0.337 | **0.438** | 0.301 | 0.124 | 0.118 | 0.121 |
| | (0.119) | (0.194) | (0.181) | (0.202) | (0.040) | (0.041) | (0.041) |
| *habPreyEnergyDensity* | 0.157 | 0.086 | 0.126 | 0.153 | 0.277 | 0.255 | 0.257 |
| | (0.046) | (0.059) | (0.114) | (0.078) | (0.054) | (0.054) | (0.052) |
| *fishSpawnProb* | 0.069 | 0.056 | 0.056 | 0.018 | 0.073 | 0.076 | 0.082 |
| | (0.028) | (0.009) | (0.019) | (0.011) | (0.030) | (0.035) | (0.035) |
| *fishFecundParamB* | **0.634** | **0.535** | **0.612** | 0.287 | 0.149 | 0.129 | 0.136 |
| | (0.138) | (0.290) | (0.186) | (0.131) | (0.047) | (0.048) | (0.047) |
| *fishRespParamB* | 0.306 | **0.610** | 0.363 | 0.295 | 0.117 | 0.079 | 0.077 |
| | (0.145) | (0.243) | (0.124) | (0.108) | (0.039) | (0.044) | (0.041) |
| *mortFishConditionK9* | **0.618** | **0.832** | **0.525** | **0.464** | **0.661** | **0.656** | **0.657** |
| | (0.160) | (0.196) | (0.198) | (0.374) | (0.087) | (0.092) | (0.091) |
| *mortFishTerrPredMin* | 0.099 | **0.557** | 0.162 | **0.445** | 0.192 | 0.173 | 0.175 |
| | (0.062) | (0.237) | (0.088) | (0.223) | (0.052) | (0.053) | (0.051) |

### 7.3. Screening of influential parameters under increased-temperature scenario

We repeated the same analyses but using a different input temperature profile, because parameters controlling effects of high temperature on reproduction, survival or metabolism may have little effect under conditions where temperatures are never extreme but the same parameters could be very important when temperatures are limiting. We created the new temperature profile by adding 3 °C to daily temperatures all year round. According to regional climate change projections, this water temperature increase is expected to occur by 2100 under the ecologically-friendly SRES scenario B2. The new sensitivity analysis was performed over the same seven demographic and genetic outputs. We selected the 36 parameters (half the number of the parameters selected for the first sensitivity analyses) identified as most influential by the Morris method using the original temperature profile. All parameters related to temperature were included in this selection. We then added an additional number of 13 parameters related to temperature that were not selected for the first sensitivity analyses. Those parameters are: *fishCmaxParamA*, *fishCmaxParamB*, *mortFishHiTT1*, *mortFishHiTT9*, *mortFishAqPredT1*, *mortFishAqPredT9*, *mortReddLoTT1*, *mortReddLoTT9*, *mortReddHiTT1*¸ *mortReddHiTT9*, *reddDevelParamA*, *reddDevelParamB*, and *reddDevelParamC*. The 49 selected parameters were varied over five levels according to ranges shown in Table A27. We chose again a value of 50 elementary effects, which led to 50 × (49 + 1) = 2500 new model runs.

**Table A27.** Range of parameter values used to conduct the global sensitivity analysis under a new temperature profile with increased daily temperatures. Parameters are displayed by alphabetical order.

| Parameter | Lower extreme | Lower median | Central | Upper median | Upper extreme |
|---|---|---|---|---|---|
| *fishCaptureParam9* | 0.375 | 0.437 | 0.5 | 0.563 | 0.625 |
| *fishCmaxParamA* | 0.314 | 0.470 | 0.628 | 0.78 | 0.942 |
| *fishCmaxParamB* | -0.24 | -0.27 | -0.3 | -0.33 | -0.36 |
| *fishDetectDistParamB* | 1.6 | 1.8 | 2.0 | 2.2 | 2.4 |
| *fishEnergyDensity* | 3900 | 4900 | 5900 | 6900 | 7900 |
| *fishFecundParamA* | 0.038 | 0.1 | 0.2 | 0.5 | 1 |
| *fishFecundParamB* | 1.7 | 2 | 2.6 | 3 | 3.3 |
| *fishFitnessHorizon* | 22 | 55 | 90 | 125 | 158 |
| *fishMaxSwimParamB* | 15.0 | 22.5 | 30.0 | 37.5 | 45.0 |
| *fishMaxSwimParamC* | -0.00375 | -0.00310 | -0.00250 | -0.0019 | -0.00125 |
| *fishMaxSwimParamD* | 0.036 | 0.054 | 0.072 | 0.09 | 0.108 |
| *fishMaxSwimParamE* | 0.250 | 0.375 | 0.500 | 0.625 | 0.750 |
| *fishMoveDistParamA* | 5 | 12.5 | 20 | 27.5 | 35 |
| *fishRespParamA* | 18 | 24 | 30 | 36 | 42 |

| | | | | | |
|---|---|---|---|---|---|
| *fishRespParamB* | 0.627 | 0.710 | 0.784 | 0.86 | 0.940 |
| *fishRespParamC* | 0.0415 | 0.0550 | 0.0693 | 0.0830 | 0.0970 |
| *fishSpawnMaxTemp* | 7 | 8.5 | 10 | 11.5 | 13 |
| *fishSpawnMinAge* | 365 | 547 | 730 | 912 | 1095 |
| *fishSpawnMinCond* | 0.9 | 0.925 | 0.95 | 0.975 | 1 |
| *fishSpawnMinLengthMeanF* | 14.5 | 15.5 | 16.5 | 17.5 | 18.5 |
| *fishSpawnMinTemp* | 2 | 3 | 4 | 5 | 6 |
| *fishSpawnProb* | 0.01 | 0.04 | 0.1 | 0.15 | 0.2 |
| *fishWeightParamA* | 0.00668 | 0.00770 | 0.00879 | 0.01135 | 0.01390 |
| *fishWeightParamB* | 2.949 | 3.022 | 3.098 | 3.155 | 3.212 |
| *habDriftConc* | 2.00E-10 | 4.00E-10 | 6.00E-10 | 8.00E-10 | 1.00E-09 |
| *habDriftRegenDist* | 100 | 300 | 500 | 700 | 900 |
| *habPreyEnergyDensity* | 1600 | 2000 | 2500 | 3500 | 5000 |
| *habSearchProd* | 1.3E-07 | 3.00E-07 | 5.00E-07 | 7.00E-07 | 8.8E-07 |
| *mortFishAngleSuccess* | 0.0001 | 0.0015 | 0.003 | 0.006 | 0.03 |
| *mortFishAqPredL1* | 2.5 | 3.25 | 4 | 4.5 | 5 |
| *mortFishAqPredMin* | 0.91 | 0.93 | 0.95 | 0.97 | 0.99 |
| *mortFishAqPredT1* | 3.1 | 4.5 | 6 | 7.5 | 9 |
| *mortFishAqPredT9* | 1 | 1.5 | 2 | 2.5 | 2.9 |
| *mortFishConditionK1* | 0.21 | 0.24 | 0.3 | 0.36 | 0.4 |
| *mortFishConditionK9* | 0.42 | 0.48 | 0.6 | 0.72 | 0.8 |
| *mortFishHiTT1* | 28.0 | 29.0 | 30.0 | 31.5 | 33.0 |
| *mortFishHiTT9* | 22.8 | 24.3 | 25.8 | 26.8 | 27.8 |
| *mortFishTerrPredH1* | 250 | 375 | 500 | 625 | 750 |
| *mortFishTerrPredMin* | 0.98 | 0.984 | 0.988 | 0.992 | 0.996 |
| *mortFishTerrPredV9* | 50 | 75 | 100 | 125 | 150 |
| *mortReddHiTT1* | 23 | 24 | 25 | 26 | 27 |
| *mortReddHiTT9* | 14 | 15 | 16 | 17 | 18 |
| *mortReddLoTT1* | -1.6 | -1.2 | -0.8 | -0.6 | -0.41 |

| | | | | | |
|---|---|---|---|---|---|
| *mortReddLoTT9* | -0.39 | -0.2 | 0 | 0.4 | 0.8 |
| *reddDevelParamA* | 0.0030674 | 0.0030987 | 0.0031300 | 0.0031613 | 0.0031926 |
| *reddDevelParamB* | 0.0000301 | 0.0000304 | 0.0000307 | 0.0000310 | 0.0000313 |
| *reddDevelParamC* | 0.0000915 | 0.0000925 | 0.0000934 | 0.0000943 | 0.0000953 |

As expected, temperature-related parameters played a pervasive role on controlling both demographic and genetic analyzed outputs under limiting water temperatures (Tables 28 and 29). This was especially true for YOY trout; eight and seven temperature-related parameters ranked amongst the 13 most influential parameters for abundance and biomass of YOYs, respectively. This was predictable as small fish are more sensitive to both extreme temperatures and temperature fluctuations than larger fish (see Elliott 1994 for details of underlying mechanisms). While *mortFishConditionK9, fishFecundParamB* and *fishRespParamB* were still the parameters exerting the strongest effects on demographic outputs of both YOY and older trout, these model outputs were also highly sensitive to parameters controlling trout and redd mortality due to high temperatures (*mortFishHiTT9* and *mortReddHiTT9*) as well as to parameters controlling temperature effects on fish swimming performance (*fishMaxSwimParamC* and *fishMaxSwimParamD*). Parameters driving temperature effects on the probability of surviving aquatic predation (*mortFishAqPredT9*) and on respiration costs (*fishRespParamC*) were additionally important for YOY's demographics. This aquatic predation survival increase function reflects how low temperatures reduce the metabolic demands and, therefore, feeding activity of piscivorous fish. Under increased temperatures, this function may no longer offer protection to small trout.

The parameters *mortFishConditionK9* and *fishRespParamB* were also the most influential for genetic outputs. However, five temperature-related parameters ranked amongst the ten most influential. Aside from the temperature-related parameters previously identified as important for demographic outputs, the parameter defining the maximum temperature at which trout are able to spawn (*fishSpawnMaxTemp*) had strong effects on all genetic outputs. By contrast, none of demographic and genetic model outputs were sensitive to any of the parameters controlling the development of eggs within the redd, despite this process being totally dependent on temperature conditions.

Despite being somewhat less influential under limiting temperatures, the habitat parameters *habDriftRegenDist, habDriftConc, habSearchProd* and *habPreyEnergyDensity*, as well as the fish parameter *mortFishTerrPredMin*, still had strong effects on model outputs, ranking amongst the twenty more determinant parameters across all model outputs. Interesting enough, the relevance of the parameter *fishFitnessHorizon* increased under increasing temperature conditions. Increased respiration costs (in both standard and activity components) and decreased probability of surviving extreme temperatures significantly affected the time horizon over which fish evaluate the tradeoffs between food intake and mortality risks to maximize their probability of surviving and reproducing under limiting temperatures.

**Table A28.** Ranking and sensitivity values (as a percentage of the maximum sensitivity) of the 24 parameters to which demographic outputs are most sensitive under a new temperature profile with increased daily temperatures.

| Parameter | Count Age0 | Parameter | Count Age1Plus | Parameter | Biomass Age0 | Parameter | Biomass Age1Plus |
|---|---|---|---|---|---|---|---|
| *fishFecundParamB* | 100.0 | *fishFecundParamB* | 100.0 | *fishRespParamB* | 100.0 | *mortFishConditionK9* | 100.0 |
| *fishRespParamB* | 82.1 | *mortFishConditionK9* | 92.4 | *fishFecundParamB* | 84.2 | *fishRespParamB* | 98.1 |
| *mortFishHiTT9* | 61.1 | *fishFitnessHorizon* | 90.2 | *mortFishHiTT9* | 83.7 | *mortFishTerrPredV9* | 95.5 |
| *mortFishConditionK9* | 59.9 | *fishRespParamB* | 84.2 | *fishFitnessHorizon* | 76.1 | *mortFishHiTT9* | 95.4 |
| *fishFitnessHorizon* | 50.7 | *mortFishHiTT9* | 75.1 | *habPreyEnergyDensity* | 72.3 | *habPreyEnergyDensity* | 82.4 |
| *mortReddHiTT9* | 43.9 | *fishMaxSwimParamC* | 68.4 | *fishMaxSwimParamD* | 47.5 | *fishMaxSwimParamC* | 79.2 |
| *fishCmaxParamB* | 41.2 | *mortFishTerrPredV9* | 67.2 | *mortReddHiTT1* | 46.1 | *habDriftRegenDist* | 76.7 |
| *fishMaxSwimParamD* | 40.0 | *habSearchProd* | 51.6 | *fishMaxSwimParamC* | 44.2 | *fishFecundParamB* | 75.1 |
| *fishMaxSwimParamC* | 39.4 | *mortFishTerrPredH1* | 49.4 | *fishFecundParamA* | 43.6 | *mortFishConditionK1* | 68.5 |
| *mortReddHiTT1* | 39.2 | *mortFishAngleSuccess* | 48.8 | *mortFishAqPredT9* | 43.5 | *habSearchProd* | 63.6 |
| *habSearchProd* | 36.4 | *habDriftRegenDist* | 48.2 | *mortFishConditionK9* | 43.1 | *mortFishTerrPredMin* | 54.6 |
| *fishRespParamC* | 36.3 | *mortFishConditionK1* | 47.5 | *fishRespParamC* | 42.0 | *fishFecundParamA* | 51.9 |
| *fishSpawnMaxTemp* | 33.3 | *fishMaxSwimParamD* | 44.7 | *mortReddHiTT9* | 39.0 | *fishRespParamA* | 51.7 |
| *fishMoveDistParamA* | 33.2 | *mortFishTerrPredMin* | 43.2 | *mortFishTerrPredV9* | 35.9 | *mortFishAngleSuccess* | 49.8 |
| *fishWeightParamB* | 31.8 | *mortReddHiTT9* | 41.1 | *fishMoveDistParamA* | 35.3 | *fishEnergyDensity* | 49.6 |
| *fishFecundParamA* | 31.7 | *fishEnergyDensity* | 38.8 | *fishSpawnProb* | 35.2 | *fishMaxSwimParamD* | 48.8 |
| *mortFishAngleSuccess* | 31.7 | *habPreyEnergyDensity* | 36.6 | *fishEnergyDensity* | 35.1 | *fishMaxSwimParamB* | 44.1 |
| *mortFishTerrPredV9* | 31.3 | *fishWeightParamB* | 36.0 | *habDriftConc* | 32.6 | *mortFishAqPredT9* | 40.6 |
| *habDriftRegenDist* | 30.5 | *fishSpawnMaxTemp* | 33.3 | *fishSpawnMinLengthMeanF* | 32.4 | *fishFitnessHorizon* | 38.1 |
| *fishSpawnProb* | 30.1 | *fishRespParamC* | 32.5 | *mortFishConditionK1* | 32.2 | *fishWeightParamB* | 37.9 |
| *mortReddLoTT1* | 28.7 | *fishMoveDistParamA* | 32.0 | *reddDevelParamB* | 32.1 | *habDriftConc* | 37.5 |
| *mortFishAqPredT9* | 28.7 | *mortFishAqPredT9* | 31.3 | *mortFishTerrPredMin* | 31.4 | *fishMoveDistParamA* | 34.1 |
| *habDriftConc* | 28.3 | *fishFecundParamA* | 30.9 | *habSearchProd* | 30.8 | *fishCaptureParam9* | 33.1 |

**Table A29.** Ranking and sensitivity values (as a percentage of the maximum sensitivity) of the 24 parameters to which genotypic outputs are most sensitive under a new temperature profile with increased daily temperatures.

| Parameter | Males GMSL | Parameter | Females GMSL | Parameter | Emergence Length |
|---|---|---|---|---|---|
| *mortFishConditionK9* | 100.0 | *mortFishConditionK9* | 100.0 | *mortFishConditionK9* | 100.0 |
| *fishRespParamB* | 67.9 | *fishRespParamB* | 68.4 | *fishRespParamB* | 72.2 |
| *fishSpawnMaxTemp* | 55.7 | *fishRespParamC* | 61.3 | *mortFishHiTT9* | 66.9 |
| *mortFishHiTT9* | 46.7 | *mortFishHiTT9* | 61.2 | *fishRespParamC* | 65.9 |
| *mortFishAqPredT9* | 45.7 | *fishSpawnMaxTemp* | 57.2 | *fishSpawnMaxTemp* | 62.1 |
| *habPreyEnergyDensity* | 45.1 | *fishMaxSwimParamE* | 54.6 | *fishMaxSwimParamE* | 60.1 |
| *fishCaptureParam9* | 45.0 | *mortFishAqPredT9* | 54.5 | *mortFishAqPredT9* | 56.3 |
| *fishFecundParamB* | 44.9 | *mortFishConditionK1* | 49.7 | *mortFishAqPredL1* | 51.6 |
| *fishRespParamC* | 43.3 | *mortFishAqPredL1* | 47.7 | *mortFishConditionK1* | 50.6 |
| *fishMaxSwimParamE* | 43.3 | *fishFecundParamB* | 47.4 | *fishFecundParamB* | 48.4 |
| *mortFishConditionK1* | 42.2 | *mortFishAqPredMin* | 45.3 | *mortFishAqPredMin* | 45.1 |
| *fishFecundParamA* | 41.5 | *habSearchProd* | 44.0 | *habSearchProd* | 44.7 |
| *fishFitnessHorizon* | 40.6 | *fishCaptureParam9* | 42.2 | *fishCaptureParam9* | 44.5 |
| *fishWeightParamB* | 39.8 | *fishMoveDistParamA* | 42.1 | *fishMoveDistParamA* | 42.9 |
| *mortFishAngleSuccess* | 39.5 | *habPreyEnergyDensity* | 41.2 | *habPreyEnergyDensity* | 41.0 |
| *mortFishAqPredL1* | 39.2 | *fishWeightParamB* | 40.8 | *fishWeightParamB* | 40.5 |
| *fishMaxSwimParamC* | 37.9 | *fishFitnessHorizon* | 39.4 | *habDriftConc* | 40.1 |
| *habSearchProd* | 36.8 | *mortFishTerrPredMin* | 38.3 | *mortFishTerrPredMin* | 39.4 |
| *fishWeightParamA* | 34.8 | *habDriftConc* | 37.3 | *fishFitnessHorizon* | 38.8 |
| *mortFishTerrPredH1* | 34.6 | *fishFecundParamA* | 35.9 | *mortReddLoTT1* | 37.7 |
| *mortFishTerrPredMin* | 33.8 | *fishSpawnProb* | 35.5 | *fishWeightParamA* | 37.7 |
| *fishDetectDistParamB* | 33.7 | *fishWeightParamA* | 35.2 | *fishSpawnProb* | 37.4 |
| *fishEnergyDensity* | 33.2 | *mortReddLoTT1* | 35.1 | *fishMaxSwimParamD* | 37.3 |

Parameters controlling respiration costs are derived from laboratory studies and are generally well-known. Parameters controlling the swimming capacity of fish are also based on laboratory studies, but their values are moderately uncertain due to variability among individuals and measurement difficulties so they should typically not be changed. Values for the parameter defining the maximum temperature at which spawning occurs are typically well-established and can be borrowed from the existing literature. However, temperature-related parameters controlling survival functions are typically quite uncertain (Table A30), so caution must be paid when selecting their values.

**Table A30.** Temperature-related parameters to which inSTREAM-Gen's assessed demographic and genetic outputs were found most sensitive in the global sensitivity analysis, in order of decreasing sensitivity.

| Parameter | Sensitivity considerations |
|---|---|
| *mortFishHiTT9* | This parameter controls fish mortality owing to the breakdown of physiological processes at high temperatures.<br><br>Models of this mortality source remain variable and uncertain because mortality varies (a) with laboratory conditions and techniques and the endpoints used to define mortality, (b) between laboratory and field conditions, and (c) among individuals. Interspecific differences in lethal temperatures are not clearly distinguishable from uncertainty and variability in the measurements. |
| *fishMaxSwimParamC* | See Table A23 |
| *fishMaxSwimParamD* | |
| *fishMaxSwimParamE* | |
| *fishRespParamC* | See Table A23 |
| *mortFishAqPredT9* | This parameter controls the aquatic predation survival increase function that describes how low temperatures reduce the metabolic demands and, therefore, feeding activity of piscivorous fish.<br><br>The function is based on the bioenergetics of the trout predators, using a decreasing logistic function that approximates the decline in maximum food consumption (*cMax*) with declining temperature. Values are from laboratory studies, but in general, *cMax* is poorly defined and difficult to measure, which adds an inherent uncertainty to this parameter. |
| *fishSpawnMaxTemp* | This parameter defines the maximum temperature at which spawning occurs.<br><br>Reliable values can be borrowed from the literature. |
| *mortReddHiTT9* | This parameter controls the fraction of eggs surviving mortality due to high temperatures.<br><br>Values for rainbow trout are from laboratory studies, but parameter values for brown trout were guestimated and arbitrarily set, so they should not be considered reliable. |

### 7.4. Prioritization of parameters under increased-temperature scenario

We selected again the eight parameters identified as most influential on both demographic and genetic outputs by the Morris method to perform a new sensitivity analysis using the Sobol method. Each parameter was varied over the following ranges: *habPreyEnergyDensity* (1600-5500), *fishFecundParamB* (1.7-3.3), *fishRespParamB* (0.627-0.94), *fishRespParamC* (0.0415-0.097), *fishMaxSwimParamC* (-0.00375 - -0.00125), *mortFishConditionK9* (0.42-0.8), *mortFishHiTT9* (22.8-27.8), and *fishFitnessHorizon* (22 - 158). We chose a sample matrix of size 400, and Sobol first-order and total-effect indices were computed for each parameter from a total number of runs of $400 \times (8 + 2) = 4000$.

The analysis of the first-order indices showed that *fishFecundParamB* and *mortFishConditionK9* had the highest contribution to the variance of abundance and biomass of both age-0 trout and trout older than one year. As it happened with the unmodified temperature scenario, *mortFishConditionK9* was the most important parameter for the three genetic outputs (Table A31). However, the sum of the first order sensitivity indices was again well below 1 for all model outputs, so the assessment of the total-effect indices was necessary.

**Table A31.** Sobol first-order indices of sensitivity for the eight parameters of inSTREAM-Gen identified as the most influential by the Morris method influencing seven demographic and genetic outputs under the increased-temperature profile scenario. Mean estimates and standard errors from 1000 bootstrap iterations are shown.

| Parameter | Count Age0 | Count Age1Plus | Biomass Age0 | Biomass Age1Plus | Males GMSL | Females GMSL | Emergence Length |
|---|---|---|---|---|---|---|---|
| *habPreyEnergyDensity* | -0.001 | -0.020 | 0.052 | 0.088 | -0.035 | -0.066 | -0.065 |
| | (0.034) | (0.037) | (0.059) | (0.059) | (0.052) | (0.058) | (0.056) |
| *fishFecundParamB* | **0.360** | **0.123** | **0.198** | 0.071 | 0.022 | -0.019 | -0.020 |
| | (0.104) | (0.072) | (0.073) | (0.037) | (0.050) | (0.055) | (0.056) |
| *fishRespParamB* | 0.032 | 0.026 | 0.061 | 0.094 | 0.068 | 0.071 | 0.075 |
| | (0.033) | (0.031) | (0.042) | (0.060) | (0.045) | (0.048) | (0.047) |
| *fishRespParamC* | 0.072 | 0.066 | 0.080 | 0.075 | 0.018 | -0.008 | -0.006 |
| | (0.040) | (0.028) | (0.043) | (0.035) | (0.042 | (0.048) | (0.049) |
| *fishMaxSwimParamC* | -0.037 | -0.029 | -0.041 | 0.009 | -0.061 | -0.070 | -0.069 |
| | (0.017) | (0.013) | (0.029) | (0.030) | (0.033) | (0.038) | (0.038) |
| *mortFishConditionK9* | **0.148** | **0.256** | **0.130** | **0.211** | **0.353** | **0.334** | **0.336** |
| | (0.054) | (0.112) | (0.060) | (0.077) | (0.098) | (0.095) | (0.101) |
| *mortFishHiTT9* | 0.087 | 0.053 | 0.061 | 0.076 | 0.071 | 0.065 | 0.067 |
| | (0.050) | (0.049 | (0.034) | (0.032) | (0.054) | (0.053) | (0.056) |
| *fishFitnessHorizon* | -0.019 | 0.003 | -0.026 | 0.014 | -0.003 | -0.039 | -0.033 |
| | (0.019) | (0.026) | (0.026) | (0.028) | (0.042) | (0.045) | (0.045) |

The parameter *fishFecundParamB* had the highest contribution to the variance of numbers and biomass of age-0 trout (Table A32). In this case, the parameters *mortFishConditionK9*, *mortFishHiTT9*, *habPreyEnergyDensity* and *fishRespParamB* had a relatively important secondary role. Numbers and biomass of trout older than one year were highly sensitive to

*mortFishConditionK9*. While variations of *mortFishHiTT9* alone had negligible effects on these model outputs, its interactive effects with other analysed parameters had a strong contribution, especially to explain numbers variability. In a lesser extent, the parameter *fishRespParamB* was also highly important (Table A32). For the three genetic outputs, *mortFishConditionK9* was again the parameter that could reduce most of the variance when fixed to its true value, but the parameter *habPreyEnergyDensity* had also a high contribution through interactions with other parameters. The parameters *fishMaxSwimParamC* and *fishFitnessHorizon* seem to have a small contribution to the variance of the seven tested model outputs.

**Table A32.** Sobol total-effect indices of sensitivity for the eight parameters of inSTREAM-Gen identified as the most influential by the Morris method influencing seven demographic and genetic outputs under the increased-temperature profile scenario. Mean estimates and standard errors from 1000 bootstrap iterations are shown.

| Parameter | Count Age0 | Count Age1Plus | Biomass Age0 | Biomass Age1Plus | Males GMSL | Females GMSL | Emergence Length |
|---|---|---|---|---|---|---|---|
| *habPreyEnergyDensity* | 0.277 | 0.304 | 0.388 | 0.287 | **0.403** | **0.440** | **0.441** |
| | (0.068) | (0.110) | (0.094) | (0.096) | (0.067) | (0.073) | (0.072) |
| *fishFecundParamB* | **0.564** | 0.274 | **0.458** | 0.163 | 0.193 | 0.235 | 0.234 |
| | (0.081) | (0.085) | (0.081) | (0.079) | (0.053) | (0.057) | (0.057) |
| *fishRespParamB* | 0.161 | 0.204 | 0.301 | **0.428** | 0.159 | 0.203 | 0.196 |
| | (0.056) | (0.108) | (0.067) | (0.078) | (0.047) | (0.054) | (0.052) |
| *fishRespParamC* | 0.137 | 0.186 | 0.131 | 0.097 | 0.114 | 0.180 | 0.175 |
| | (0.067) | (0.104) | (0.070) | (0.063) | (0.049) | (0.054) | (0.053) |
| *fishMaxSwimParamC* | 0.035 | 0.036 | 0.070 | 0.052 | 0.116 | 0.160 | 0.157 |
| | (0.037) | (0.050) | (0.054) | (0.068) | (0.035) | (0.040) | (0.039) |
| *mortFishConditionK9* | 0.348 | **0.470** | 0.272 | **0.429** | **0.570** | **0.586** | **0.591** |
| | (0.084) | (0.090) | (0.089) | (0.092) | (0.084) | (0.087) | (0.087) |
| *mortFishHiTT9* | 0.337 | **0.605** | 0.283 | 0.364 | 0.246 | 0.237 | 0.234 |
| | (0.077) | (0.100) | (0.073) | (0.088) | (0.056) | (0.056) | (0.061) |
| *fishFitnessHorizon* | 0.117 | 0.191 | 0.047 | 0.078 | 0.156 | 0.189 | 0.181 |
| | (0.039) | (0.055) | (0.040) | (0.051) | (0.046) | (0.053) | (0.045) |

- Conclusions:

1. Values for the habitat parameters *habDriftRegenDist*, *habDriftConc* and *habSearchProd*, as well as the fish parameters controlling terrestrial and aquatic predation mortality *mortFishTerrPredMin* and *mortFishAqPredMin*, must be estimated via calibration because (1) all model outputs are highly sensitive to their variations, (2) they are typically unknown and highly uncertain, and (3) they are typically site-specific.

2. Values for the habitat parameter *habPreyEnergyDensity* should be calibrated when no information is available for the studied rivers since it is highly site-specific and all model outputs are very sensitive to its variations.

3. The fish parameter controlling the probability of surviving starvation, *mortFishConditionK9*, is a key parameter irrespective of the temperature profile used in the sensitivity analysis, influencing all model outputs. Values are not well known and changes in them are likely to have widespread, complex, and unexpected effects. Therefore, we recommend not to change the default values.

4. Parameters defining the fecundity (*fishFecundParamA* and *B*) and length-weight (*fishWeightParamA* and *B*) relationships are strongly influential to all model outputs under any temperature profile. They are highly site-specific population parameters, so their values should be known for the study population before calibration.

5. Parameters driving respiration costs (*fishRespParamA*-*C*) and fish swimming capacity (*fishMaxSwimParamA*-*E*) are strongly influential to all model outputs irrespective of the temperature profile. Further, the influence of the parameters involved on the temperature functions significantly increased under limiting water temperatures. Values are relatively well-known from laboratory studies, and typically should not be changed.

6. Parameters defining the conditions under which spawning occurs, *fishSpawnMinAge*, *fishSpawnMinCond*, *fishSpawnProb* and *fishSpawnMaxTemp*, have strong effects on genetic outputs. The first three parameters are highly influential under no temperature limitation, while on the contrary, the latter one was important only under increased temperature conditions. Values can be uncertain and site-specific so they should be selected for each study site, before calibration.

7. Temperature-related parameters controlling trout and redd mortality (*mortFishHiTT9*, *mortFishAqPredT9* and *mortReddHiTT9*) influence all model outputs under limiting temperatures. Values are typically quite uncertain, so caution must be paid when changing their values; it is not recommended.

8. Sensitivity of inSTREAM-Gen's model outputs to *fishFitnessHorizon* was higher than previously reported for inSTREAM. What is more, its relevance increased under increasing temperature conditions. Further investigation on this parameter is required.

# 8 Model output corroboration

**This TRACE element provides supporting information on**: How model predictions compare to independent data and patterns that were not used, and preferably not even known, while the model was developed, parameterized, and verified. By documenting model output corroboration, model users learn about evidence which, in addition to model output verification, indicates that the model is structurally realistic so that its predictions can be trusted to some degree.

**Summary:**

**So far inSTREAM-Gen's predictions have not been compared to independent data. We summarize, nevertheless, the numerous ecological patterns successfully reproduced by inSTREAM, which should be accordingly mimicked by inSTREAM-Gen.**

In the section 5 ("Implementation verification") of this document, we proved that inSTREAM-Gen and inSTREAM produced the same results (i.e., results did not statistically differed) when run under the same simulation scenarios (same model inputs and parameter

values, with no genetic transmission of heritable traits). We have not tested so far how inSTREAM-Gen's predictions compare to independent data or qualitative patterns described in the literature. Nevertheless, Railsback and colleagues have shown along the way that inSTREAM is capable of reproducing numerous ecological qualitative patterns described in the literature regarding stream-dwelling trout populations (Table A33). Here, we summarized all these ecological patterns successfully reproduced by inSTREAM, which should be accordingly mimicked by inSTREAM-Gen.

- Habitat selection and foraging behaviour:

Railsback and Harvey (2002) showed that inSTREAM (using input data and parameters representing a resident cutthroat trout *Oncorhynchus clarki* population) was able to reproduce six habitat selection patterns observed in real trout populations; patterns that (1) are general responses to relatively well-understood changes in growth and risk conditions, (2) are documented in the literature, and (3) occur over spatial and temporal scales compatible with the model. Importantly, the authors showed that those patterns were only reproduced by the IBM when modelled trout selected habitat to maximize "Expected Reproductive Maturity", but no when habitat-selection objectives were to maximize either growth rate or probability of survival. The tested and successfully reproduced patterns are:

1) Hierarchical feeding in heterogeneous habitat: this pattern is defined by (a) a consistent preference for specific feeding sites, (b) dominant fish displacing others from the most preferred sites, and (c) subdominant fish occupying the most preferred sites when the dominant fish are removed.

2) Response to high flows: trout move to stream margins during flood flows and return to previous locations as flows recede.

3) Response to interspecific competition: competition with a larger species produces a shift in habitat selection by age-0 trout toward higher velocities and shallower depths.

4) Response to predatory fish: the presence of piscivorous fish results in a shift by age-0 trout to faster and shallower habitat.

5) Variation in velocity preference with season: trout prefer higher velocities in summer compare to winter.

6) Changes in habitat use with food availability and energy reserves: trout move to habitat that provides higher food intake, at the cost of lower survival probability, when food availability is reduced.

Railsback and Harvey (2005) performed simulation experiments (modelling a trout assemblage comprised by brown trout *Salmo trutta* and rainbow trout *Oncorhynchus mykiss*) that showed that the IBM reproduces eight diverse diel behavior patterns observed in real trout populations. A key feature of the simulation experiment was that the model was able to explain all the following patterns of variation in diel foraging behaviour without assuming that populations or individuals vary in how inherently nocturnal or diurnal they are. The reproduced patterns were:

1) Diel activity (whether foraging occurs during day and/or night) varies among a population's individuals, and from day to day for each individual.

2) Salmonids use shallower and slower habitat for nocturnal feeding than for daytime feeding.

3) Local densities of trout in the best habitat are higher when feeding at night.

4) Salmonids feed relatively more at night if temperatures (and, therefore, metabolic demands) are low. That is, the relative frequency of nocturnal feeding decreases as temperature increases.

5) Daytime feeding is more common for life stages in which potential fitness increases more rapidly with growth.

6) Competition for feeding or hiding sites can shift foraging between day and night: competition from larger, night-feeding fish increases the fraction of feeding by smaller fish that occurs in daytime.

7) Daytime feeding is more common when food availability or fish condition is low.

8) Diel activity patterns are affected by the availability of good habitat for feeding or hiding.

- Population dynamics:

Railsback et al. (2002) illustrated the ability of inSTREAM to reproduce five patterns of population-level behaviour observed in real trout. The modelled cutthroat trout population (same as in Railsback and Harvey 2002) followed the next theoretically-expected and/or observed patterns:

1) A "self-thinning" relationship, a negative power relationship between mean weight and mean abundance among age classes.

2) The “critical survival time”, the duration of intense, density-dependent mortality in newly hatched trout.

3) Age-specific quantitative patterns in population variation over time observed in a trout stream similar to the modelled one: (a) fourfold interannual variation in abundance of age 0 trout; (b) age 1 had the most stable abundance, with the highest abundance only twice the lowest; (c) age 2+ was the most variable age class, with sixfold interannual variation; (d) no correlation between the number of age 1 fish one year and the number of age 2+ fish the following year; (e) a weak correlation between peak flow in winter and abundance of age 1 trout the following summer; (f) no correlation between summer low flow and trout abundance.

4) Density-dependent growth.

5) Fewer large adult trout in the absence of deep pool habitat.

Harvey and Railsback (2014) additionally showed that inSTREAM successfully predicted differences in adult trout growth and how growth was affected by stream flow as observed in empirical studies.

Harvey et al. (2014) applied inSTREAM to stream reaches above and below a diversion that have been monitored on their biophysical properties for 4 years. The model accurately predicted the observed difference in fish biomass between control and diversion reaches at the ends of the dry seasons. Instream also reproduced the large seasonal differences in growth, small differences between reaches in individual growth, and natural distributions of growth among individuals.

**Table A33.** Patterns theoretically expected or observed in real trout populations reproduced by the inSTREAM IBM.

| Pattern | Reference |
|---|---|
| Habitat selection behaviour: | |
| Hierarchical feeding in heterogeneous habitat, responses to high flow, interspecific competition and predatory fish, seasonal shifts in velocity preferences, and changes in habitat use with food availability and energy reserves | Railsback and Harvey (2002) |
| Diel foraging behaviour: | |
| Variations in individual diel activity and habitat use, and responses to temperature, competition, food availability and habitat quality | Railsback et al. (2005) |
| Demographic and life-history population-level behaviour: | Railsback et al. (2002) |
| Self-thinning, the critical survival time after emergence, density-dependent growth, and age-specific quantitative patterns in population variation over space and time | |
| Adult trout individual growth rates and streamflow effects on growth rates | Harvey and Railsback (2014) |
| Population biomass below vs. above a flow diversion | Harvey et al. (2014) |

# 9 References

Alexander, G.R., 1979. Predators of fish in coldwater streams. Predator-prey systems in fisheries management, in Clepper, H. (Editor). Sport Fishing Institutes, Washington, D. C, pp. 153-170.

Almodóvar, A., Nicola, G.G., Elvira, B., Ayllón, D., Leal, S., Parra, I., 2006. Analysis of population dynamics and angling impacts on the brown trout populations of Navarre. Carrying capacity modelling for brown trout population conservation and management. Study of the genetic variability of brown trout in Navarre. (In Spanish). Government of Navarre, Final Report, 3369 pp.

Almodóvar, A., Nicola, G.G., Ayllón, D., Elvira, B., 2012. Global warming threatens the persistence of Mediterranean brown trout. Glob. Change Biol. 18, 1549-1560.

Alsop, D. H., Wood, C.M., 1997. The interactive effects of feeding and exercise on oxygen consumption, swimming performance and protein usage in juvenile rainbow trout (*Oncorhynchus mykiss*). J. Exp. Biol. 200, 2337-2346.

Armstrong, J.D., Kemp, P.S., Kennedy, G.J.A., Ladle, M., Milner, N.J., 2003. Habitat requirements of Atlantic salmon and brown trout in rivers and streams. Fish. Res. 62, 143-170.

Aulstad, D., Skjervol, H., Gjedrem, T., 1972. Genetic and environmental sources of variation in length and weight of rainbow trout (*Salmo gairdneri*). Journal of the Fisheries Research Board of Canada 29, 237-241.

Ayllón, D., Almodóvar, A., Nicola, G.G., Elvira, B., 2009. Interactive effects of cover and hydraulics on brown trout habitat selection patterns. River Res. Appl. 25, 1051-1065.

Ayllón, D., Almodóvar, A., Nicola, G.G., Elvira, B., 2010a. Ontogenetic and spatial variations in brown trout habitat selection. Ecol. Freshw. Fish 19, 420-432.

Ayllón, D., Almodóvar, A., Nicola, G.G., Elvira, B., 2010b. Modelling brown trout spatial requirements through physical habitat simulations. River Res. Appl. 26, 1090-1102.

Ayllón, D., Almodóvar, A., Nicola, G.G., Parra, I., Elvira, B., 2012a. Modelling carrying capacity dynamics for the conservation and management of territorial salmonids. Fisheries Research 134-136, 95-103.

Ayllón, D., Almodóvar, A., Nicola, G.G., Parra, I., Elvira, B., 2012b. A new biological indicator to assess the ecological status of Mediterranean trout type streams. Ecol. Indic. 20, 295-303.

Ayllón, D., Railsback, S.F., Vincenzi, S., Groeneveld, J., Almodóvar, A., Grimm, V., 2015. InSTREAM-Gen: modelling eco-evolutionary dynamics of trout populations under anthropogenic environmental change. Ecological Modelling.

Baltz, D.M., Moyle, P.B., 1984. Segregation by species and size classes of rainbow trout, *Salmo gairdneri*, and Sacramento sucker, *Catostomus occidentalis,* in three California streams. Environ. Biol. Fishes10, 101-110.

Baltz, D.M., Vondracek, B., Brown, L.R., Moyle, P.B., 1987. Influence of temperature on microhabitat choice by fishes in a California stream. Trans. Am. Fish. Soc. 116,12-20.

Bartell, S.M., Breck, J.M., Gardner, R.H., Brenkert, A.L., 1986. Individual parameter perturbation and error analysis of fish bioenergetics models. Can. J. Fish. Aquat. Sci.
43, 160-168.

Battarbee, R.W., Kernan, M., Livingstone, D., et al., 2008. Euro-limpacs Position Paper: Impact of climate change on European freshwater ecosystems: consequences, adaptation and policy. Euro-limpacs Deliverable No. 301.

Bell, G., González, A., 2011. Adaptation and Evolutionary Rescue in Metapopulations Experiencing Environmental Deterioration. Science 332, 1327-1330.

Blanc, J.M., 2005. Contribution of genetic and environmental variance components to increasing body length in juvenile brown trout Salmo trutta. J. World Aquac. Soc. 36, 51-58.

Booker, D.J., Dunbar, M.J., Ibbotson, A., 2004. Predicting juvenile salmonid drift-feeding habitat quality using a three-dimensional hydraulic-bioenergetic model. Ecol. Mod. 177, 157-177.

Bradford, M. J., Higgins, P. S., 2001. Habitat-, season-, and size-specific variation in diel activity patterns of juvenile chinook salmon (*Oncorhynchus tshawytscha*) and steelhead trout (*Oncorhynchus mykiss*). Can. J. Fish. Aquat. Sci. 58, 365-374.

Brown, H.W., 1974. Handbook of the effects of temperature on some North American fishes. Canton, Ohio: American Electric Power Service Corp.

Brown, L.R., Moyle, P.B., 1991. Changes in habitat and microhabitat partitioning within an assemblage of stream fishes in response to predation by Sacramento squawfish (*Ptychocheilus grandis*). Can. J. Fish. Aquat. Sci. 48, 849-856.

Brunet, M., Casado, M.J., de Castro, M., et al., 2009. Regional climate change scenarios for Spain (in Spanish). Spanish Meteorological Agency.

Butler, P.J., Day, N., Namba, K.,1992. Interactive effects of seasonal temperature and low pH on resting oxygen uptake and swimming performance of adult brown trout *Salmo trutta*. J. Exp. Biol. 165,195-212.

Campolongo, F., Cariboni, J., Saltelli, A., 2007. An effective screening design for sensitivity analysis of large models. Environ. Mod. Softw. 22, 1509-1518.

Carlson, S.M., Seamons, T.R., 2008. A review of quantitative genetic components of fitness in salmonids: implications for adaptation to future change. Evol. Appl. 1, 222-238.

Carnell, R. 2012. Lhs: Latin Hypercube Samples. R Package Version 0.10.

Comte, L., Grenouillet, G., 2013. Do stream fish track climate change? Assessing distribution shifts in recent decades. Ecography 36 1236-1246.

Cunningham, P. M. 2007. A sensitivity analysis of an individual-based trout model. Master thesis, Department of Mathematics, Humboldt State University, Arcata, California.

Cutts, C.J., Brembs, B., Metcalfe, N.B., Taylor, A.C., 1999. Prior residence, territory quality and life-history strategies in juvenile Atlantic salmon (*Salmo salar* L.). J.Fish Biol. 55, 784-794.

DeVries, P., 1997. Riverine salmonid egg burial depths: review of published data and implications for scour studies. Can. J. Fish. Aquat. Sci. 54, 1685-1698.

Diana, J.S., Hudson, J. P., Richard, J., Clark, D., 2004. Movement patterns of large brown trout in the mainstream Au Sable River, Michigan. Trans. Am. Fish. Soc. 133, 34-44.

Dickerson, B.R., Vinyard, G.L., 1999. Effects of high chronic temperatures and diel temperature cycles on the survival and growth of Lahontan cutthroat trout. Trans. Am. Fish. Soc. 128, 516-521.

Dickerson, B.R., Willson, M.F., Bentzen, P., Quinn, T.P., 2005. Heritability of life history and morphological traits in a wild pink salmon population assessed by DNA parentage analysis. Trans. Am. Fish. Soc. 134, 1323-1328.

Dunlop, E.S., Heino, M., Dieckmann, U., 2009. Eco-genetic modeling of contemporary life-history evolution. Ecol. Appl. 19, 1815-1834.

Einum, S., Fleming, I.A., 1999. Maternal effects of egg size in brown trout (Salmo trutta): norms of reaction to environmental quality. Proc. R. Soc. Lond. B 266, 2095-2100.

Elliott, J.M., 1982. The effects of temperature and ration size on growth and energetics of salmonids in captivity. Comp. Biochem. Physiol. 73, 81-91.

Elliott, J.M., 1984. Numerical changes and population regulation in young migratory trout Salmo trutta in a Lake District stream, 1966-83. J. Anim. Ecol. 53, 327-350.

Elliott, J.M., 1994. Quantitative ecology and the brown trout. Oxford University Press, New York.

Essington, T.E., Quinn, T.P., Ewert, V.E., 2000. Intra- and inter-specific competition and the reproductive success of sympatric Pacific salmon. Can. J. Fish. Aquat. Sci. 57, 205-213.

Falconer, D.S., Mackay, T.F.C., 1996. Introduction to quantitative genetics. Fourth edition. Longman, Essex, UK.

Fishback, A.G., Danzmann, R.G., Ferguson, M.M., Gibson, J.P., 2002. Estimates of genetic parameters and genotype by environment interactions for growth traits of rainbow trout (*Oncorhynchus mykiss*) as inferred using molecular pedigrees. Aquaculture 206, 137-150.

Frank, B.M., Baret, P.V., 2013. Simulating brown trout demogenetics in a river/nursery brook system: The individual-based model DemGenTrout. Ecol. Mod. 248, 184-202.

Fraser, N., Metcalfe, N.B., 1997. The costs of becoming nocturnal: feeding efficiency in relation to light intensity in juvenile Atlantic salmon. Funct. Ecol. 11, 385-391.

From, J., Rasmussen, G., 1984. A growth model, gastric evacuation, and body composition in rainbow trout, *Salmo gairdneri* Richardson, 1836. Dana 3, 61-139.

Funk, W.C., Tyburczy, J.A., Knudsen, K.L., Lindner, K.R., Allendorf, F.W., 2005. Genetic basis of variation in morphological and life-history traits of a wild population of pink salmon. J. Heredity 96, 24-31.

García-Vázquez, E., Morán, P., Martínez, J., Pérez, B., de Gaudemar, B., Beall, E., 2001. Alternative mating strategies in Atlantic salmon and brown trout J. Heredity 92, 146-149.

Gjerde, B., Gjedrem, T., 1984. Estimates of phenotypic and genetic parameters for carcass traits in Atlantic salmon and rainbow trout. Aquaculture 36, 97-110.

Gjerde, B., Simianer, H., Refstie, T., 1994. Estimates of genetic and phenotypic parameters for body-weight, growth-rate and sexual maturity in Atlantic salmon. Livestock Prod. Sci. 38, 133-143.

Gortázar, J., de Jalón, D.G., Alonso-González, C., Vizcaíno, P., Baeza, D., Marchamalo, M., 2007. Spawning period of a southern brown trout population in a highly unpredictable stream. Ecol. Freshw. Fish 16, 515-527.

Gortázar, J., Alonso, C., de Jalón, D.G., 2012. Brown trout redd superimposition in relation to spawning habitat availability. Ecol. Freshw. Fish 21, 283-292.

Grimm, V., Berger, U., Bastiansen, F., Eliassen, S., Ginot, V., Giske, J., Goss-Custard, J., Grand, T., Heinz, S.K., Huse, G., Huth, A., Jepsen, J.U., Jørgensen, C., Mooij, W.M., Müller, B., Pe'er, G., Piou, C., Railsback, S.F., Robbins, A.M., Robbins, M.M., Rossmanith, E., Rüger, N., Strand, E., Souissi, S., Stillman, R.A., Vabø, R., Visser, U., DeAngelis, D.L., 2006. A standard protocol for describing individual-based and agent-based models. Ecol. Mod. 198, 115-126.

Grimm, V., Berger, U., DeAngelis, D.L., Polhill, J.G., Giske, J., Railsback, S.F., 2010. The ODD protocol: A review and first update. Ecol. Mod. 221, 2760-2768.

Grimm, V., Railsback, S., 2005. Individual-based Modeling and Ecology. Princeton University Press, Princeton, NJ.

Groot, C., Margolis, L. (Editors), 1991. Pacific salmon life histories. UBC Press, Vancouver, Canada.

Grost, R.T., Hubert, W.A., Wesche, T.A., 1990. Redd site selection by brown trout in Douglas Creek, Wyoming. J.Freshw. Ecol. 5, 365-371.

Hanson, P., Johnson, T., Kitchell, J., Schindler, D.E., 1997. Fish Bioenergetics 3.0. University of Wisconsin Sea Grant Institute, Madison, Wisconsin.

Harvey, B.C., Stewart, A.J., 1991. Fish size and habitat depth relationships in headwater streams. Oecologia 87, 336-342.

Harvey, B.C., Marti, C.D., 1993. The impact of dipper, *Cinclus mexicanus*, predation on stream benthos. Oikos 68, 431-436.

Harvey, B.C., Nakamoto, R.J., White, J.L., 1999. Influence of large woody debris and a bankfull flood on movement of adult resident coastal cutthroat trout (*Oncorhynchus clarki*) during fall and winter. Can. J. Fish. Aquat. Sci. 56, 2161-2166.

Harvey, B.C., Nakamoto, R.J., 2013. Seasonal and Among-Stream Variation in Predator Encounter Rates for Fish Prey. Trans. Am. Fish. Soc. 142, 621-627.

Harvey, B.C., Railsback, S.F., 2014. Feeding modes in stream salmonid population models: is drift feeding the whole story? Environ. Biol. Fishes 97, 615-625.

Harvey, B.C., Nakamoto, R.J., White, J.L., Railsback, S.F., 2014. Effects of streamflow diversion on a fish population: combining empirical data and individual-based models in a site-specific evaluation. N. Am. J. Fish. Manage. 34, 247-257.

Haschenburger, J.K., 1999. A probability model of scour and fill depths in gravel-bed channels. Water Resour. Res. 35, 2857-2869.

Hawkins, D.K., Quinn, T.P., 1996. Critical swimming velocity and associated morphology of juvenile coastal cutthroat trout (*Oncorhynchus clarki clarki*), steelhead trout (*Oncorhynchus mykiss*), and their hybrids. Can. J. Fish. Aquat. Sci. 53, 1487-1496.

Healey, M.C., 1991. Life history of chinook salmon (*Oncorhynchus tshawytscha*). Pacific Salmon Life Histories: in Groot, C., Margolis, L. (Editors). UBC Press, Vancouver pp. 564.

Henryon, M., Jokumsen, A., Berg, P., Lund, I., Pedersen, P.B., Olesen, N.J., Slierendrecht, W.J., 2002. Genetic variation for growth rate, feed conversion efficiency, and disease resistance exists within a farmed population of rainbow trout. Aquaculture 209, 59-76.

Hill, J., Grossman, G.D., 1993. An energetic model of microhabitat use for rainbow trout and rosyside dace. Ecology 74, 685-698.

Hodgens, L.S., Blumenshine, S.C., Bednarz, J.C., 2004. Great blue heron predation on stocked rainbow trout in an Arkansas tailwater fishery N. Am. J. Fish. Manage. 24, 63-75.

Hughes, J.B., Daily, G.C., Ehrlich, P.R., 1997. Population diversity: its extent and extinction. Science 278, 689-692.

Hughes, N.F., 1992a. Ranking of feeding positions by drift-feeding arctic grayling (*Thymallus arcticus*) in dominance hierarchies. Can. J. Fish. Aquat. Sci. 49, 1994-1998.

Hughes, N.F., 1992b. Selection of positions by drift-feeding salmonids in dominance hierarchies: Model and test for arctic grayling (*Thymallus arcticus*) in subarctic mountain streams, interior Alaska. Can. J. Fish. Aquat. Sci. 49, 1999-2008.

Hughes, N.F., Dill, L.M., 1990. Position choice by drift-feeding salmonids: Model and test for arctic grayling (*Thymallus arcticus*) in subarctic mountain streams, interior Alaska. Can. J. Fish. Aquat. Sci. 47, 2039-2048.

Hughes, N.F., Hayes, J.W., Shearer, K.A., Young, R.B., 2003. Testing a model of drift-feeding using 3-dimensional videography of wild brown trout in a New Zealand river. Can. J. Fish. Aquat. Sci. 60, 1462-1476.

Hutchings, J.A., 1991. Fitness consequences of variation in egg size and food abundance in brook trout *Salvelinus fontinalis*. Evolution 45, 1162-1168.

Iványi, M., Beckman, R., Conover, W., 1979. A comparison of three methods for selecting values of input variables in the analysis of output from a computer code. Technometrics 21, 239-245.

Jenkins, A.R., Keeley, E.R., 2010. Bioenergetic assessment of habitat quality for stream-dwelling cutthroat trout (*Oncorhynchus clarkii bouvieri*) with implications for climate change and nutrient supplementation. Can. J. Fish. Aquat. Sci. 67, 371-385.

Jensen, H., Bøhn, T., Amundsen, P.-A., Aspholm, P.E., 2004. Feeding ecology of piscivorous brown trout (*Salmo trutta* L.) in a subarctic watercourse. Annales Zoologici Fennici 41, 319-328.

Johnson, T., Barton, N., 2005. Theoretical models of selection and mutation on quantitative traits. Philos. Trans. R. Soc. B-Biol. Sci. 360, 1411-1425.

Johnsson, J.I., Forser, A., 2002. Residence duration influences the outcome of territorial conflicts in brown trout (*Salmo trutta*). Behav. Ecol. Sociobiol. 51, 282-286.

Johnsson, J. I., Nobbelin, F., Bohlin, T., 1999. Territorial competition among wild brown trout fry: effects of ownership and body size. J. Fish Biol. 54, 469-472.

Jonsson, B., Jonsson, N. (Editors), 2011. Ecology of Atlantic Salmon and Brown Trout: Habitat as a Template for Life Histories. Springer, Dordrecht, Netherlands.

Jørgensen, C., Enberg, K., Dunlop, E.S., Arlinghaus, R., Boukal, D.S., Brander, K., Ernande, B., Gardmark, A., Johnston, F., Matsumura, S., Pardoe, H., Raab, K., Silva, A., Vainikka, A., Dieckmann, U., Heino, M., Rijnsdorp, A.D., 2007. Ecology: managing evolving fish stocks. Science 318, 1247-1248.

June, J.A.. 1981. Life history and habitat utilization of cutthroat trout (Salmo clarki) in a headwater stream on the Olympic Peninsula, Washington. MS thesis, College of Fisheries, University of Washington, Seattle.

Keeley, E.R., Grant, J.W.A., 2001. Prey size of salmonid fishes in streams, lakes, and oceans. Can. J. Fish. Aquat. Sci. 58, 1122-1132.

Klemetsen, A., Amundsen, P.A., Dempson, J.B., Jonsson, B., Jonsson, N., O'Connell, M.F., Mortensen, E., 2003. Atlantic salmon *Salmo salar* L., brown trout *Salmo trutta* L. and Arctic charr *Salvelinus alpinus* (L.): a review of aspects of their life histories. Ecol. Freshw. Fish 12, 1-59.

Kopp, M., Gavrilets, S., 2006. Multilocus genetics and the coevolution of quantitative traits. Evolution 60, 1321-1336.

Laaser, C, Leipprand, A, de Roo, C, et al., 2009. Report on good practice measures for climate change adaptation in river basin management plans. EEA Internal report.

Lien, L., 1978. The energy budget of the brown trout population of Øvre Heimdalsvatn. Holarctic Ecol. 1, 279-300.

Louhi, P., Maki-Petays, A. and Erkinaro, J., 2008. Spawning habitat of atlantic salmon and brown trout: General criteria and intragravel factors. River Res. Appl. 24, 330-339.

Lynch, M., Walsh, J.B., 1998. Genetics and Analysis of Quantitative Traits. Sinauer Associates Inc., Sunderland, MA, USA.

MacNutt, M.J., Hinch, S.G., Farrell, A.P., Topp, S., 2004. The effect of temperature and acclimation period on repeat swimming performance in cutthroat trout. J. Fish Biol. 65, 342-353.

Magee, J.P., McMahon ,T.E., Thurow, R.F., 1996. Spatial variation in spawning habitat of cutthroat trout in a sediment-rich stream basin. Trans. Am. Fish. Soc. 125, 768-779.

McKay, L.R., Ihssen, P.E., Friars, G.W., 1986a. Genetic parameters of growth in rainbow trout, *Salmo gairdneri*, as a function of age and maturity. Aquaculture 58, 241-254.

Metcalfe, N.B., Fraser, N.H.C., Burns ,M.D., 1999. Food availability and the nocturnal vs. diurnal foraging trade-off in juvenile salmon. J. Anim. Ecol. 68, 371-381.

Milhous, R.T., Waddle T.J., 2012. Physical Habitat Simulation (PHABSIM) Software for Windows (v.1.5.1). Fort Collins, CO: USGS Fort Collins Science Center.

Miller, T.J., Crowder, L.B., Rice, J.A., Marschall, E.A., 1988. Larval size and recruitment mechanisms in fishes: toward a conceptual framework. Can. J. Fish. Aquat. Sci. 45, 1657-1670.

Morris, M.D., 1991. Factorial sampling plans for preliminary computational experiments. Technometrics 33, 161-174.

Moyle, P.B., Baltz, D.M., 1985. Microhabitat use by an assemblage of California stream fishes: Developing criteria for instream flow determinations. Trans. Am. Fish. Soc. 114, 695-704.

Myrick, C.A., 1998. Temperature, genetic, and ration effects on juvenile rainbow trout (Oncorhynchus *mykiss*) bioenergetics. PhD Thesis. University of California, Davis, Davis, CA.

Myrick, C.A., Cech, J.J. Jr., 2000. Temperature influences on California rainbow trout physiological performance. Fish Physiol. Biochem. 22, 245-254.

Myrick, C.A., Cech, J.J. Jr., 2003. The physiological performance of golden trout at water temperatures of 10 - 19°C. California Fish and Game 89, 20-29.

Nelson, R.L., Platts, W.S., Casey, O., 1987. Evidence for variability in spawning behavior of interior cutthroat trout in response to environmental uncertainty. Great Basin Naturalist 47, 480-487.

Olsen, E.M., Vøllestad, L.A., 2001. Within-stream variation in early life-history traits in brown trout. J. Fish Biol. 59, 1579-1588.

Parra, I., Nicola, G.G., Vøllestad, L.A., Elvira, B., Almodóvar, A., 2014. Latitude and altitude differentially shape life history trajectories between the sexes in non-anadromous brown trout. Evol. Ecol. 28, 707-720.

Pacific Gas and Electric Company (PG&E), 1994. Evaluation of factors causing variability in habitat suitability criteria for Sierra Nevada trout. Report 009.4-94.5. Pacific Gas and Electric Company, Department of Research and Development, San Ramon, CA.

Palkovacs, E.P., Hendry, A.P., 2010. Eco-evolutionary dynamics: intertwining ecological and evolutionary processes in contemporary time. F1000 Biology Reports 2.

Parmesan, C., 2006. Ecological and Evolutionary Responses to Recent Climate Change. Annu. Rev. Ecol. Evol. Syst. 37, 637-669.

Pimm, S.L., Jenkins, C.N., Abell, R., Brooks, T.M., Gittleman, J.L., Joppa, L.N., Raven, P.H., Roberts, C.M., Sexton, J.O., 2014. The biodiversity of species and their rates of extinction, distribution, and protection. Science 344.

Piou, C., Prévost, E., 2012. A demo-genetic individual-based model for Atlantic salmon populations: Model structure, parameterization and sensitivity. Ecol.Mod.231, 37-52.

Post, J.R., Parkinson, E.A., Johnston, E.A., 1998. Spatial and temporal variation in risk to piscivory of age-0 rainbow trout: patterns and population level consequences. Trans. Am. Fish. Soc. 127, 932-942.

Power, M.E., 1987. Predator avoidance by grazing fishes in temperate and tropical streams: importance of stream depth and prey size. Predation, Direct and Indirect Impacts on Aquatic Communities: in Kerfoot, W.C., Sih, A., (Editors). University Press of New England, Hanover, pp. 333-352.

Pujol, G., Iooss, B., Janon, A., 2013. Sensitivity: Sensitivity analysis. R Package Version 1.7.

Quinn, T.P., Buck, G.B., 2001. Size- and sex-selective mortality of adult sockeye salmon: bears, gulls, and fish out of water. Trans. Am. Fish. Soc. 130, 995-1005.

Railsback, S.F., Grimm, V., 2012. Agent-Based and Individual-Based Modeling: A Practical Introduction. Princeton University Press, Princeton, New Jersey.

Railsback, S., and B. Harvey. 2001. Individual-based model formulation for cutthroat trout, Little Jones Creek, California. General Technical Report PSW-GTR-182, Pacific Southwest Research Station, Forest Service, U. S. Department of Agriculture, Albany, CA.

Railsback, S.F., Harvey, B.C., 2002. Analysis of habitat selection rules using an individual-based model. Ecology 83, 1817-1830.

Railsback, S.F., Harvey, B.C., 2013. Trait-mediated trophic interactions: is foraging theory keeping up? Trends Ecol. Evol., 28, 119-125.

Railsback, S.F., Rose ,K.A., 1999. Bioenergetics modeling of stream trout growth: temperature and food consumption effects. Trans. Am. Fish. Soc. 128, 241-256.

Railsback, S.F., Lamberson, R.H., Harvey, B.C. and Duffy, W.E., 1999. Movement rules for individual-based models of stream fish. Ecol. Mod.123, 73-89.

Railsback, S.F., Harvey, B.C., Lamberson, R.H., Lee, D.E., Claasen, N.J., Yoshihara, S., 2002. Population-level analysis and validation of an individual-based cutthroat trout model. Nat. Resour. Mod. 15, 83-110.

Railsback, S.F., Stauffer, H.B., Harvey, B.C., 2003. What can habitat preference models tell us? Tests using a virtual trout population. Ecol. Appl. 13,1580-1594.

Railsback, S.F., Harvey, B.C., Hayes, J.W., LaGory, K.E., 2005. Tests of theory for diel variation in salmonid feeding activity and habitat use. Ecology 86, 947-959.

Railsback, S. F., Hayes, J.W., LaGory, K.E., 2006. Simulation analysis of within-day flow fluctuations on trout below Flaming Gorge Dam. Argonne National Laboratory, ANL/EVS/TM/06-01, Argonne, Illinois.

Railsback, S.F., Harvey, B.C., Jackson, S.K., Lamberson, R.H., 2009. InSTREAM: the individual-based stream trout research and environmental assessment model., U.S. Department of Agriculture, Forest Service, Pacific Southwest Research Station, Albany, CA.

Railsback, S.F., Harvey, B.C., Sheppard, C., 2013. inSTREAM-SD: The Individual-based Stream Trout Research and Environmental Assessment Model with Sub-Daily Time Step, Version 6.0.

Raleigh, R.F., Zuckerman, L.D., Nelson ,P.C., 1986. Habitat suitability index models and instream flow suitability curves: brown trout. Biological Report 82, U.S. Department of Interior.

Rand, P.S., Stewart, D.J., Seelbach, P.W., Jones, M.L., Wedge, L.R., 1993. Modeling steelhead population energetics in lakes Michigan and Ontario. Trans. Am. Fish. Soc. 122, 977-1001.

Reed, T.E., Schindler, D.E., Hague, M.J., Patterson, D.A., Meir, E., Waples, R.S., Hinch, S.G., 2011. Time to evolve? Potential evolutionary responses of fraser river sockeye salmon to climate change and effects on persistence. PLoS ONE 6, e20380.

Reiser, D.W., White, R.G.. 1983. Effects of complete redd dewatering on salmonid egg-hatching success and development of juveniles. Trans. Am. Fish. Soc. 112, 532-540.

Rosenfeld, J.S., Taylor, J., 2009. Prey abundance, channel structure and the allometry of growth rate potential for juvenile trout. Fish. Manage. Ecol. 16, 202-218.

Saltelli, A., Ratto, M., Andres, T., Campolongo, F., Cariboni, J., Gatelli, D., Saisana, M., Tarantola, S., 2008. Global Sensitivity Analysis, The Primer. Wiley, Chichester, UK.

Sánchez-Hernández, J., Cobo, F., 2012. Summer differences in behavioural feeding habits and use of feeding habitat among brown trout (Pisces) age classes in a temperate area. Ital. J. Zool. 79, 468-478.

Schmidt, D., O'Brien, W.J., 1982. Planktivorous feeding ecology of Arctic grayling (*Thymallus arcticus*). Can. J. Fish. Aquat. Sci. 39, 475-482.

Schneider, M.J., Connors, T.J., 1982. Effects of elevated water temperature on the critical swimming speeds of yearling rainbow trout, *Salmo gairdneri*. J. Therm. Biol. 7, 227-229.

Serbezov, D., Bernatchez, L., Olsen, E.M., Vøllestad, L.A., 2010a. Mating patterns and determinants of individual reproductive success in brown trout (*Salmo trutta*) revealed by parentage analysis of an entire stream living population. Mol. Ecol. 19, 3193-3205.

Serbezov, D., Bernatchez, L., Olsen, E.M., Vøllestad, L.A., 2010b. Quantitative genetic parameters for wild stream-living brown trout: heritability and parental effects. J. Evol. Biol. 23, 1631-1641.

Simpkins, D.G., Hubert, W.A., Martinez Del Rio, C., Rule, D.C., 2003a. Physiological responses of juvenile rainbow trout to fasting and swimming activity: effect of body composition and condition indices. Transactions of the American Fisheries Society 132, 576-589.

Simpkins, D.G., Hubert, W.A., Martinez Del Rio, C., Rule, D.C., 2003b. Interacting effects of water temperature and swimming activity on body composition and mortality of fasted juvenile rainbow trout. Can. J. Zool. 81, 1641-1649.

Smoker, W.W., Gharrett, A. J., Stekoll, M.S., Joyce, J.E., 1994. Genetic analysis of size in an anadromous population of pink salmon. Can. J. Fish. Aquat. Sci. 51, 9-15.

Sobol, I., 1993. Sensitivity analysis for non-linear mathematical model. Mathematical Modeling and Computational Experiment 1, 407-414.

Stearley, R.F., 1992. Historical ecology of Salmoninae, with special reference to Oncorhynchus. Systematics, historical ecology, and North American freshwater fishes: in Mayden, R.L. (Ed.). Stanford University Press, Stanford, CA, pp. 622-658.

Taylor, S.E., Egginton, S., Taylor, E.W., 1996. Seasonal temperature acclimatisation of rainbow trout: cardiovascular and morphometric influences on maximal sustainable exercise level. J. Exp. Biol. 199, 835-845.

Thiele, J.C., Kurth, W., Grimm, V., 2014. Facilitating Parameter Estimation and Sensitivity Analysis of Agent-Based Models: A Cookbook Using NetLogo and 'R'. J. Artif. Soc. Soc. Simulat. 17, 11.

Thorpe, J., Mangel, M., Metcalfe, N., Huntingford, F., 1998. Modelling the proximate basis of salmonid life-history variation, with application to Atlantic salmon, *Salmo salar* L. Evol. Ecol. 12, 581-599.

Valdimarsson, S.K., Metcalfe, N.B., Thorpe, J.E., Huntingford, F.A., 1997. Seasonal changes in sheltering: Effect of light and temperature on diel activity in juvenile salmon. Anim. Behav. 54, 1405-1412.

Van Winkle, W., Jager, H.I., Holcomb, B.D., 1996. An individual-based instream flow model for coexisting populations of brown and rainbow trout. EPRI TR-106258, Electric Power Research Institute, Palo Alto, CA.

Vedder, O., Bouwhuis, S. and Sheldon, B.C., 2013. Quantitative Assessment of the Importance of Phenotypic Plasticity in Adaptation to Climate Change in Wild Bird Populations. PLoS Biol. 11, e1001605.

Verdonschot, P., Keizer-Vlek, H., Spears, B., et al., 2012. Final report on impact of catchment scale processes and climate change on cause-effect and recovery-chains. WISER Deliverable D6.4-3

Vincenzi, S., De Leo, G.A. and Bellingeri, M., 2012. Consequences of extreme events on population persistence and evolution of a quantitative trait. Ecol. Inform. 8, 20-28.

Vincenzi, S., 2014. Extinction risk and eco-evolutionary dynamics in a variable environment with increasing frequency of extreme events. J. R. Soc. Interface 11, 20140441.

Wiegand, T., Jeltsch, F., Hanski, I. and Grimm, V., 2003. Using pattern-oriented modeling for revealing hidden information: a key for reconciling ecological theory and application. Oikos 100, 209-222.

Wootton, R.J., 1998. Ecology of Teleost Fishes, 2nd edn. Kluwer, London.

Wilensky, U., 1999. NETLOGO. Centre for Connected Learning and Computer-Based Modelling. Northwestern University, Evanston, IL. See. http://ccl.northwestern.edu/netlogo.

# References to further TRACE documents


Ayllón, D., Railsback, S.F., Vincenzi, S., Groeneveld, J., Almodóvar, A., Grimm, V. 2016. InSTREAM-Gen: Modelling eco-evolutionary dynamics of trout populations under anthropogenic environmental change. Ecological Modelling 326: 36-53.

Backmann, P., Grimm, V., Jetschke, G., Lin, Y., Vos, M., Baldwin, I.T., van Dam, N.M. 2019. Delayed Chemical Defense: Timely Expulsion of Herbivores Can Reduce Competition with Neighboring Plants. The American Naturalist 193: 125-139.

Boult, V.L., Quaife, T., Fishlock, V., Moss, C.J., Lee, P.C., Sibly, R.M. 2018. Individual-based modelling of elephant population dynamics using remote sensing to estimate food availability. Ecological Modelling 387: 187-195.

Boyd, R., Roy, S., Sibly, R., Thorpe, R., Hyder, K. 2018. A general approach to incorporating spatial and temporal variation in individual-based models of fish populations with application to Atlantic mackerel. Ecological Modelling 382: 9-17.

Dey, C. J., Richardson, E., McGeachy, D., Iverson, S.A., Gilchrist, H.G., Semeniuk, C.A. 2017. Increasing nest predation will be insufficient to maintain polar bear body condition in the face of sea ice loss. Global Change Biology 23: 1821-1831.

Dick, D.D.C., Ayllón, D. 2017. FloMan-MF: Floodplain Management for the Moor Frog — a simulation model for amphibian conservation in dynamic wetlands. Ecological Modelling 348: 110-124.

Erickson, R.A., Thogmartin, W.E., Diffendorfer, J.E., Russell, R.E., Szymanski, J.A. 2016. Effects of wind energy generation and white-nose syndrome on the viability of the Indiana bat. PeerJ 4: e2830.

Erickson, R.A., Eager, E.A., Brey, M.K., Hansen, M.J., Kocovsky, P.M. 2017. An integral projection model with YY-males and application to evaluating grass carp control. Ecological modelling 361: 14-25.

Galic, N. , Grimm, V., Forbes, V. E. 2017. Impaired ecosystem process despite little effects on populations: modeling combined effects of warming and toxicants. Global Change Biology 23: 2973-2989.

Kułakowska, K.A., Kułakowski, T.M., Inglis, I.R., Smith, G.C., Haynes, P.J., Prosser, P., Thorbek, P., Sibly, R.M. 2014. Using an individual-based model to select among alternative foraging strategies of woodpigeons: Data support a memory-based model with a flocking mechanism. Ecological Modelling 280: 89-101.

Langtimm, C.A., Kendall, W.L., Beck, C.A., Kochman, H.I., Teague, A.L., Meigs-Friend, G., Peñaloza, C.L. 2016. Model Description and Evaluation of the Mark-Recapture Survival Model Used to Parameterize the 2012 Status and Threats Analysis for the Florida Manatee (*Trichechus manatus latirostris*). Report No. 2016-1163. US Geological Survey.

Liukkonen, L., Ayllón, D., Kunnasranta, M., Niemi, M., Nabe-Nielsen, J., Grimm, V., Nyman, A.-M. 2018. Modelling movements of Saimaa ringed seals using an individual-based approach. Ecological Modelling 368: 321-335.

McClure, C.J., Pauli, B.P., Mutch, B., Juergens, P. 2017. Assessing the importance of artificial nest-sites in the population dynamics of endangered Northern Aplomado Falcons Falco femoralis septentrionalis in South Texas using stochastic simulation models. Ibis 159: 14-25.

Nabe-Nielsen, J., Beest, F.M., Grimm, V., Sibly, R.M., Teilmann, J., Thompson, P.M. 2018. Predicting the impacts of anthropogenic disturbances on marine populations. Conservation Letters 11: e12563.

Pauli, B.P., Spaul, R.J., Heath, J.A. 2017. Forecasting disturbance effects on wildlife: tolerance does not mitigate effects of increased recreation on wild lands. Animal Conservation 20: 251-260.

Schmolke, A., Brain, R., Thorbek, P., Perkins, D., Forbes, V. 2017. Population modeling for pesticide risk assessment of threatened species — A case study of a terrestrial plant, *Boltonia decurrens*. Environmental Toxicology and Chemistry 36: 480-491.

Watermeyer, K.E., Jarre, A., Shannon, L.J., Mulumba, P., Botha, J. 2018. A frame-based modelling approach to understanding changes in the distribution and abundance of sardine and anchovy in the southern Benguela. Ecological Modelling 371: 1-17.

Weller, F., Sherley, R.B., Waller, L.J., Ludynia, K., Geldenhuys, D., Shannon, L.J., Jarre, A. 2016. System dynamics modelling of the Endangered African penguin populations on Dyer and Robben islands, South Africa. Ecological modelling 327: 44-56.